

Evaluation of Microcracking and Chemical
Deterioration in Concrete Pavements

Final Report

October 31, 1995

S. Schlorholtz

J. Amenson

Iowa DOT PROJECT HR-358

ERI PROJECT 3711

ISU-ERI-96402

Sponsored by the Highway Division of the Iowa Department of
Transportation and the Iowa Highway Research Board

"The opinions, findings and conclusions expressed in this publication are those of the authors and not necessarily those of the Highway Division of the Iowa Department of Transportation."

TABLE OF CONTENTS

ABSTRACT	iii
INTRODUCTION	1
Background	1
RESEARCH APPROACH	6
Cores Available for Analysis	7
Other Samples for Analysis	8
Equipment	8
Shale Counts	10
SAMPLE PREPARATION	10
Procedure Used for Specimen Preparation	11
SEM INVESTIGATION ROUTINES	11
Basics	11
Standard Operating Procedure	13
Potential Errors	14
RESULTS AND DISCUSSION	17
Results of Different Sample Prep. Techniques	17
CMI Cores	29
Highway US 20 Cores	35
I-35 Cores	51
I-80 Cores	59
Fast-track Pavement at Bettendorf	65
Assorted Other Cores	72
SUMMARY AND CONCLUSIONS	81
RECOMMENDATIONS	85
Field Concrete	85
Concrete Materials	86
Additional Research	87
CLOSING COMMENTS	88
ACKNOWLEDGEMENTS	90
REFERENCES	90
APPENDICES	
Appendix A - Summary of Core Logs	93
Appendix B - Summary of Shale Counts	148
Appendix C - DSC Results, Preliminary	171

ABSTRACT

The major objective of this research project was to investigate the chemistry and morphology of portland cement concrete pavements in Iowa. The integrity of the various pavements was evaluated qualitatively, based on the presence or absence of microcracks, the presence or absence of sulfate minerals, and the presence or absence of alkali-silica gel(s).

Major equipment delays and subsequent equipment replacements resulted in significant delays over the course of this research project. However, all these details were resolved and the equipment is currently in place and fully operational. The equipment that was purchased for this project included: (1) a LECO VP 50, 12-inch diameter, variable speed grinder/polisher; (2) a Hitachi S-2460N variable pressure scanning electron microscope; and (3) a OXFORD Instruments Link ISIS microanalysis system with a GEM (high-purity germanium) X-ray detector.

This study has indicated that many of the concrete pavements contained evidence of multiple deterioration mechanisms; and hence, the identification of a single reason for the distress that was observed in any given pavement typically had to be based on opinion rather than empirical evidence.

INTRODUCTION

Concrete is typically a very durable building material. However, there are a few instances where special precautions must be taken to ensure that it does not exhibit premature deterioration. For instance, when concrete is exposed to cyclical freezing and thawing it is normally desirable to use an air-entraining admixture to increase the durability of the mortar fraction of the concrete. Also, when concrete is to be exposed to soluble salts (sulfates, alkalis, etc.) it is wise to use a mix design that produces a concrete with a very low permeability (i.e., low water/cement ratio), high cement content (using the proper ASTM cement type), and one that incorporates aggregates that are not prone to alkali-induced expansion. However, the deterioration of concrete is still a fact of life. Any composite material like concrete can fail because of a wide variety of different circumstances. The key to understanding and avoiding future occurrences of similar failures is to be able to identify the true cause of the problem, whether it is related to design parameters, constituent materials or construction processes.

This report summarizes the research activities conducted on Iowa Department of Transportation Project HR-358. The objective of this research project was to investigate the chemistry and morphology of core specimens that were taken from portland cement concrete pavements throughout Iowa. The pavements that were cored exhibited a wide range of field performance; and hence, have helped to contrast how microstructure relates to the observed performance of field concrete. The goal of the project was to enhance the ability of engineers to diagnose the reason(s) for materials related failures in concrete pavement systems.

Background

Recent field observations of deteriorating concrete pavements in Wisconsin, Minnesota, Nebraska and Iowa have indicated that several different forms of

chemical and/or physical attack may have been involved in the degradation process [1, 2, 3, 4]. The major deterioration mechanisms that have been identified were alkali-aggregate (silicate) reaction (ASR), delayed ettringite formation (DEF), and freeze-thaw damage. It is pertinent to point out that mixed mode failure (i.e., ASR or DEF coupled with freeze-thaw attack) are quite probable in pavement concrete due to the severe exposure conditions. Each mode of deterioration produces microcracks that grow as the degradation proceeds. Only a brief description of these degradation mechanisms will be discussed here because both the macroscopic and microscopic perspectives have been addressed in previous reports [5, 6].

Alkali-aggregate reactions occur because some types of aggregates react with the alkaline pore solution in concrete to produce a gel. The gel tends to imbibe water and expand. The expansion, which typically occurs within the aggregate particle, eventually causes cracking in the surrounding paste. The kinetics of the process (i.e., the time required for the onset of deterioration) are very complicated and researchers are still working to find reliable correlations between laboratory testing and actual field performance. However, many of the aggregates that exhibit sensitivity to alkalis have been (or are currently being) cataloged [7, 8].

Cracking of portland cement based materials due to delayed ettringite formation (DEF) is considerably less well defined than alkali-aggregate reactivity [9]. In fact, some researchers still insist that such a phenomenon cannot occur in concretes subjected to normal curing (for a literature survey on this topic please refer to reference 9). The cracking is typically observed several years after construction is completed. This process is different from normal (external) sulfate attack because the external source of sulfates is not required. The chemical product evident in both cases is the same, namely ettringite (although gypsum may also form in some situations).

Weathering (freezing and thawing) often plays a major role in the deterioration of concrete pavements. This is due to the severe exposure conditions (i.e., continuous wetting and drying coupled with large temperature fluctuations), plus the routine application of deicing salts. Freeze-thaw durability failure (i.e., cracking) can occur in the mortar phase of the concrete or in the coarse aggregate fraction of the concrete. The durability of the mortar can be improved by entraining air voids in the concrete. Likewise, selective quarrying and proper materials specifications (based on service record) generally help to avoid coarse aggregate durability failures.

There are several other processes that may cause cracking in portland cement based products. The interested reader should refer to [8] for a general overview of these processes and a description of the cracking patterns that may be observed in field investigations. However, the point of the previous discussion is that the various deterioration mechanisms produce different distortions in the concrete specimens. Johansen, Thaulow and Sklany [10], list the following possibilities for the expansion of concrete in the field:

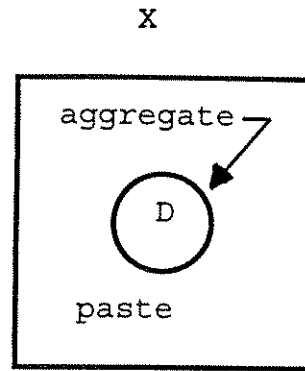
1. Both cement paste and aggregate expand.
2. Cement paste expands, aggregate does not expand.
3. Aggregate expands, cement paste does not expand.

These idealized expansion processes are illustrated in Figure 1. Keep in mind, that cracking typically occurs when the expansion pressure exceeds the tensile strength of the constituent.

ASR produces expansion in reactive aggregate particles (see possibility 3 above and Fig. 1d). The expansion eventually causes cracking. Deleterious expansion occurs when these cracks propagate through the cement paste. Note, that often the paste-aggregate interface will remain intact during alkali-induced deterioration because the cement paste does not expand. Hence, ASR induced deterioration includes cracked aggregates, cracks extending from aggregates into the paste, and gel material.

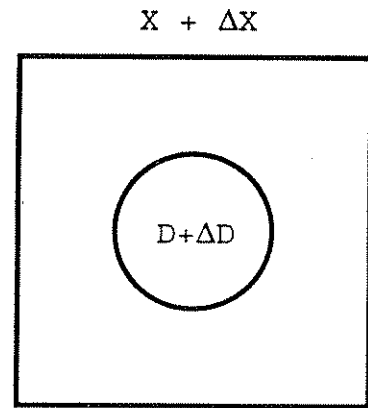
1a - Idealized concrete in its initial state.

Y



1b - Cement paste expands, aggregate expands.

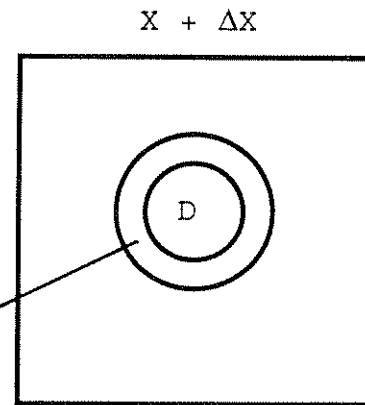
$Y + \Delta Y$



1c - Cement paste expands, aggregate does not.

$Y + \Delta Y$

note gap



1d - Aggregate expands, cement paste does not.

Y

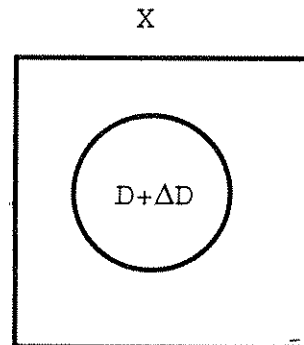


Figure 1. Idealization of expansion mechanisms in field concrete.

Secondary ettringite formation (or, also, external sulfate attack) occurs in the paste fraction of concrete; and hence, causes the paste to expand. This process is illustrated in Figure 1c (thinking in terms of cylindrical or spherical coordinates, rather than the Cartesian coordinates depicted in the figure, greatly simplifies the idealization process). Note that since the aggregate does not expand there may be a noticeable gap between the aggregate and the cement paste.

Frost damage is more complicated because it can occur in the coarse aggregate, the cement paste, or both; and it depends on whether a constituent reaches critical saturation (about 90% saturated, give or take a few percent). Freeze-thaw attack in the coarse aggregate (durability cracking or d-cracking) creates the situation depicted in Fig. 1d. Freeze-thaw attack in the paste fraction of the concrete creates the situation depicted in Fig. 1c. Obviously, the use of poor coarse aggregate and poor air entrainment in concrete could lead to expansion in both the aggregate and the paste (see Fig. 1b).

It is important to understand the concepts illustrated in Figure 1 because they describe the fabric (morphology) that should be observed in specimens of concrete obtained from the field. These observations of fabric, coupled with information about the chemical composition, essentially lead to petrographic examination as defined by Katharine Mather [11].

For the purpose of this report several terms will be used rather loosely. The terms macrocracks and microcracks need some explanation because they will not be used in a quantitative sense in this report. Instead, macrocracks refer to cracks that are visible to the eye or at very low (2X) magnification. Microcracks refer to cracks that require a microscope for observation. Also, the terms ettringite and sulfate-bearing material will often be used interchangeably, and the term ettringite will denote a mineral group (i.e., similar crystal structures but with varying chemical composition, as is often observed in real systems; however, the deviations from the pure endmember appear small in this study).

RESEARCH APPROACH

Petrographic methods were the major analytical methods that were chosen to investigate the characteristics of the concrete core specimens that were obtained for this study. These techniques generally produce information that helps to identify the distress mechanisms(s) present in concrete materials [8, 11, 12, 13, 14].

The core samples were cut into sections (see Fig. 2) to produce specimens for analysis. Normally, the sections denoted as B and C were used in this study so that information pertaining to the top and bottom of the pavement slab could be obtained. However, all of the sections were inspected (the longitudinal sections were particularly informative) over the course of this investigation. Also, some of the core specimens (see IA 25 and US 169 described later in this report) were in such a deteriorated state that the sectioning using the normal techniques was impossible.

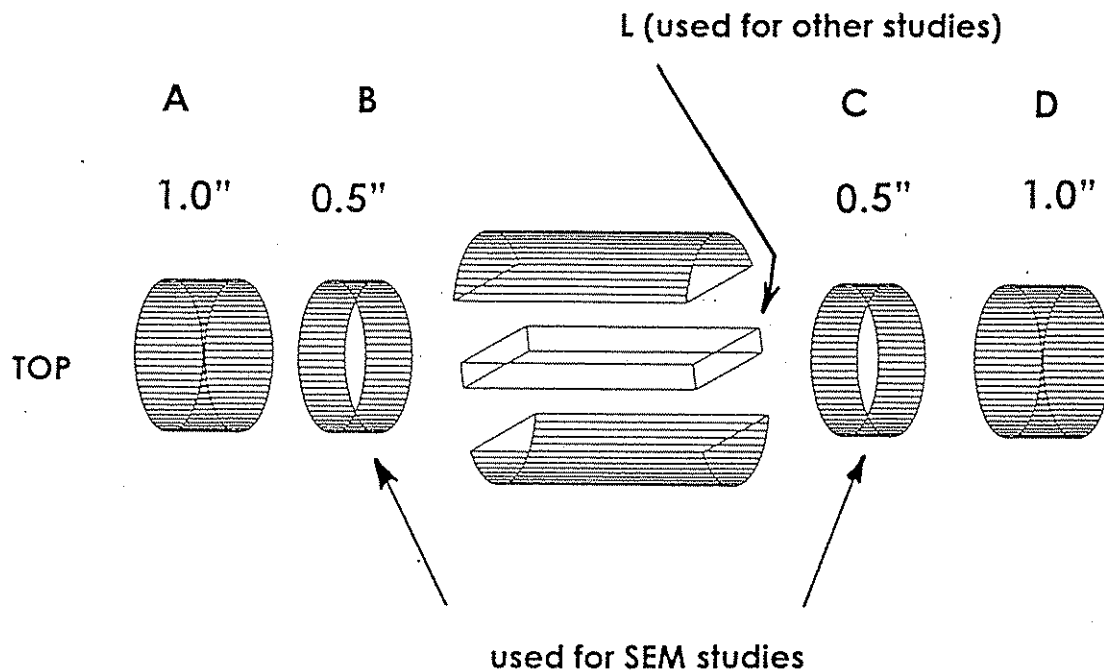


Figure 2. Illustration depicting the sectioning of the core specimens.

Typically, the investigation began with a quick visual inspection of the core specimen using the naked eye or a low-power (2X) magnifying lens. This was followed by a more detailed investigation using conventional light microscopy and scanning electron microscopy. The scanning electron microscope (SEM) featured the ability to operate at variable pressures (to minimize specimen cracking that normally occurs in high-vacuum systems) and it was equipped with an energy dispersive X-ray analyzer. The specific details pertaining to these procedures will be described in more detail below.

Cores Available for Analysis

Core specimens were drilled from a variety of different portland cement concrete pavements across Iowa. The core samples were taken by Iowa Department of Transportation (IDOT) personnel and then transported to the Materials Analysis and Research Laboratory (MARL) at Iowa State University, for specimen preparation and analysis. Core logs are listed in Appendix A.

The various pavement cores were assigned priority numbers, ranging from 1 through 6, at a subsequent meeting with IDOT engineers and geologists (see Table 1). Priority numbers were assigned to indicate the order that the samples should be analyzed (highest priority = 1, lowest priority =6).

Table 1. Summary of cores taken for this project.

Priority Number	Description	Number of Cores
1	Cores from the Materials Quality Task Force study at the Iowa DOT	6 cores 2 beams
2	US 520 in Webster County	12
3	I-35 in Story County	8
4	I-80 in Dallas County	4
5	Bettendorf street in Scott County	4
6	Assorted cores from Louisa, Madison, Hamilton, Union and Buchanan Counties	25

Other Samples for Analysis

A wide variety of mortar bar specimens and several concrete beam specimens were also available for analysis. All of the mortars and concretes were taken from a chemical durability research project that had recently been completed [6]. Hence, all of the mortars and concretes were proportioned, mixed and cured in a laboratory environment. All of these samples had been exposed to very severe environments which should have accelerated the alkali silica reaction or sulfate deterioration processes. Also, the various test specimens had been monitored for various physical properties (i.e., length change, etc.) as a function of exposure time. These specimens were selected because they would allow a more quantitative evaluation of the level of deterioration that is present in the mortar fraction of the specimens. However, due to the many procurement and equipment related delays that plagued this project, most of these specimens still need to be analyzed. Unfortunately, all of the concrete specimens were inadvertently discarded and will not be available for future studies.

Equipment

A Hitachi S-2460N, variable pressure SEM was used for this project. This SEM was selected because it would accept large specimens (up to 6-inches in diameter) and had a stage movement capable of traversing a four inch specimen. The SEM can be operated at pressures ranging from 0.01 to 2 Torr (1 to 270 pascals), in the variable pressure mode. The "variable pressure" mode (also referred to as "low-vacuum") allows researchers to analyze difficult specimens, like concrete or portland cement mortars, in their natural state, without the tedious sample preparation techniques that are normally mandatory for conventional scanning electron microscopes [14, 15, 16]. The scanning electron microscope was equipped with a Robinson backscattered electron detector and an Oxford Instruments GEM energy dispersive X-ray detector. The GEM X-ray detector has a higher resolution than most typical X-ray detectors

(111 eV in best resolution mode, measured at our laboratory, for Mn K_{α} radiation; as compared to about 140 to 150 eV for most conventional Si(Li) detectors). The detector was generally operated in optimum acquisition rate mode. This caused the resolution to drop to about 133 eV but allowed X-ray spectrums and maps to be obtained relatively quickly since they could be acquired at a rate of 10,000 counts per second (about 20 to 25 percent deadtime).

A LECO variable speed grinder/polisher (model VP-50) was used to prepare the core specimens for detailed microscopic investigation. The grinder/polisher was equipped with a 12-inch diameter brass wheel. Fixed grit silicon carbide paper was used throughout the study.

Several different microscopes were used for the light microscopy phase of this study. Thin sections were viewed with an Olympus BH-2 transmitted light microscope or a Unitron polarizing microscope. Bulk or polished specimens were viewed in reflected light with an Olympus BH reflected light microscope or an Olympus SZH stereo microscope.

A Buehler LAPRO slab saw (18 inch model) was used to cut the cores into pieces for analysis. The saw was equipped with an 18-inch diameter notched-rim diamond blade. Propylene glycol (reagent grade from Fisher Scientific Company) was used as the lubricant/coolant for the blade during the cutting process.

A TA-Instruments differential scanning calorimeter (DSC, Model 2910) was used to analyze portions of the paste that were extracted from some of the core specimens. A typical experiment was conducted on a 10 milligram specimen that was heated from 25°C to about 550°C using a heating rate of 10 degrees per minute. All specimens were sealed in aluminum specimen containers prior to analysis. A pinhole was punched through the top of the specimen container prior to analysis. Nitrogen was purged through the system to avoid oxidation of the DSC cell.

A Siemens D-500 X-ray diffractometer was used to analyze portions of the paste that were extracted from some of the core specimens. A typical experiment used a copper X-ray tube (excitation conditions: 50kV and 27 mA) and a diffracted beam monochromator. Specimens were front-loaded into a silicon sample holder for analysis. Scanning rates were generally below 0.5 degrees per minute due to the very poor crystalline nature of the hydrates commonly observed in portland cement pastes.

Shale Counts

Prior investigators had indicated that shale particles were a major factor in the premature deterioration of some of the concrete included in this study [2]. Hence, the shale content of selected cores was estimated by counting shale particles on the interior surfaces of the core specimens using a low power magnifying glass. The total area that was inspected for shale particles amounted to about 170 square inches (i.e., all the sawn faces shown in Fig. 2). Total number of shale particles, maximum size and distance from the top of the core (in 1-inch increments), are tabulated in Appendix B.

SAMPLE PREPARATION

Sample preparation for the low-vacuum scanning electron microscope used in this study, is considerably simpler than the techniques that are commonly employed for conventional scanning electron microscopes because there is no need to coat the sample with a conductive film. Several different sample preparation methods have been used during different stages of this project. They included fractured surfaces, sawn surfaces, ground and polished surfaces and thin sections. Examples of each different sample preparation technique will be illustrated and discussed in detail later in this report.

Procedure Used for Specimen Preparation

The method that was most commonly employed in this project consisted of: (1) sawing off a section of the concrete; (2) rinsing off the propylene glycol; (3) grinding the sample surface flat by using fixed grit paper (grit sizes listed in Table 2, water used as a lubricant); and (4) cleaning the surface of the sample with petroleum ether (Skelly B) or acetone to remove any residual debris from the final grinding/polishing step. This sample preparation method is similar to the method that is commonly used to prepare specimens for air void analysis by standard ASTM procedures [7].

Table 2. Grinding and polishing procedure for the concrete cores.

Step	Current method grit size (micron equiv.)	ASTM C 457 (see [7]) grit size (micron equiv.)
1	180 (70 μ m)	100 (150 μ m) optional
2	320 (30 μ m)	220 (75 μ m)
3	600 (17 μ m)	320 (35 μ m)
4	800 (12 μ m)	600 (17.5 μ m)
5	1200 (2 to 5 μ m)	800 (12.5 μ m)
6	optional 1 μ m diamond paste	optional 5 μ m Alumina

SEM INVESTIGATION PROCEDURES

Basics

As mentioned above, two types of information have been collected in this project. First, the macroscopic and microscopic features from each core have been collected by means of pictures. And secondly, the chemistry of the core specimens has been investigated by collecting digital X-ray maps of various features that were observed in the pictures. Obviously, as the title of this research project suggests, the regions of interest will normally contain cracks. The basic details pertinent to the collection process are illustrated in Figure 3. It is

important to note that the imaging process employed two entirely separate detectors. The pictures were generated from a backscattered electron detector that was located directly above the specimen. The elemental maps were constructed using the signal from the GEM X-ray detector.

The pictures consist of the normal (analog) format and a more modern, computer readable format (digital, this format was available only for work conducted using the SEM). The analog format currently offers more resolution (about 2000 by 1500 lines per picture) than the digital format (digital images can be collected at 256 by 192 pixels, 512 by 384 pixels or 1024 by 768 pixels). However, the digital format will surely be the media of the future because: (1) computer storage media costs are falling rapidly,; (2) the resolution of digital images is constantly being increased (second source vendors already boast 4096 by 4096 pixel images); and (3) the images can be manipulated (i.e., magnified or processed using image analysis) and cataloged (e.g. an image

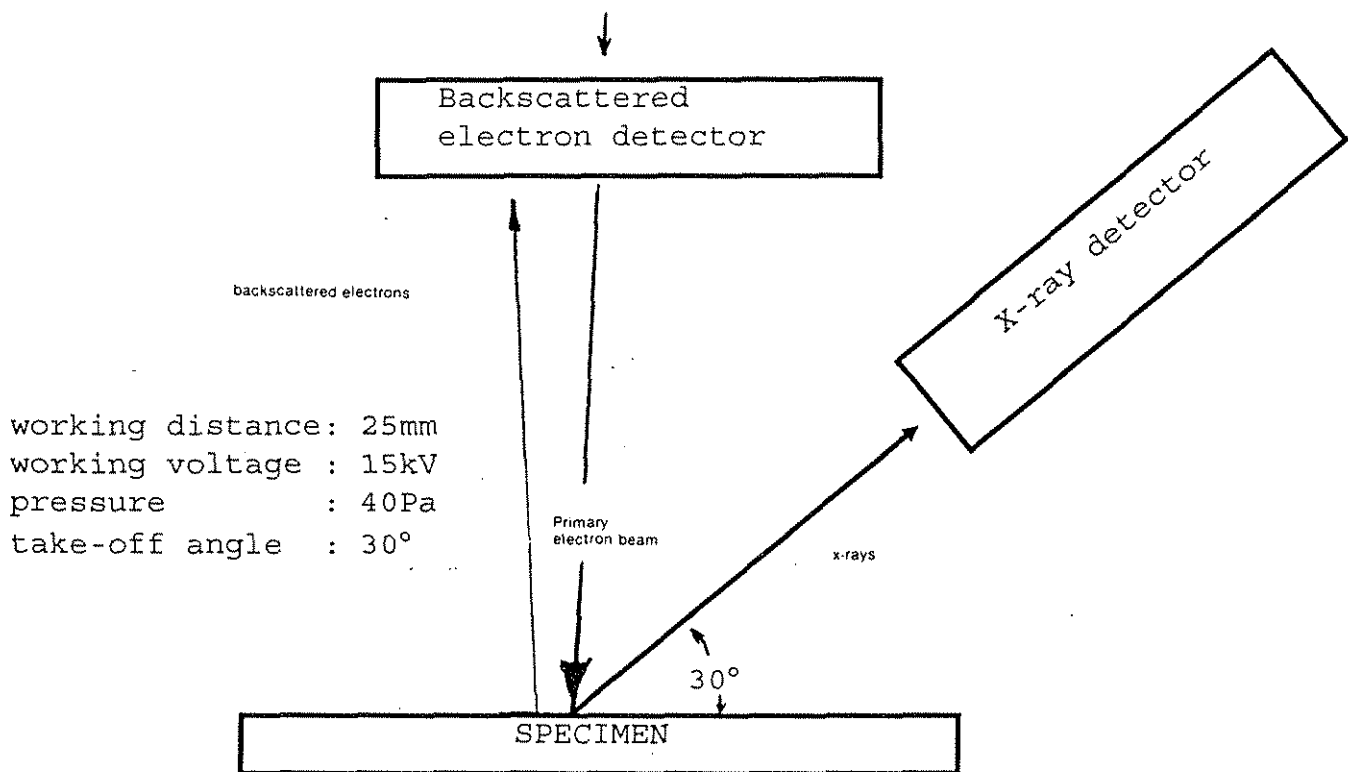


Figure 3. Illustration of details pertaining to the SEM study.

database) using less resources than is required for conventional pictures. For the purpose of this research project both media formats have been used. Typically, pictures were taken using Polaroid Type 55 film because it has a negative that can be used for enlargements. The digital images were normally collected using the high resolution (1024 by 768 pixels) mode; however, some lower resolution images were also collected.

The Link ISIS program SPEEDMAP was used to collect the digital X-ray maps for this project. This particular program allows researchers to collect information on 30 different elements, simultaneously. The major elements of interest in this project were oxygen (O), sodium (Na), magnesium (Mg), aluminum (Al), silicon (Si), sulfur (S), chlorine (Cl), potassium (K), calcium (Ca) and iron (Fe). Occasionally, after special treatments, other elements were also measured (i.e., uranium). Digital X-ray maps were normally collected at a resolution of 256 by 192 pixels; however, occasionally higher resolution maps were collected (512 by 384 pixels).

Standard Operating Procedure

Test specimens were normally seated in the specimen holder and then marked with reference points so that they could be removed and then reinserted into the SEM at the same nominal location (i.e., easy location of the features of interest). The study of a specimen began by scanning rapidly over the surface of the specimen at a magnification of 15X to 20X. This process was conducted as shown in Figure 4. The process was videotaped so that gross details could be permanently recorded. The videotaping, which took about 10 to 15 minutes per specimen to complete, provides a good record of approximately 65% of the surface of each specimen. It also provides preliminary indications of void (entrapped and entrained air) content, homogeneity of the specimen, and cracking in the aggregate and/or paste fraction of the concrete. During the videotaping session the microscopist recorded the x-y coordinates of interesting features that could be investigated in more detail.

Another source of error in the X-ray maps was due to topography in the specimens. Since all of the concrete cores contained entrained air voids (these voids are huge on a microscopic scale) one can often see shadows in the X-ray maps (see Fig. 6). These shadows result from the fact that the X-ray detector had a take-off angle of 30 degrees relative to the specimen surface. A comparison of the backscattered electron image and the oxygen X-ray map normally allows one to quickly identify when shadowing may distort the X-ray image. For the convenience of the operator no attempt was made to tilt the specimen towards the detector to minimize this error.

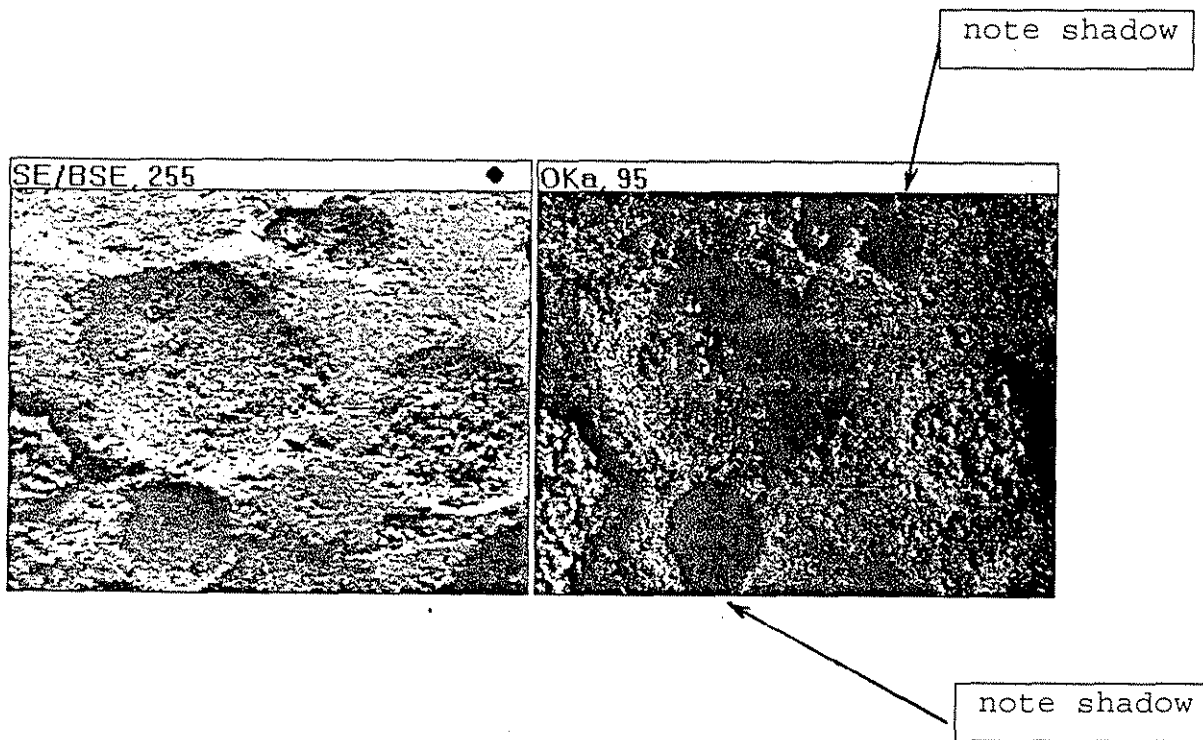


Figure 6. Illustration of how specimen morphology distorts the X-ray images.

RESULTS AND DISCUSSION

The results from this study will be discussed in detail; however, due to the nature of the data collected in this research project (i.e., pictures or images), it is difficult to display the results in a text-based report. Also, since this report has been published without using color it lacks many of the sophisticated image processing techniques that can be used to enhance and clarify subtle details. These techniques are available and can be used to manipulate the digital data; however, publishing costs prohibited their use in this report. Hence, much of the information has been reduced to tabular form. This is a great disservice because it limits the information that can be presented. However, it is not currently possible to create and distribute a multimedia based report that can incorporate all of the digital data (although this will be possible in the near future). The original photographs, hard copies of the X-ray maps, and copies of the exploratory videotapes were submitted to the Iowa Department of Transportation upon completion of the project. The availability and distribution of the original information is left to their discretion.

Results of Different Sample Preparation Techniques

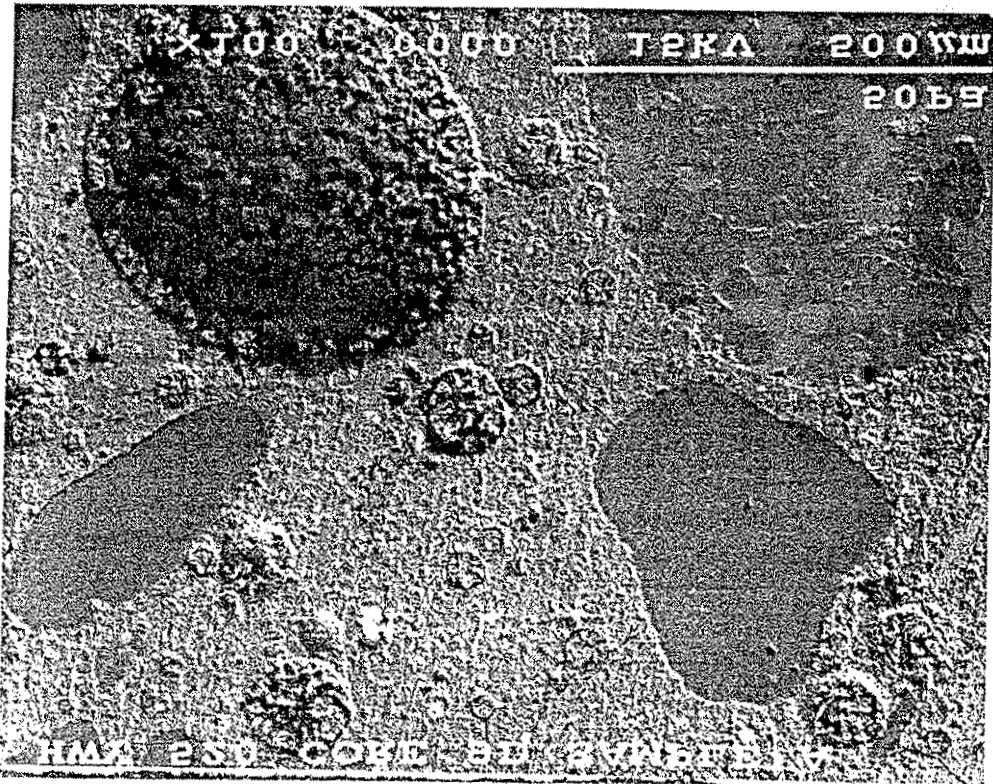
Sample preparation is critical to the interpretation petrographic examinations; and hence, this study has briefly evaluated the use of four different common sample preparation techniques. These techniques included the observation of freshly fractured surfaces, sawn surfaces, ground and polished surfaces, and standard thin section surfaces.

The thin sections were prepared by a commercial petrographic consultant (Spectrum Petrographics, Winston, Oregon) using both standard techniques and special techniques that are often employed for water and heat sensitive samples. There were no apparent differences between the specimens prepared by the standard or sensitive materials procedures. Backscattered electron images obtained from a typical thin section are shown in Figure 7. The

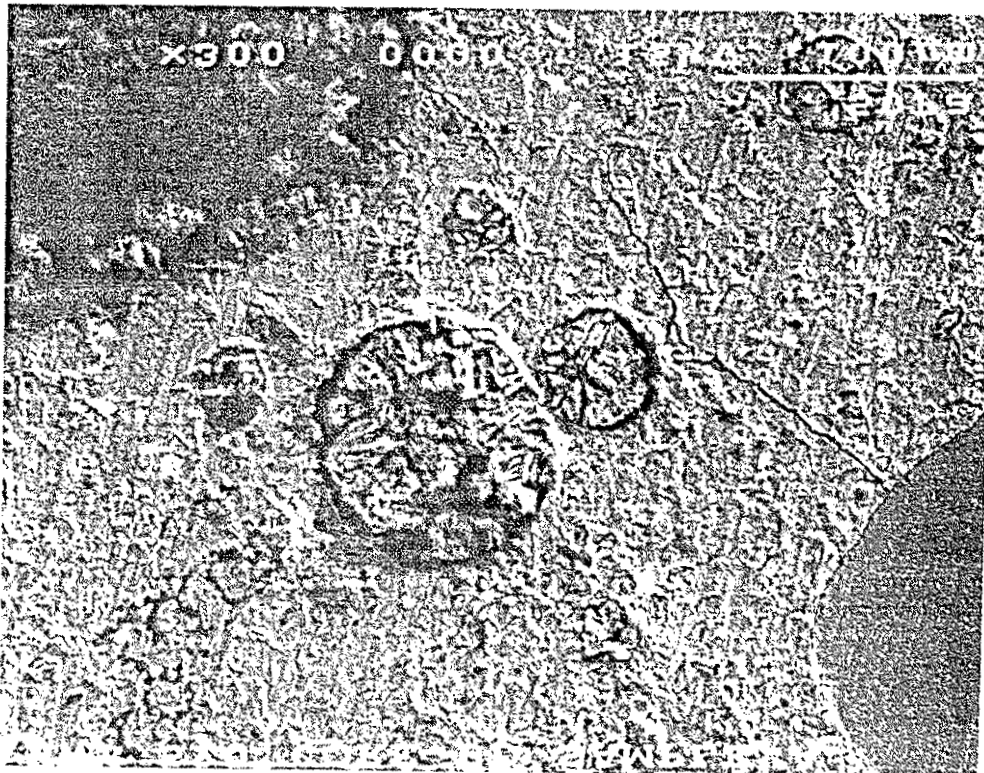
image clearly indicates the presence of material in the air voids. In fact, many of the smaller voids have been completely filled. Fine hair line cracks were also evident in the paste portion of the specimen. Most of the features remained intact during the preparation of the thin section; however, some of the shale particles were destroyed by the process.

Backscattered electron images obtained from the normal sample preparation method used in this study (ground and polished surfaces), which was described earlier in this report, are shown in Figure 8. The images have been oriented so that the area shown in Figure 7 corresponds closely to the area shown in Figure 8. The images shown in Figure 8 were obtained before the samples were sent to be made into thin sections. This allowed the laboratory that made the thin sections to prepare a specimen of nearly the same area that had been viewed on the bulk specimen (except for the 30 micron thickness of the thin section).

Overall, Figures 7 and 8 contain essentially the same information. The surface polish is a little better in Figure 8 than in Figure 7, but the major features, particularly the filled voids, have been preserved in both sample preparation techniques. The voids are filled with a sulfate bearing mineral (see Fig. 9). The X-ray map indicates that only a small amount of aluminum is present in the material in the voids, this suggests that the material's composition has been altered to some extent by the sample preparation process because the material started out as ettringite. If the thin section is viewed in transmitted light using a petrographic microscope the voids appear to be nearly empty. This may help to explain why these features were not mentioned in previous studies of similar cores [2,17]. The distinct morphology of the ettringite is easily recognized when using a scanning electron microscope. In addition, the visual information can easily be supplemented with chemical information (via an X-ray spectrum or an X-ray map). This allows one to better estimate the identity of the object that is being observed.



Magnification = 100X



Magnification = 300X

Figure 8. US 20, polished specimen, normal preparation technique.

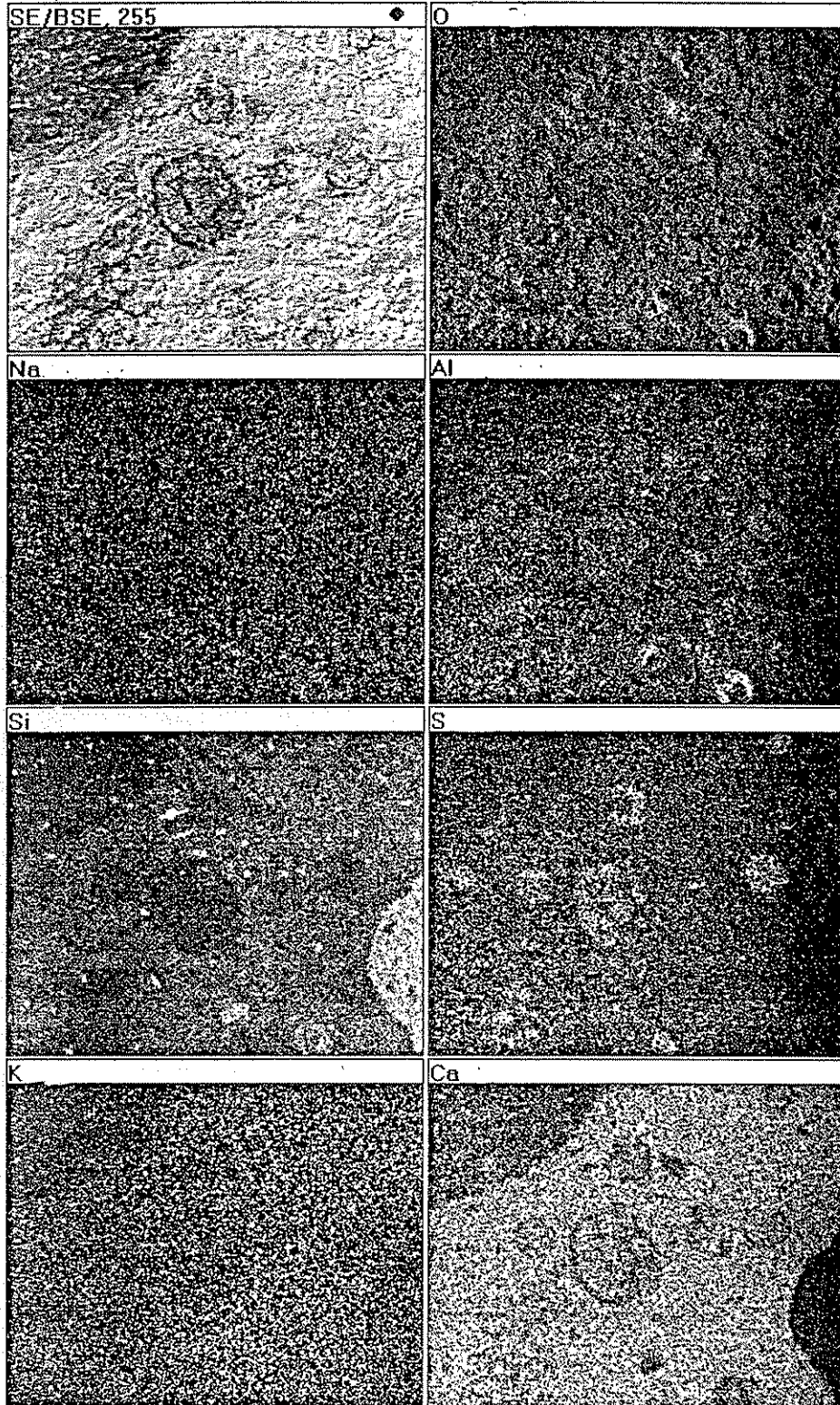
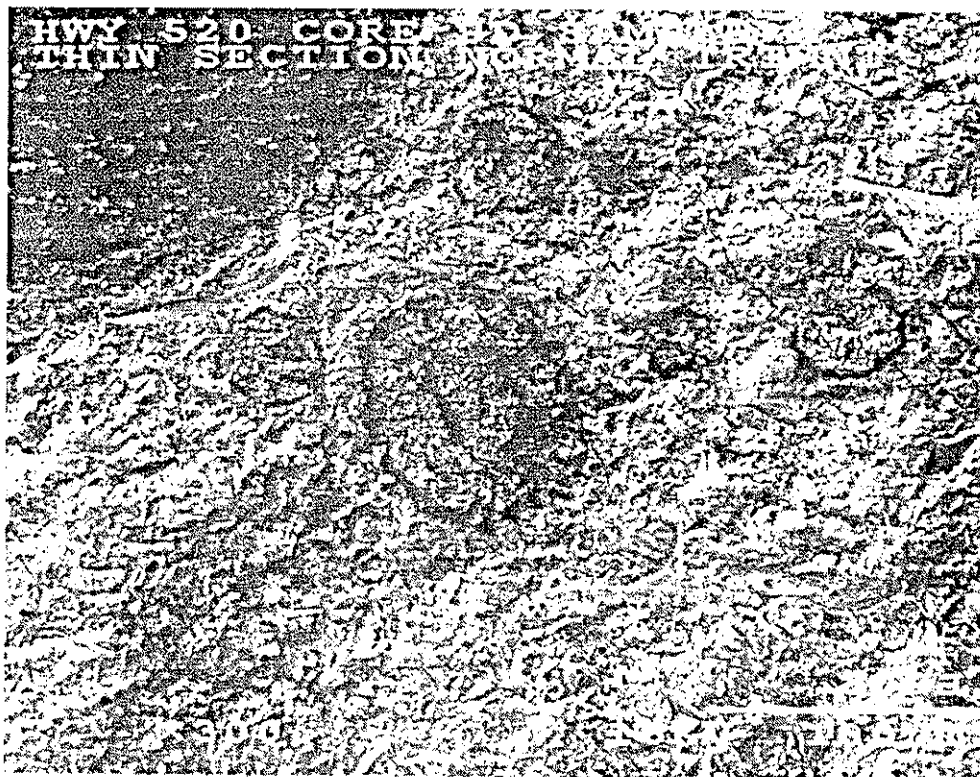


Figure 9. X-ray map of the region shown in Fig. 7B, 300X magnification.



Magnification = 100X



Magnification = 300X

Figure 7. US 20, thin section specimen, normal preparation technique.

Images obtained from the sawn surface of the specimen are shown in Figures 10 and 11. Note the poor contrast between adjacent minerals in Figure 10. The sawing process has smeared debris over the surface of the specimen, this has distorted the information in both the backscattered electron image and the X-ray map. This also makes it difficult to identify microcracks in the specimen. However, both figures still indicate the presence of filled air voids. Higher magnification (see Fig. 12) helps to discern features but it also indicates that specimen topography will interfere with accurate X-ray mapping.



Figure 10. US 20, sawn surface, magnification =100X..

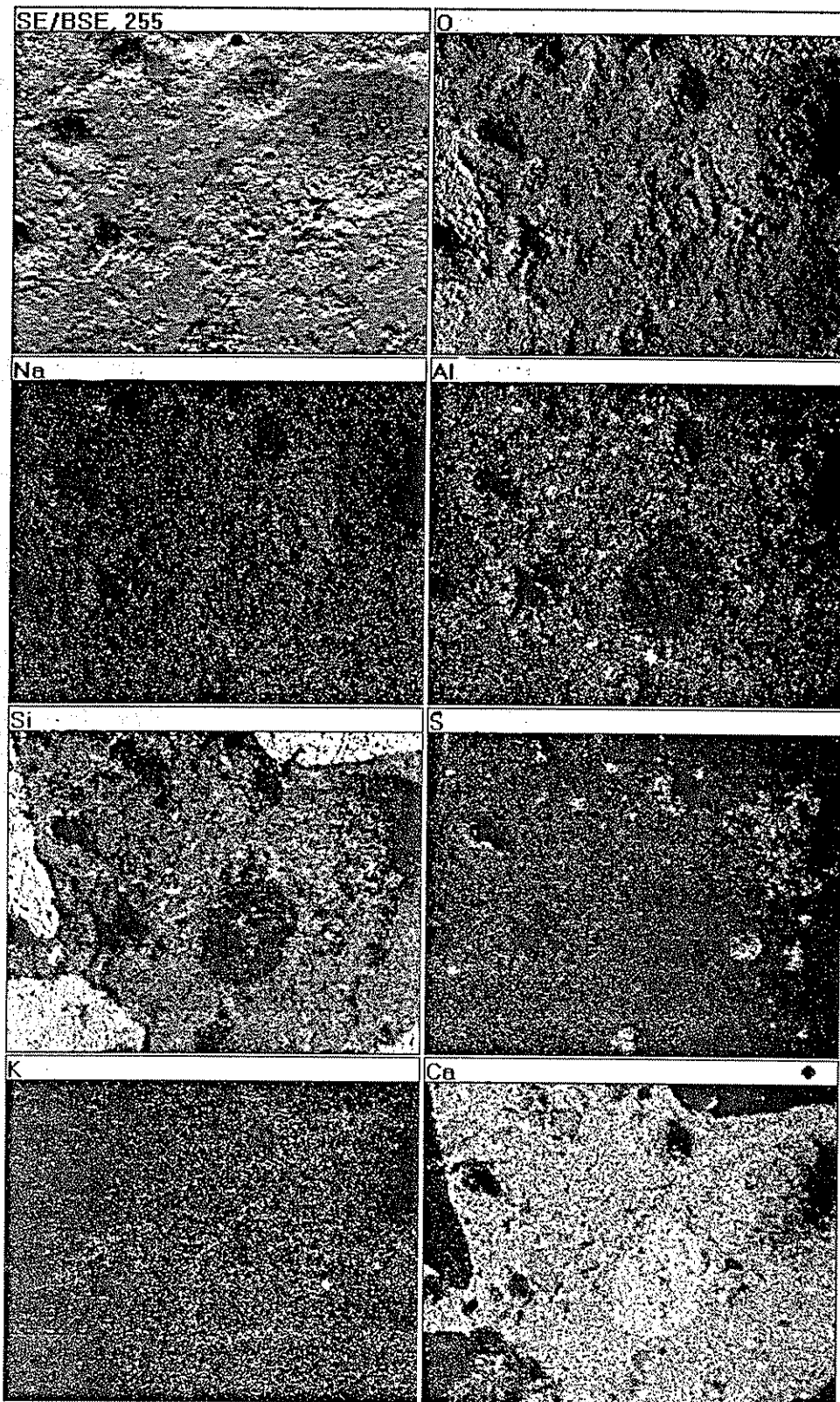


Figure 11. X-ray map of the region shown in Fig. 10; 100X magnification.

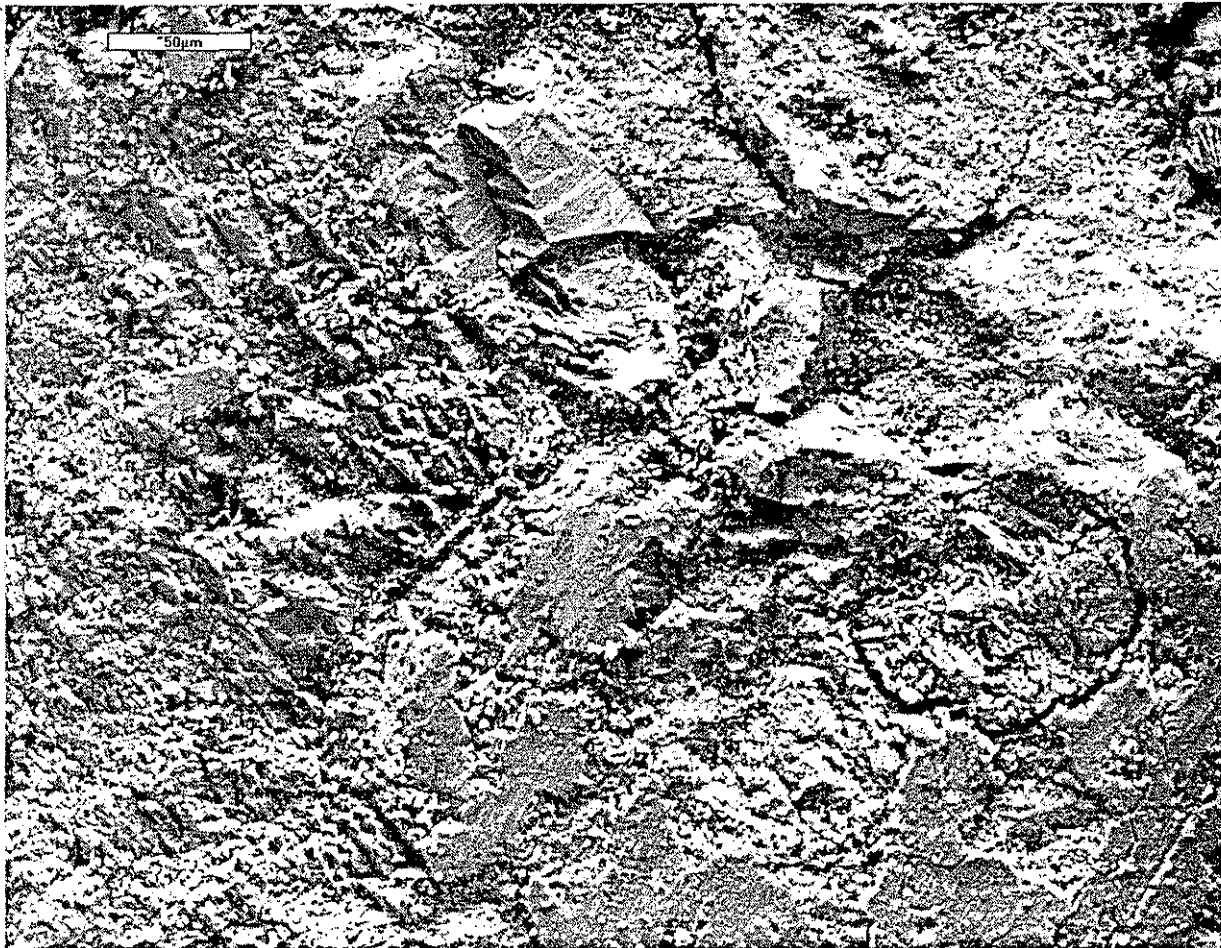


Figure 12. US 20, sawn surface; 300X magnification.

Images from a freshly fractured specimen surface are shown in Figures 13 through 17. The first two figures clearly illustrate the presence of filled air voids. In fact, the images give a better illustration of the three dimensional nature of the air voids. The X-ray map (see Fig. 15) contains many shadows (due to topography) which make interpretation difficult. Figures 16 and 17 show a large shale particle that was uncovered during the fracturing process. The shale particle is surrounded by voids that have been filled with ettringite. None of the voids give any evidence of being filled with alkali-silica gel. However, this statement must be tempered by the fact that surface topography has distorted both the image (this is why the lower-right half of the image is poorly focused) and the elemental map.

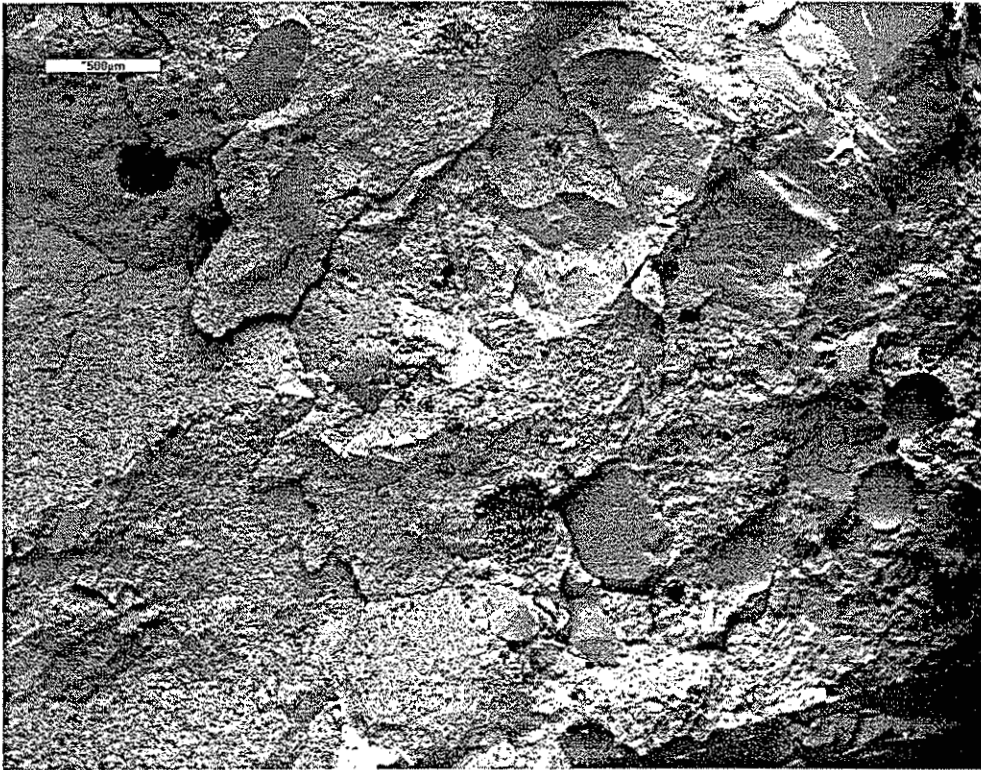


Figure 13. US 20, fractured surface, 30X magnification.

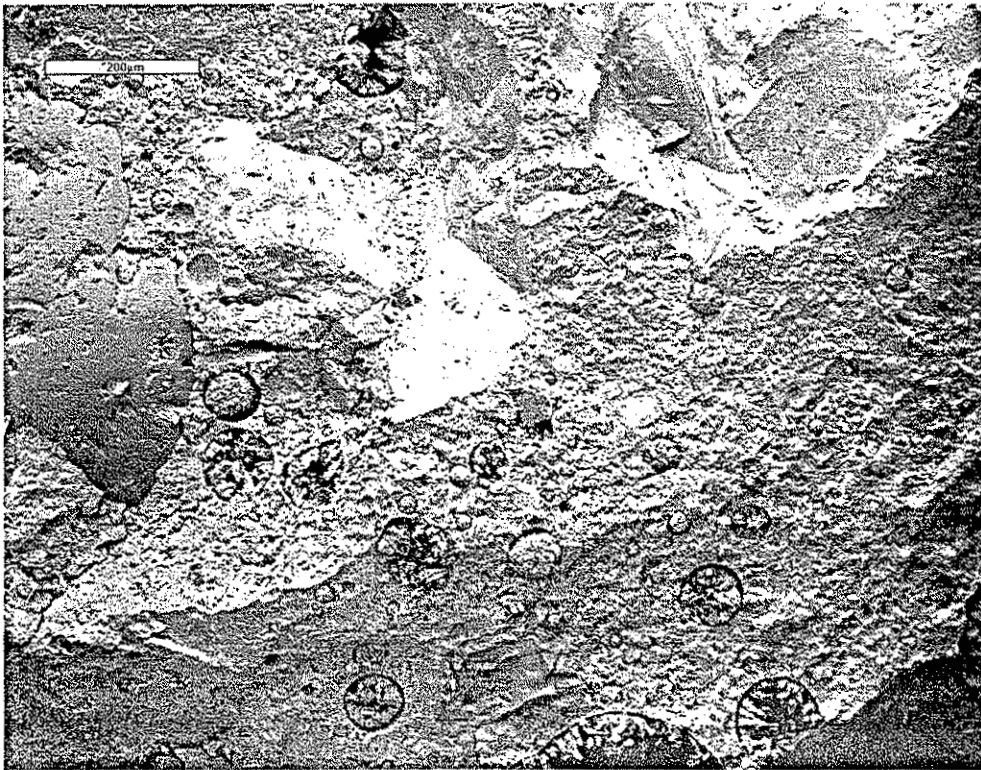


Figure 14. US 20, fractured surface, 100X magnification.

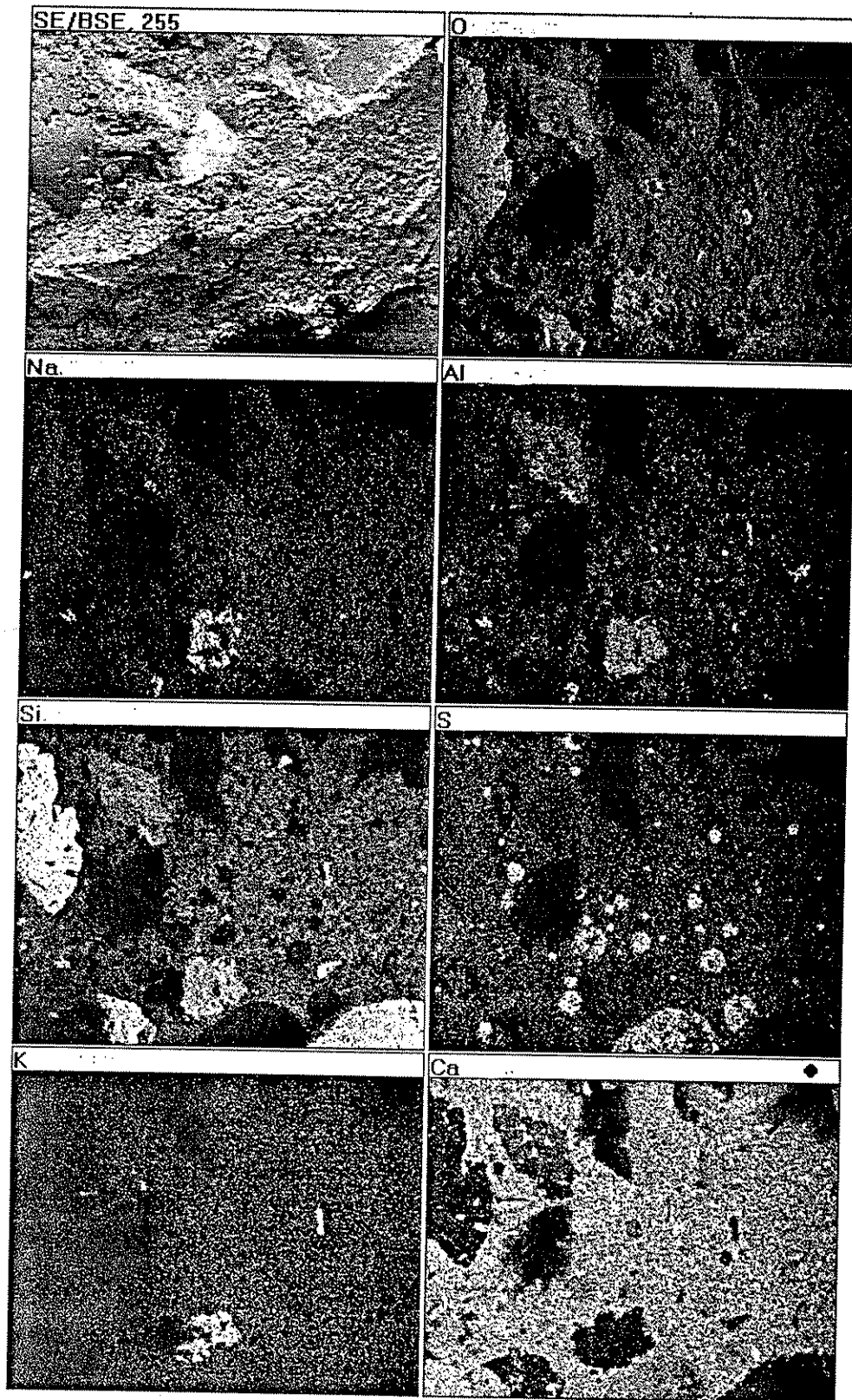


Figure 15. X-ray map of the region shown in Fig. 14; 100X magnification.

The preceding discussion has illustrated some of the strengths and weaknesses of the various sample preparation techniques that were available for use in this project. Obviously, there is no single technique that fits all situations. However, the fractured surface and sawn surface sample preparation techniques were not deemed to be adequate since the observation of cracking was a fundamental requirement for this project. The thin section technique produced excellent specimens but the delicate and time consuming sample preparation procedure, plus the small specimen size (about 1 inch by 2 inches), did not meet the needs of the project. Hence, the use of bulk specimens, that had been ground flat and then polished to #1200 grit, appeared to provide the most reliable information with only a moderate amount of time invested for specimen preparation.



Figure 16. US 20, fractured surface, shale particle, 50X magnification.

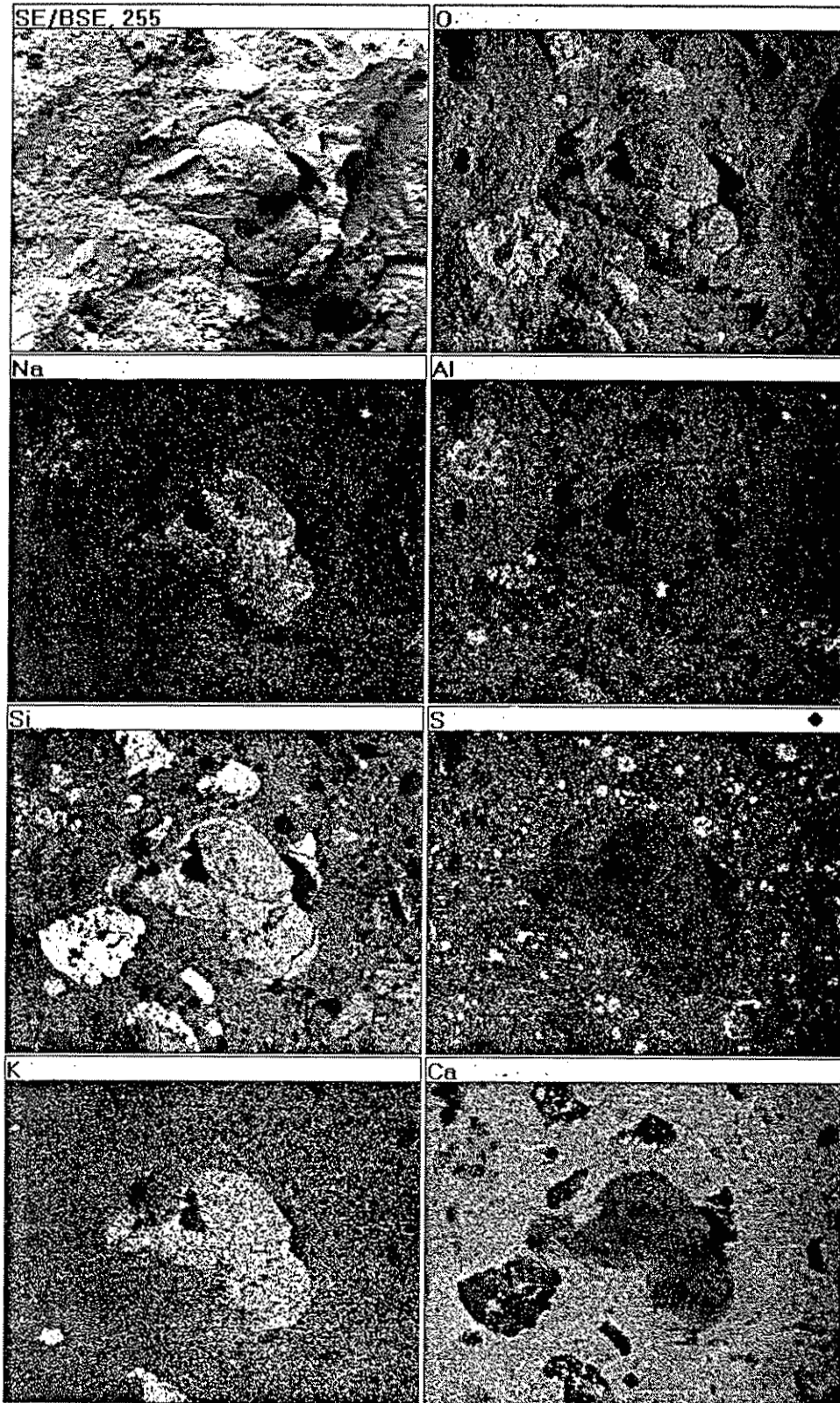


Figure 17. X-ray map of the region shown in Fig. 16; 50X magnification.

CMI Cores

The concrete samples denoted as priority 1 in Table 1, all consisted of sections of cores that had been studied earlier by the Materials Quality Task Force [17]. The results of the petrographic examination are summarized in Table 3. A detailed discussion of the first four core specimens (i.e., specimens from I-80, I-35 and US 20) will be delayed until later in this report so that all observations from a single pavement site can be considered as a whole. At this time, it is sufficient to say that the results are roughly similar to those reported by Concrete Microscopy, Inc. [17].

The samples denoted as CMI-11 and CMI-12 both exhibited very little cracking; however, they did contain features that help to illustrate points that will be mentioned later in this report. The CMI report [17] indicated that the two specimens contained similar amounts of entrained air (7.9% and 7.5%, respectively), and that the air voids were only thinly lined with ettringite. This investigation revealed major differences in the distribution of air voids (compare Figures 18 and 19), and it also indicated that many of the small air voids in the CMI-11 sample had been filled with ettringite (compare Figures 20 and 21).

The specimens denoted as CMI-14 and CMI-15 both exhibited severe cracking at the edges of the specimens. The corners of the specimens were quite fragile and crumbled during normal handling. This was due to the fact that both specimens had been submerged in a concentrated sodium sulfate solution (10% by mass) for almost two years. Visual inspection indicated that the sulfate-induced cracking penetrated about 0.5" to 1" into concrete specimens. Again, the CMI report acknowledges only thin ettringite linings in the air voids near the edges of the specimens. This study indicated that many of the small air voids near the edges of the specimens had been completely filled with ettringite (see Figure 22). The frequency of the filled voids decreases as one travels towards the interior of the specimen, this is in agreement with the CMI report. The ettringite filled voids appeared to be more prevalent in the

Table 3. Summary of observations from the CMI cores

Observations: Visual inspection and light microscopy

Core No.	Location & Details	Aggregates	Voids	Cracks	Comments
CMI-1	I-80 EB Dallas Co.	Alden stone 0.75" max Van Meter sand 0.2" max	many entrapped voids, some air voids lined	cracked shale; other cracks minimal	fly ash present air looks OK
CMI-2	I-35 NB Story Co.	Alden stone 1" max Ames sand 0.2" max	many entrapped voids, some air voids lined	cracked shale; other cracks minimal	fly ash present air looks OK
CMI-5	US 520 EB, C ash	Ft. Dodge 1" max Yates sand 0.2" max	little entrapped air; air looks low	cracked shale; macrocracks roughly subparallel to top of core, go through paste	most voids lined with white material; small voids filled; fly ash present
CMI-6	US 520 WB, no ash	Ft. Dodge 1" max Croft sand 0.2" max	little entrapped air	cracked shale; other cracks minimal	most voids lined with white material; no fly ash present
CMI-11	Fast track Benton Co.	Lee Crawford 0.75" max Cedar Rapids sand, 0.2" max	little entrapped air; air looks odd	none evident	all voids lined with white material; no fly ash but considerable angular debris in paste
CMI-12	Co. Road B Hancock Co.	Garner North 0.75" max Sankey sand 0.2" max	little entrapped air; air content looks high	cracked shale; some cracked fine aggregate particles	some gel evident lining voids near cracked shale particles
CMI-14	Lab sample HR-327 no ash	Montour 1.0" max Bellevue 0.25" max	few entrapped voids; air content looks good	cracks evident at surface of specimen, some large	microcracking extensive in outside 0.5" of specimen
CMI-15	Lab sample HR-327 15% C ash	Montour 1.0" max Bellevue 0.25" max	few entrapped voids; air content looks marginal	cracks evident at surface of specimen	fly ash present; microcracking less apparent than in CMI- 14 specimen

specimen containing Class C fly ash. However, the specimen containing only Type I cement appeared to exhibit more internal distress, this distress was particularly evident at the paste-aggregate interface (see Figure 23). This observation was consistent with the results of the expansion tests that had been conducted on the specimens during research project HR-327 (see Figure 24).

Table 3. (continued) Summary of observations from the CMI cores

Observations: scanning electron microscopy

Core No.	Location & Details	Matrix	Voids	Cracks	Fly Ash	Comments
CMI-1	I-80 EB Dallas Co.	good paste/agg bond, air looks good	some small voids filled with ettringite	cracked shale; very fine microcracks connecting air voids	yes	some ASR gel in voids near shale particles
CMI-2	I-35 NB Story Co.	good paste/agg bond, air looks low	small voids filled with ettringite in some areas	cracked shale; microcracks travel thru paste, often connect air voids	yes	
CMI-5	US 520 EB, C ash	paste/agg bond varies; air looks low	many entrapped voids; many small air voids filled with ettringite	cracked shale; microcracks common in paste, go around aggregates	yes	paste looks very poor in some regions
CMI-6	US 520 WB, no ash	paste/agg. bond ?; air may be low	many entrapped voids; many voids lined with ettringite	cracked shale; few microcracks in paste	no	paste looks poor in some regions
CMI-11	Fast track Benton Co.	paste/agg. bond OK, air looks low	large voids lined with ettringite, small voids often filled	fine microcracks go thru paste, connect air voids	no	
CMI-12	Co. Road B Hancock Co.	paste/agg. bond OK; too much air	some entrapped voids; some voids lined with ettringite	cracked shale; some microcracks in paste	no	
CMI-14	Lab sample HR-327 no ash	paste/agg. bond poor at exterior surface of specimen	air content OK; some voids lined but few filled with ettringite	microcracks extensive in paste fraction of specimen	no	paste and the paste/ coarse aggregate bond look poor
CMI-15	Lab sample HR-327 15% C ash	paste/agg. bond poor at exterior surface of specimen	air content looks OK; some voids lined, small voids filled with ettringite	microcracks extensive in paste fraction of specimen	yes	paste and the paste/ coarse aggregate bond look poor

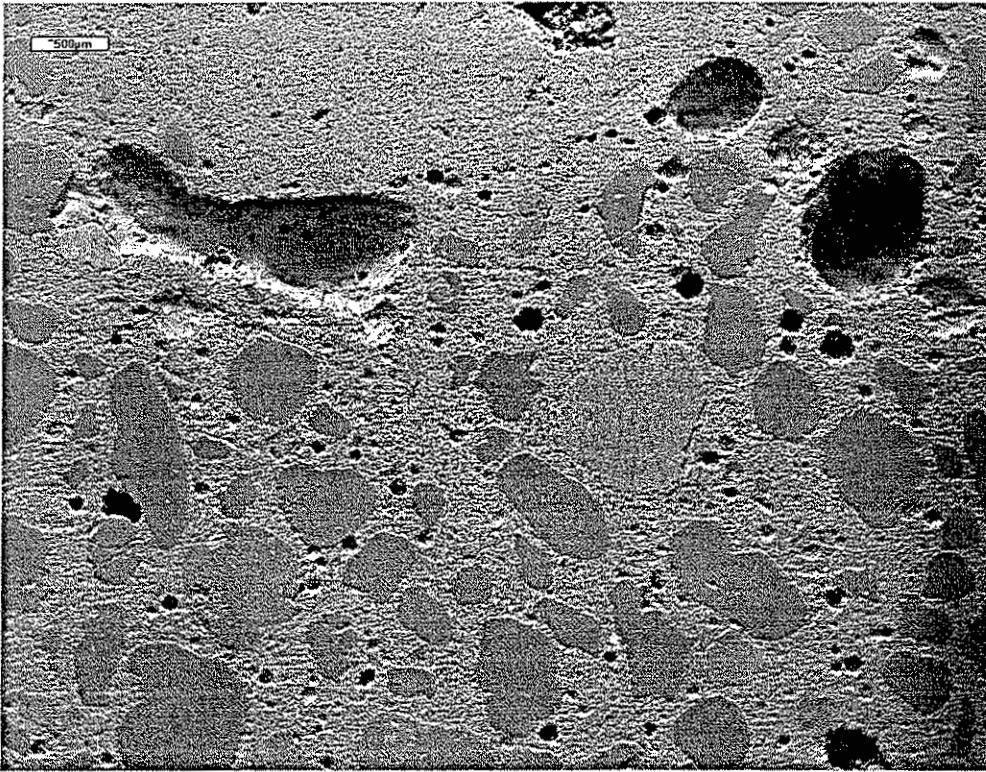


Figure 18. Fast track, Benton County (CMI-11), 20X magnification.

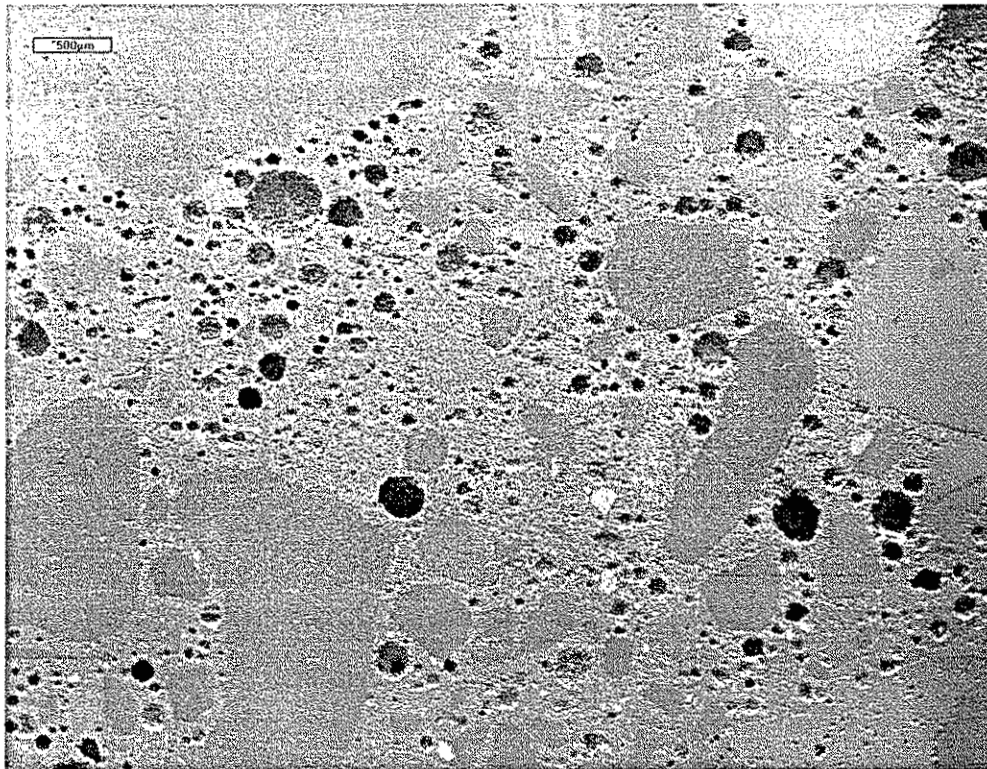


Figure 19. County Road B, Hancock Co. (CMI-12), 20X magnification.

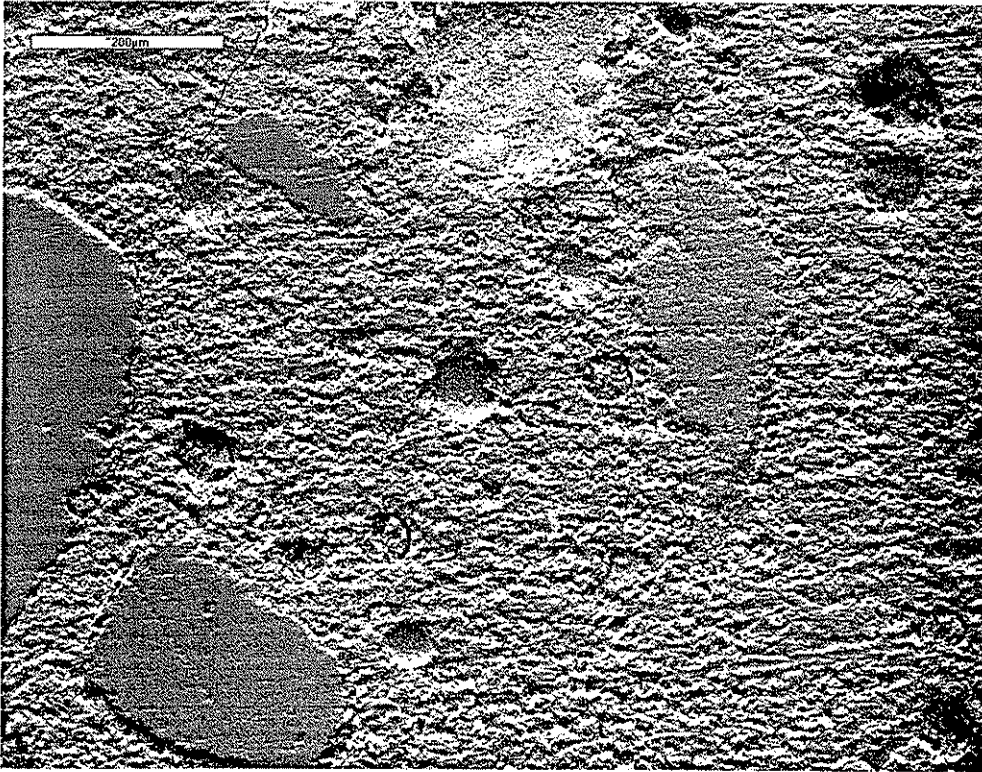


Figure 20. Fast track, Benton County (CMI-11), 125X magnification.

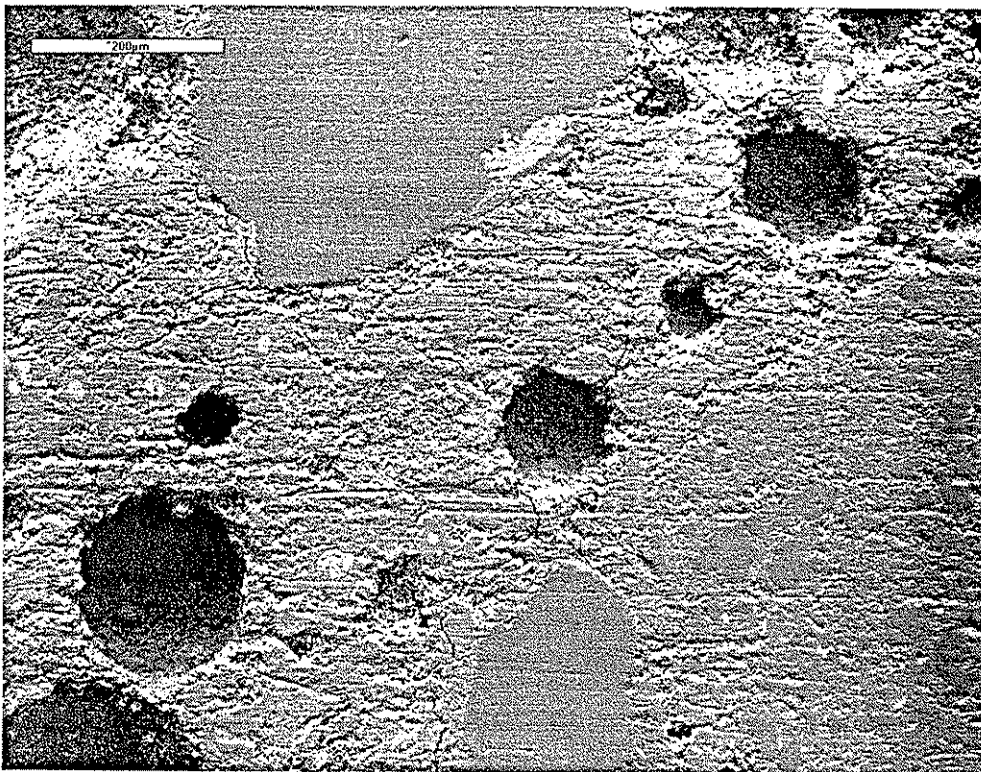


Figure 21. County Road B, Hancock Co. (CMI-12), 125X magnification..

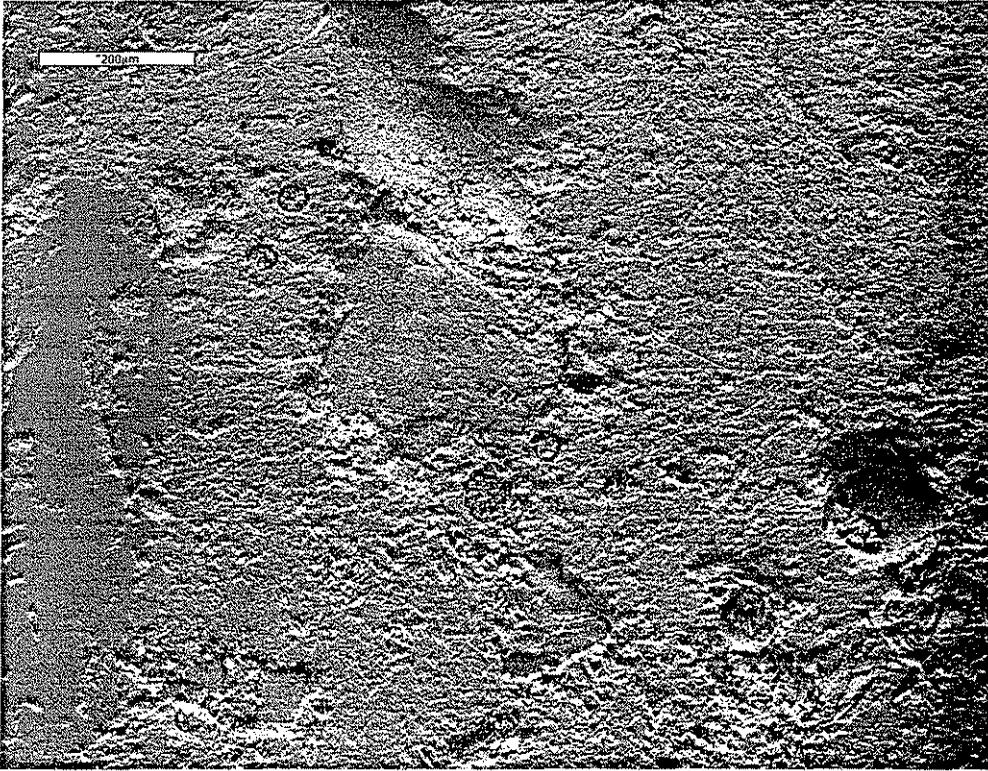


Figure 22. Lab concrete exposed to sulfate solution, 100X magnification;
(Beam 55 from HR-327, Type I cement with 15% C fly ash).

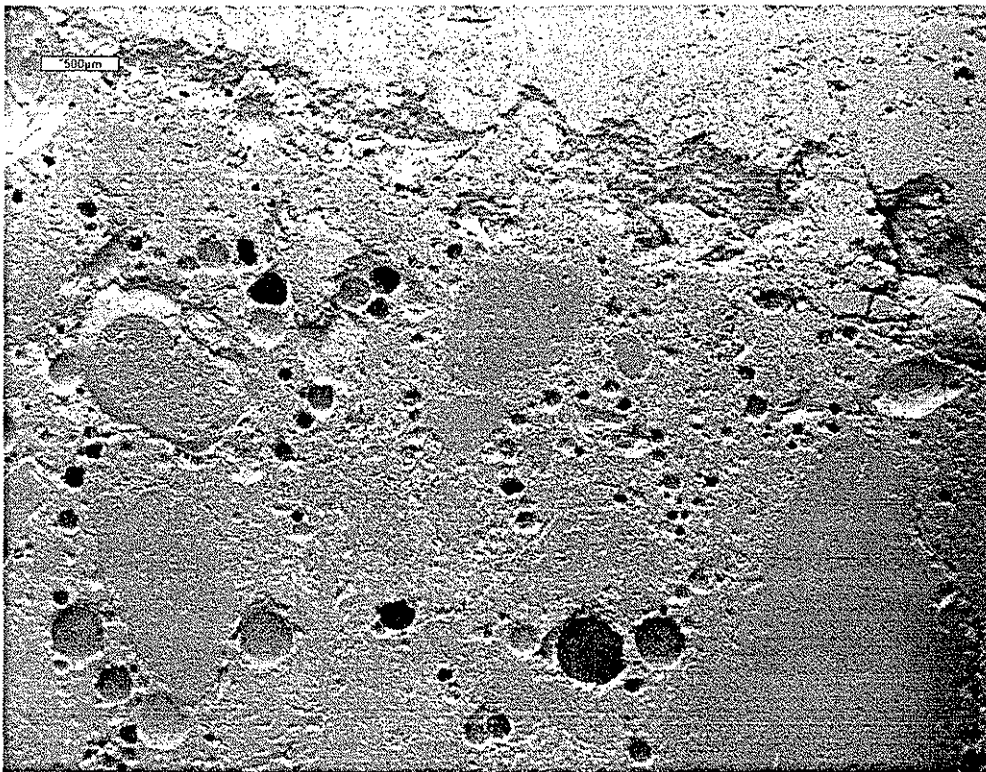


Figure 23. Lab concrete exposed to sulfate solution, 20X magnification;
(Beam 53 from HR-327, Type I cement, no fly ash).

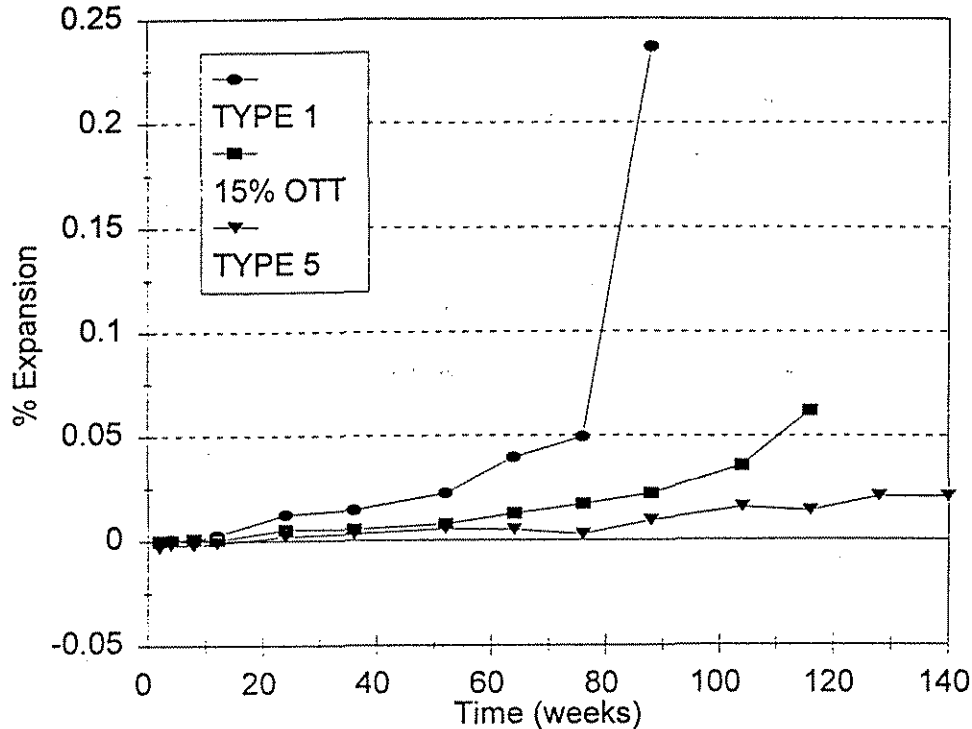


Figure 24. Results of a laboratory sulfate resistance study using Ottumwa fly ash.

Highway US 20 Cores

The concrete samples in the priority 2 group were all taken from US 20. The results of the petrographic examination are summarized in Tables 4, 5 and 6. The cores have been split into distinct groups based on the mix design used during construction of the pavement. These details have been described thoroughly by Jones [18] in a earlier investigation of the deterioration observed on US 20. Observations from the two CMI cores that were taken from US 20 (CMI-5 and CMI-6, respectively), will also be discussed in this section.

The major type of distress that was observed in the specimens consisted of cracking oriented subparallel to the top of the pavement. The number and severity of the cracking varied considerably from core to core. This type of cracking was apparent (i.e., by visual inspection only) in cores 10, 11, 12, 17, 19, 20, and the core denoted as CMI-5. The horizontal cracks tended to propagate through the paste fraction of the concrete. The cracks often reached widths of 0.5 millimeters (or more in some instances) and they were typically open (i.e., not filled with alkali-silica gel or ettringite).

Table 4. Summary of observations from the cores taken from US 20 (mix#1).

Highway: US 20, paved 1987, proj. #.?
 Mix details: C3WRC, Mix#1
 Coarse Aggregate (CA) : Ft. Dodge Mine crushed limestone
 Fine Aggregate (FA) : Croft
 Cement : Lehigh
 Fly Ash : Ottumwa

Observations: Visual inspection and light microscopy

Core No.	Location & Details	Aggregates	Voids	Cracks	Comments
9	midpanel, no vibrator trail	CA sound max. = 1.0" FA max.=.3" shale not measured	many entrapped air voids; many air voids lined	cracked shale particles	few cracks observed
10	joint, no vibrator trail	CA sound max. = 1.25" FA max.=.3" shale = 1.1%	many entrapped air voids; many air voids lined	extensive in top of core; also cracked shale particles	steel observed in lower third of sample
11	joint, vibrator trail	CA sound max. = 1.0" FA max.=.3" shale = 0.6%	entrapped air voids; many air voids lined, some filled	extensive, full depth; subparallel to top of pavement	air looks low cracked shale particles
12	midpanel, vibrator trail	CA sound max. = 1.25" FA max.=.3" shale not measured	entrapped air voids; many air voids lined, some filled	extensive, in top of core; subparallel to top of pavement	some regions in top of core exhibit segregation; cracked shale particles

Observations: Scanning electron microscopy

Core No.	Location & Details	Matrix	Voids	Cracks	Fly Ash	Comments
9	midpanel, no vibrator trail	Good cement/agg. bond	many large voids; small voids filled with ettringite	few, except for cracked shale	yes	ASR evident near shale particles
10	joint, no vibrator trail	some regions poorly consol- idated	many large voids; small voids filled with ettringite	common in paste, often connect air voids; cracked shale	yes	more air and less void filling in bottom specimen
11	joint, vibrator trail	some paste areas have excess fly ash or poor mixing	many large voids; small voids filled with ettringite	common, some cracks contain ASR gel; cracked shale	yes	air looks low in top specimen
12	midpanel, vibrator trail	paste looks poor or distorted in some regions	many large voids; small voids filled with ettringite	common, some were caused by a reactive aggregate; cracked shale	yes	air looks low in top specimen

Table 5. Summary of observations from the cores taken from US 20 (mix#2).

Highway: US 20, paved 1986, proj. #.?

Mix details: C3WR, Mix#2

Coarse Aggregate (CA) : Ft. Dodge Mine crushed limestone

Fine Aggregate (FA) : Croft

Cement : Lehigh

Fly Ash : None

Observations: Visual inspection and light microscopy

Core No.	Location & Details	Aggregates	Voids	Cracks	Comments
13	midpanel, no vibrator trail	CA sound max. = 1.0" FA max.=.25" shale = 1.2%	some entrapped air voids; some air voids lined	not evident except for cracked shale particles	looks sound
14	joint, no vibrator trail	CA sound max. = 1.0" FA max.=.25" shale = 1.4%	large entrapped air voids; many air voids lined	not evident except for cracked shale particles	air looks low; perhaps some segregation in some areas
15	joint, vibrator trail	CA sound max. = 1.25" FA max.=.3" shale = 0.9%	entrapped air voids common near center of core	not evident except for cracked shale particles	steel observed in lower third of core
16	midpanel, vibrator trail	CA sound max. = 1.25" FA max.=.25" shale = 0.8%	entrapped air voids common near center of core	not evident except for cracked shale particles	clumps of air voids observed in some areas

Observations: Scanning electron microscopy

Core No.	Location & Details	Matrix	Voids	Cracks	Fly Ash	Comments
13	midpanel, no vibrator trail	good paste/agg. bond	many voids lined with ettringite	few except for cracked shale particles	no	air looks low in some areas
14	joint, no vibrator trail	good paste/agg. bond	some voids lined with ettringite	few except for cracked shale particles	no	? low air in top of core; higher in bottom
15	joint, vibrator trail	good paste/agg. bond	many large voids; some voids lined with ettringite	common in paste; cracked shale particles	no	shale may be producing ASR gel
16	midpanel, vibrator trail	good paste/agg. bond	many large voids; some voids lined with ettringite	some radiate from air voids others from shale particles	no	

Table 6. Summary of observations from the cores taken from US 20 (mix#3).

Highway: US 20, paved 1986, proj. #.?
 Mix details: C3C, Mix#3
 Coarse Aggregate (CA) : Ft. Dodge Mine crushed limestone
 Fine Aggregate (FA) : Yates
 Cement : Lehigh
 Fly Ash : Port Neal 4

Observations: Visual inspection and light microscopy

Core No.	Location & Details	Aggregates	Voids	Cracks	Comments
17	joint, no vibrator trail	CA sound max. = 1.0" FA max.=.3" shale = 0.8%	many entrapped voids; many air voids lined	extensive in top of core; subparallel to top of pavement	steel observed in middle of core; cracked shale
18	midpanel, no vibrator trail	CA sound max. = 1.0" FA max.=.3" shale = 0.5%	air content looks low	not evident except for cracked shale particles	some oversize in fine aggregate
19	midpanel, vibrator trail	CA sound max. = 1.25" FA max.=.25" shale = 0.9%	some entrapped air voids; many lined voids	extensive in top of core; subparallel to top of pavement	cracked shale; ? segregation and mortar cracking near top of core
20	joint, vibrator trail	CA sound max. = 1.0" FA max.=.3" shale = 0.7%	air content looks low in top of core; many lined voids	extensive in top of core; subparallel to top of pavement	some oversize in fine aggregate cracked shale

Observations: Scanning electron microscopy

Core No.	Location & Details	Matrix	Voids	Cracks	Fly Ash	Comments
17	joint, no vibrator trail	air content looks low	many ettringite filled voids	cracked shale; some cracks go thru paste around agg.	yes	some ASR observed near shale particles
18	midpanel, no vibrator trail	air content looks low	many ettringite filled voids	cracked shale; some cracks go thru paste around agg.	yes	some ASR observed near shale particles
19	midpanel, vibrator trail	air content looks low	many large voids, many ettringite filled voids	cracked shale; some cracks go thru paste around agg.	yes	some areas distorted, ? poor mixing or consol- idation
20	joint, vibrator trail	air content looks low in top of core, high in bottom	many large voids, many ettringite filled voids	often join large voids; cracked shale	yes	minor evidence of ASR

The coarse aggregate (Ft. Dodge crushed limestone) was found in all of the cores. The fine aggregate contained some reactive particles that had produced alkali-silica gel. Most of the reactive aggregates were shale particles and all of the core specimens (cores 9 through 20 plus CMI-5 and CMI-6) contained cracked shale particles. Some of the cracked shale particles had produced alkali-silica gel while many others had not. The cracks associated with the shale particles were extremely fine and typically did not propagate far into the cement paste (see Figures 25 through 27). Other reactive aggregates were only very rarely observed in the fourteen core samples. Sand-sized dolomite particles were observed in all of the cores from US 20.

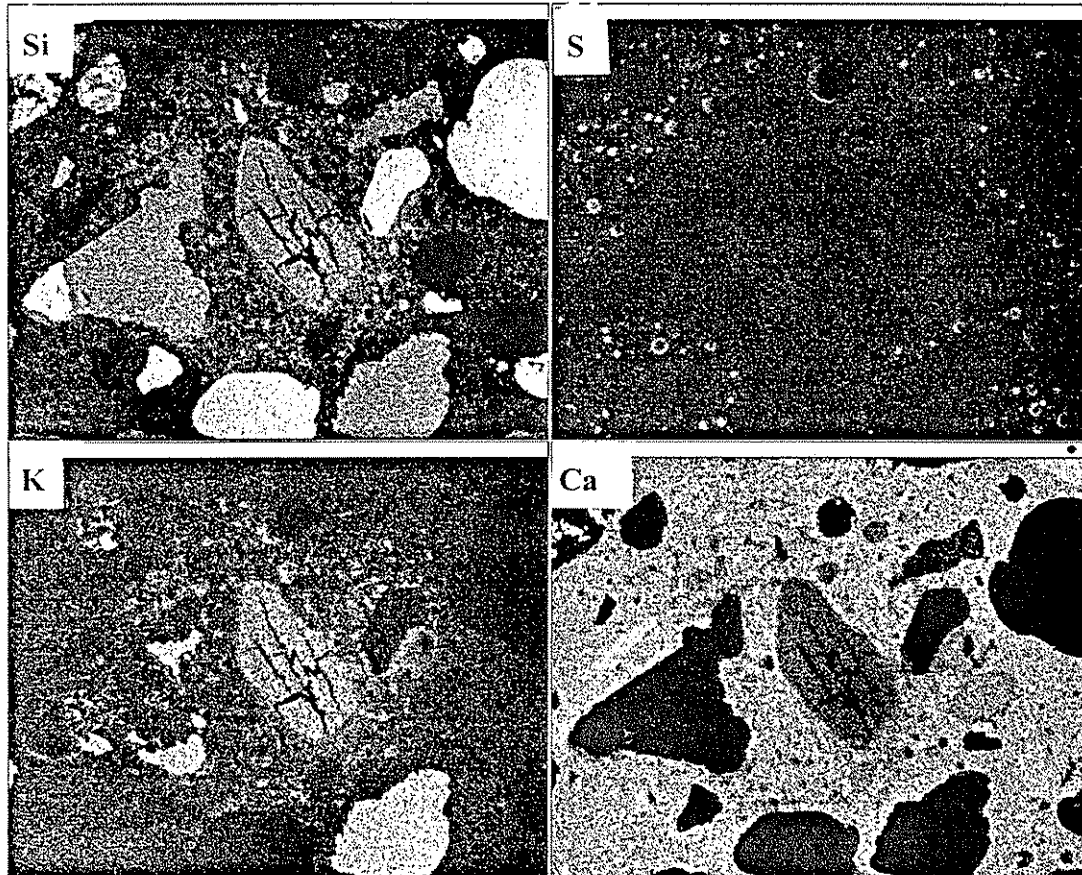


Figure 25. US 20, core 17B, ASR near shale particle; 50X magnification.

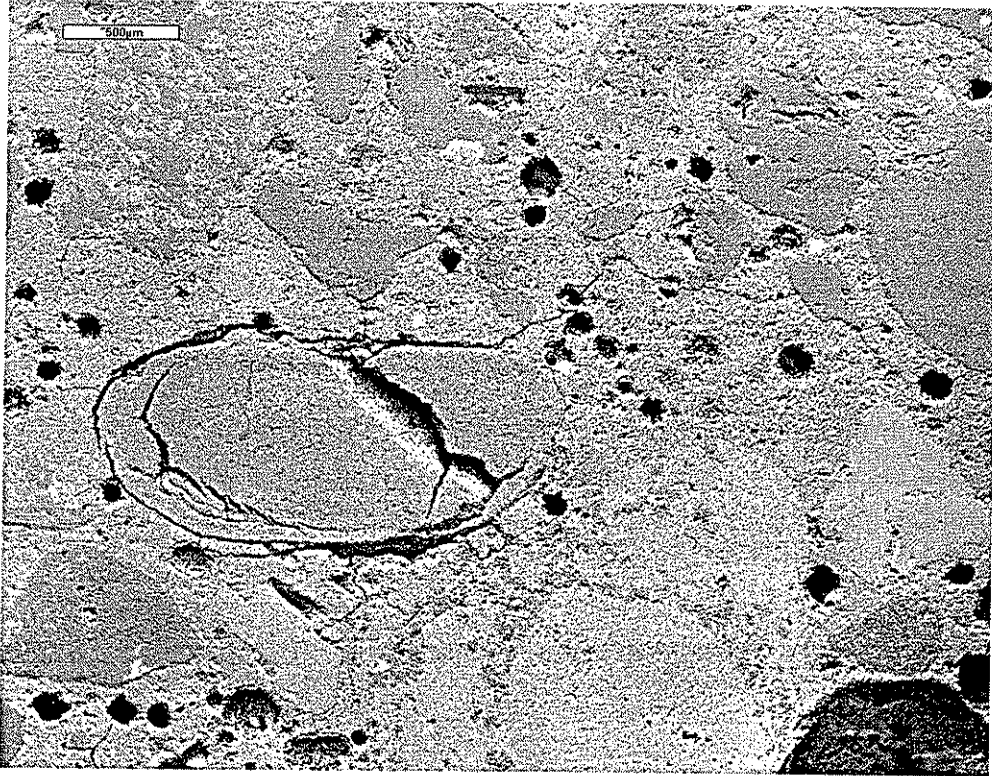


Figure 26. US 20, core 15B, 30X magnification (mix#2, no fly ash).

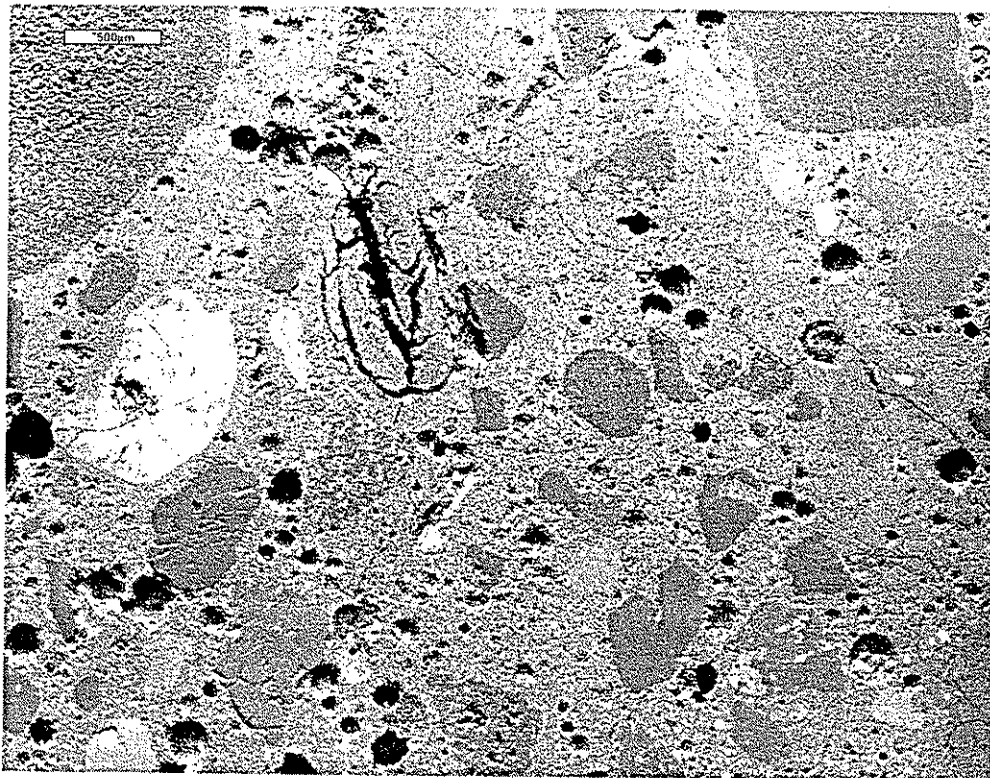


Figure 27. US 20, core 12B, 25X magnification (mix#1, 15% fly ash)

A reactive particle, which had produced disruptive expansion by the production of alkali-silica gel, was found in the top specimen of core 12 (see Figures 28 and 29). This particular particle is an excellent example of alkali-silica reaction and it will be used to demonstrate how alkali-reactive aggregates can be identified using the scanning electron microscope. First, notice in Figure 28, that a cracked aggregate is present in the field-of-view. The cracks tend to radiate from the reactive particle into the cement paste (several millimeters in this instance, they actually pass out of the field-of-view). Several cracks appear to be filled with a material that has a "mud-cracked" appearance, this is the normal morphology of alkali-silica gel in a scanning electron microscope.

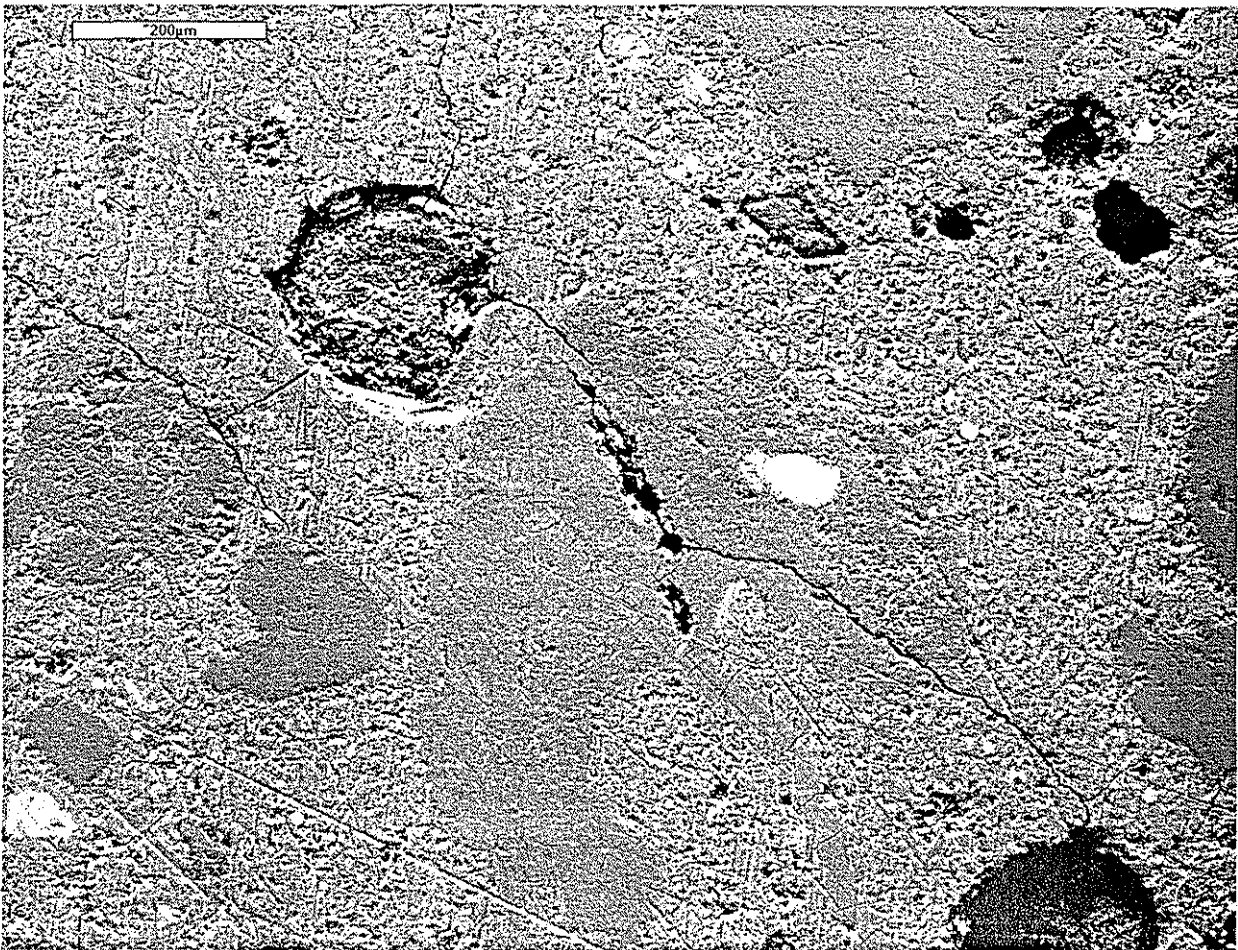


Figure 28. US 20, core 12B, deleterious ASR cracking; 100X magnification.

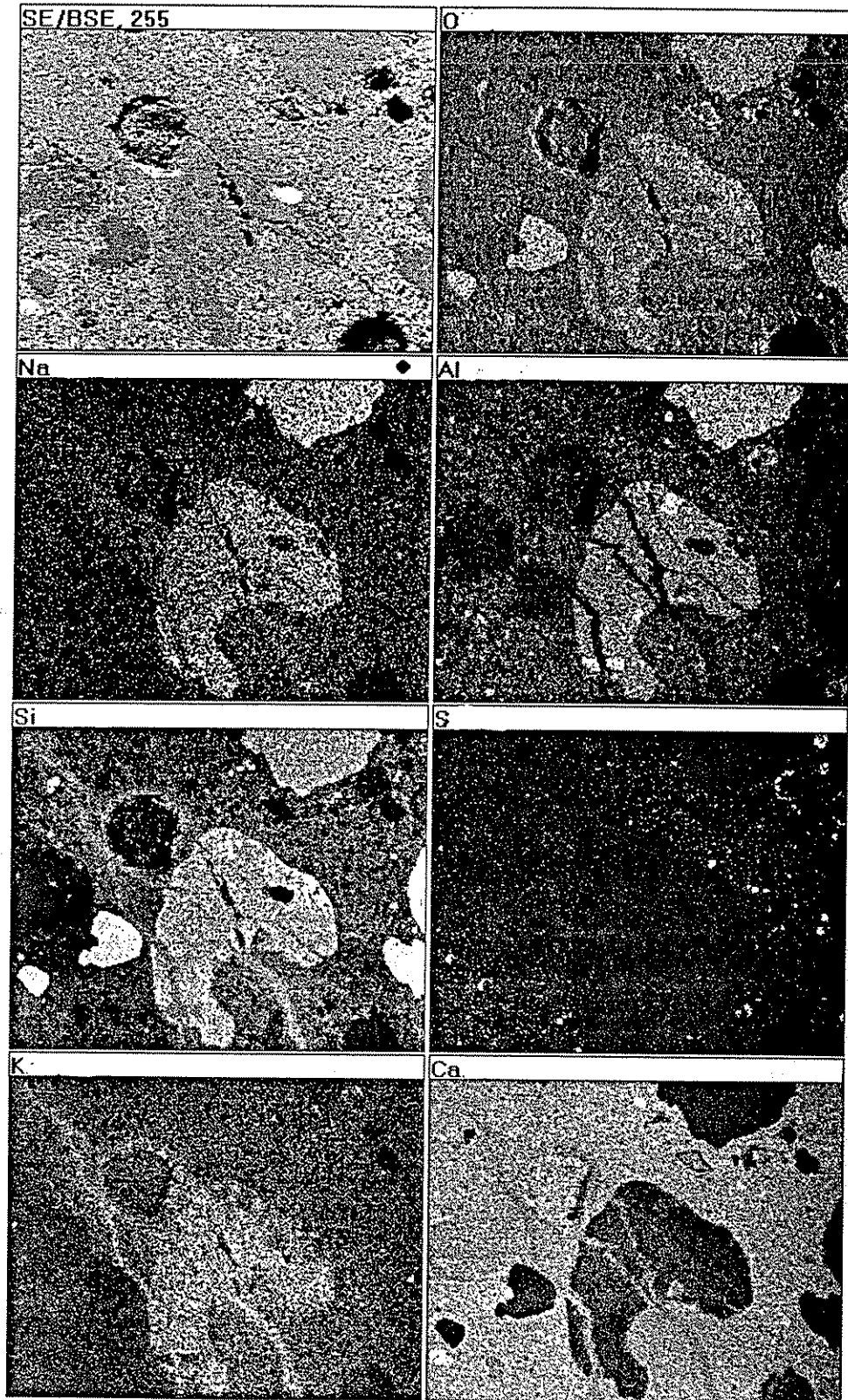
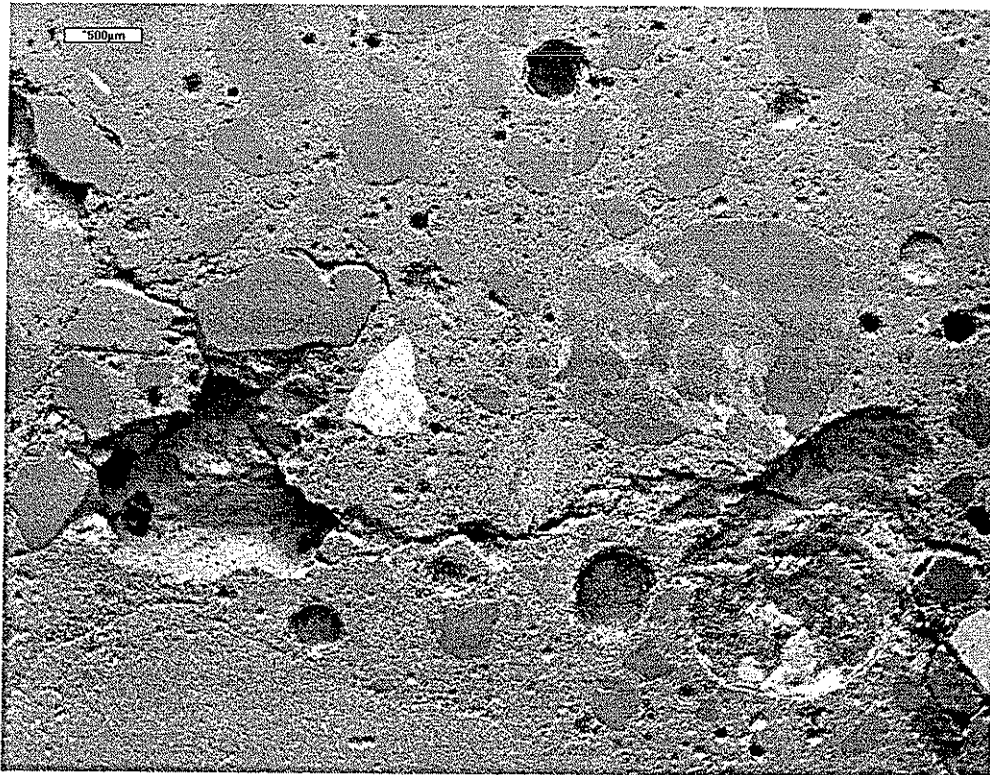


Figure 29. X-ray map of the area shown in Fig. 28; 100X magnification.

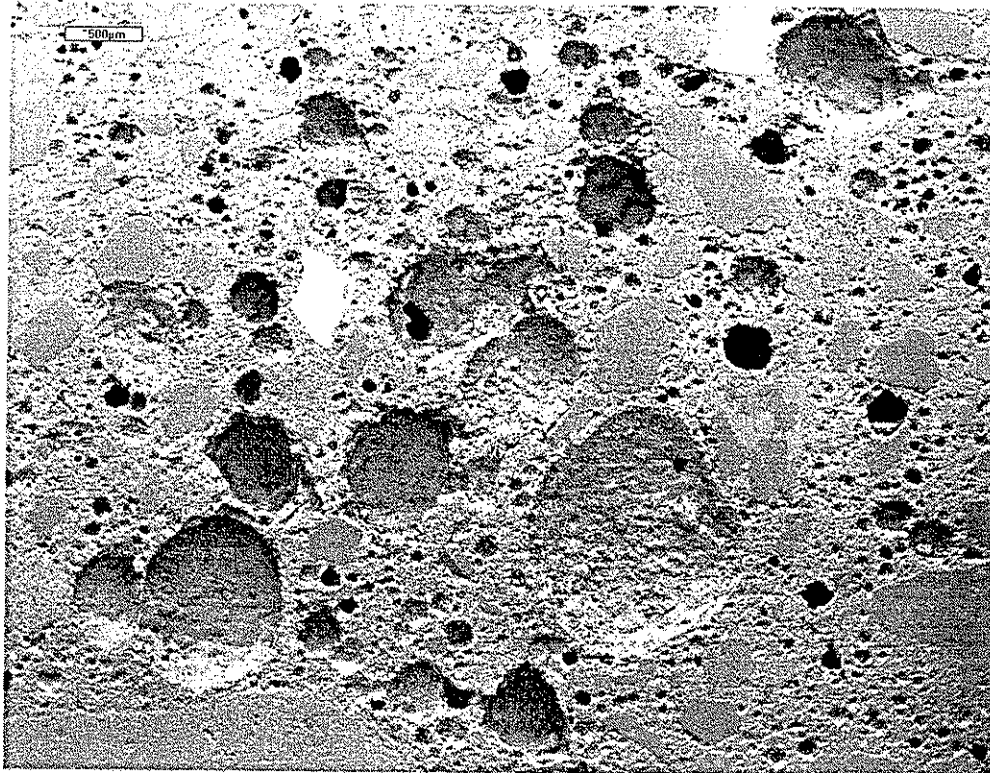
The visual information can immediately be supplemented with elemental information from the energy dispersive X-ray analyzer. This could consist of an elemental scan of the gel material or an X-ray map of the region of interest. In this instance, an X-ray map was collected because it provides a more comprehensive view of the region of interest. Figure 29 is the X-ray map that was collected from the region shown in Figure 28. The oxygen map indicates that the sample was reasonably flat with little topography (i.e., few shadows are apparent in the oxygen map). The silicon, potassium and sodium maps clearly indicate that the material in the cracks is primarily composed of these elements (plus oxygen). The calcium map indicates that regions of the gel contain only small amounts of calcium. However, as is readily apparent in the calcium X-ray map, the concentration of calcium varies considerably in different parts of the crack, this suggests a variety of alkali-silica gels with different compositions (and perhaps with different swelling potentials). One important thing to note is that the aggregate, which appeared to contain only a single well defined crack in the backscattered electron image, now clearly indicates severe distress in the X-ray maps (refer to aluminum or calcium maps which indicate about five distinct cracks). This is in better agreement with the amount of gel that was observed in the region.

The paste fraction of many of the concrete cores taken from US 20 was often distorted in one way or another. One of the most commonly observed distortions was a large number of entrapped air voids. The diameter of the entrapped voids ranged in size from 1" (uncommon but observed), to about 0.2" (very common in all of the cores). The entrapped voids were observed in both the top and bottom sections of cores taken from either the pavement joint or midpanel region. No attempt was made to quantify these observations.

The entrained-air void system varied considerably from core to core. It also varied from the top to the bottom of the core in many instances (see Figure 30 for an example). Again, the discussion that follows will hinge on qualitative



Top of Core



Bottom of Core

Figure 30. US 20, core 20, 20X magnification; note difference in air voids.

comparisons rather than strict quantitative comparisons. The distribution of air voids throughout the paste often appeared to be very poor when compared to laboratory concrete specimens. However, a closer inspection of the paste generally indicated that ettringite had filled many of the small (<100 microns) air voids (see Fig. 31). Even closer inspection (see Fig. 32) appeared to indicate that the air voids had been filled from smallest to largest (note the linings on the larger voids while the small voids have been filled). Often the air voids that had been filled were difficult to see without careful inspection (even though ettringite has a very unique morphology in the scanning electron microscope). X-ray maps, particularly the sulfur and silicon maps, were useful for detecting the ettringite filled voids (see Fig. 31). Sometimes very fine cracks were observed to pass through the filled air voids into the adjacent paste (or perhaps to another filled air void).

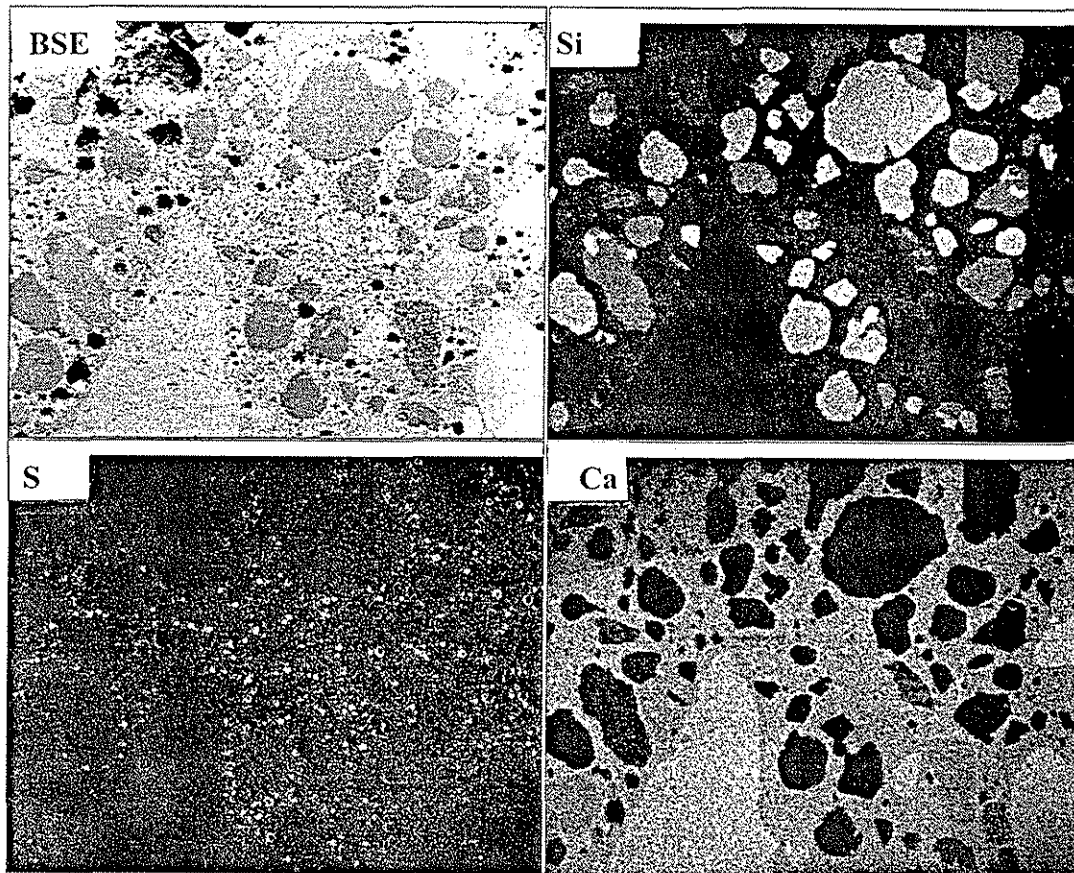


Figure 31. X-ray map of US 20, core 10B, note filled voids; 20X magnification.

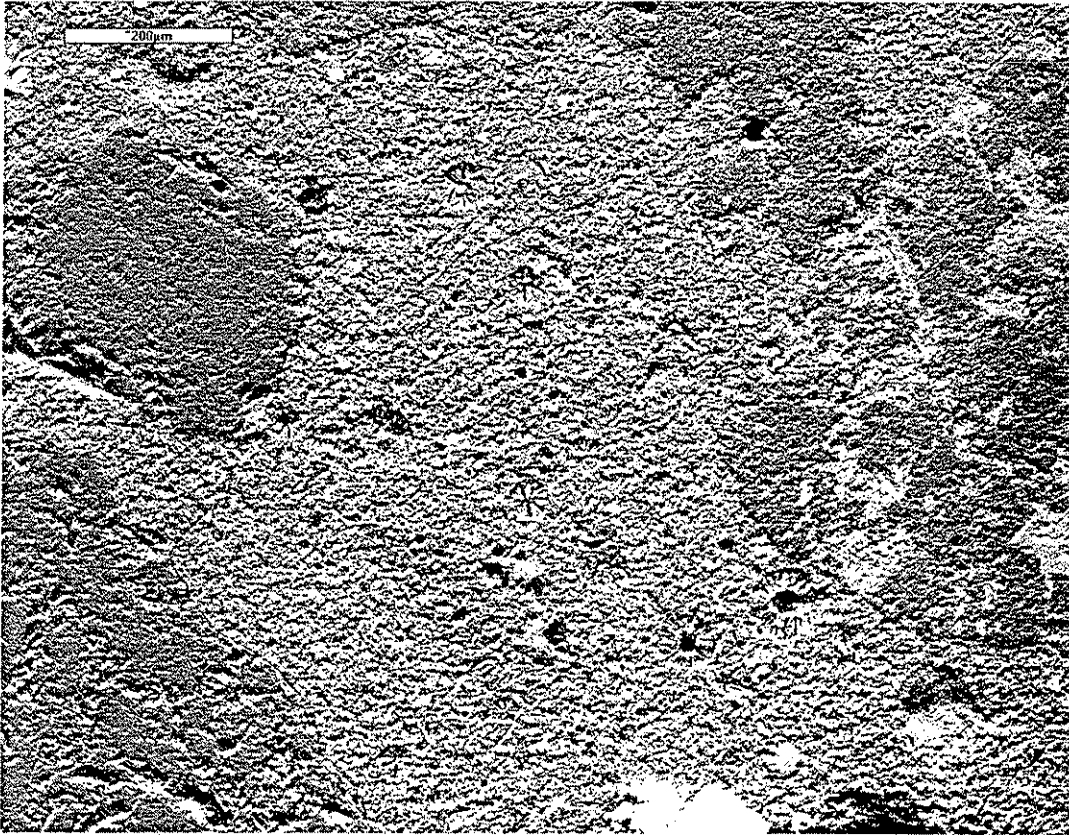


Figure 32. US 20, core 10B, void filling and microcracking; 100X magnification.

The observation of ettringite filled voids was common throughout all the cores taken from US 20. The cores from mixes that contained fly ash (mixes 1 and 3) appeared to contain considerably more filled voids than the cores taken from the mix without fly ash (mix 2); however, this observation is only qualitative at this time. Future work will be suggested to quantify this matter. It is also important to remember that the cements used in the different mixes were not the same. They had been produced by a single manufacturer but at different times.

In an attempt to shed more light on the chemistry of the paste fraction of the cores from US 20, all the cores were analyzed using differential scanning calorimetry (DSC). Also, selected samples were subjected to X-ray diffraction analysis (XRD).

The preliminary specimens for DSC analysis were obtained by using a masonry bit to remove mortar from the exterior of the concrete cores, this allowed one to avoid sampling the coarse aggregate fraction of the concrete. The extracted material was then sieved through a #100 mesh sieve and then ground to a fine particle size for the DSC experiments. However, this sampling procedure also tended to sample material that had been altered due to exposure to the atmosphere. Hence, additional samples were removed from fresh surfaces of specific core specimens, to evaluate the influence of the sampling technique. The fresh surfaces were tested with phenolphthalein to evaluate the depth of carbonation (which was less than 0.5 millimeters in all the cores that were tested). All of the results of the DSC study have been appended to this report (see Appendix C). For the purpose of brevity only three core specimens will be discussed in detail. It is important to note, however, that the DSC experiments appear to sort the cores into groups based on the calcium hydroxide content of the mortar -- but beware of making any conclusions based on these results because of the potential for sample alteration that was described above. The exposure of the core samples to the atmosphere appears to magnify the differences observed between the cores. These tests are currently being repeated on fresh surfaces to see if the grouping is repeated.

Three core specimens were selected from the fourteen cores from US 20 that were available for study. To aid the comparison, all three of the cores were obtained from the joint region of the pavement slab, and they represented all three of the concrete mixes that were available. Two of the cores represented concrete that contained vibrator trails (cores 15 and 20), the remaining sample (core 11) did not contain vibrator trails.

The results of DSC analysis are shown in Figures 33 and 34. Figure 33 depicts results obtained from the outside surface of the concrete cores (i.e., the specimen was not indicative of the mortar fraction of the concrete specimen

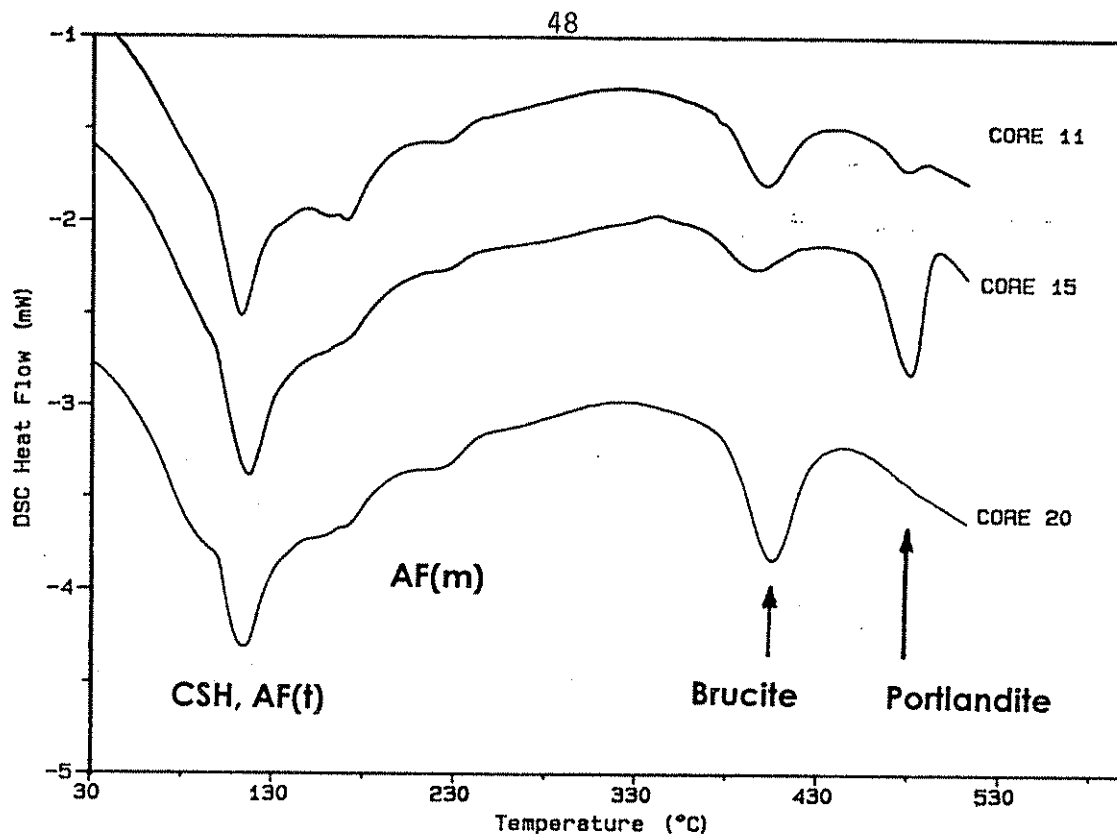


Figure 33. Results of DSC analysis on the mortar fraction of US 20 cores, (sample from exterior of core specimen, significant carbonation).

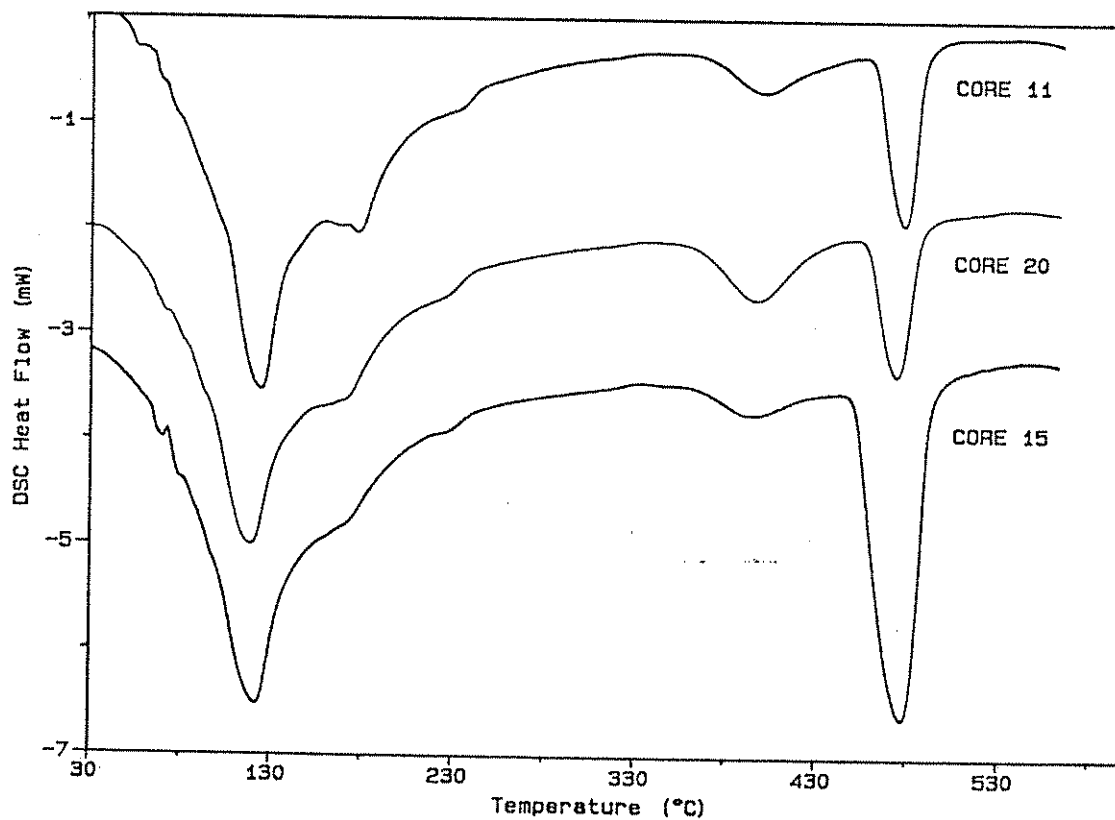


Figure 34. Results of DSC analysis on the fresh mortar fraction of US 20 cores.

since it had been exposed to the air for a considerable amount of time). The test results obtained from a fresh surface are shown in Figure 34, this should give a better indication of the composition of the mortar fraction of the concrete cores. The results were in rough agreement since they identified the same major constituents in the mortar fraction; however, the quantitative details (i.e., the area of the peaks that represented different decomposition events) varied considerably.

The major compounds that were indicated by the DSC study included: (1) calcium silicate hydrate gel and ettringite (or another AF(t) phase with a composition close to ettringite) - these compounds decomposed at temperatures between 50 and 120°C; (2) monosulfoaluminate hydrate (or another AF(m) phase of similar composition) - this compound decomposed at about 170°C; (3) magnesium hydroxide (brucite) - this compound decomposed at about 390°C; and (4) calcium hydroxide (portlandite) - this compound decomposed at about 470°C. The presence of brucite was also indicated by XRD (see Fig. 35). The XRD study indicated that the calcite content was similar in each core specimen, this suggests similar amounts of carbonation.

Why the drastic difference in brucite and portlandite contents of the mortar fractions from the different cores? The answer to this question is not readily evident; however, one can speculate on why this was observed.

Portlandite (calcium hydroxide) is a common by-product from the hydration of the calcium silicate phases in portland cement (fly ashes typically produce negligible amounts of portlandite when compared to cements, especially when only 15% fly ash is substituted for an equivalent amount of cement). The use of fly ash would have reduced the amount of portlandite present in the cores because of: (1) direct substitution; and (2) consumption of portlandite via the pozzolanic reaction. However, the reduction of the amount of portlandite by roughly 50%, which was evident in the DSC results (see Figure 34), cannot be explained adequately by either of these processes. Remember

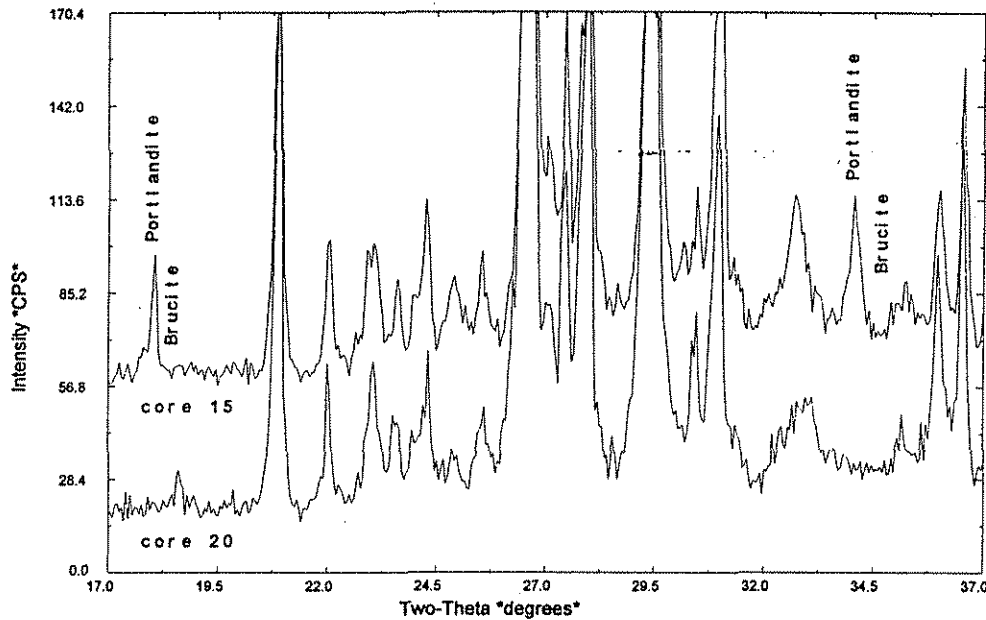


Figure 35. Results of XRD analysis on the mortar fraction of US 20 cores.

that Class C fly ashes tend to be poor pozzolans but good cements, this is the reason why they often do not mitigate the occurrence of alkali-silica reaction like a Class F fly ash. Supporting evidence can be found in the DSC results for the laboratory concrete specimens (see samples IO-1 #53 and 115-1 #55 in Appendix C). These laboratory test specimens were made in 1991 and showed only about a 20% reduction in portlandite content for a 15% level of fly ash replacement. It seems unlikely that several additional years of curing would have doubled the consumption of portlandite in the specimens.

Brucite (magnesium hydroxide) is normally formed from the hydration of periclase (magnesium oxide), and the periclase could have entered the system via the cement or the Class C fly ash. The hydration of periclase tends to occur slowly and may cause soundness problems. However, this does not seem to provide a reliable answer because, as was stated by Jones [18], the materials used in the project all met the appropriate specifications (i.e., the materials would have passed an autoclave expansion test).

The relative solubility of the two minerals may be the key factor to understanding the test results. Brucite is nearly insoluble in water. Portlandite is

slightly soluble in water but it is still many times more soluble than Brucite. Hence, if water had been allowed to leach the samples one would expect Portlandite to leave the bulk sample while Brucite would be retained. The dissolved Portlandite would travel to a free surface where it would probably precipitate as a carbonate, due to exposure to atmospheric carbon dioxide. This would produce efflorescence on the surface of the sample. Analysis of the leached specimen would indicate an elevated concentration of Brucite and a reduction in the amount of Portlandite. Hence, one may speculate that the DSC results simply indicate the relative amounts of deterioration present in the core specimens. Internal cracking drastically increased the amount of water that could penetrate into the concrete, and the relative solubility of the two compounds dictated which would be removed.

I-35 Cores

The concrete samples in the priority 3 group were all taken from I-35 in Story County. The results of the petrographic studies are summarized in Table 7. Observations from the CMI core that was taken from I-35 (CMI-2), will also be discussed in this section.

The major type of distress that was observed consisted of cracking oriented subparallel to the top of the pavement (cores 1 and 2), and cracking oriented perpendicular to the top of the pavement (cores 7 and 8). The cracks were severe and often caused portions of the cores to break apart during normal sample preparation procedures. The other samples (cores 3, 4, 5, 6 and CMI-2) did not exhibit macroscopic cracking (except for cracked shale particles). However, closer inspection of the cores indicated that they all exhibited similar features on a microscopic level.

The coarse aggregate (Alden crushed limestone) was sound in all of the cores. The fine aggregate contained shale particles that had cracked; however, little, if any, alkali-silica gel had been produced. The cracked shale particles rarely appeared to be causing much distress in the paste fraction of

the concrete. Core 8 contained more shale (2.1%) than any of the other cores. Sand-sized dolomite particles were observed in all the I-35 cores.

The paste fraction of the concrete cores often looked poor. The paste contained many entrapped voids (especially in the cores obtained from the pavement joints), and often the entrained air content varied considerably from the top to the bottom of the cores (see Figures 36 and 37). Again, the joints appeared to look the worst. The air content often appeared to be low in both the top and bottom of some cores. Occasionally, clumps of what appeared to be fly ash were observed in the paste (see Fig. 38). The significance of such features is difficult to ascertain; however, such features would typically suggest problems in the mixing cycle of the concrete.

Closer inspection of the paste typically indicated microcracking that tended to migrate around aggregates and through adjacent air voids (see Fig. 39). Small air voids were often completely filled with ettringite and were very difficult to observe without careful inspection because of poor contrast between the air voids and the bulk paste. Often it was easiest to refer to the sulfur X-ray map to locate the air voids. An alternative method of identifying the filled voids was to look for "holes" (dark regions) in the silicon X-ray map. Cracks, plus gaps between the cement paste and the aggregate particles, were also occasionally observed. Often these features tended to be filled with ettringite (see Figures 40 and 41). These features generally passed through several millimeters of paste. They suggest that the paste has expanded away from the aggregate. Plastic concrete problems, such as poor consolidation, could also leave similar gaps around aggregates; however, they could not account for the cracks that were observed adjacent to the gaps. It is difficult to say if the ettringite helped to create the cracks or if it simply was deposited there during the normal wetting and drying cycles experienced by the concrete pavement.

Table 7. Summary of observations from the cores taken from I-35.

Highway: I-35 north bound, paved 1985, proj. #IR-35-5(40)121

Mix details : C-3-C

Coarse Aggregate (CA) : Alden crushed limestone

Fine Aggregate (FA) : Ames, Hallett

Cement : Lehigh, Type I

Fly Ash : Port Neal #4

Observations: Visual inspection and light microscopy

Core No.	Location & Details	Aggregates	Voids	Cracks	Comments
1	1' from joint	CA sound max. = 1" FA max.=.25" shale = 1.1%	many filled with white material	Subparallel to surface of pavement	cracks pass through paste
2	4" from joint	CA sound max. = 1" FA max.=.3" shale = 0.9%	many entrapped voids, some air voids filled	Subparallel to surface of pavement	sample broke about 4" below surface
3	midpanel	CA sound max. = 1" FA max.=.25" shale = 1.9%	few entrapped voids, air voids filled	evident only in the shale particles	sample looks good
4	midpanel	CA sound max. = 1" FA max.=.25" shale = 1.0%	many entrapped voids, some air voids filled	evident only in the shale particles	some entrapped voids go all the way thru specimen
5	8" from vibrator trail crack	CA sound max. = 1" FA max.=.3" shale = 1.4%	some entrapped voids, many voids filled	evident only in shale particles	one entrapped void goes all the way thru specimen
6	8" from vibrator trail crack	CA sound max. = 1" FA max.=.3" shale = 1.1%	few entrapped voids, many voids filled	evident only in shale particles	
7	in vibrator trail crack	CA sound max. = 1" FA max.=.3" shale = 1.4%	many entrapped voids, many voids filled	cracked the length of the core specimen (from bottom to top)	cracks go around aggregates
8	in vibrator trail crack	CA sound max. = 1" FA max.=.25" shale = 2.1%	many entrapped voids, many voids filled	cracked from the bottom up about 5", some cracked shale	cracks go around aggregates

Table 7. (continued) Summary of observations from the cores taken from I-35.

Observations: Scanning electron microscopy

Core No.	Location & Details	Matrix	Voids	Cracks	Fly Ash	Comments
1	1' from joint	few cracked aggs.	air voids filled with ettringite in top of core, open in bottom	extensive in paste, often leading from air voids	yes	air content varies from top to bottom of core
2	4" from joint	one area contains alot of fly ash, paste looks poor	many entrapped voids; many ettringite filled voids	present in paste	yes	air content varies from top to bottom
3	midpanel	few cracked aggs.	many entrapped voids; many ettringite filled voids	extensive in paste; some cracked shale	yes	some shale showing ASR gel
4	midpanel	few cracked aggs.	ettringite fills many air voids in top and bottom of core	mostly in paste; some cracked shale	yes	
5	8" from vibrator trail crack	few cracked aggs.	ettringite fills air voids in top and bottom of core	mostly in paste; some cracked shale	yes	air content looks low
6	8" from vibrator trail crack	few cracked aggs.	many entrapped voids; ettringite fills many small air voids	some cracks in paste; some cracked shale	yes	air content looks low
7	in vibrator trail crack	? paste/agg bond, few cracked aggs.	many entrapped voids; ettringite fills small air voids	extensive in paste; some cracked shale	yes	air content looks low
8	in vibrator trail crack	? paste/agg bond, few cracked aggs.	many entrapped voids; ettringite fills small air voids	extensive in paste; some cracked shale	yes	air content looks low



Figure 36. I-35, core 2B, 25X magnification.

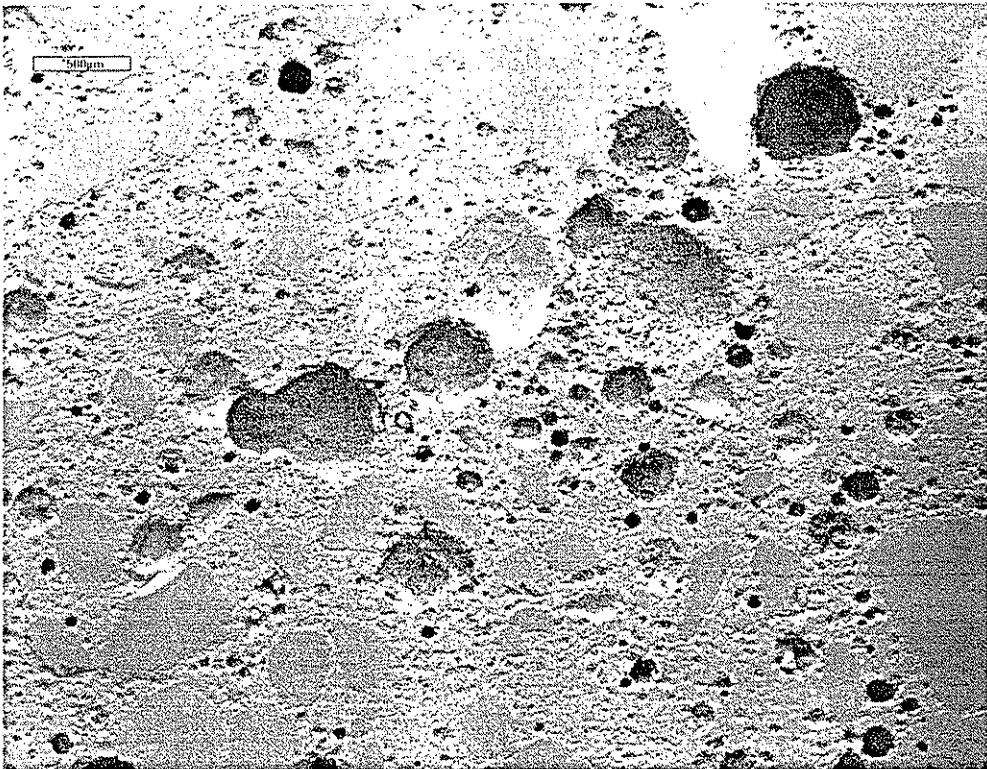


Figure 37. I-35, core 2C, 25X magnification; compare air voids to Fig. 36.

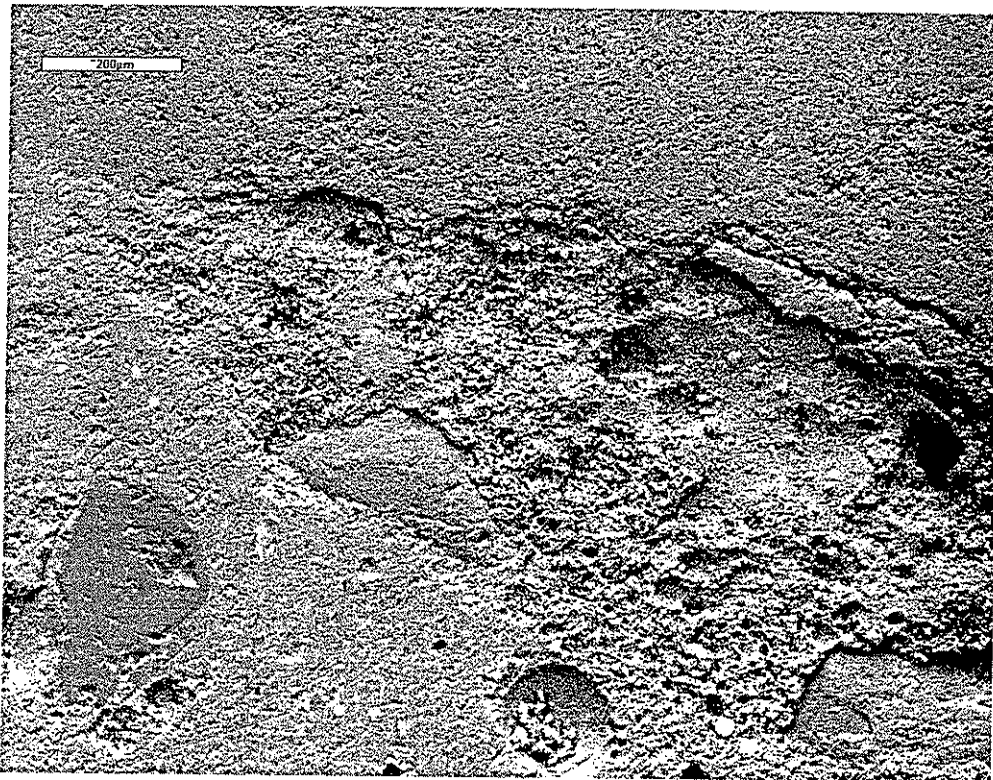


Figure 38. I-35, core 2B, 90X magnification; note clump of fly ash.

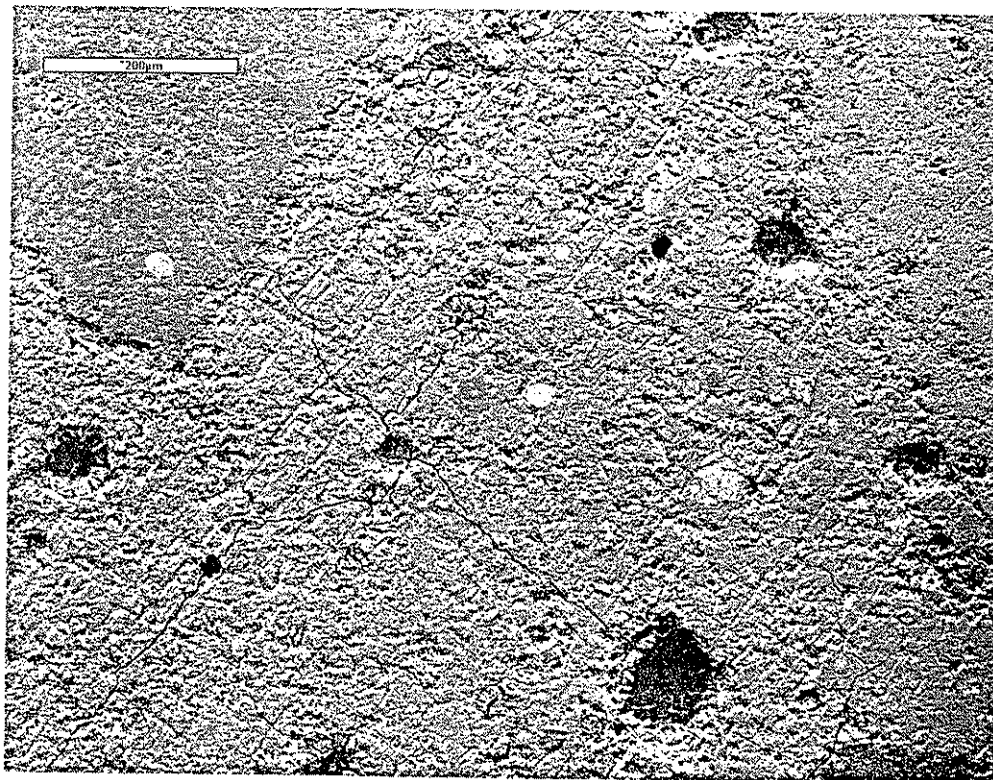


Figure 39. I-35, core 3B, 125X magnification; note general paste cracking.

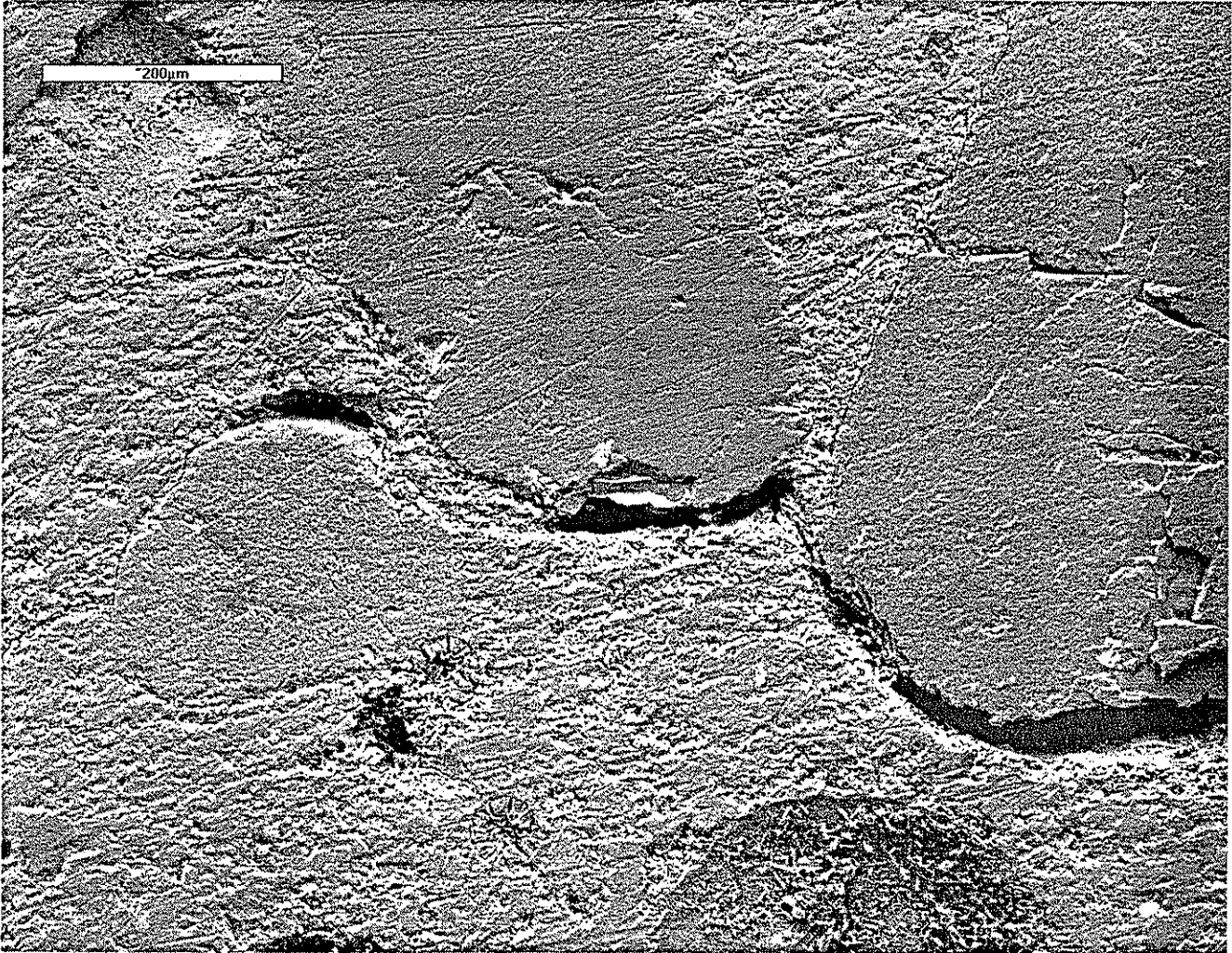


Figure 40. I-35, core 7B, 125X magnification; note gaps around aggregate particles that have been filled with ettringite.

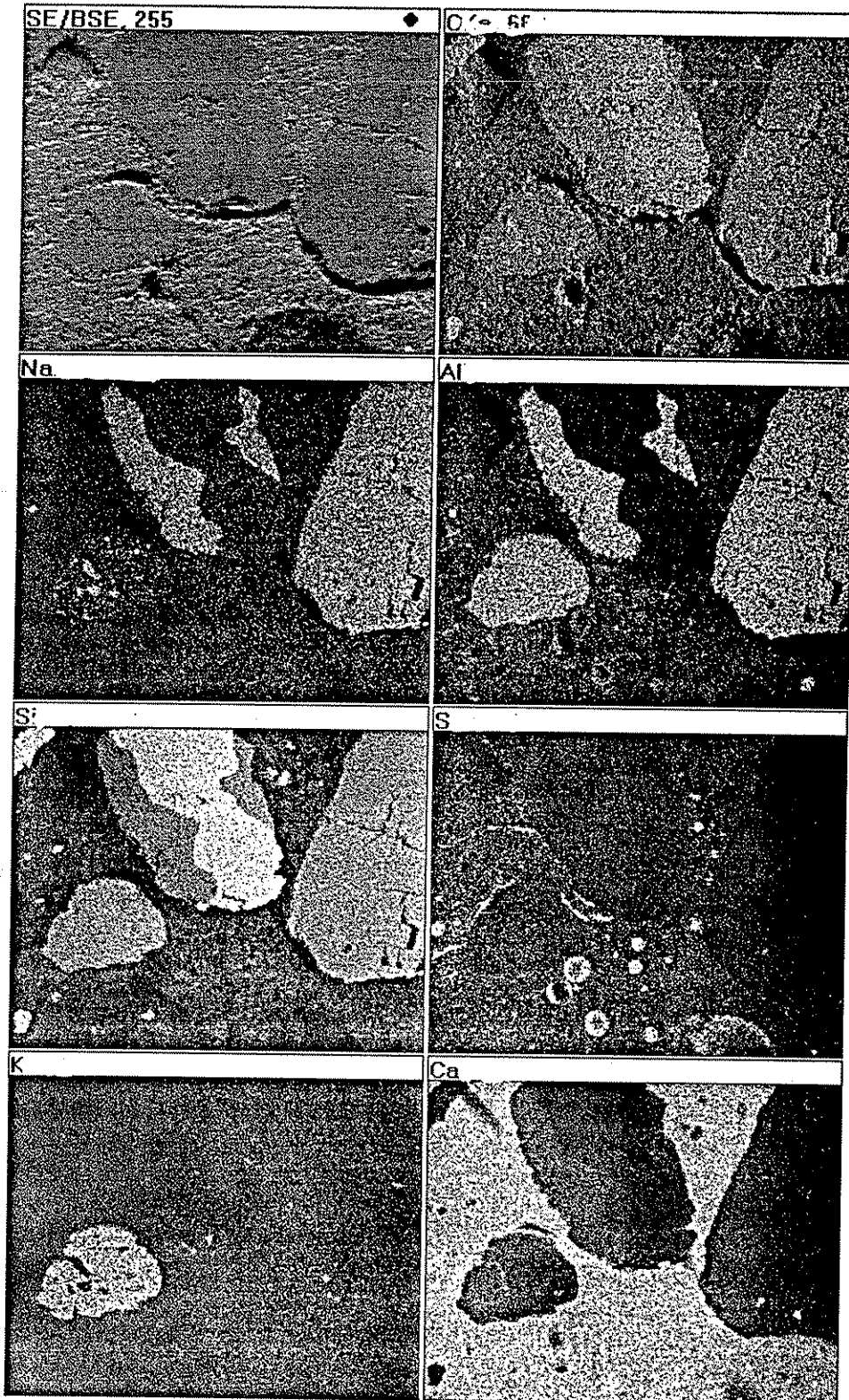


Figure 41. X-ray map of the region shown in Fig. 40; 125X magnification.

I-80 Cores

The concrete samples in the priority 4 group were all taken from I-80 in Dallas County. The results of the petrographic examination are summarized in Table 8. Observations from the CMI core that was taken from I-80 (CMI-1), will also be discussed in this section.

Distress was observed in several of the cores from I-80; however, the severity of the cracking was considerably less than that which was noted in US 20 and I-35. The cracking was most evident in cores taken from regions that exhibited vibrator trails (cores 21 and 22, note that core 21 also appeared to contain some mortar-rich regions (segregation) in the top few inches of the core). Most of the cracks were randomly oriented; however, occasionally they appeared to orient subparallel to the top of the pavement. The remaining samples (cores 23, 24 and CMI-1) did not exhibit extensive cracking (except for the cracked shale particles that were evident in all of the cores).

The coarse aggregate appeared to be sound. The fine aggregate contained shale particles that were causing popouts, this was due to the formation of alkali-silica gel (see Figure 42). Needle-like crystals, which were primarily composed of sodium and oxygen (perhaps sodium hydroxide?), were observed during detailed investigation of the popout region (see Figure 43). The exact significance of these crystals is not clear; however, it was noted that the composition of the alkali-silica gel tended to be enriched in potassium and low in sodium.

The paste fraction of the concrete was highly variable. Both entrapped and entrained air voids tended to be poorly dispersed throughout the paste. Some regions had virtually no air voids (see Figure 44), while other regions contained many air voids but they were not dispersed uniformly (see Figure 45). Also, it appeared that the tops of the cores from pavement sections containing vibrator trails contained less entrained air than similar cores without vibrator trails (compare Figures 44 and 45 with Figures 46 and 47, note the small change in

Table 8. Summary of observations from the cores taken from I-80.

Highway: I-80, Dallas Co., EB, paved 1989, proj. #IR-80-3(57)106

Mix details : C-4WR-C

Coarse Aggregate (CA) : Alden crushed limestone

Fine Aggregate (FA) : Van Meter, Hallett

Cement : Davenport, Type I

Fly Ash : Council Bluffs

Observations: Visual inspection and light microscopy

Core No.	Location & Details	Aggregates	Voids	Cracks	Comments
21	joint, vibrator trail	CA sound max. = 1" FA max.=.25" shale = 1.4%	few entrapped voids but some large	fine cracks, subparallel to surface of pavement	excess mortar near top of core; gel near cracked shale particles; air looks low
22	midpanel, vibrator trail	CA sound max. = 1" FA max.=.2" shale = 0.7%	many entrapped voids, some go thru specimen	fine cracks in mortar, random orientation ;some cracked shale	some areas appear to have low air content
23	joint, no vibrator trail	CA sound max. = 1" FA max.=.25" shale = 1.1%	some entrapped voids	evident only in the shale particles	sample looks good; air content looks good
24	midpanel, no vibrator trail	CA sound max. = 1.25" FA max.=.25" shale = 0.9%	some entrapped voids	evident only in the shale particles	sample looks good; air content looks good

Observations: scanning electron microscopy

Core No.	Location & Details	Matrix	Voids	Cracks	Fly Ash	Comments
21	joint, vibrator trail	good paste/agg bond, air looks low	many clustered voids; small voids filled with ettringite	extensive in paste; cracked shale	yes	bottom of core has more air than top of core
22	midpanel, vibrator trail	good paste/agg bond, air looks low	small voids filled with ettringite in top of core, bottom open	extensive in paste; cracked shale	yes	fly ash appears to be poorly dispersed
23	joint, no vibrator trail	good paste/agg bond, air looks good	many entrapped voids; most air void open	few cracks in paste; cracked shale	yes	fly ash appears to be poorly dispersed
24	midpanel, no vibrator trail	good paste/agg bond, air looks good	many entrapped voids; most air void open	few cracks in paste; cracked shale	yes	fly ash appears to be poorly dispersed

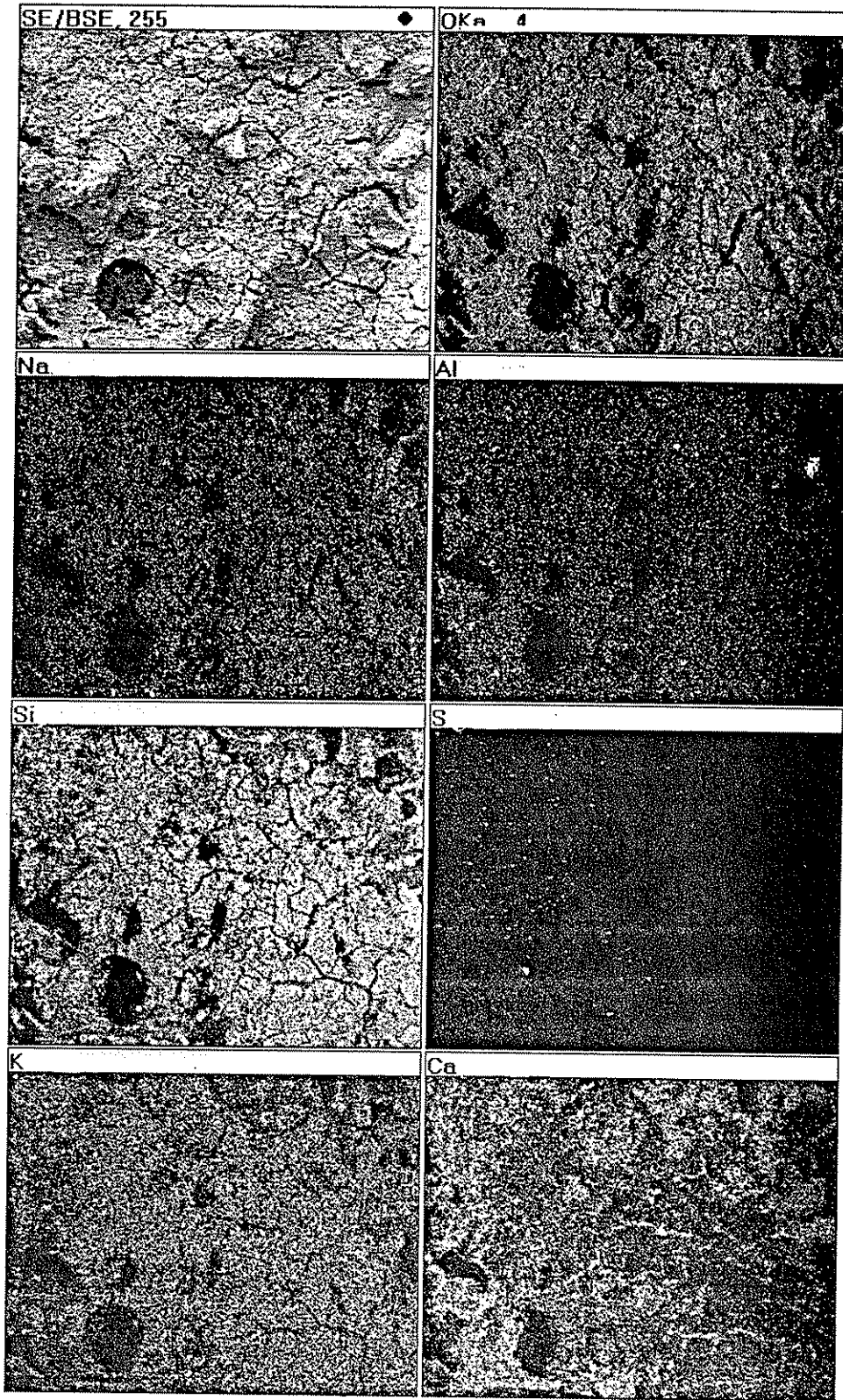


Figure 42 X-ray map of shale pop-out from I-80, core 24; 100X magnification.

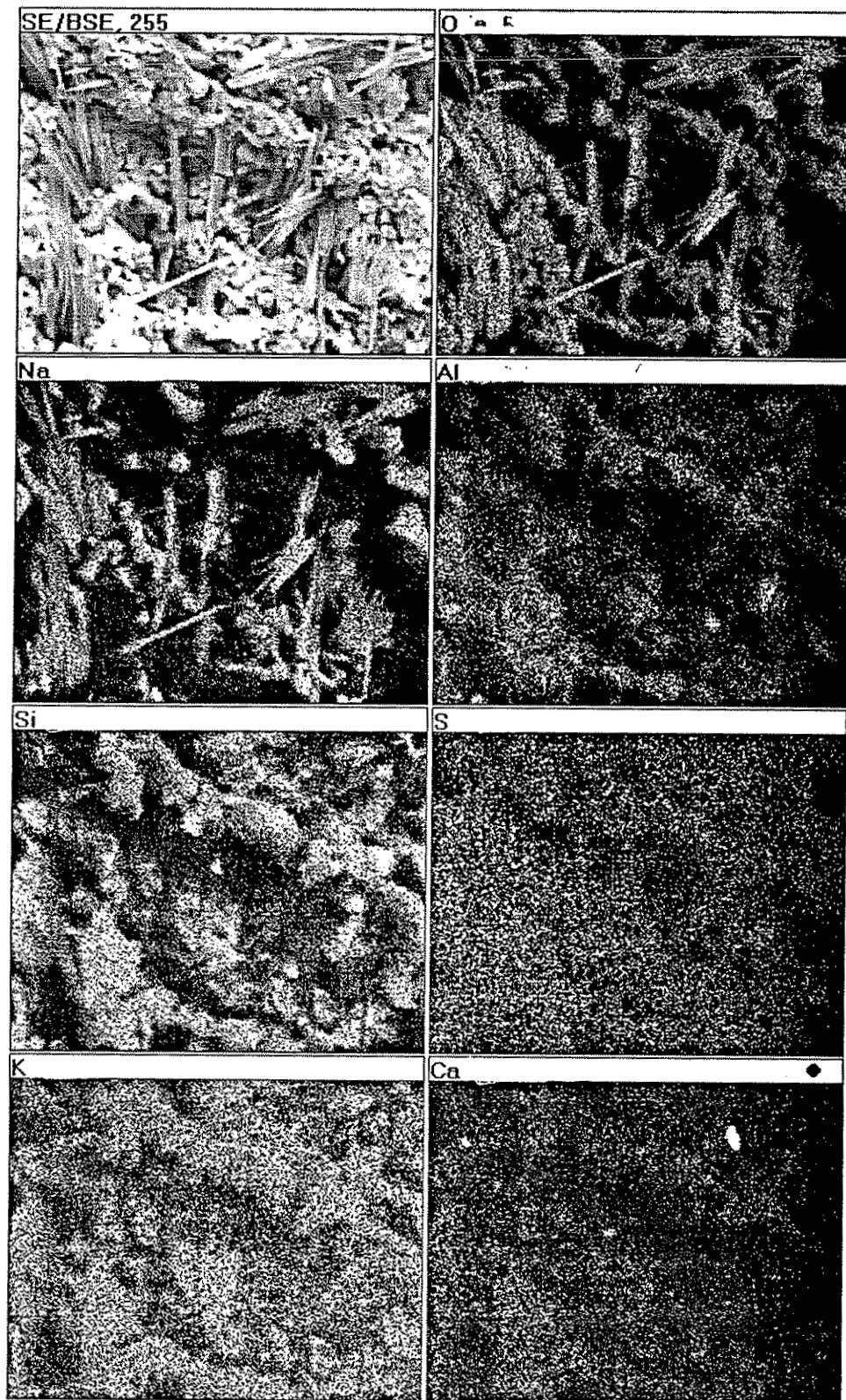


Figure 43 X-ray map of shale pop-out from I-80, core 24; 2000X magnification.

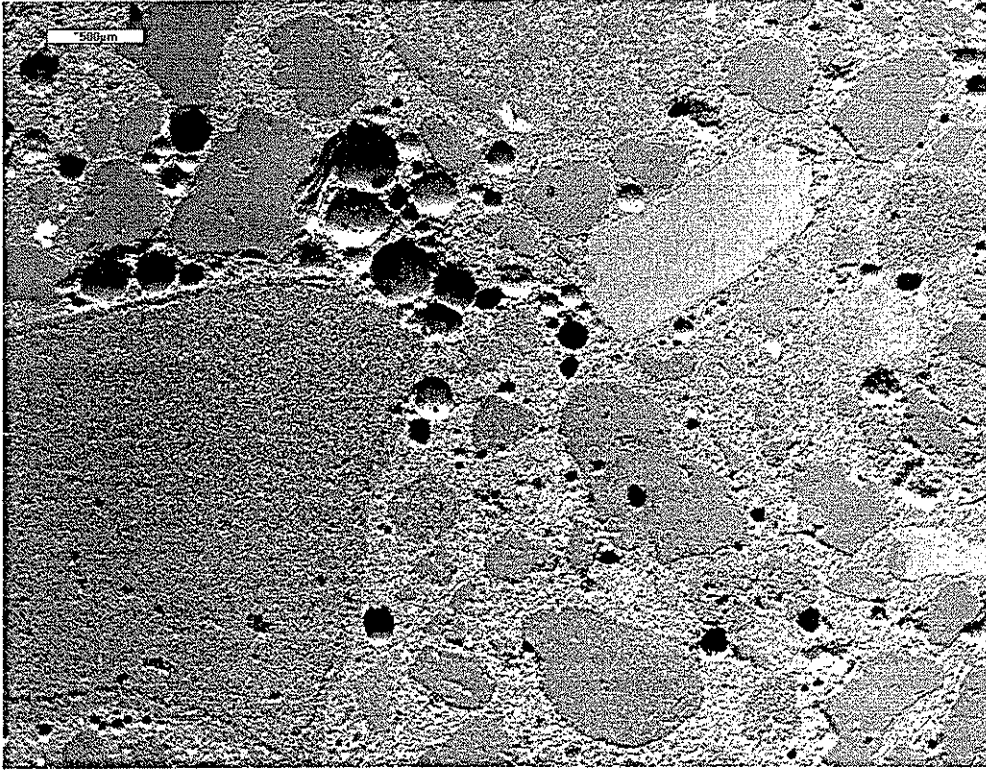


Figure 44. I-80, core 21B, 25X magnification.

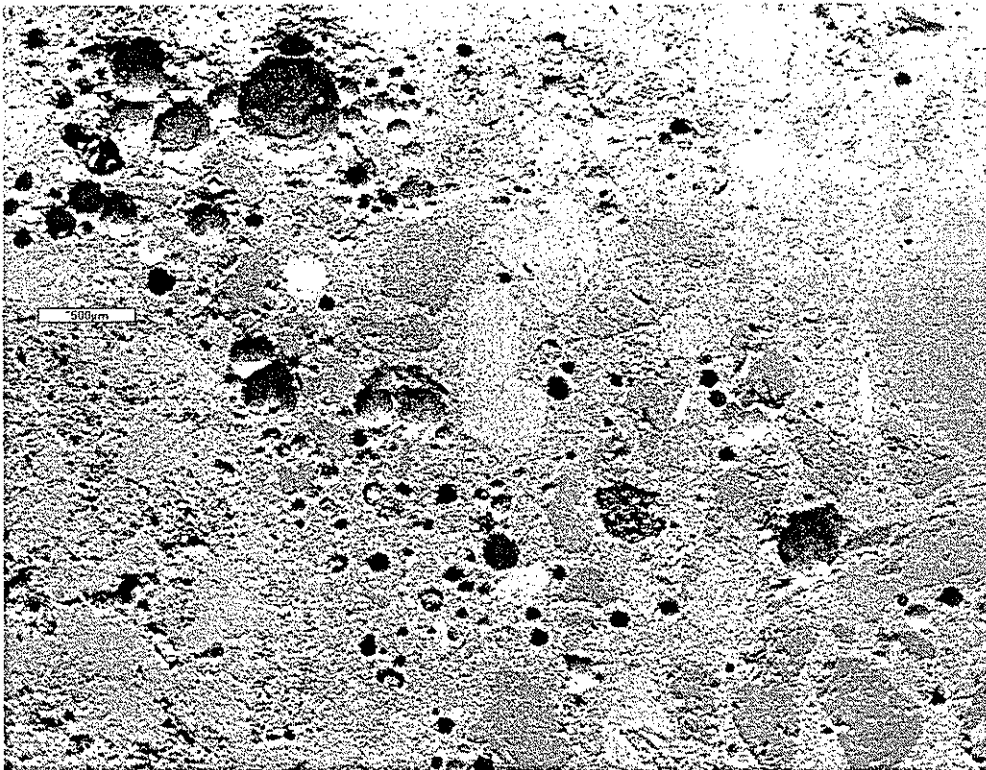


Figure 45. I-80, core 22B, 25X magnification.

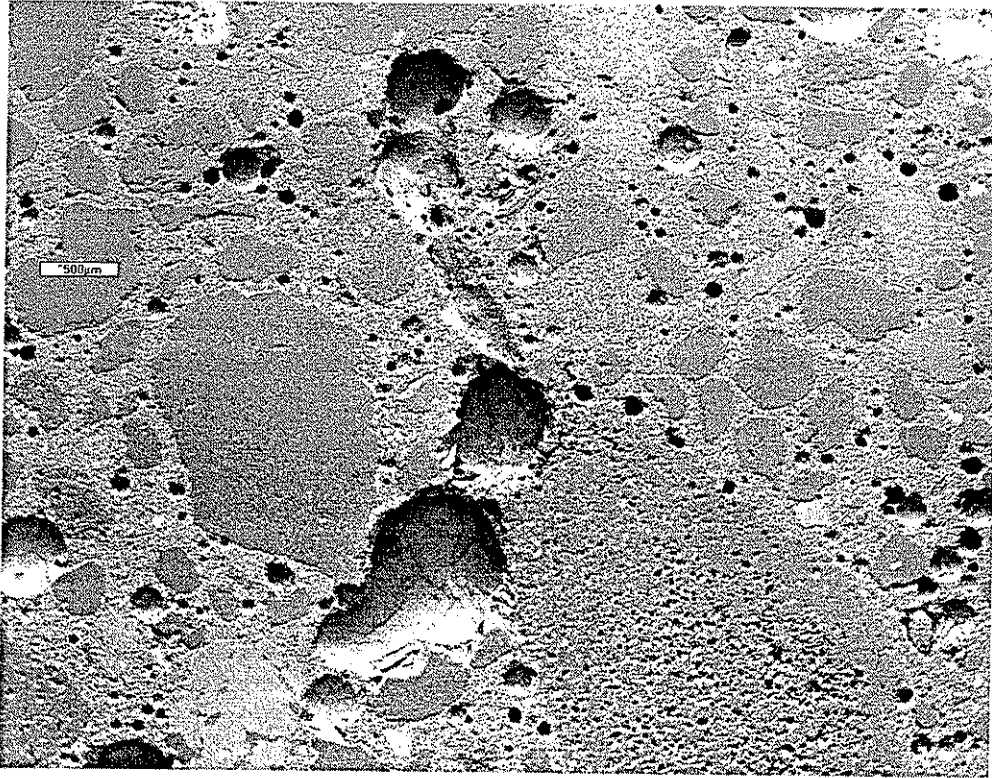


Figure 46. I-80, core 23B, 20X magnification.

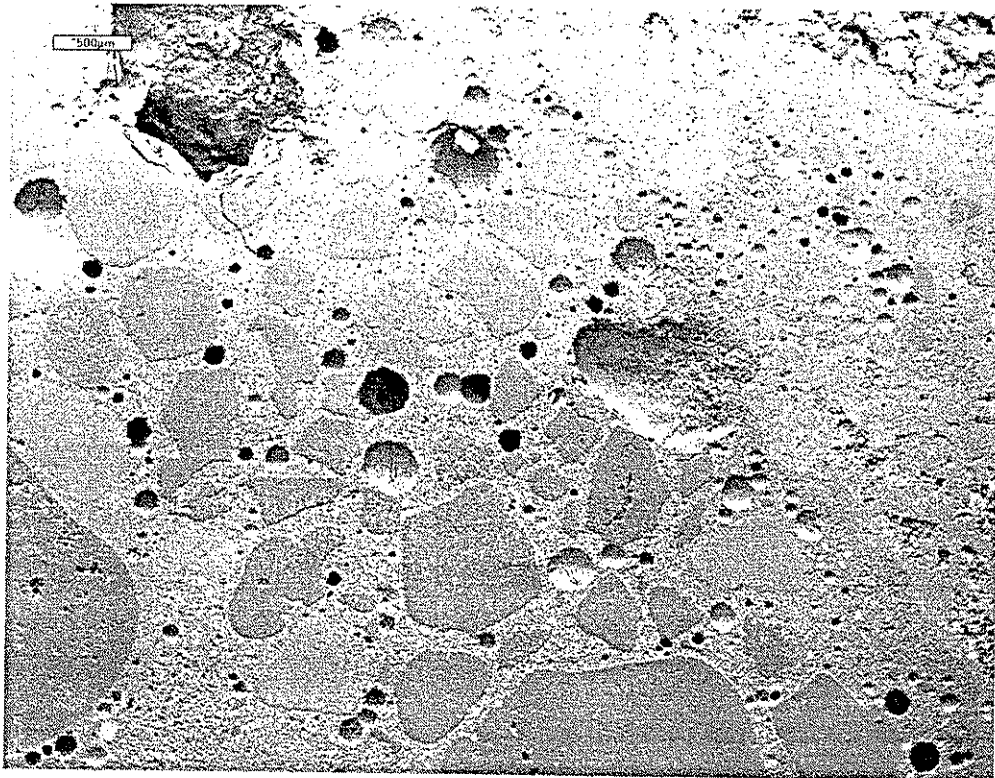


Figure 47. I-80, core 24B, 20X magnification.

magnification). Also, the small air voids tended to be filled with ettringite in the top sections of the two cores taken from pavement sections exhibiting vibrator trails. In general, however, the cores from I-80 exhibited considerably less ettringite filled voids than the cores from I-35 and US 20.

Fly ash also appeared to be poorly distributed in the paste (see Fig. 48). An alternative explanation for the number of fly ash spheres that were observed would be that too much fly ash was batched into the concrete. However, this explanation does not seem as plausible as poor mixing because other paste regions appear to contain virtually no fly ash.

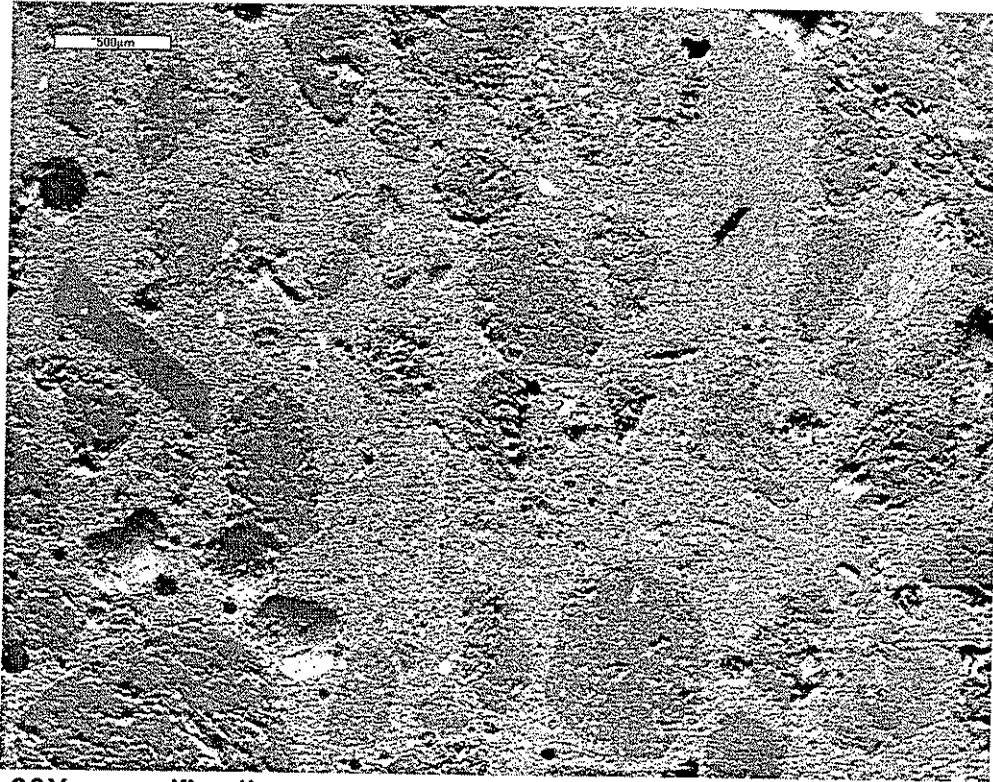
Fast-track Pavement at Bettendorf

The concrete samples in the priority 5 group were all taken from a street in Bettendorf, Iowa. The results of the visual inspection, light and scanning electron microscopy studies are summarized in Table 9.

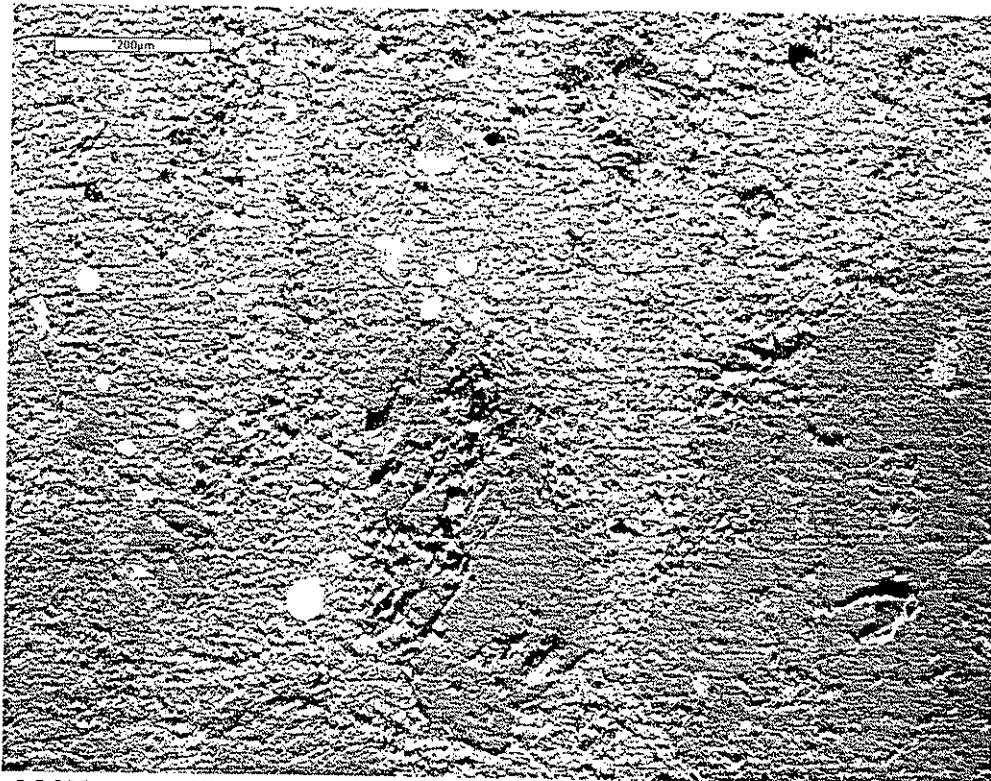
Moderate distress was observed in only one of the cores (number 27, cored from the joint area) from the Bettendorf fast track pavement. Again, the severity of the cracking was considerably less than that which was noted in US 20 and I-35. The cracking was oriented subparallel to the top of the pavement and was located about half way down the core. The remaining samples (cores 25, 26 and 27) did not exhibit macroscopic cracking (except for an occasional chert particle, these were evident in all of the cores).

The coarse aggregate appeared to be sound. The fine aggregate contained some reactive particles that were in the early stages of alkali-silica related deterioration (see Figures 49 and 50). Cracking related to the formation of alkali-silica gel was minimal; however, some voids lined with gel were observed. Sand-sized dolomite particles were observed in all of the cores.

The paste fraction of the concrete cores looked poor, this was especially true for cores 27 and 28. Air contents looked low; however, this was simply due



30X magnification



100X magnification

Figure 48. 180, core 22B; note excess fly ash.

Table 9. Summary of observations from the cores taken from Bettendorf.

Highway: Bettendorf Fast Track, Spruce Hill, paved 1987.
 Coarse Aggregate (CA) : Linwood crushed limestone
 Fine Aggregate (FA) : ?
 Cement : Continental, Type III
 Fly Ash : Louisa

Observations: Visual inspection and light microscopy

Core No.	Location & Details	Aggregates	Voids	Cracks	Comments
25	East bound lane	CA sound 1.25" max FA max=.2"	some entrapped voids; many lined	none evident	fly ash present
26	East bound lane	CA sound 1.25" max FA max=.2"	some entrapped voids; many lined	none evident	fly ash present
27	West bound lane	CA sound 1.25" max FA max=.4" ;some FA particles reactive	some entrapped voids; many lined	subparallel to surface of pavement, about half way down core	fly ash present; paste looks poor in some regions; some gel material in voids near reactive aggregates
28	West bound lane	CA sound 1.0" max FA max=.2" ;some FA particles reactive	many entrapped voids; many lined	none evident	fly ash present; paste looks poor in some regions

Observations: Scanning electron microscopy

Core No.	Location & Details	Matrix	Voids	Cracks	Fly Ash	Comments
25	East bound lane	good paste/agg. bond; air looks OK in top but low in bottom	many voids lined with ettringite; small air voids sometimes filled, especially in bottom	few present; some cracked shale particles	yes	some ASR gel near shale
26	East bound lane	air appears to vary from top to bottom	many entrapped voids, many air voids lined with ettringite, some entirely filled	more cracking than was observed in core 25, typically cracks go thru paste	yes	regions with low air tend to have small voids entirely filled
27	West bound lane	air content looks low; paste/agg. bond poor in some regions	air voids appear distorted; voids as large as 200 microns filled with ettringite	extensive cracking; some cracks filled with ettringite; some cracked FA	yes	ASR gel evident near reactive fine aggregate particles
28	West bound lane	air content looks better than in core 27	air voids appear distorted; many filled with ettringite	much cracking in paste; some cracks filled with ettringite; few cracked FA	yes	some ASR gel evident in entrapped air voids

to the fact that many of the entrained air voids had been filled with ettringite (see Figures 51 and 52). Also, cracks were often filled with ettringite (note the bright lines in the sulfur and aluminum maps in Fig. 52). Sometimes the air voids even appeared as if they had been distorted during the placement process (note the asymmetric voids in Figure 53). Microcracking was common in the paste and typically went around aggregates and through air voids. Again, in a manner very similar to that which was observed in the cores from I-35, the ettringite-filled cracks tended to propagate several millimeters through the cement paste.

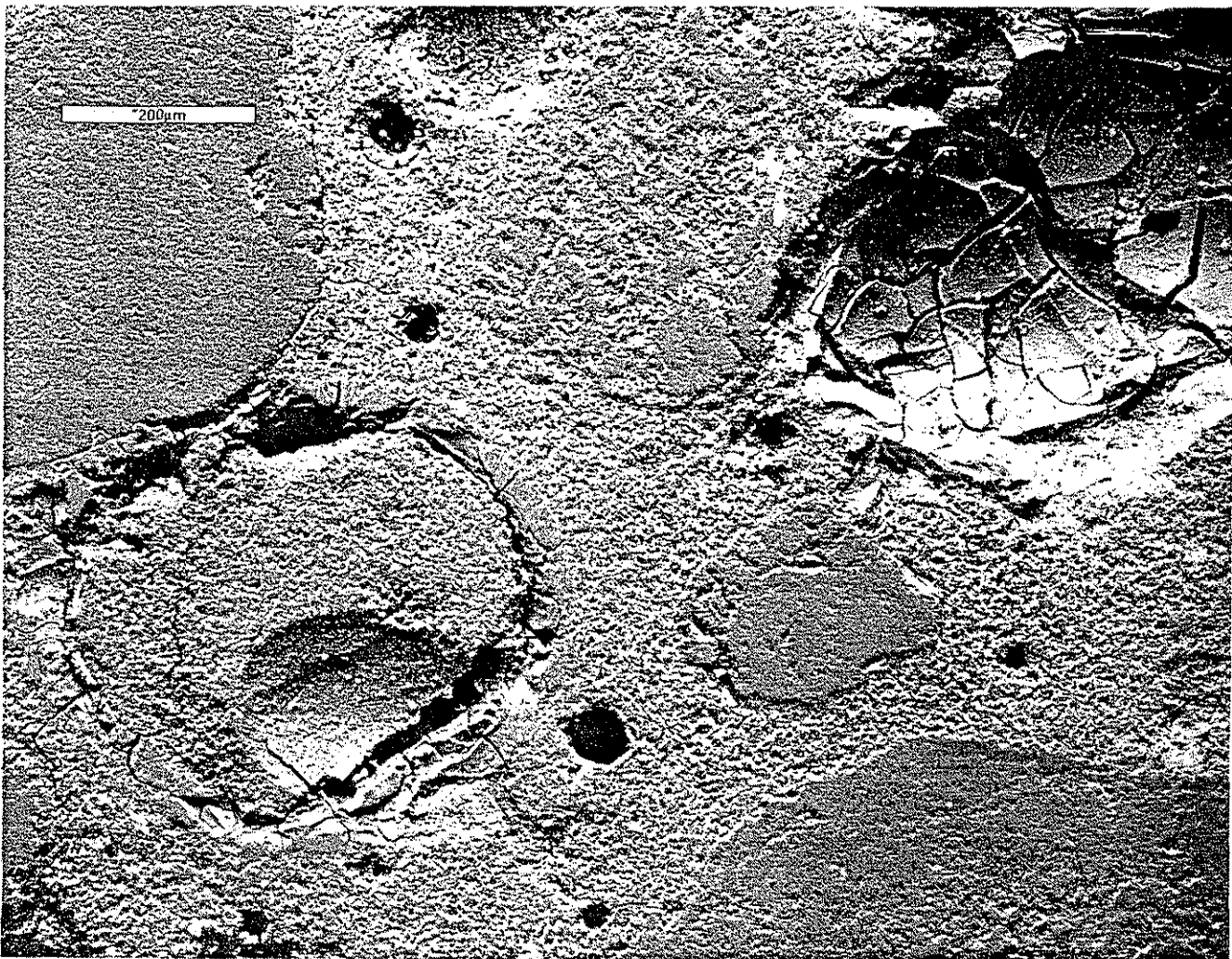


Figure 49. Bettendorf fast track, core 25B, 100X magnification.

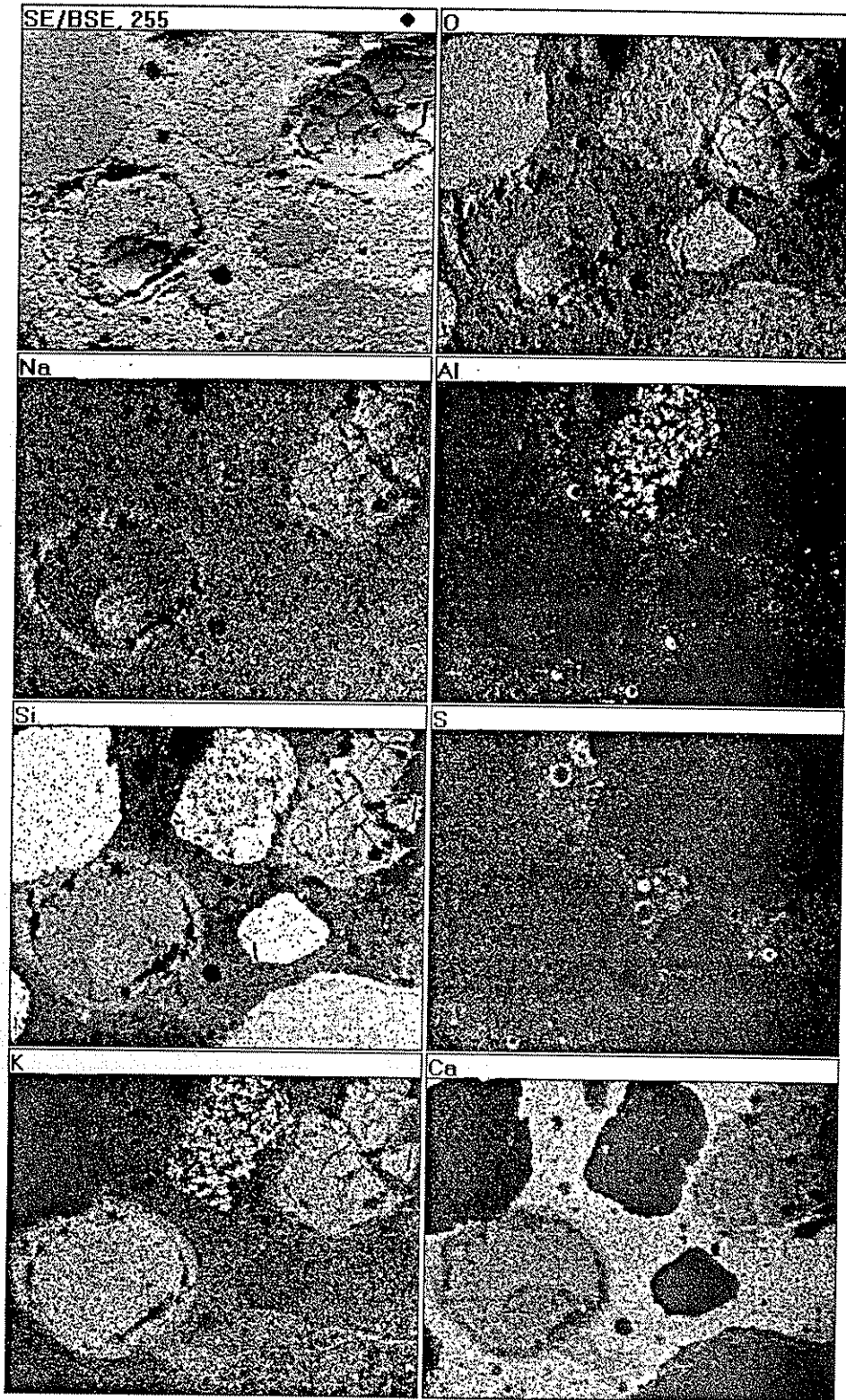


Figure 50. X-ray map of the region shown in Fig. 49; 100X magnification.

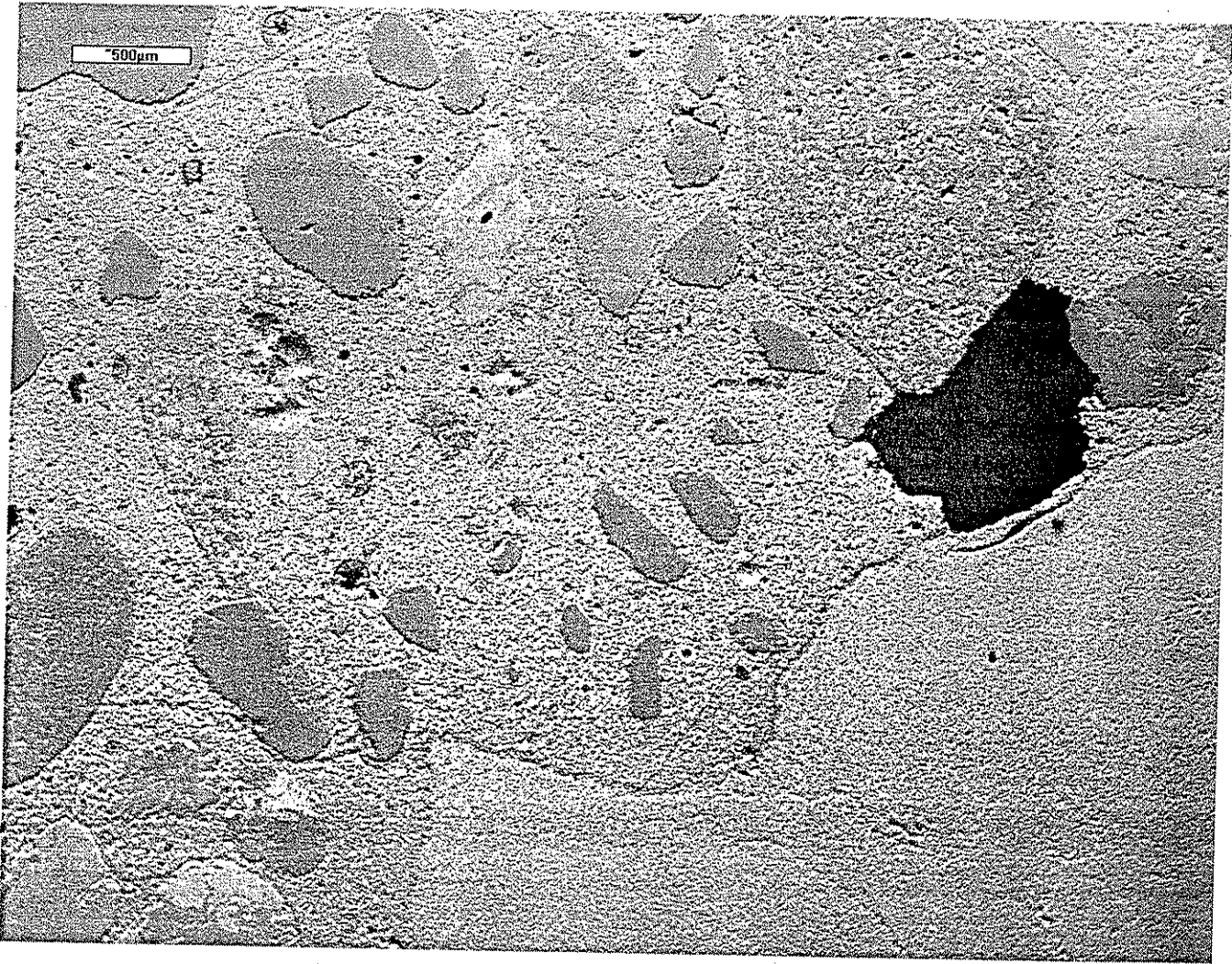


Figure 51. Bettendorf fast track, core 27B, 25X magnification.

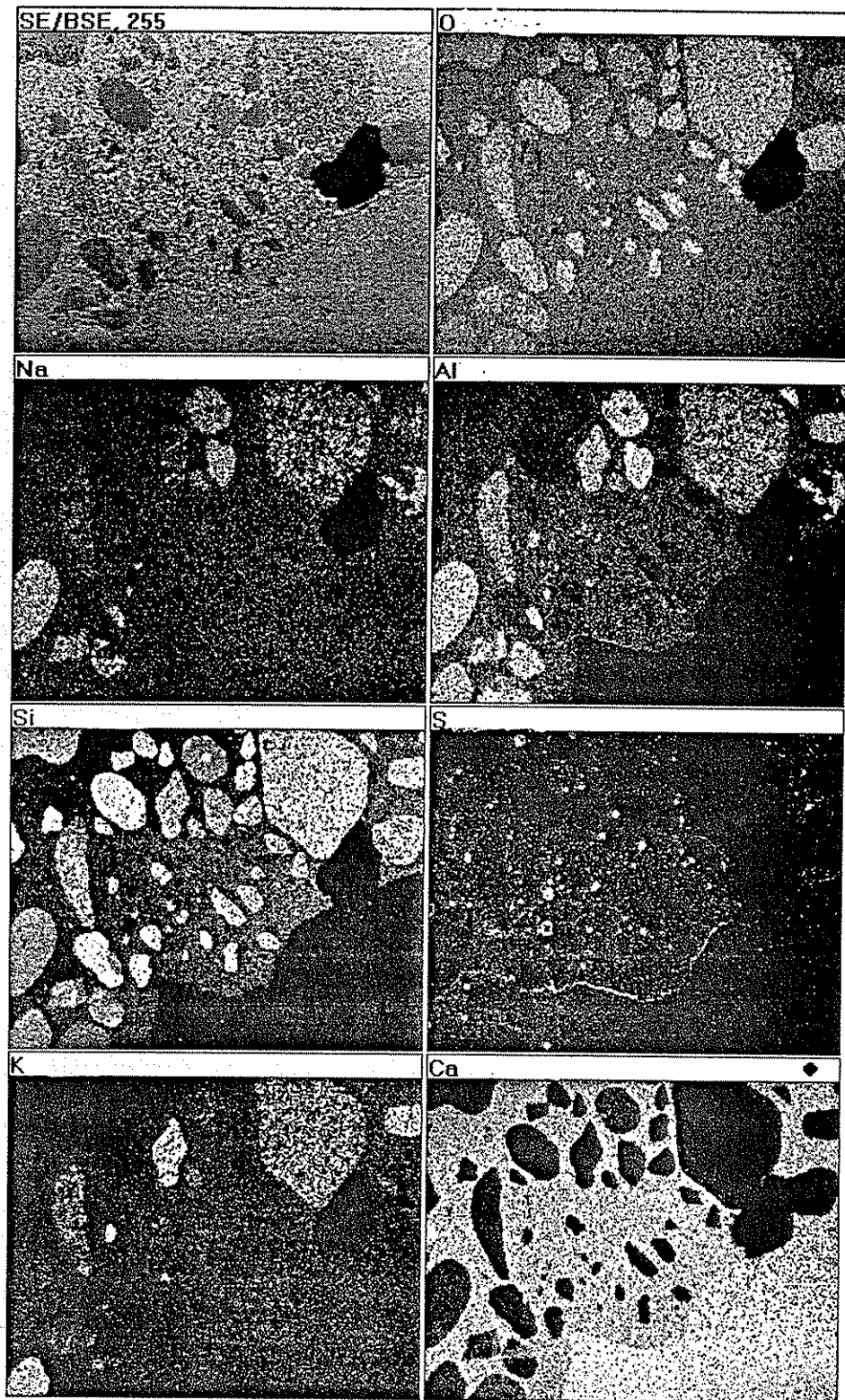


Figure 52. X-ray map of the region shown in Fig. 51; 25X magnification.

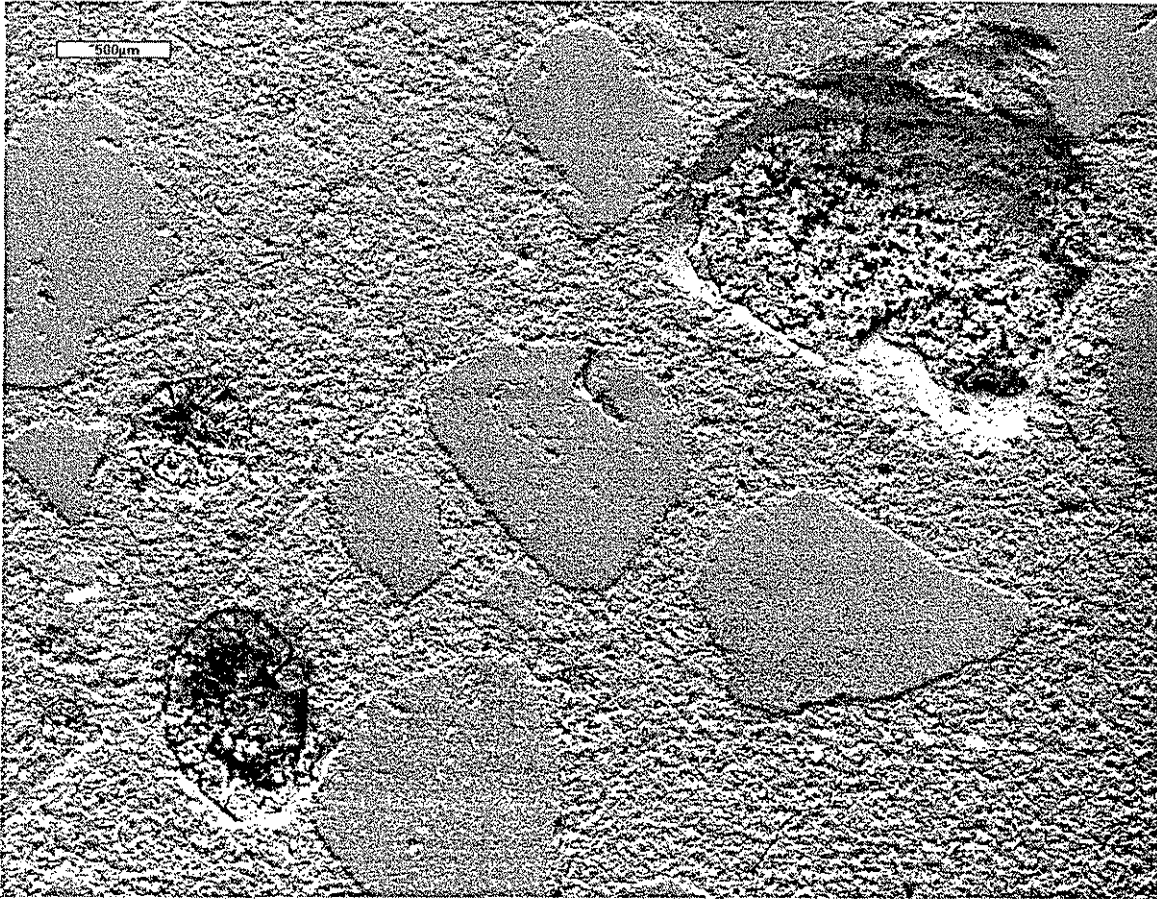


Figure 53. Bettendorf fast track, core 28C, 70X magnification.

Assorted Other Cores

The concrete samples in the priority 6 group consisted of cores obtained from three different locations. The first set of cores was from Highway 175 in Hamilton county. The results of the petrographic studies are summarized in Table 10. The second set of cores was from US 169 in Madison county. The results of the petrographic examination are summarized in Table 11. The final set of cores that were inspected for this project were obtained from Highway 25 in Union county, and the results of the petrographic examination are summarized in Table 12. Time and funding were insufficient to allow for the examination of cores from Buchanan and Louisa counties.

Very little distress was observed in the cores taken from Highway 175. Five different cores were studied; however, only two are listed in the core log in Appendix A. The three additional cores were obtained from Iowa Department

Table 10. Summary of observations from the cores taken from IA 175.

Highway: Highway 175, paved 1980, proj.# F-175-7(13)-20-40.

Mix details: C-3 control mix, A-3 for fly ash mixes

Coarse Aggregate (CA) : Moberly mine crushed limestone

Fine Aggregate (FA) : Hallet sand

Cement : Penn Dixie, Type I

Fly Ash : varies, see below

Observations: Visual inspection and light microscopy

Core No.	Location & Details	Aggregates	Voids	Cracks	Comments
not in log	control section (no ash)	CA sound max.=1.25" FA max.=.25"	some entrapped voids; most voids clean, few lined	cracked shale particles	ASR gel evident near shale particles and adjacent voids
not in log	C - ash section (Council Bluffs)	CA sound max.=1.25" FA max.=.25"	some voids lined	cracked shale particles	ASR gel evident near shale particles and adjacent voids
not in log	F - ash section (Port Neal)	CA sound max.=1.25" FA max.=.25"	few voids lined	cracked shale particles	no ASR gel evident
41	midpanel fly ash	CA sound max.=1.0" FA max.=.25"	some voids with thick linings	cracked shale particles	no ASR gel evident
42	joint fly ash	CA sound max.=1.25" FA max.=.20"	some voids lined	cracked shale particles	ASR gel evident near shale particles and adjacent voids

Observations: Scanning electron microscopy

Core No.	Location & Details	Matrix	Voids	Cracks	Fly Ash	Comments
not in log	control section (no ash)	good paste/agg. bond	often lined with ettringite; some voids near shale filled with ASR gel	cracked shale particles; very fine microcracks in paste	no	ASR gel evident near shale particles
not in log	C - ash section	good paste/agg. bond	often lined with ettringite; some voids near shale filled with ASR gel	cracked shale particles; very fine microcracks in paste	yes	ASR gel evident near shale particles
not in log	F - ash section	good paste/agg. bond	some voids lined with ettringite	cracked shale; few cracks in paste	yes	No ASR observed

of Transportation personnel, the cores were extracted from the pavement in 1991. These three cores were taken from pavement sections that contained Class C fly ash, Class F fly ash, and no fly ash (i.e., a control section). Two of the cores (cores 41 and 42, which both contained fly ash) were not studied in the scanning electron microscope because the visual investigation indicated that they were very similar to the cores taken in 1991.

The coarse aggregate used in the Highway 175 project (Moberly mine crushed limestone) was sound in all of the cores. The fine aggregate contained some shale particles that had produced alkali-silica gel. All of the core specimens (cores 41 and 42 plus the three other cores described above) contained cracked shale particles. Some of the cracked shale particles in the

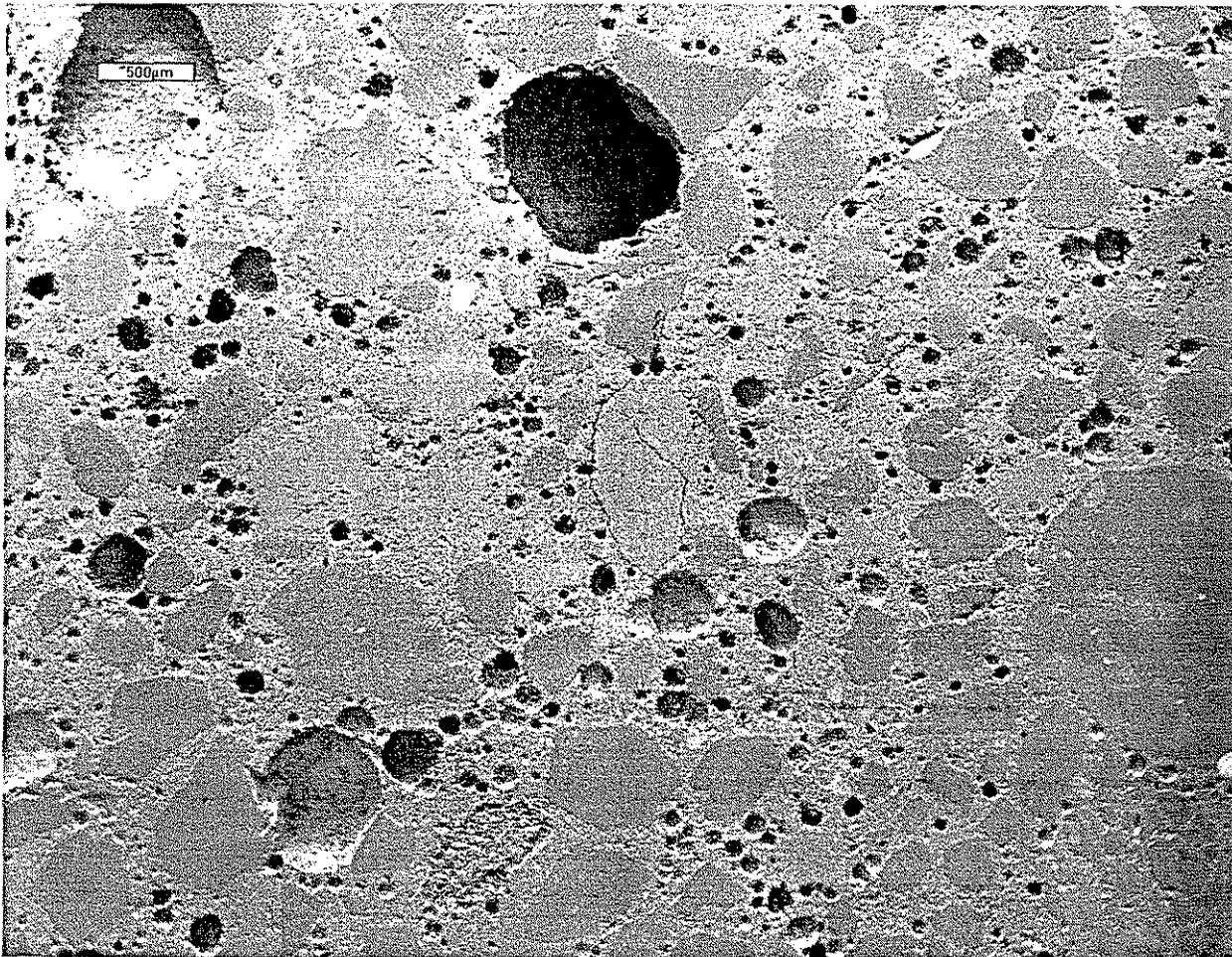


Figure 54. Highway 175, class F fly ash, 20X magnification.

pavement cores that did not contain fly ash, or that contained Class C fly ash, had produced alkali-silica gel. None of the shale particles in the section containing Class F fly ash exhibited any signs of alkali-silica gel. The cracks associated with the shale particles (see Figure 54) were small and typically did not propagate far into the cement paste. Other reactive aggregates were not observed in the five core samples. Sand-sized dolomite particles were observed in all of the cores taken from Highway 175.

The paste fraction of the cores taken from Highway 175 appeared reasonably uniform. It did contain some very fine microcracks that could be observed at magnifications of about 100X (or more); however, they appeared randomly oriented. The samples contained entrapped air voids, but few exceeded about 3 millimeters in diameter. The entrained-air voids were often lined with ettringite (see Fig. 55); however, they were never totally filled (even the small air voids).



Figure 55 Highway 175, core containing no ash; 100X magnification.

The remaining cores, those from US 169 and Highway 25, arrived at the laboratory in very poor shape. In fact, several of the cores consisted primarily of rubble. Hence, it was decided to do the majority of the studies using sawn specimens of various sizes. Some studies were also conducted on small samples that had been ground and polished as was described earlier in this report. The two sets of pavement cores will be discussed at the same time since they exhibit nearly identical types of deterioration.

Table 11. Summary of observations from the cores taken from US 169.

Highway: US 169, paved 1977, proj. #. FN-169-3(18)--21-6
 Mix details: ?
 Coarse Aggregate (CA) : Early Chapel crushed limestone
 Fine Aggregate (FA) : ?
 Cement : ?

Observations: Visual inspection and light microscopy

Core No.	Location & Details	Aggregates	Voids	Cracks	Comments
37	near joint South Bound	CA cracked max.=.75" FA=0.25" max	many entrapped voids; air looks low	severe; subparallel to top of pavement	sample basically rubble
38	midpanel South Bound	CA cracked max.=.75" FA=0.25" max	some entrapped voids; some voids lined	extensive; subparallel to top of pavement	some randomly oriented cracks were also observed
39	near joint South Bound	CA cracked max.=.75" FA=0.25" max	some voids lined	extensive; subparallel to top of pavement	all cracks intersect coarse aggregate
40	midpanel South Bound	CA cracked max.=.75" FA=0.2" max	some entrapped voids; many voids lined	severe; subparallel to top of pavement	all cracks intersect coarse aggregate

Observations: Scanning electron microscopy

Core No.	Location & Details	Matrix	Voids	Cracks	Fly Ash	Comments
37	near joint South Bound	distorted due to cracking, sample preparation	often filled with ettringite	extensive; often intersect coarse agg.	?	much fine Mg observed in paste
38	midpanel South Bound	distorted due to cracking, sample preparation	often filled with ettringite	extensive; often intersect coarse agg.	no	much fine Mg observed in paste
39	near joint South Bound	distorted due to cracking, sample preparation	many voids lined, small voids filled	extensive; often intersect coarse agg.	no	much fine Mg observed in paste
40	midpanel South Bound	distorted due to cracking, sample preparation	many voids lined	extensive; often intersect coarse agg.	no	some dolomite in sand fraction

Distress was observed in all of the cores taken from the two pavements. Cracking was nearly always oriented subparallel to the top of the pavement. The cracks tended to pass through coarse aggregate particles as they traversed across the samples. Cracking was always severe (this was the most deteriorated concrete that was studied in this project) handling during viewing in a stereo microscope often resulted in specimen breakage.

Table 12. Summary of observations from the cores taken from IA 25.

Highway: IA 25, paved 1964, proj. # F-451 (8)
 Mix details: A*3
 Coarse Aggregate (CA) : Stanzel (Schildberg)
 Fine Aggregate (FA) : Conc. materials
 Cement : Lone Star Type I
 Fly Ash : none

Observations: Visual inspection and light microscopy

Core No.	Location & Details	Aggregates	Voids	Cracks	Comments
43	midpanel South bound	CA cracked max.= 1.0" FA=0.25" max	some voids lined	severe; subparallel to top of pavement	12 of 20 coarse aggregate particles cracked
44	midpanel South bound	CA cracked max.= 1.0" FA=0.25" max	some voids lined; some voids filled	severe; subparallel to top of pavement	13 of 15 coarse aggregate particles cracked
45	midpanel South bound	CA cracked max.= 1.0" FA=0.25" max	some voids lined; many voids filled	severe; subparallel to top of pavement	10 of 15 coarse aggregate particles cracked

Observations: Scanning electron microscopy

Core No.	Location & Details	Matrix	Voids	Cracks	Fly Ash	Comments
43	midpanel South bound	distorted due to cracking, sample preparation	some voids lined	extensive; often intersect coarse agg.	no	air system difficult to see
44	midpanel South bound	distorted due to cracking, sample preparation	many small voids filled with ettringite	extensive; often intersect coarse agg.	no	air system difficult to see
45	midpanel South bound	distorted due to cracking, sample preparation	many small voids filled with ettringite	extensive; often intersect coarse agg.	no	air system difficult to see

The coarse aggregate was extensively cracked in both sets of cores. This was most frequent in the cores from Highway 25, where over 50% of the coarse aggregate particles exhibited cracks. The cracks in the coarse aggregate particles were not filled (i.e., little evidence of ettringite or gel products). The fine aggregate looked sound and very few shale particles were observed. Sand-sized dolomite particles were observed in all the cores from IA 25, and core number 40 from US 169.

The paste fraction of the concrete cores was difficult to view because of the poor surface preparation that was used. Hence, it was difficult to assess details of the entrained-air system that was present in the specimens. Ettringite filled voids were present in both series of cores; although the cores from US 169 appeared to be filled more frequently (see Figures 56 and 57). Microcracks could not be reliably detected in the specimens, this was due to the way that the specimens had been prepared.

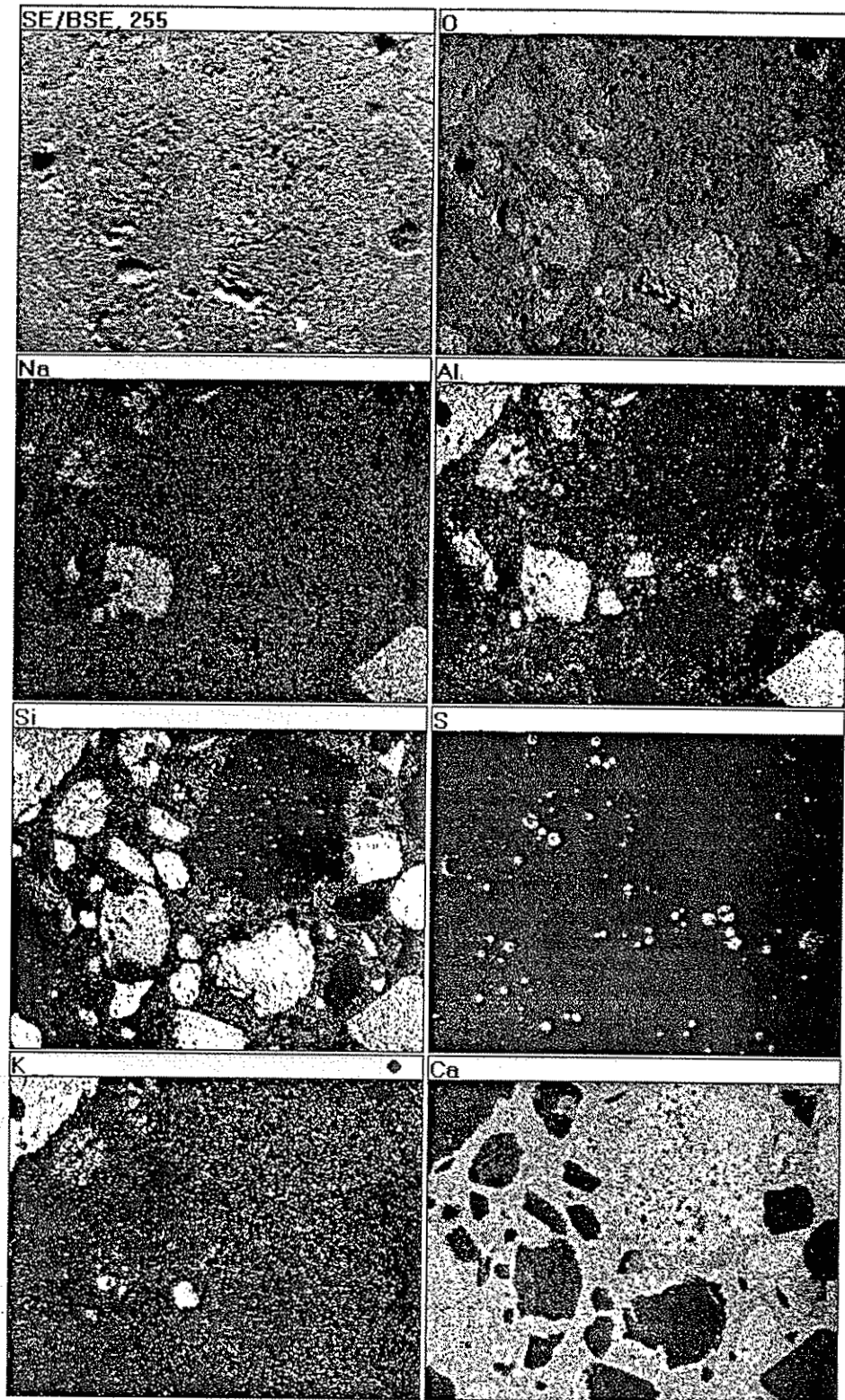


Figure 56. X-ray map from US 169, core 37B; 30X magnification.

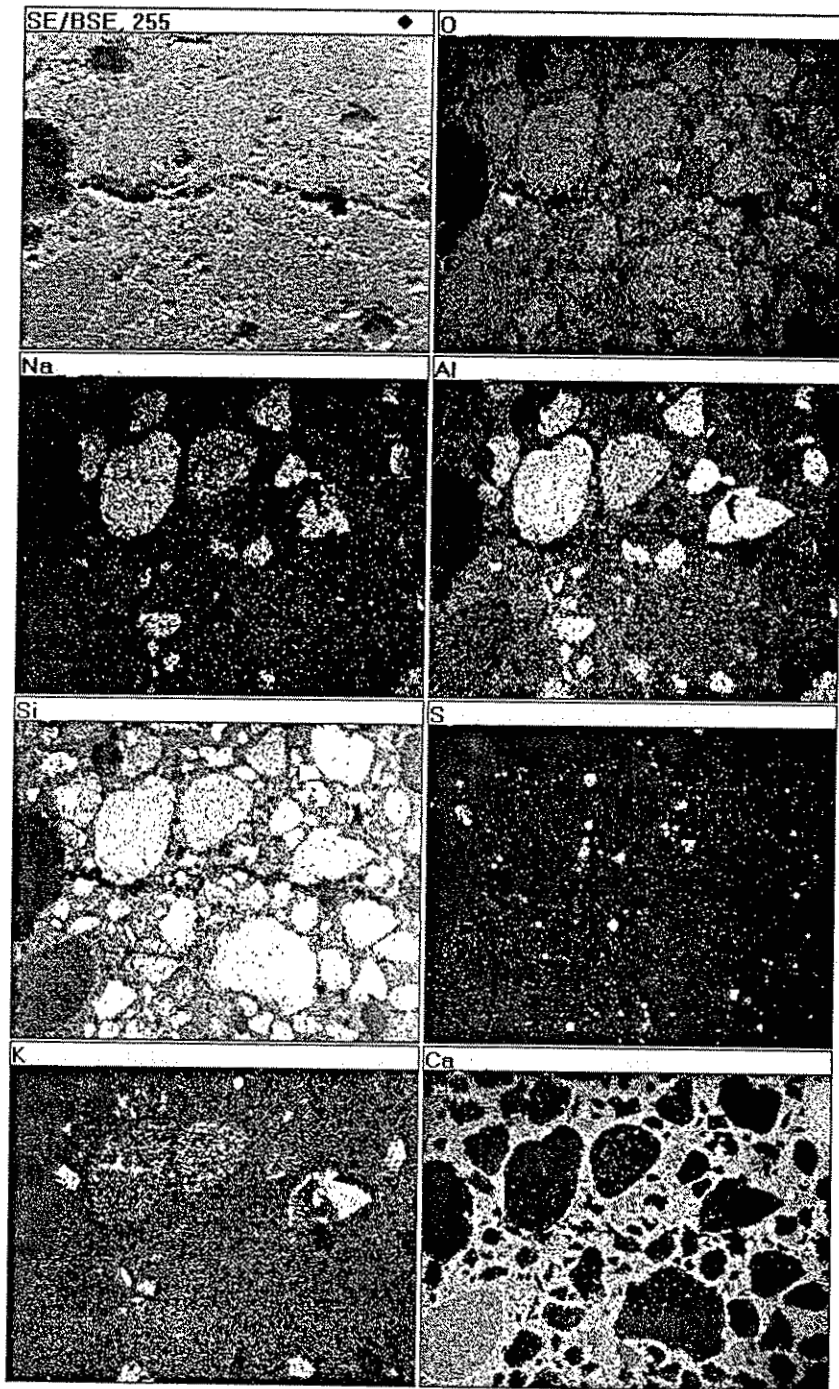


Figure 57. X-ray map from IA 25, core 45B; 20X magnification.

SUMMARY AND CONCLUSIONS

In summary, a detailed investigation has been conducted on core specimens from nine different concrete pavements located in Iowa. The investigation used scanning electron microscopy, coupled with energy dispersive X-ray analysis, to document the deterioration processes that were observed in the cores. Visual inspection and light microscopy techniques were also used to study the cores. Selected fractions of some cores were also subjected to thermal analysis (differential scanning calorimetry) and X-ray diffraction analysis to help identify the constituents that were present.

The results of the study indicated that there were typically two or more deterioration processes acting simultaneously in many of the core specimens. Hence, one must use judgment to ascertain which process initiated the deterioration and which process contributed most to the observed degradation. There is no sound reason to assume that a single process accounts for both of these observations. This is very difficult because petrographic techniques still lack much of the quantitative methods that are needed to sort out the relative significance of multiple distress features. Hence, one must rely on opinion to diagnose the situation and that is what the reader will be exposed to in the remainder of this report. The facts (observations) that allowed the formulation of the opinion will be interspersed as needed; however, much of the information was presented earlier in this report.

1. Freeze-thaw damage appears to be the most probable explanation for the deterioration observed in cores from US 20 in Webster County. This deterioration was only observed in concrete cores taken from pavement sections using mix formulations denoted as Mix#1 and Mix#3 (see Tables 4 through 6 for details). Cores from sections denoted as Mix#2 exhibited little distress, they also exhibited much more coherent paste fractions than did the other two mixes. The void system of the deteriorated concrete often appeared to be odd. Entrained-air voids, especially voids smaller than 100 μm in diameter, were often filled with a sulfate bearing mineral that had a chemical composition close to ettringite. The concrete also tended to

contain a large proportion of entrapped air voids. Alkali-silica reaction was observed in all of the core specimens from US 20. This was almost entirely related to the presence of shale particles in the fine aggregate (only one other reactive fine aggregate particle (nonshale) was observed in the 14 cores that were studied, this particular particle was a site of alkali-silica gel expansion and subsequent paste cracking). The shale content of the cores was less than 2% in all of the specimens that were measured. The coarse aggregate was sound in all of the core samples. Very little alkali-silica gel was observed in any of the cores. The macroscopic cracking patterns observed in the cores tended to follow the periphery of aggregate particles and rarely intersected the shale particles. Hence, alkali-silica reaction appeared to play a minor part in the deterioration. Some of the microcracking in the paste, coupled with the observation of filled air voids and general paste expansion, suggested the presence of an additional deterioration mechanism; however, this research has not explicitly defined such a mechanism.

2. Freeze-thaw damage appears to be the most probable explanation for the deterioration observed in cores from I-35 in Story County. This deterioration was most severe in cores taken from near the pavement joints and near a crack in a vibrator trail. The paste portion of the deteriorated concrete often appeared to be odd. Entrained-air voids, especially voids smaller than 100 μm in diameter, were often filled with a sulfate bearing mineral that had a chemical composition similar to ettringite. The concrete also tended to contain a large proportion of entrapped air voids. Some paste regions exhibited extensive microcracking plus sulfate-filled gaps around fine aggregate particles. It is currently unclear if these observations indicate that the freeze-thaw deterioration caused the paste expansion, which then allowed the transport of sulfates to the site, or if the sulfates initiated the paste expansion which caused cracking and subsequent critical saturation of the pavement. Alkali-silica reaction was observed in all of the core specimens from I-35. This was due to the presence of shale particles in the fine aggregate. The maximum shale content observed in the cores was 2.1%. The coarse aggregate was sound in all of the core samples. Very little alkali-silica gel was observed in any of the cores. The macroscopic cracking patterns observed in the cores tended to follow the periphery of aggregate particles and rarely intersected aggregate particles. Hence, alkali-silica reaction appeared to play a minor part in the deterioration.
3. The concrete specimens taken from I-80 exhibited only minor deterioration. Few macrocracks were observed during inspection, most of which appeared to be related to the presence of vibrator trails (or segregation) in the concrete. Alkali-silica reaction was observed in all of the core specimens from I-80. This was due to the presence of shale particles in the fine

aggregate. The maximum shale content observed in the cores was 1.4%. The coarse aggregate was sound in all of the core samples. Microcracking was common in the cores taken from areas with vibrator trails. Some cracks appeared to be related to the cracked shale particles while other cracks tended to follow the periphery of the aggregate particles. Sulfate-filled air voids were also observed in these specimens; however, they were considerably less prevalent than in other pavements (i.e., US 20 or I-35). Many features were observed that suggested poor mixing or plastic concrete problems. Hence, it is difficult to pinpoint which of these factors has played a major role in the minor amount of deterioration that was observed.

4. Only one of the cores from the Bettendorf fast-track project in Scott County, exhibited macrocracks (core 27). Three of the cores (26, 27 and 28) exhibited moderate to extensive microcracking. Some of the microcracks were filled with ettringite and sometimes ettringite-filled gaps were observed between aggregates and the cement paste. The cement paste appeared to be highly distorted and air voids as large as 200 μm were totally filled with ettringite. Alkali-silica gel was also observed in three of the cores (25, 27 and 28). The reactive aggregate appeared to be some shale particles in core 25. The reactive aggregate appeared to be chert particles in cores 27 and 28. Some distress was related to the presence of alkali-silica reaction. However, the microcracks related to reactive aggregates tended to stop after a few hundred microns while the ettringite filled microcracks extended millimeters through the cement paste. This suggests that the cracking induced by alkali-silica reaction did not play a major role in the distress. However, in this particular case one may legitimately argue that any one of three different mechanisms may have started the cracking (freeze and thaw, alkali-silica reaction or sulfate expansion).
5. The cores from IA 175 exhibited virtually no distress (no macrocracking). Alkali-silica reaction was noted in three of the cores. This was due to the presence of shale particles in the fine aggregate. The distress adjacent to the shale particles was similar to that which was observed in the other cores studied in this project. The void system looked excellent, air content and distribution looked good, and few voids were filled with ettringite. Microcracks tended to be very fine and typically propagated randomly through the cement paste.
6. The cores from US 169 were all severely macrocracked. The macrocracks tended to connect coarse aggregate particles. The cracks were not filled in nearly all instances. No alkali-silica gel was observed in any of the samples. Hence, this suggests that the most probable cause for the deterioration was freeze-thaw damage in a frost-sensitive coarse aggregate (classic d-cracking). Many of the air voids appeared to be filled with sulfate minerals;

however, the use sawn specimens, rather than ground and polished specimens, restricted the observation of microcracking in the various specimens.

7. The cores from IA 25 were all severely macrocracked. The macrocracks tended to connect coarse aggregate particles. No alkali-silica gel was observed in the samples. Hence, the most probable cause for the deterioration appears to be freeze-thaw damage in a frost-sensitive coarse aggregate (classic d-cracking). Many of the small air voids present in the specimen appeared to be filled with sulfate minerals; however, the use sawn specimens, rather than ground and polished specimens, restricted the observation of microcracking in the various specimens.
8. The core from the fast-track project in Benton County (CMI-11) exhibited virtually no distress (no macrocracking). The void system looked marginal to adequate; however, the small entrained-air voids were filled with ettringite. Microcracks tended to be fine and typically propagated randomly through the cement paste, sometimes connecting adjacent air voids.
9. The cores from County Road B in Hancock County, exhibited virtually no distress (no macrocracking). Alkali-silica reaction was noted in the core. This was mostly due to the presence of shale particles in the fine aggregate; however, some other fine aggregate particles had cracked. The distress adjacent to the shale particles was similar to that which was observed in the other cores studied in this project. The void system looked good, air content looked high but distribution looked good, and few voids were filled with ettringite. Microcracks tended to be very fine and typically propagated randomly through the cement paste.
10. Little evidence was found of deicer (road salt) induced distress in any of the cores specimens. X-ray analysis rarely indicated the presence of significant amounts of chlorine in the specimens. However, it must also be stressed that this study concentrated on specimens that were taken about one-inch, or lower, below the top surface of the pavement cores; and hence, additional work is needed to totally validate this claim.
11. Construction practices (i.e., mixing, placement and curing techniques) and the associated quality of concrete that was produced, appeared to vary significantly throughout the cores investigated in this study. Cores from US 20, I-35, I-80, and the Bettendorf fast-track project, tended to contain many artifacts (e.g., segregation or vibrator trails, clusters of air voids, clusters of fly ash and a large fraction of entrapped-air voids), that suggest that things simply did not go well in the field during construction. It is currently difficult to ascertain how large of an influence this had on the deterioration processes

that were noted in the various pavements. However, in most instances, one would expect that these construction related problems would accelerate the onset of any given deterioration mechanism.

12. Many of the concrete specimens that were studied for this project contained a considerable amount of small air voids ($<150\mu\text{m}$) that were filled with a sulfate mineral that had a chemical composition close to ettringite. Hence, accurate air-void content determinations would not be obtained with the epoxy impregnation technique that is commonly used to increase the contrast between the air voids and the cement paste. Note, that this same bias would apply to any of the common automated image analysis techniques that use air-void filling, via a powder or fluid, for contrast enhancement. An accurate air-void determination should either account for these voids by some type of direct measurement (i.e., a staining technique for light microscopy or elemental mapping for scanning electron microscopy), or the voids should be cleaned prior to analysis. Our research has indicated that it is often difficult to differentiate between filled air voids and bulk cement paste as the size of the features decrease, this was especially true for light microscopy using polished sections (however, scanning electron microscopy suffered similar limitations). Without these refinements the specimens will simply produce test results that indicate low air contents; however, one will not be able to ascertain from such an analysis if the air content is really low or if the voids have simply been filled.

RECOMMENDATIONS

Field Concrete

It is strongly recommended that every effort should be made to ensure the proper mixing and placement of the concrete used for the construction of pavement slabs. Some of the deterioration processes that were noted in the concrete core specimens, could be interpreted as having been significantly influenced by the mixing, placement and finishing procedures employed during construction. This research project has documented instances of segregation (probable cause: excessive vibration), clumping of air voids (probable causes: poor mixing, retempering or admixture incompatibility), and clumping of fly ash (probable cause: poor mixing). All efforts must be directed at ensuring that a homogeneous, workable concrete mixture reaches the paver.

Much of the distortion that was observed in the concrete cores appeared to be related to the void distribution that was created during the paving

process. Hence, it is strongly recommended that efforts should be made to obtain estimates of the hardened air content and the distribution of entrained-air voids present in concrete pavements. Refinement of the procedures developed for this research project should produce rapid measurements that could be used to provide feedback to contractors. This would provide an additional mechanism for improving the quality of field concrete.

Finally, it is recommended that the protocol described in reference 8 should be followed when sampling concrete for routine analysis. The procedures and technical details pertinent to the selection and description of test specimens have been outlined in detail, and they should provide a high level of assurance that the core samples represent the concrete in question.

Concrete Materials

Distress was noted in some of the materials that were present in the cores studied for this project. However, the distress was not convincing enough to abandon the information that is currently contained in existing service record files. Service record is still the most reliable estimate of durability. However, one must temper the service record information (which was generated over the course of tens of years) with the following facts: (1) cement production techniques have changed significantly in the past two decades; (2) incorporation of chemical admixtures and fly ash into concrete pavements has become routine; and (3) deicer salts are liberally applied to pavements during inclement weather. These facts indicate a need for laboratory testing (to verify performance, compatibility, etc.); however, it is very difficult to find quick laboratory tests that yield accurate information about field performance. This was case for many of the pavements that were included in this study, all of the materials independently passed the designated specifications but yet the concrete deteriorated prematurely. Why? For the simple reason that the laboratory experiments never simulated the field concrete. This is another good reason to spend more time inspecting and evaluating the properties of specimens obtained from real (field) concrete pavements.

Extensive laboratory testing has been conducted during the last 15 years concerning the use of Class C fly ashes in concrete products. We have studied how these fly ashes influence air void properties, strength, freeze-thaw durability, sulfate resistance and alkali-silicate reactivity; and each study has generally indicated that these fly ashes can play a beneficial role in concrete that is

properly proportioned with portland cements commonly available in Iowa. Yet the reader should note that many of the pavements that exhibit premature distress also contain fly ash. It is not known if this is due to the fact that we now mandate the use of fly ash in pavement projects (and hence, all good and bad pavements contain fly ash - so why don't they all fail?) or if some other unforeseen (or unmeasured) factor is contributing to the deterioration. Hence, it is recommended that a serious attempt should be made to correlate field performance with laboratory performance. The study should contain detailed petrographic examinations because the results of this research (HR-358) have indicated gross differences between concrete specimens prepared in a laboratory and those cored from concrete pavements.

Also, some of the field related problems were probably caused (or at least exacerbated) by materials problems involving poor workability or premature stiffening (false set). Our experience has indicated that these problems can typically be attributed to an improper gypsum content in the cement (note that the total sulfur trioxide content of the cement can be within specification limits but the partitioning of sulfur among several different compounds may cause problems). It is important to mention that Class C fly ashes can also have a detrimental influence on these types of plastic concrete problems; however, cements typically have a much greater influence than fly ashes. Hence, it is recommended that efforts be made to provide routine quantification of the amount of gypsum (and other sulfate bearing phases for that matter) present in cements. Differential scanning calorimetry and X-ray diffraction would be suitable for performing these types of analysis. Both types of equipment could provide rapid information (less than one hour for analysis) that could help identify problematic cements.

Additional Research

This research project was of a preliminary nature; and hence, it has posed many questions that need further research. For the purpose of brevity they will simply be listed.

- Refinement of the procedures described in this report to provide quantitative information pertaining to void content and distribution plus information pertaining to the quantity and orientation of cracks in concrete.

- Quantification and categorization of the different ASR gels that have been observed over the course of this study. This may lead to a better understanding of the swelling potentials of different gels and how they relate to the deterioration observed in field concrete specimens.
- Quantification of the amount of ettringite filled voids in concrete and how this influences the rate at which concrete becomes critical saturated with water. Does this play a major role in the freeze-thaw resistance of the concrete?
- Do soluble alkalis (particularly sodium and potassium sulfates and chlorides) influence the movement of ettringite through the pore solution of concrete to the entrained-air voids?
- Influence of the soluble aluminum and sulfates in Class C fly ashes on the presence of ettringite in the entrained-air voids of concrete. How much of a role does the glass phase of the fly ash play in the amount of soluble aluminum that is liberated?

CLOSING COMMENTS

One feature that was common in many of the concrete cores exhibiting distress was the presence of sulfate minerals in the entrained-air voids. The chemical composition of the material in the air voids was often quite close to that which is characteristic of ettringite and the material typically exhibited a fibrous morphology. Experts indicated that such an observation was not uncommon and most petrographic examination guides also suggested that such observations should be documented because they may be important to understanding the deterioration mechanism. So we documented our observations. However, such documentation was not considered a relevant explanation for deterioration by some experts, while others failed to observe such features in companion cores. Hence, our early observations were ignored.

The amount of void filling that was observed varied considerably from sample to sample. Some of the samples had few air voids that were completely filled (e.g. highway 175), while others had nearly all air voids smaller than 100 microns completely filled. In extreme cases air voids as large as 250 microns had been completely filled. Hence, in some samples, void filling occurred on both a macroscopic and a microscopic level. Occasionally, sulfates were also

found around the periphery of some aggregate particles. Alkali-silica reaction cannot cause features of this type. Instead, these types of features are normally attributed to a cement paste matrix that has expanded (possibly due to frost damage or sulfate related reactions). Such features may also be attributed to poor consolidation during field construction.

Many of the cracks that were observed in the concrete core specimens appeared to be open (i.e., no apparent material filling the cracks). This was true regardless of the sample preparation method that was employed prior to observation. Often, the general cracking pattern tended to go around the aggregate particles and through the cement paste and air voids. Little aggregate related cracking was apparent, except for the notorious shale particles (cracked shale particles, in close proximity with small amounts of ASR gel, were observed in nearly all of the pavement cores in this study, even the pavements which exhibited no deterioration).

Sometimes the cracking pattern around air voids suggested that expansion had taken place within the air void. These voids were typically filled with ettringite, as was noted by Marks and Dubberke [3]. Such features suggest that secondary ettringite formation contributed to the microcracking. However, an alternative interpretation of the feature can be formulated. Such an interpretation would maintain that the void had become filled with water and then subjected to freezing and thawing. Hence, the cracks were generated by the expansion of water and then the ettringite precipitated in the void. This alternative interpretation fails to account for the fact that the microcracks often remain empty while only the air void has been filled with ettringite, such preferential filling seems odd under such circumstances.

It is sad to say that this research project has shed little light on the potential for secondary ettringite formation in concrete pavements. However, the observations still stand, the voids are still filled, and it appears that the general consensus about what this observation means may have changed during the course of this research project. More investigators appear to be observing similar features. A direct link to premature deterioration is still not evident but at least questions are being raised.

New and more powerful equipment, such as that used in this study, was not needed to make these observations. The new equipment did make the observations easier to obtain, more fun to recheck, and simpler to document. However, careful observations using light microscopy, coupled with some

detailed chemical analysis of the material filling the voids, would have yielded very similar results. The best way to express my optimism about what modern analytical techniques can do for the study of concrete is to quote Katharine Mather [11, see 169-A]; however, it is extremely troubling to note that the use of these techniques have not migrated from concrete science to concrete practice after thirty years. Why?

"The measure of progress and the results of the use of newer techniques including X-ray diffraction, differential thermal analysis, electron microscopy and electron diffraction are that the questions listed above, and others, are obvious to me in 1965, although I could not have formulated them in 1955."

ACKNOWLEDGMENTS

We would like to thank all of the people who helped to contribute to this project. A special thanks to Iowa DOT personnel who spent many days coring concrete pavements to produce the samples that were analyzed in this project. Also, a special thanks to all the MARL staff and students who contributed time and effort to this project.

REFERENCES

1. Deicer Distress, by S. Wolter, T.E. Swor, R.D. Stehly and M. Lukkarila; personal communication by R.D. Stehly, 1991.
2. Investigation of Pavement Cracking in US 20 and I 35, Central Iowa, by D. Stark, Construction Technology Laboratory, September, 1992.
3. V. Marks and W. Dubberke, Investigation of PCC Pavement Deterioration, Interim Report for Iowa DOT Research Project HR-2074 January, 1995.

4. Skalny, J.P., Evaluation of Concrete Cores, State of Wisconsin, Dept. of Transportation, Prepared for the Portland Cement Association, November 15, 1994. (RJ Lee Group, Inc. was a subcontractor).
5. Schlorholtz, S. and J. Amenson, Evaluation of Microcracking and Chemical Deterioration in Concrete Pavements, Phase II Report, HR-358, ISU-ERI-Ames-95-411, February, 1995
6. Schlorholtz, S. and K. Bergeson, Evaluation of the Chemical Durability of Iowa Fly Ash Concretes, Final Report, HR-327, ISU-ERI-AMES-93-411 March, 1993.
7. American Society for Testing and Materials, Annual Book of ASTM Standards, Vol. 4.02, ASTM:Philadelphia, 1994. See C 33 and also C 294, C 295 and C 856.
8. British Cement Association, The Diagnosis of Alkali-Silica Reaction, Second Edition, Wexham Springs, Slough, 1992.
9. Day, R.L., The Effect of Secondary Ettringite Formation on the Durability of Concrete: A Literature Analysis, Portland Cement Association Research and Development Bulletin RD108T, PCA, 1992.
10. Johansen, V., Thaulow, N., and Skalny, J., "Simultaneous presence of alkali-silica gel and ettringite in concrete," Advances in Cement Research, Vol. 5, No. 17, 1993, pp. 23-18.
11. Mather, K., Petrographic Examination, in ASTM STP 169, 1956, pp. 68-80. (see also later versions of the article in STP 169A and C).
12. Erlin, B. The Magic of Investigative Petrography: The Practical Basis for Resolving Concrete Problems, in ASTM STP 1061, 1990, pp. 171-181.
13. Mielenz, R. C., Petrography Applied to Portland Cement Concrete, in Reviews in Engineering Geology, Vol. 1, Geological Society of America, 1962, pp. 1-38.

14. Struble, L. and P. Stutzman, "Epoxy Impregnation of Hardened Cement for Microstructural Characterization", *Journal of Materials Science Letters*, Vol. 8, ,1989 pp. 632-634.
15. Stutzman, P. and J. R. Clifton, Microstructural Features of Some Low Water/Solids, Silica Fume Mortars Cured at Different Temperatures, NISTIR 4790, National Institute for Standards and Technology, Gaithersburg, MD, April 1992.
16. Diamond, S., S. Mindess, A. Bentur and J. Lovell, Development and Applications of Devices to Study Cracking Within the SEM, in Proceedings of the Sixth International Conference on Cement Microscopy, Held March 26-29 in Albuquerque, New Mexico, 1984, pp.438-452.
17. Kofoed, D.E., CMI Report 793-587, submitted to Mr. Gordon Smith of the Iowa Concrete Paving Association, September 27, 1993.
18. Jones, K., Evaluation of Deterioration on U.S. 20 in Webster County, Final Report for MLR-91-1, Iowa Department of Transportation, January, 1991.

APPENDIX A (SUMMARY OF CORE LOGS)



358 Concrete Cores 1994

SAMPLE IDENTIFICATION: # 1, STORY. I35, STA 5462+36, NB LANE

GENERAL SAMPLE OBSERVATIONS:

Sample Dimensions: 10.1 CM DIAMETER, 25cm LENGTH

FULL SLAB THICKNESS

Surface condition:

Top- TRES. 2mm MAX DEPTH, 5mm MAX WIDTH

Bottom- CAST ON COMPACTED SAND

SPACED @ 1 TO 2 CM INTERVALS

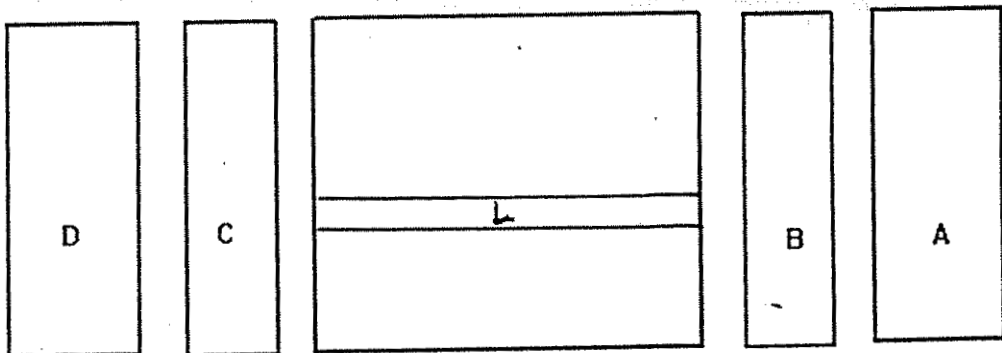
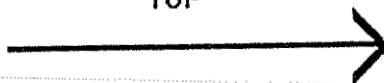
Reinforcement: NONE PRESENT

Cracks and Other

Distinctive Features: NO VISIBLE CRACKING

LIMESTONE AGGREGATE

TOP



OK

HR - 358 Concrete Cores 1994

SAMPLE IDENTIFICATION: #2, STORY, I-35, STA. 5462+37 NB LANE

GENERAL SAMPLE OBSERVATIONS:

Sample Dimensions: 10.1 CM DIAMETER, APPROX 25 CM LENGTH, FULL SLAB THICKNESS.

Surface condition:

Top- TINES, 2MM MAX DEPTH, 5MM MAX WIDTH, @ INTERVALS OF .15 TO 2 CM

Bottom- CAST ON GRAVEL, UN EVEN SURFACE: VARIES BY APPROX. 1.5 CM IN PLACES

Reinforcement: NONE PRESENT

Cracks and Other

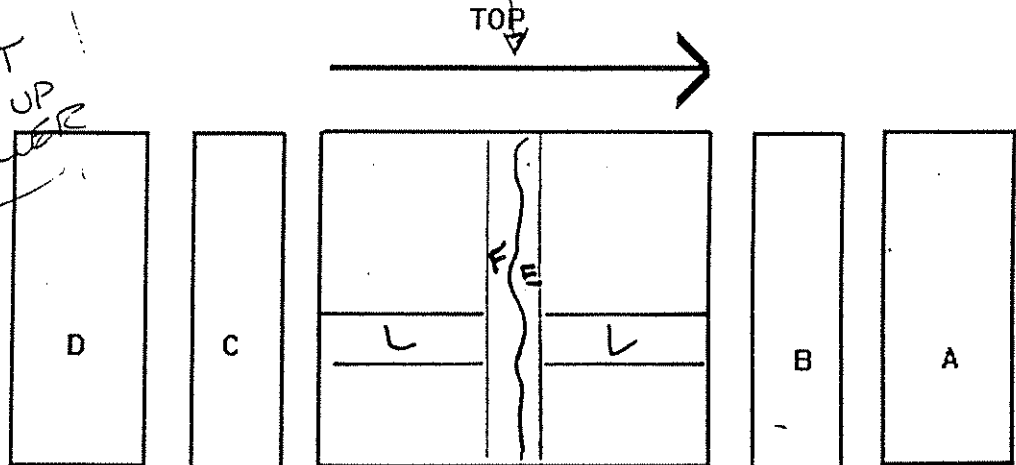
Distinctive Features: BROKEN COMPLETELY @ 11 CM

FROM TOP. ALSO, MAJOR CRACKS @ 14 CM AND 24 CM FROM TOP.

- BESIDES NORMAL SAMPLE CUTS,

TOOK A SAMPLE ABOVE AND BELOW THE MAJOR BREAKS. SOME SHALE.

SAW PAINT SHOWING UP IN SMALLER VOIDS



OK

HR - 358 Concrete Cores 1994

SAMPLE IDENTIFICATION: #3, STORY, I-35, STA 5462+46, NB LANE

GENERAL SAMPLE OBSERVATIONS:

Sample Dimensions:

DIAMETER 10.1 CM, LENGTH 25 CM

FULL SLAB THICKNESS

Surface condition:

Top- TINES, 3mm MAX DEPTH, 5mm MAX LENGTH

1 to 1.5 INTERVALS

Bottom- CAST ON GRAVEL

Reinforcement:

NONE PRESENT

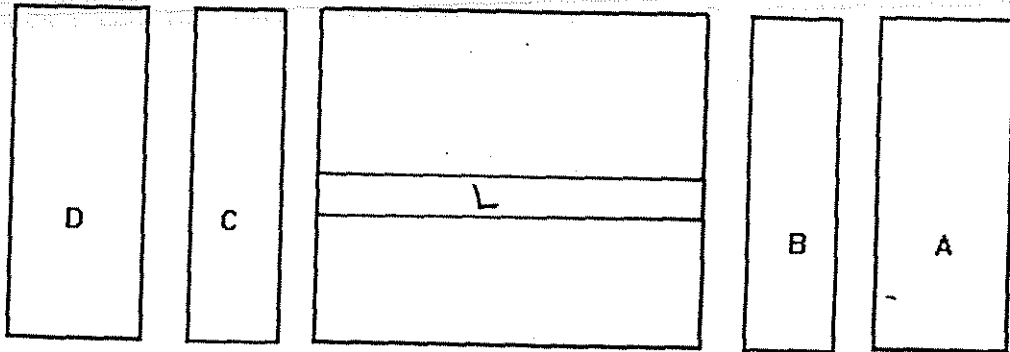
Cracks and Other

Distinctive Features:

NUMEROUS VOIDS APPROX

1 CM DIAMETER, SOME SHALE.

TOP



OK

HR - 358 Concrete Cores 1994

SAMPLE IDENTIFICATION: #4, STORY, STA 5462+47, NB LANE

GENERAL SAMPLE OBSERVATIONS:

Sample Dimensions: 10.1 cm DIAMETER, 25.5 cm LENGTH

FULL SLAB THICKNESS

Surface condition:

Top- TINES, MAX DEPTH 4mm, MAX WIDTH 5mm,

@ 1.5 to 2 cm INTERVALS

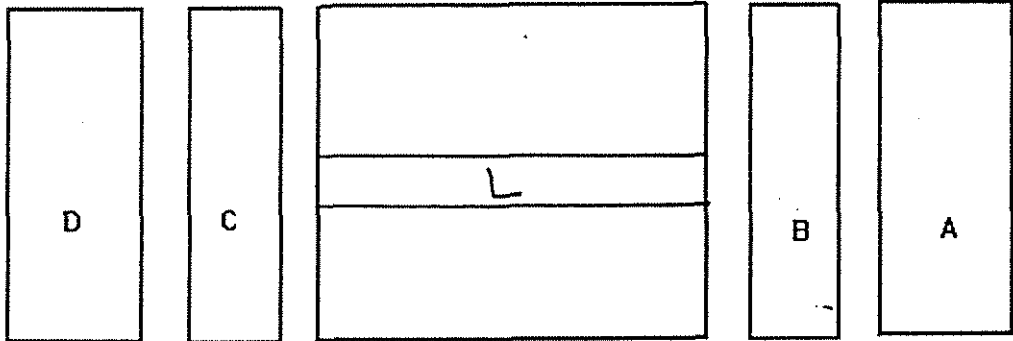
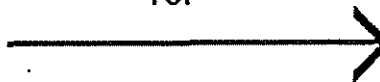
Bottom- CAST ON GRAVEL SUB GRADE

Reinforcement: NONE PRESENT

Cracks and Other Distinctive Features: NUMEROUS HOLES UP TO 1cm

DIAMETER, SHALE INCLUSIONS

TOP



OK

HR - 358 Concrete Cores 1994

SAMPLE IDENTIFICATION: #5, STORY, J-35, STA 15471+90 NB LANE

GENERAL SAMPLE OBSERVATIONS:

Sample Dimensions: 10.1 cm DIAMETER, 25 cm LENGTH

FULL SLAB THICKNESS

Surface condition:

Top- FINES, MAX DEPTH 1mm MAX WIDTH 5mm

@ 1.5 TO 2 cm INTERVALS

Bottom- CAST ON GRAVEL SUBGRADE

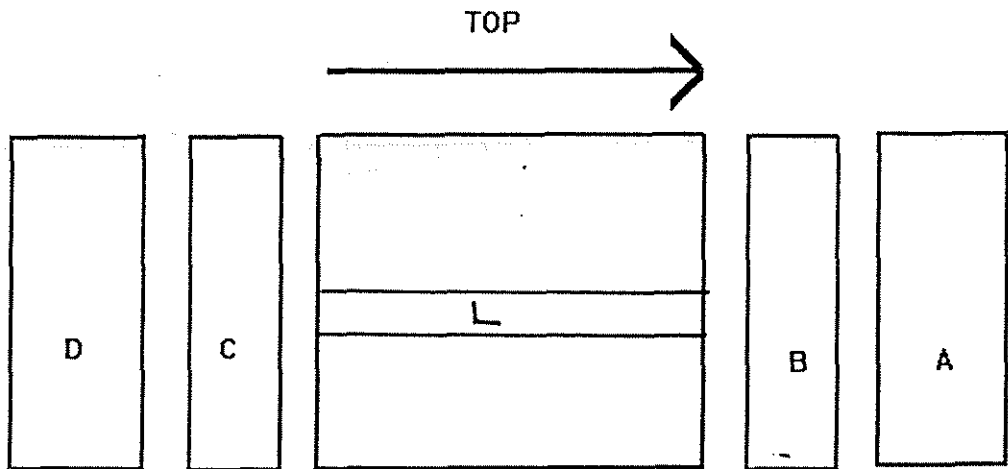
Reinforcement: NONE PRESENT

Cracks and Other Distinctive Features:

NO VISIBLE CRACKING

LARGE VOIDS UP TO 1.5cm ACROSS

SOME SMALL INCLUSIONS



OK

HR - 358 Concrete Cores 1994

SAMPLE IDENTIFICATION: # 6, STORY, 1-35, STA 5471+94, NBLANE

GENERAL SAMPLE OBSERVATIONS:

Sample Dimensions: 10.1cm DIAMETER, 25cm LENGTH

FULL SLAB THICKNESS

Surface condition:

Top- TINES. MAX DEPTH 1mm, MAX WIDTH 5mm

@ INTERFACES OF 17cm TO 2cm

Bottom- CAST ON GRAVEL SUB GRADE

Reinforcement:

NONE PRESENT

Cracks and Other
Distinctive Features:

NO VISIBLE CRACKING, MANY

LARGE AIR VOIDS UP TO 1.5cm ACROSS,

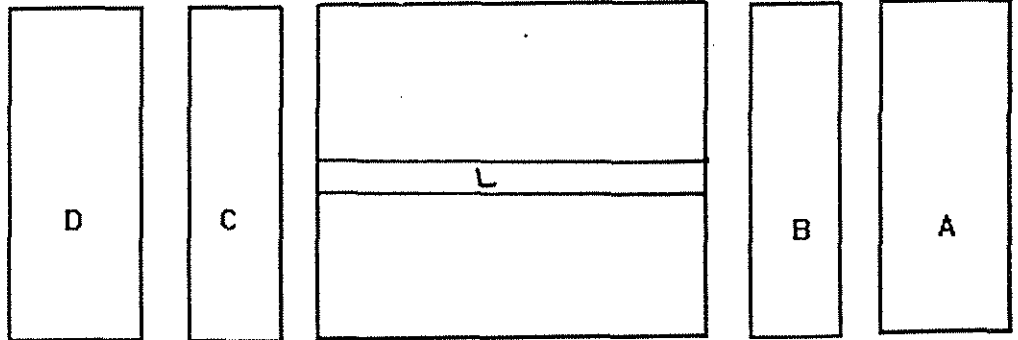
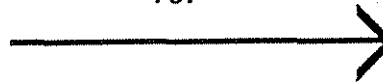
SHALE INCLUSIONS,

* THESE SAMPLES MAY HAVE BEEN

CONTAMINATED W/ SULFUR FROM EXPERIM

TOP

CUT.



OK

HR - 358 Concrete Cores 1994

SAMPLE IDENTIFICATION: #7, STORY, I-35, STA 5471+97, NBLANE

GENERAL SAMPLE OBSERVATIONS:

Sample Dimensions: 10.1 CM DIAMETER, 25 CM LENGTH

FULL SLAB THICKNESS

Surface condition:

Top- TINES, MAX DEPTH 2MM, MAX WIDTH 5MM,

@ 1.2 TO 2 CM INTERVALS

Bottom- CAST ON GRAVEL SUBGRADE

Reinforcement:

NONE PRESENT

Cracks and Other Distinctive Features:

CRACKED THE ENTIRE THICKNESS

OF SLAB. APPEARS TO BE WIDEST @ BASE,

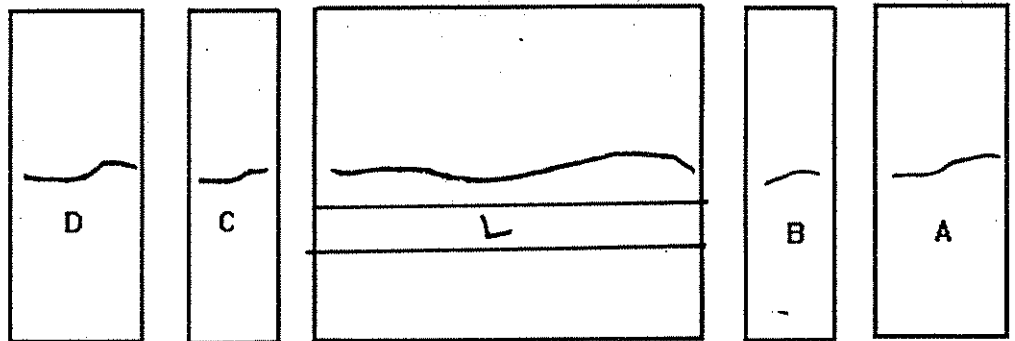
APPROXIMATELY 0.5 MM WIDTH. SMALL SECONDARY

CRACK 6 CM FROM BASE EXTENDING 4 CM UP @

30° FROM VERTICAL. AIR VOIDS UP TO 2 CM ACROSS,

SHALE INCLUSIONS

TOP



OK

HR - 358 Concrete Cores 1994.

SAMPLE IDENTIFICATION: # 2, STORY, I-35, STA 5472+01, NB LANE

GENERAL SAMPLE OBSERVATIONS:

Sample Dimensions: 10.1 CM DIAMETER, 25.3 CM LENGTH

FULL SLAB THICKNESS

Surface condition:

Top- TINES MAX DEPTH 2MM, MAX WIDTH 4mm

1.5 CM INTERVALS

Bottom- CAST ON GRAVEL SUBGRADE

Reinforcement:

NONE PRESENT

Cracks and Other
Distinctive Features:

CRACKED VERTICALLY FROM

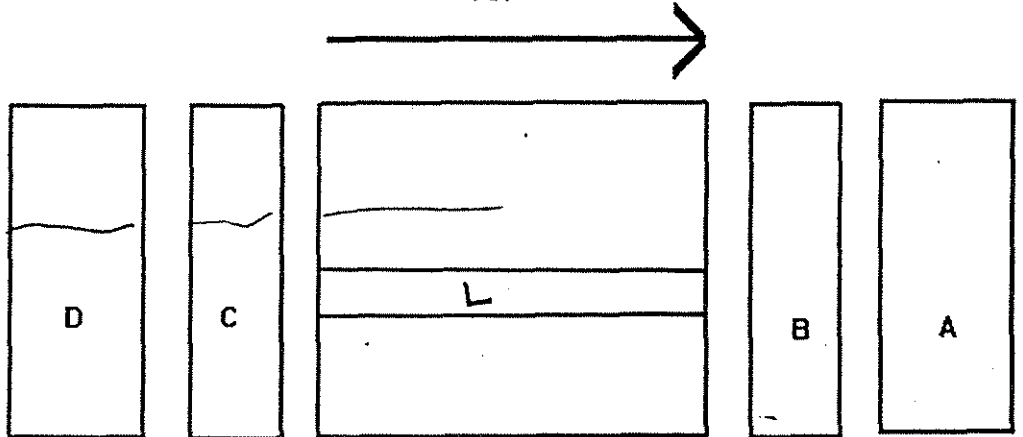
BASE, EXTENDS 10 CM ON ONE SIDE AND

14 CM ON OTHER. OCCURS ± 1 CM FROM BISECTING

SAMPLE. SOME SPACE PRESENT, MOSTLY

CALCIUM CARBONATE AGGREGATES

TOP



OK

HR - 358 Concrete Cores 1994

SAMPLE IDENTIFICATION: #9, WEBSTER, U.S. 520, STA 2004, EB LANE

GENERAL SAMPLE OBSERVATIONS:

Sample Dimensions: 10.1 cm. diameter ; 23 cm. length

Full slab thickness

Surface condition:

Top-

Tines 4mm Max width, 3 mm max depth

located 1 to 2 cm apart.

Bottom-

Cast on non-soil material

Reinforcement:

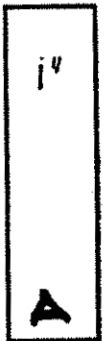
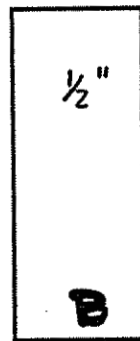
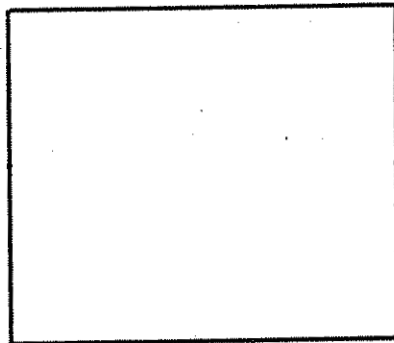
None present

Cracks and Other Distinctive Features:

No large cracks visible,

large voids noted

TOP →



OK

HR - 358 Concrete Cores 1994

SAMPLE IDENTIFICATION: #10 WEBSTER, US 520, STA 2004, EB LANE

GENERAL SAMPLE OBSERVATIONS:

Sample Dimensions: 10.1 cm diameter; 23 cm length; FULL SLAB thickness

Surface condition:

Top- Tines, 3.5 mm MAX depth, 4 mm MAX width located 1 to 2 cm apart

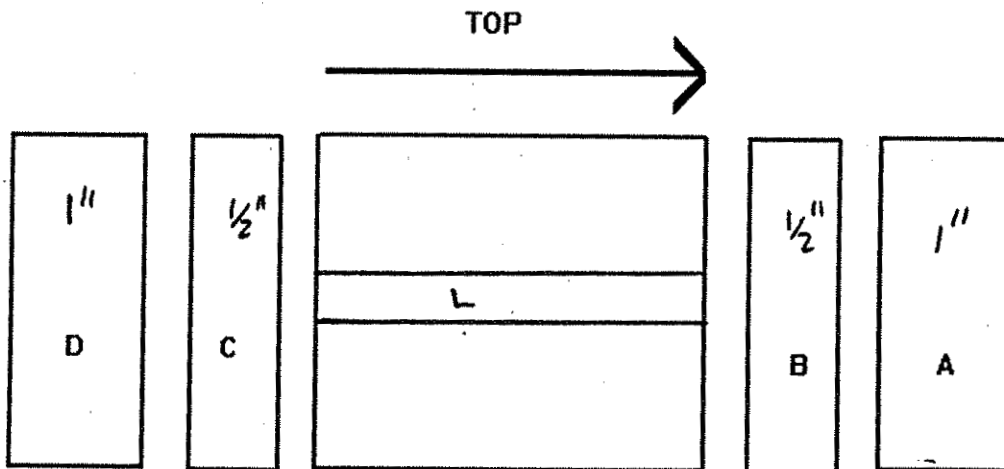
Bottom- Cast on non-soil material

Reinforcement: Present, approx 9-9.5 cm from bottom

Cracks and Other Distinctive Features:

No large cracks visible, large void spaces noted.

CUT LONGITUDINAL SECTION L. MARCH 95.



IR - 558 Concrete Cores 1994

SAMPLE IDENTIFICATION: #11 WEBSTER, U.S. 520, STA 2004, EB LANE

GENERAL SAMPLE OBSERVATIONS:

Sample Dimensions: 10.1 cm diameter, 23.5 cm length
Full slab thickness

Surface condition:

Top- Tines, max depth 3mm max. width

6mm SPACING 2 TO 1 CM APART

Bottom- CAST ON NON-SOIL MATERIAL, APPEARED

to be an impression from reinforcement bar on bottom.

Reinforcement:

Present approx 9 cm from bottom

Cracks and Other

Distinctive Features:

LARGE (UP TO 2.5cm) VOIDS NOTED,

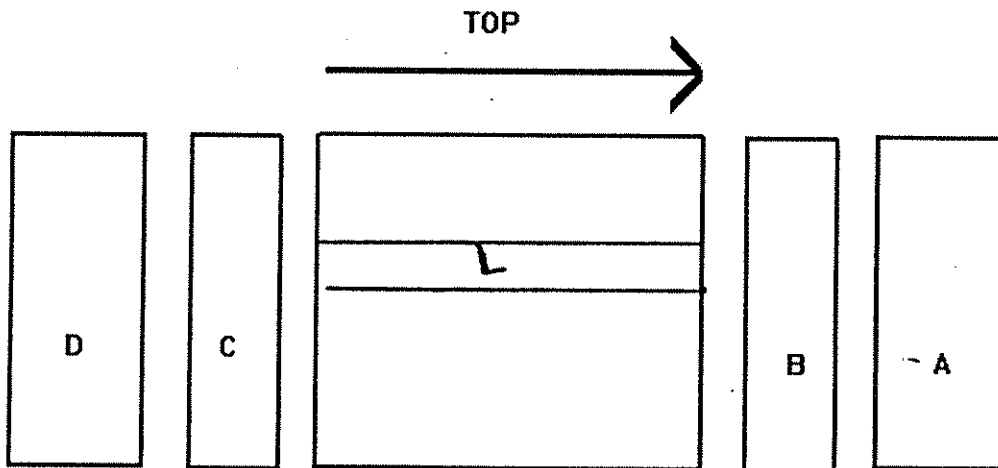
NO LARGE CRACKS, SMALL CRACKS NOTED ON

BOTTOM SURFACE EXTENDING ALONG SIDES OF SECTION D.

MOST OF AGGREGATE CALCIUM CARB. SOME SHALE

INCLUSIONS.

CUT LONGITUDINAL SECTION MARCH 1995



HR - 358 Concrete Cores 1994

SAMPLE IDENTIFICATION: #12, WEBSTER, U.S. 520, STA 2004, EB LANE

GENERAL SAMPLE OBSERVATIONS:

Sample Dimensions: 10.1 cm diameter, 23 cm length
Full slab thickness

Surface condition: Top- Tines, Max depth 6 cm (disappears in some spots)

Max width 5 cm spaced at 1 to 2 cm intervals

Bottom- Cast on non-soil material

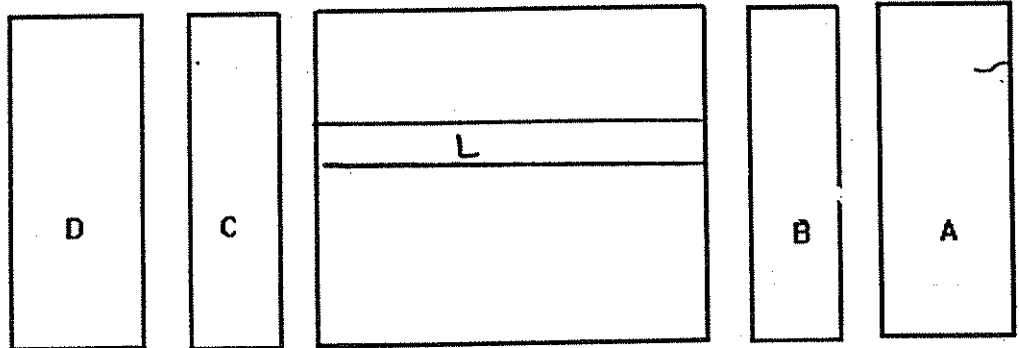
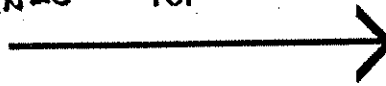
Reinforcement: None Present

Cracks and Other Distinctive Features: Crack ^(< 1 mm width) across the length of the top surface extending 2.0 cm under surface

Crack is running PERPENDICULAR TO TINES.

MOST OF AGGREGATE CALCIUM CARBONATE w/ small amount of shale present. Voids up to 1 cm diameter.

CUT LONGITUDINAL SECTION TOP MARCH 1995.



HR - 358 Concrete Cores 1994

SAMPLE IDENTIFICATION: # 13, WEBSTER, U.S. 520, STA 2020, WB LANE

GENERAL SAMPLE OBSERVATIONS:

Sample Dimensions: 10.1cm, diameter; 23.5cm length

FULL SLAB THICKNESS

Surface condition:

Top-

TYES, MAX DEPTH 4MM, MAX WIDTH 5MM

SPACES @ 1 TO 2 CM INTERVALS

Bottom-

CAST ON SAND SUBGRADE

Reinforcement:

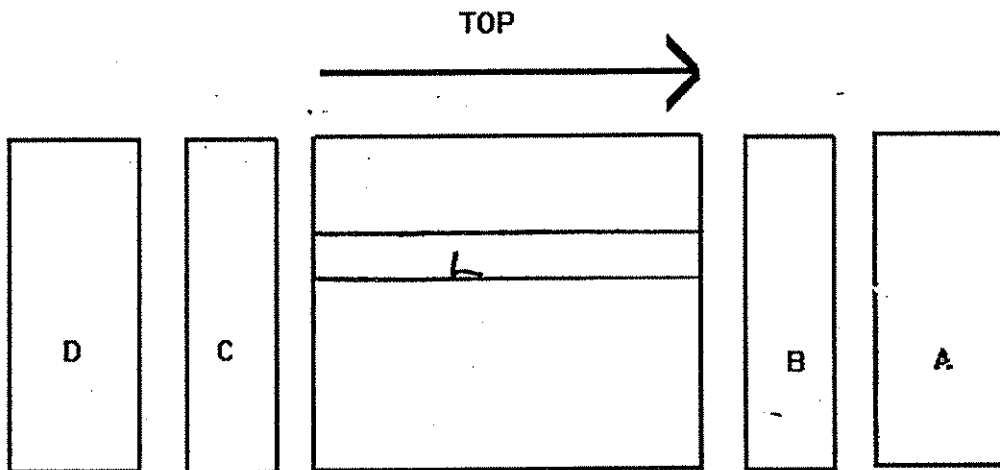
NON PRESENT

Cracks and Other
Distinctive Features:

NO VISIBLE CRACKING; VOIDS UP

TO 2 CM DIAMETER, CONCENTRATED IN THE
TOP HALF OF SPECIMEN.

CUT LONGITUDINAL SECTION MARCH 1995



HR - 358 Concrete Cores 1994

SAMPLE IDENTIFICATION: #14, WEBSTER, U.S. 520, STA 2020, WB LANE

GENERAL SAMPLE OBSERVATIONS:

Sample Dimensions:

10.1 cm diameter; 23.5 cm length

Full SLAB THICKNESS

Surface condition:

Top-

TINES ON \approx 1/2 SAMPLE; MAX DEPTH 4MM

MAX WIDTH 50MM @ 1 TO 2 CM INTERVALS

Bottom-

CASTON SAND SUBGRADE

Reinforcement:

PRESENT ON BOTTOM OF SAMPLE

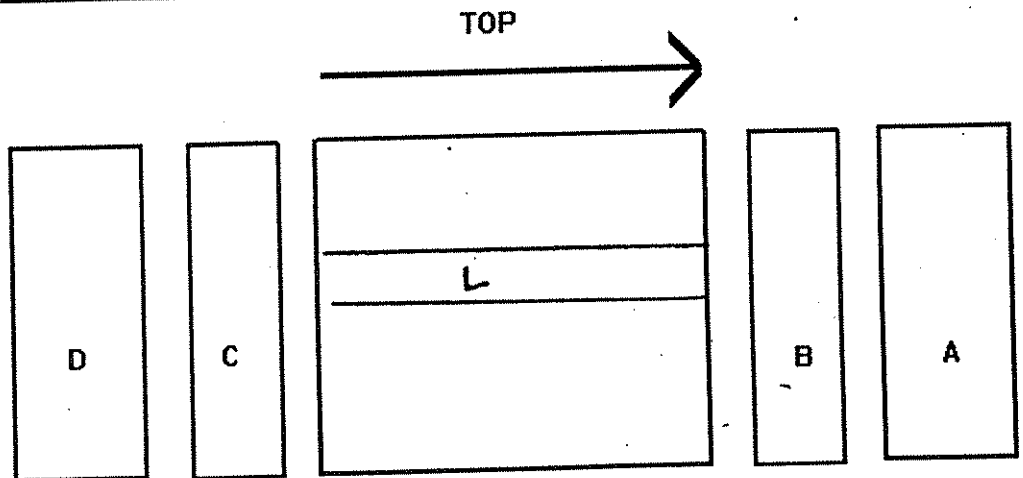
Cracks and Other Distinctive Features:

NO VISIBLE CRACKING, VOIDS

UP TO 1.5 CM DIAMETER, NOT A LARGE

AMOUNT OF JOIDS PRESENT.

CUT LONGITUDINAL SECTION MAR 14 1995



HR - 358 Concrete Cores 1994

SAMPLE IDENTIFICATION: #15, US 520, WEBSTER, STA 2020 WB LANE

GENERAL SAMPLE OBSERVATIONS:

Sample Dimensions: 10.1 cm diameter; 25.3 cm length

FULL SLAB THICKNESS

Surface condition:

Top- TINES, MAX DEPTH 3MM, MAX WIDTH 5MM

@ 1752 CM SPACING

Bottom- IRREGULAR, RUST ON SAND

SUBGRADE

Reinforcement:

PRESENT, APPROXIMATELY 9CM FROM BOTTOM

Cracks and Other

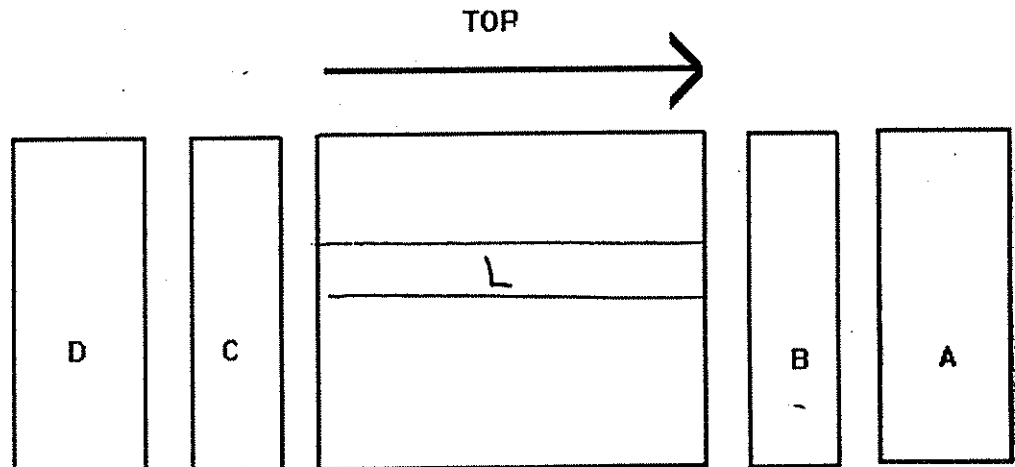
Distinctive Features:

NO VISIBLE CRACKS, LARGEST

VOID 1cm DIAMETER, NOT A LARGE AMOUNT

OF VOIDS PRESENT.

CUT LONGITUDINAL SECTION MARCH 1995.



HR - 358 Concrete Cores 1994

SAMPLE IDENTIFICATION: #16, WEBSTER, U.S. 520, STA 2020, WB LANE

GENERAL SAMPLE OBSERVATIONS:

Sample Dimensions:

10.1 cm diameter, 24.5 cm length

FULL SLAB THICKNESS

Surface condition:

Top- TINES, MAX DEPTH 2mm MAX r

WIDTH 5mm @ 1 TO 2cm SPACING

Bottom- CAST ON SUBGRADE

Reinforcement:

NONE PRESENT

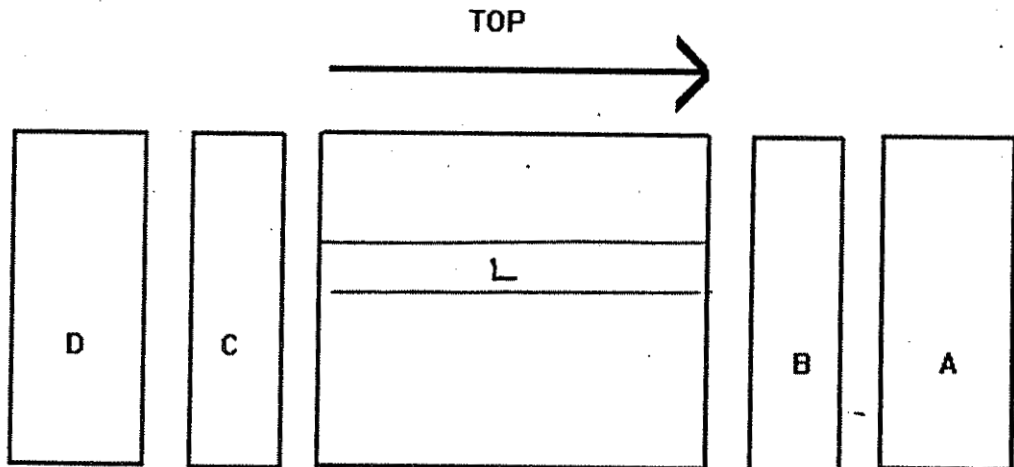
Cracks and Other

Distinctive Features:

NO CRACKS VISIBLE, VOIDS

UP TO 2cm ACROSS. MANY PRESENT.

CUT LONGITUDINAL SECTION MARCH 1995.



HR - 358 Concrete Cores 1994

SAMPLE IDENTIFICATION: #17, WEBSTER, U.S. 520, STA 2209, WB LANE

GENERAL SAMPLE OBSERVATIONS:

Sample Dimensions: 10.1 CM DIAMETER, 23.2 CM LENGTH,

FULL SLAB THICKNESS

Surface condition:

Top- TINES, MAX DEPTH 8mm, MAX WIDTH

1cm, @ 1 TO 2 CM SPACING

Bottom- CAST ON NON-SOIL MATERIAL

Reinforcement: PRESENT, @ 10.5 CM FROM BASE

Cracks and Other

Distinctive Features: NO VISABLE CRACKING LARGE

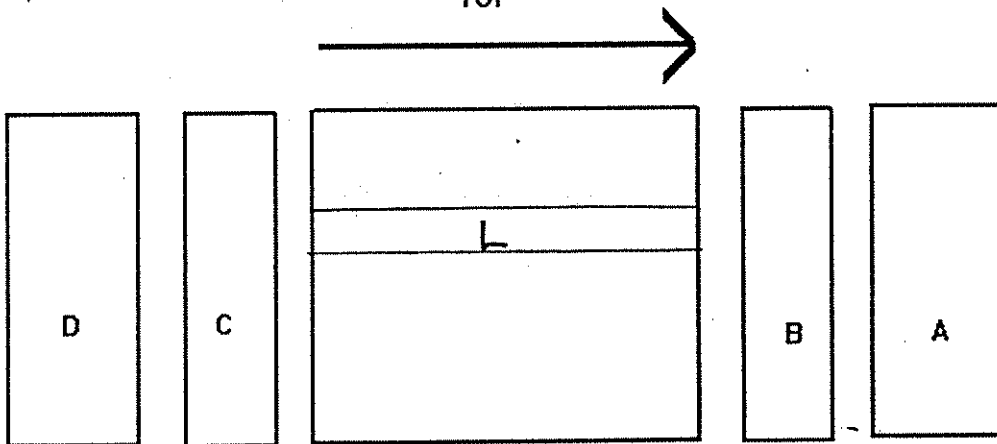
VOIDS (2cm MAX) SCATTERED THROUGHOUT SPECIMEN,

MOST AGGREGATE CALCIUM CARBONATE WITH SOME

SHALE

CUT LONGITUDINAL SECTION MARCH 1995.

VERY LARGE VOIDS NOTED WITH CRACK EXTENDING FROM THEM PARALLEL TO TOP SURFACE TOP



HR - 358 Concrete Cores 1994

SAMPLE IDENTIFICATION: # 20 WEBSTER, U.S. 520, STA 2209, WB LANE

GENERAL SAMPLE OBSERVATIONS:

Sample Dimensions: 10 CM WIDTH, 23.5 CM DEPTH

FULL SLAB THICKNESS

Surface condition:

Top- TINES, MAX DEPTH 9MM MAX WIDTH 5MM

LOCATED AT VARYING INTERVALS OF 1 TO 2CM.

Bottom- CAST ON NON SOIL SMOOTH MATERIAL

Reinforcement: NON PRESENT

Cracks and Other

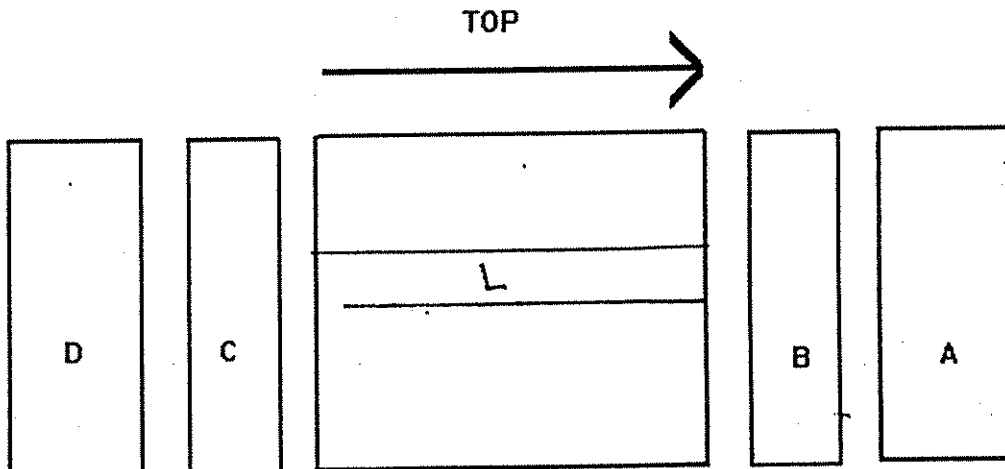
Distinctive Features: CRACKS LOCATED ON

TOP OF SAMPLE PERPENDICULAR TO

TINES. THEY RUN ABOUT 6CM LOCATED IN

CENTER OF SAMPLE TOP. LIMESTONE AGGREGATE

CUT LONGITUDINAL SECTION MARCH 1995.



HR - 358 Concrete Cores 1994

SAMPLE IDENTIFICATION: # 21, DALLAS Co., I-80, STA 726+60 EB LANE

GENERAL SAMPLE OBSERVATIONS:

Sample Dimensions: 10.1 CM DIAMETER, 29.6 CM LENGTH

FULL SLAB THICKNESS

Surface condition:

Top- TINES, MAX DEPTH 1mm, MAX WIDTH 4mm

@ 1.5-2.5 CM INTERVALS

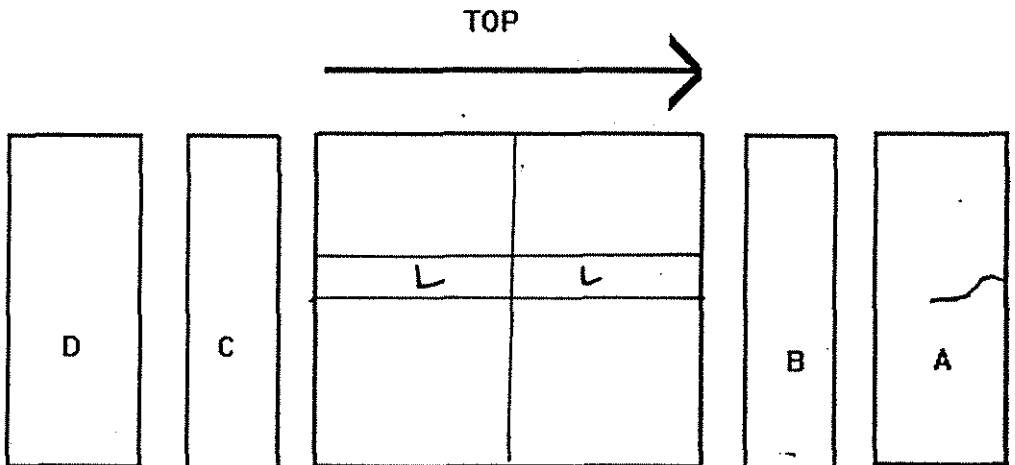
Bottom- CAST ON GRAVEL SUBGRADE

Reinforcement:

NONE PRESENT

Cracks and Other
Distinctive Features:

CRACKED THROUGH CENTER OF
TOP SURFACE EXTENDING $\hat{=}$ 3cm INTO SAMPLE.



OK

HR - 358 Concrete Cores 1994

SAMPLE IDENTIFICATION: #22, DALLAS CO., I-80, STA 726+60, EB LANE

GENERAL SAMPLE OBSERVATIONS:

Sample Dimensions: 10.1 cm DIAMETER, 30.5 cm LENGTH

FULL SLAB THICKNESS

Surface condition:

Top- FINES, MAX DEPTH 1 mm, MAX WIDTH 4 mm

@ 1.5-2.5 cm INTERVALS

Bottom- CAST ON GRAVEL SUBGRADE

Reinforcement:

NONE PRESENT

Cracks and Other

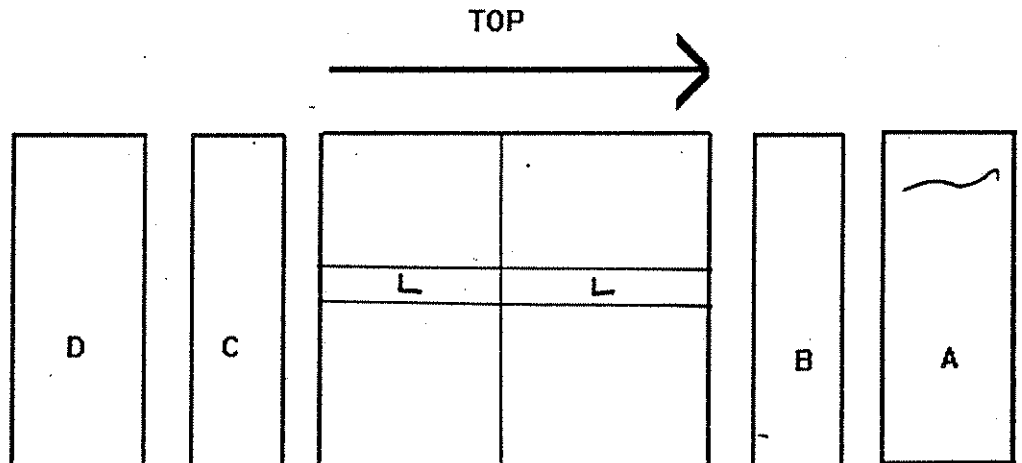
Distinctive Features:

CRACK THROUGH TOP SURFACE

EXTENDING 3 cm INTO SAMPLE, SAMPLE

HAS AREAS WHERE IT IS SPALLING OFF @

10 cm FROM TOP, 8 cm & 20 cm ALSO.



OK

HR - 358 Concrete Cores 1994

SAMPLE IDENTIFICATION: #23, DALLAS Co., I-80, STA 726+60 EB LANE

GENERAL SAMPLE OBSERVATIONS:

Sample Dimensions: 10.1 cm DIAMETER, 29.5 cm LENGTH

FULL SLAB THICKNESS

Surface condition:

Top- FINES, MAX DEPTH 1mm, MAX WIDTH 4mm

@ 1.5-2.5 cm INTERVALS

Bottom- CAST ON GRAVEL SUBGRADE

Reinforcement:

NONE PRESENT

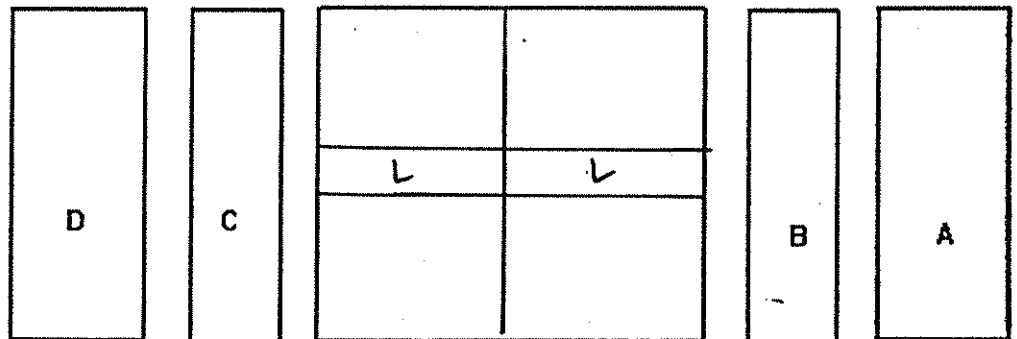
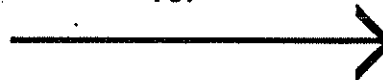
Cracks and Other

Distinctive Features:

NO CRACKS NOTED, VOIDS

AROUND MUCH OF THE LARGER AGGREGATES.

TOP



OK

HR - 358 Concrete Cores 1994

SAMPLE IDENTIFICATION: #24, DALLAS CO., I-80, STA 726+60, EB LANE

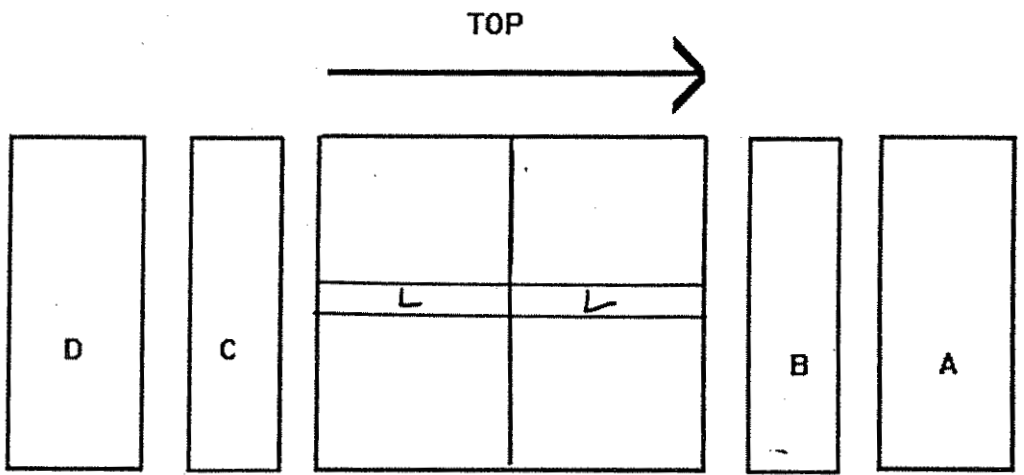
GENERAL SAMPLE OBSERVATIONS:

Sample Dimensions: 101 cm DIAMETER, 29.5 cm LENGTH
FULL SLAB THICKNESS

Surface condition:
Top- TINES, NOT MEASURABLE DEPTH, 2 4mm WIDTH
@ 1.5 - 2.5 cm INTERVALS
Bottom- CAST ON GRAVEL SUBGRADE

Reinforcement: NONE PRESENT

Cracks and Other Distinctive Features: NO CRACKS NOTED,
SOME SPALLING NOTED @ 11cm FROM TOP
OF SAMPLE.



OK

HR - 358 Concrete Cores 1994

SAMPLE IDENTIFICATION: #25, SCOTT Co., BETTENDORF, STA 120B, EB LANE

GENERAL SAMPLE OBSERVATIONS:

Sample Dimensions: 10.1 cm DIAMETER, 26cm LENGTH

FULL SLAB THICKNESS

Surface condition:

Top- TINES @ 4mm SPACING, VERY FAINT

Bottom- CAST ON GRAVEL SUBGRADE

Reinforcement:

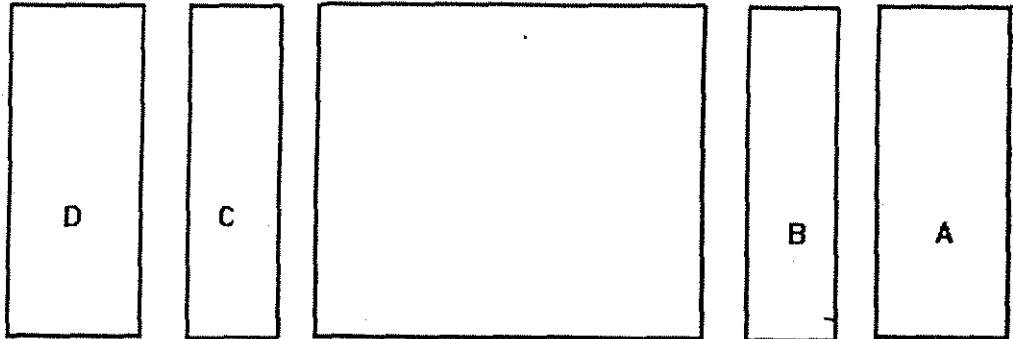
NONE PRESENT

Cracks and Other

Distinctive Features:

NO CRACKS NOTED

TOP



OK

HR - 358 Concrete Cores 1994

SAMPLE IDENTIFICATION: #26, SCOTT CO, BETTENDORF STA 1209 FBLANE

GENERAL SAMPLE OBSERVATIONS:

Sample Dimensions: 10.1 cm DIAMETER, 26 cm LENGTH

FULL SLAB THICKNESS

Surface condition:

Top- FINES, FAINT, RANDOM SPACING @ 4mm-8mm

Bottom- CAST ON GRAVEL SUBGRADE

Reinforcement:

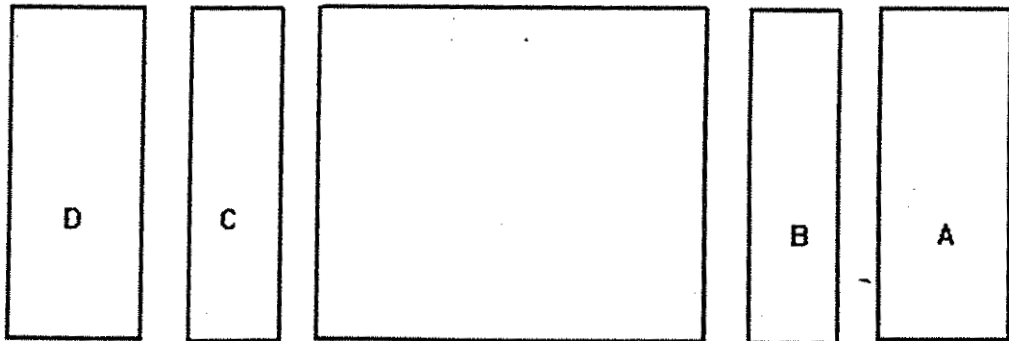
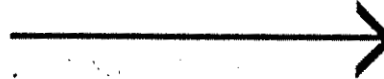
NONE PRESENT

Cracks and Other

Distinctive Features:

NO CRACKS NOTED

TOP



DK

HR - 358 Concrete Cores 1994

SAMPLE IDENTIFICATION: # 27, SCOTT Co., BETTENDORF STA 1208, WB LANE

GENERAL SAMPLE OBSERVATIONS:

Sample Dimensions: 10.1 cm DIAMETER, 25.5 cm LENGTH

FULL SLAB THICKNESS

Surface condition:

Top- TINES, TOO WORN DOWN TO MEASURE

Bottom- CAST ON GRAVEL SUBGRADE

Reinforcement:

NONE PRESENT

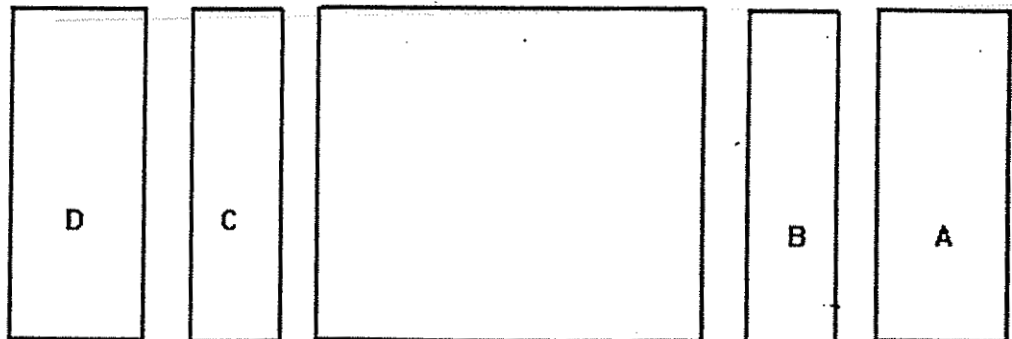
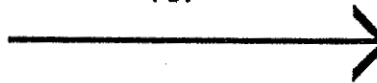
Cracks and Other

Distinctive Features: CRACKED ON TOP SURFACE

PARALLEL TO TINES, NOT EXTENDING

APPRECIABLY INTO SAMPLE.

TOP



OK

HR - 358 Concrete Cores 1994

SAMPLE IDENTIFICATION: # 28, Scott Co. BETENDORF, STA 1208, WB LANE

GENERAL SAMPLE OBSERVATIONS:

Sample Dimensions:

101 cm WIDTH, 23 cm LENGTH

FULL SLAB THICKNESS

Surface condition:

Top- TINES 2 mm MAX WIDTH, 0.5 mm DEPTH,

1 cm TO 3 mm INTERVALS

Bottom- CAST ON GRAVEL SUB GRADE

Reinforcement:

NONE PRESENT

Cracks and Other

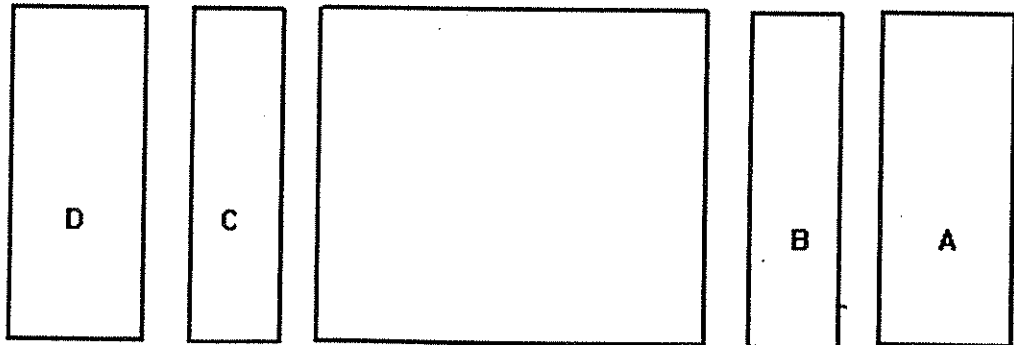
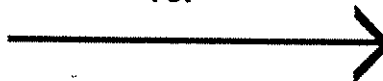
Distinctive Features:

NO CRACKS NOTED

MORE VOIDS IN TOP 1/2 OF SAMPLE

THOUGH NOT VERY LARGE (1/2 cm diameter).

TOP



OK

HR - 358 Concrete Cores 1994 .

SAMPLE IDENTIFICATION: # 29, LOUISA Co., G-62, WB LANE

GENERAL SAMPLE OBSERVATIONS:

Sample Dimensions: 10.1cm DIAMETER, 14.7cm LENGTH

FULL SLAB THICKNESS

Surface condition:

Top- TINES: 3mm MAX DEPTH, 5mm MAX WIDTH

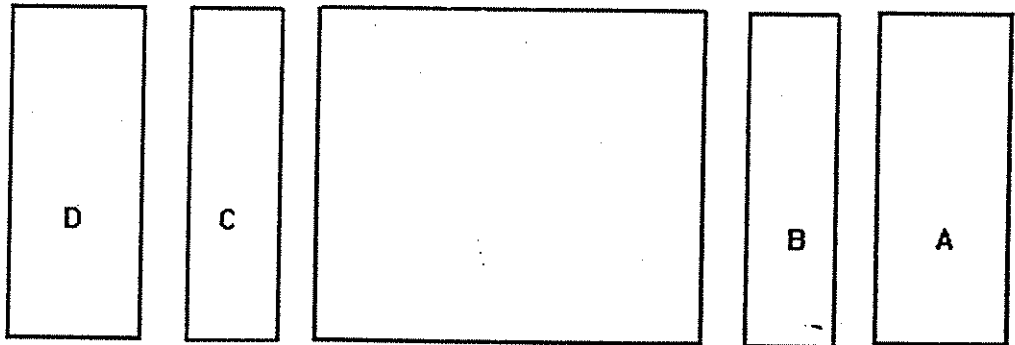
@ 1.5 - 2cm INTERVALS

Bottom- CAST ON ASPHALT

Reinforcement: NONE PRESENT

Cracks and Other Distinctive Features: NO CRACKING NOTED.

TOP



AK

HR - 358 Concrete Cores 1994

SAMPLE IDENTIFICATION: 30, LEVISO CO, G-62, WBLANE

GENERAL SAMPLE OBSERVATIONS:

Sample Dimensions: 10.1 cm WIDTH x 16.6 cm LENGTH, Full Slab

Surface Conditions:

Top- TINES, 6mm MAX DEPTH 6mm MAX WIDTH

⊙ 0.2 TO 3.5 CM INTERVALS

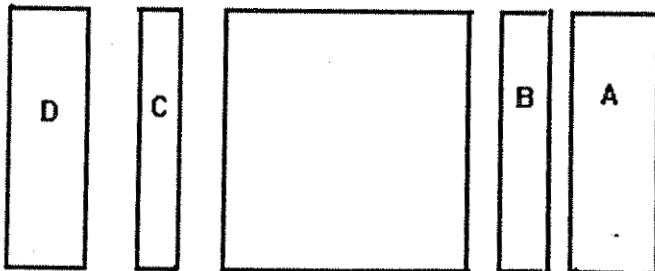
Bottom- CAST ON ASPHALT

Reinforcement: NONE PRESENT

Cracks and Other Distinctive Features: NO CRACKS PRESENT

Note rims on aggregates

TOP



OK

HR - 358 Concrete Cores 1994

SAMPLE IDENTIFICATION: 31, LOUISA Co., G-62, WB LANE

GENERAL SAMPLE OBSERVATIONS:

Sample Dimensions: 10.1cm WIDTH X 16.7cm LENGTH, FULL SLAB

Surface Conditions:

Top- TINES, 2mm MAX DEPTH X 5mm MAX WIDTH

② 1-205 cm INTERVALS

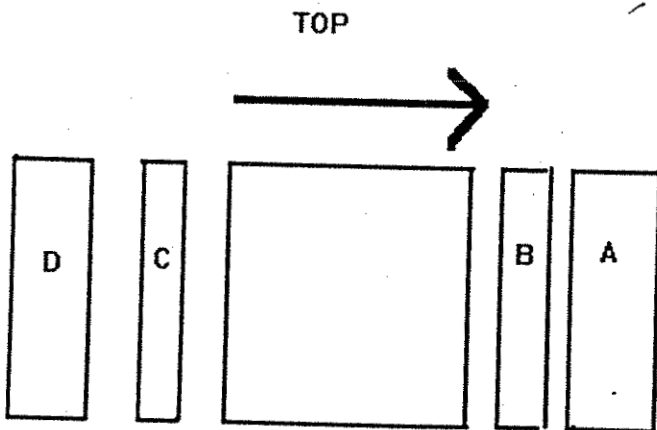
Bottom- CAST ON ASPHALT

Reinforcement: NONE PRESENT

Cracks and Other

Distinctive Features: NO CRACKS NOTED, CHIP TAKEN OUT OF TOP (MAY HAVE OCCURRED WHILE DRILLING)

Note discoloration around course agg.



OK

HR - 358 Concrete Cores 1994

SAMPLE IDENTIFICATION: 32, LOUISA CO., G-62, WB LANE

GENERAL SAMPLE OBSERVATIONS:

Sample Dimensions: 101cm WIDTH, 115cm LENGTH, FULL SLAB

Surface Conditions:

Top- TINES, 4mm MAX DEPTH X 5mm MAX WIDTH

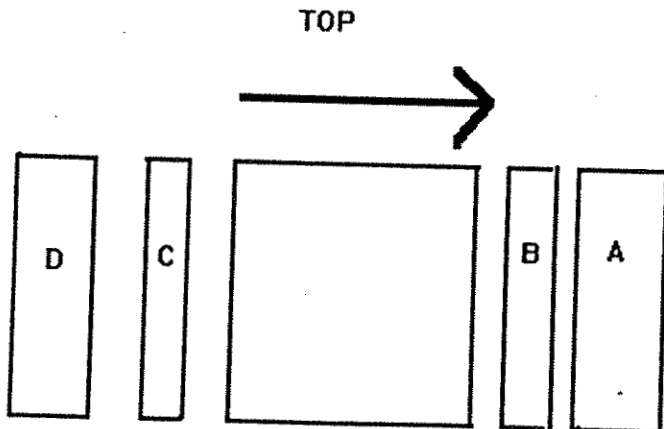
@ 1-2 cm INTERVALS

Bottom- CAST ON ASPHALT

Reinforcement: NONE PRESENT

Cracks and Other

Distinctive Features: NO CRACKS NOTED



OK

HR - 358 Concrete Cores 1994

SAMPLE IDENTIFICATION: 33 LOUISA CO., G-62, EB LANE, BAD AREA

GENERAL SAMPLE OBSERVATIONS:

Sample Dimensions: 10.1 cm WIDTH, 16.5 cm LENGTH FULL SLAB

Surface Conditions:

Top- TILES, BADLY WORN SURFACE.

Bottom- CAST ON ASPHALT

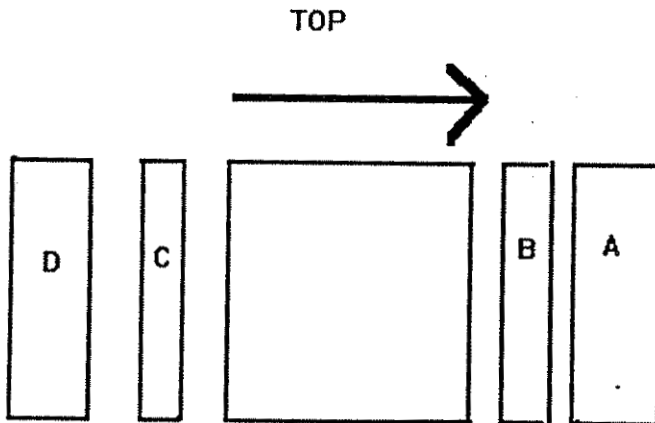
Reinforcement: NONE PRESENT

Cracks and Other

Distinctive Features: NO CRACKS NOTED, MANY

SMALL VOIDS AROUND AGGREGATE

Extremely soft!! - simple sawing plucked out
Note rims around aggregates; *material*



OK

HR - 358 Concrete Cores 1994

SAMPLE IDENTIFICATION: 34, LOUISA Co., G-62, WB LANE, BED AREA

GENERAL SAMPLE OBSERVATIONS:

Sample Dimensions: 10.1 CM WIDTH, 16 CM LENGTH, FULL SLAB

Surface Conditions:

Top- TINES, BADLY WORN SURFACE

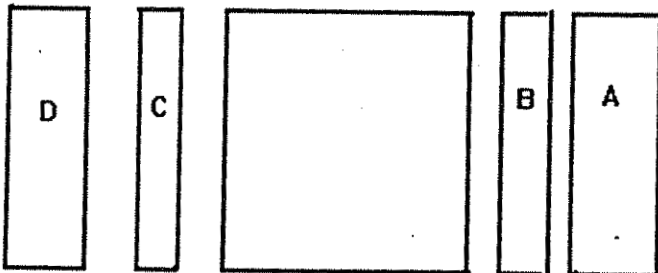
Bottom- CAST ON ASPHALT

Reinforcement: NONE PRESENT

Cracks and Other

Distinctive Features: NO CRACKS NOTED, NUMEROUS SMALL HOLES

TOP



OK

HR - 358 Concrete Cores 1994

SAMPLE IDENTIFICATION: 35, LOUISA Co., G-02, WB LANE, BAD DREG

GENERAL SAMPLE OBSERVATIONS:

Sample Dimensions: 10.1 cm WIDTH, 13 cm LENGTH, Full SLAB

Surface Conditions:

Top- TINES, BADLY WORN, LARGE PITS DEVELOPED

≅ 1cm x 4cm & 1cm x 1cm

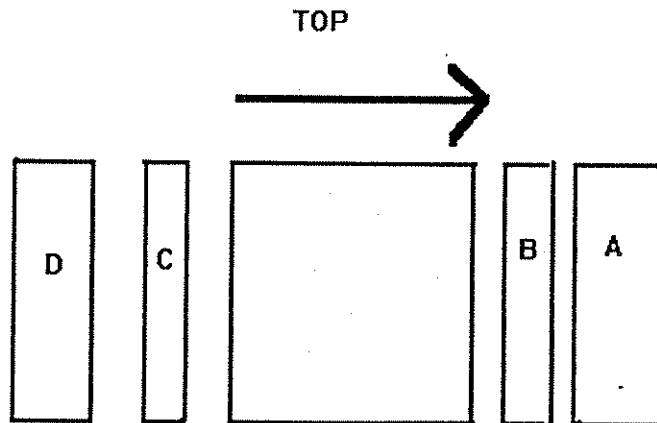
Bottom- CAST ON ASPHALT

Reinforcement: NONE PRESENT

Cracks and Other

Distinctive Features: NO CRACKS NOTED, NUMEROUS SMALL VORES

Four horizontal lines for additional notes.



OK Check mix design on these cores

HR - 358 Concrete Cores 1994

SAMPLE IDENTIFICATION: 36, LOUISA CO., G-62, WB LANE, BAD AREA

GENERAL SAMPLE OBSERVATIONS:

Sample Dimensions: 10.1 CM WIDTH, 16 CM LENGTH, FULL SWAB

Surface Conditions:

Top- TINES BADLY WORN, PITTING \approx 2CM X 2CM

Bottom- CAST ON ASPHALT

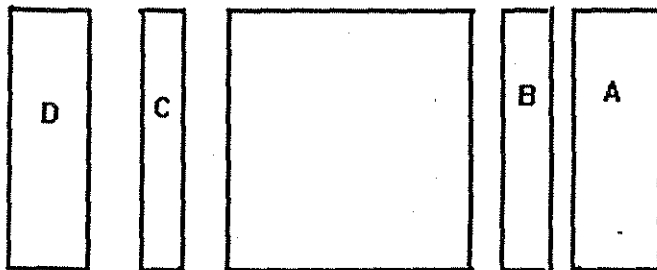
Reinforcement: NONE PRESENT

Cracks and Other

Distinctive Features: NO CRACKS, NUMEROUS SMALL PITS

NEARLY ALL IN TOP 1/3 OF SAMPLE.

TOP



OK

HR - 358 Concrete Cores 1994

SAMPLE IDENTIFICATION: 37, MADISON Co., U.S. 169, STA 224+20, SB LANE
(joint, bad area)

GENERAL SAMPLE OBSERVATIONS:

Sample Dimensions: 10.1 cm WIDTH, APPROX 19.5 cm LENGTH, FULL SLAB

Surface Conditions:

Top-TINES, WORN SLEELY

Bottom- CAST ON GRAVEL SUBGRADE

Reinforcement:

NONE PRESENT

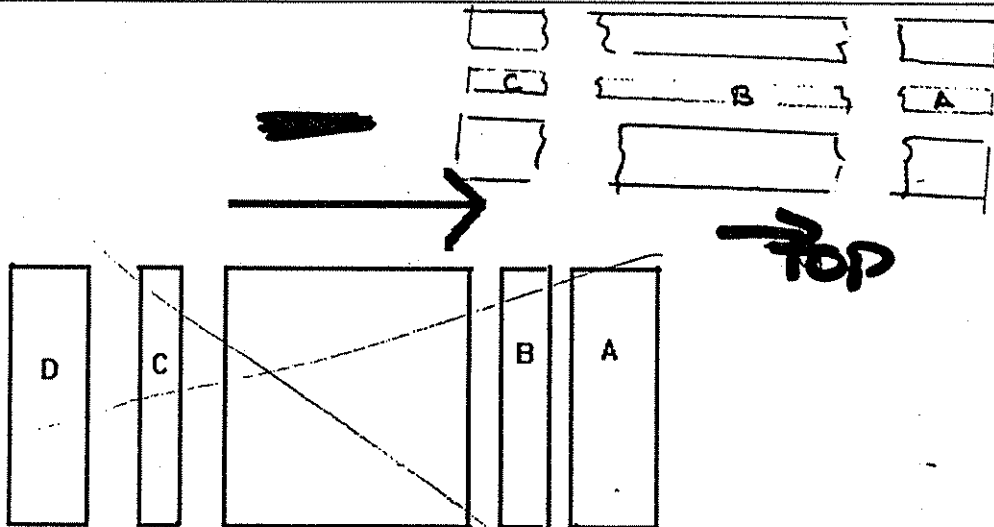
Cracks and Other

Distinctive Features: COMPLETELY BROKEN INTO THREE PIECES

BREAK #1 @ \approx 5cm FROM TOP & #2 @ \approx 15cm FROM TOP

NUMEROUS OTHER CRACKS, ALL PARALLEL TO TOP SURFACE.

TOOK SAMPLE PERPENDICULAR TO TOP SURFACE.



OK

HR - 358 Concrete Cores 1994

SAMPLE IDENTIFICATION: 38, MADISON CO., U.S. 169, STA 224+20, SB LANE
(mid panel, end)

GENERAL SAMPLE OBSERVATIONS:

Sample Dimensions: 101 cm WIDTH, 20 cm LENGTH FULL SLAB

Surface Conditions:

Top- TINES, BADLY WORN

Bottom- CAST ON GRAVEL SUBGRADE

Reinforcement: NONE PRESENT

Cracks and Other

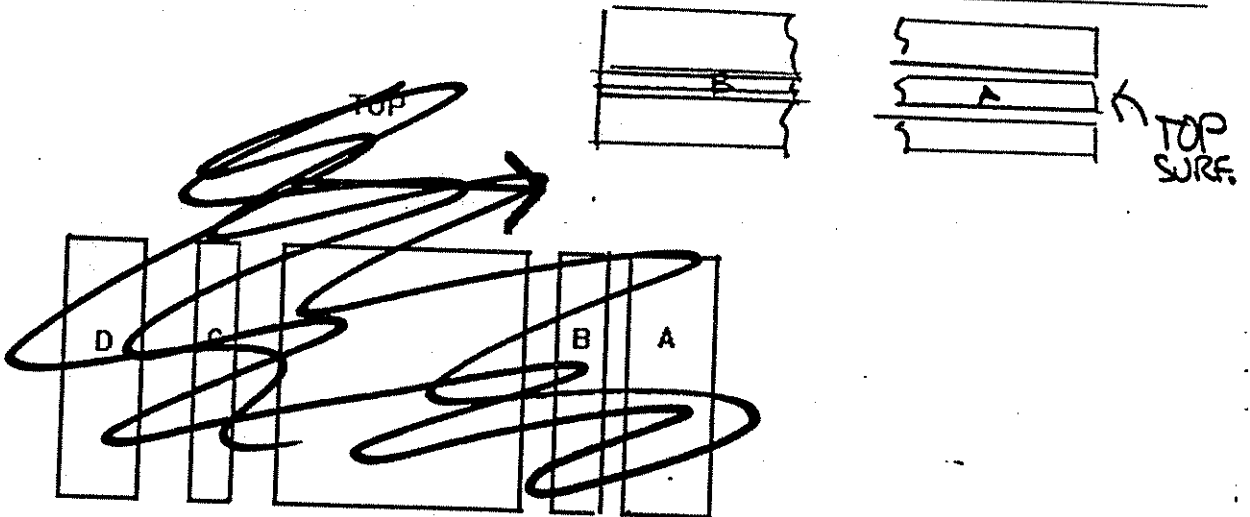
Distinctive Features: BROKEN @ 29.5 cm FROM TOP SURFACE.

OTHER CRACKS NOTED THROUGHOUT SAMPLE

PARALLEL TO TOP SURFACE. ALSO, A

CRACK IN TOP SURFACE PERPENDICULAR TO

TINES, NOT EXTENDING DOWN INTO SAMPLE.



OK

HR - 358 Concrete Cores 1994

SAMPLE IDENTIFICATION: 39, MADISON CO., U.S. 169, STA 220+00, SB LANE
(JOINT area, less bad) THEIR NOTE

GENERAL SAMPLE OBSERVATIONS:

Sample Dimensions: 10.1 cm WIDTH, 21.5 cm LENGTH, FULL SCAB

Surface Conditions:

Top- TINES, CLOSELY SPACED, BADLY WORN
2-3mm

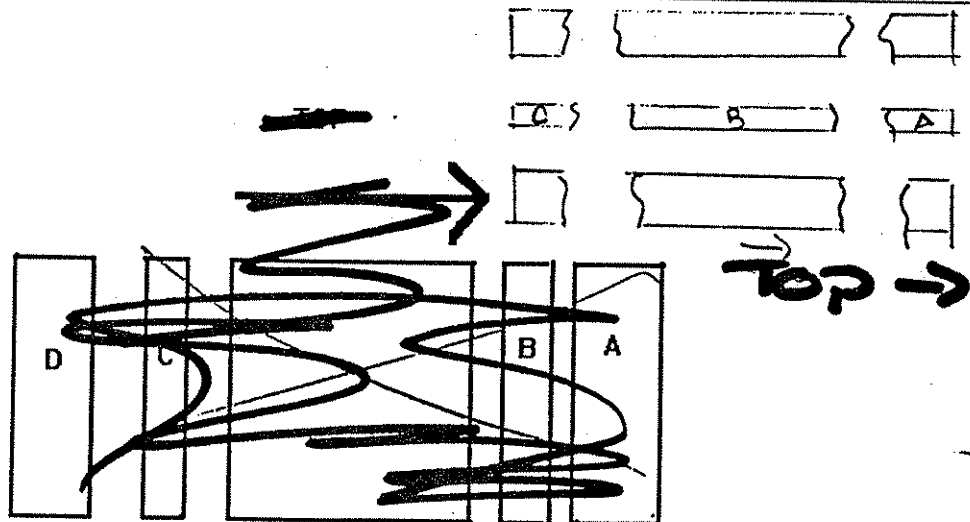
Bottom- CAST ON GRAVEL SUBGRADE

Reinforcement: NONE PRESENT

Cracks and Other

Distinctive Features: CRACKS PARALLEL TO TOP SURFACE

THROUGHOUT SAMPLE. BROKEN @ APPROX 5 + 13 CM FROM TOP SURFACE. A SMALL CRACK IN TOP SURFACE PERPENDICULAR TO TINES.



OK

HR - 358 Concrete Cores 1994

SAMPLE IDENTIFICATION: 40, MADISON CO., U.S. 169, STA 220+00, SB LANE
(MID PANEL, LEES EAD)

GENERAL SAMPLE OBSERVATIONS:
Sample Dimensions: 10 cm WIDTH, 21 cm LENGTH, FULL SLAB

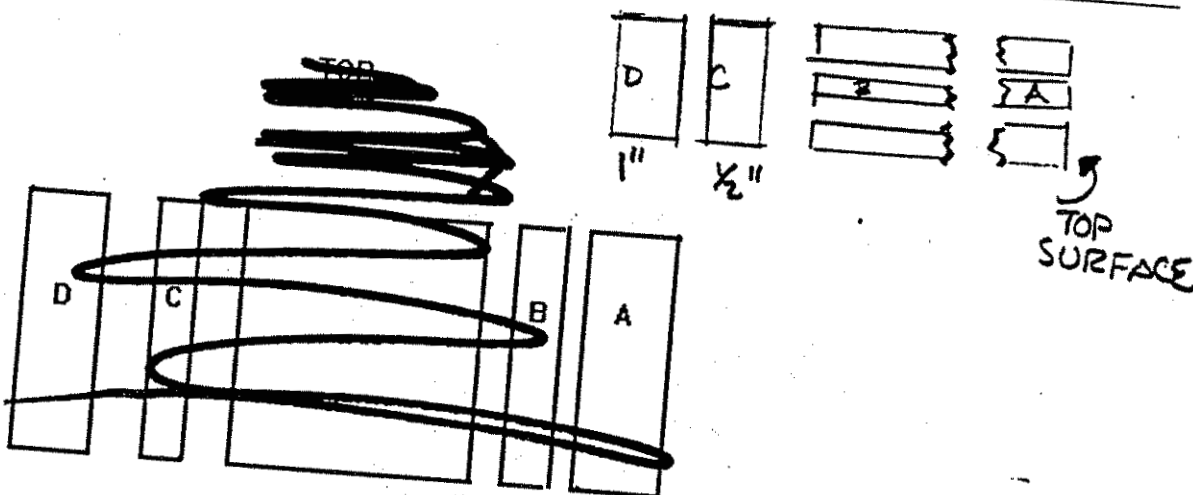
Surface Conditions:
Top: TINES, BADLY WORN, PITTING STARTING

Bottom: CAST ON GRAVEL SUBGRADE

Reinforcement: NONE PRESENT

Cracks and Other Distinctive Features: ONE CRACK COMPLETELY THROUGH SAMPLE

@ 7cm DOWN FROM TOP SURFACE. CORE IS IN TWO PIECES AS A RESULT ALSO, CRACK STARTING @ 7cm FROM BOTTOM SURFACE. BOTH CRACKS RUN PARALLEL TO TOP SURFACE.



OK

HR - 358 Concrete Cores 1994

SAMPLE IDENTIFICATION: 41, HAMILTON Co., IA 175, STA 190, EB LANE
(mid panel, good, fly ash)

GENERAL SAMPLE OBSERVATIONS:

Sample Dimensions: 10.1 cm WIDTH, 20.2 cm LENGTH, FULL SLAB

Surface Conditions:

Top- TINES, 7mm MAX DEPTH, 11mm MAX WIDTH

@ 1-1.5 cm INTERVALS

Bottom- CAST ON GRAVEL SUBGRADE

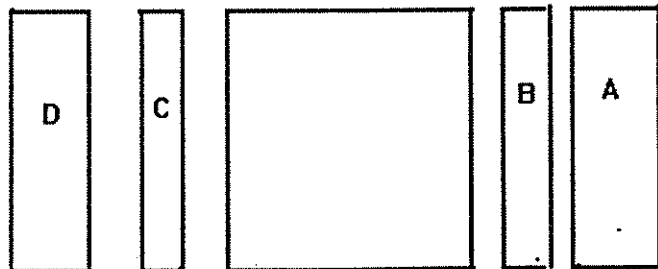
Reinforcement: NONE PRESENT

Cracks and Other

Distinctive Features: NO CRACKS NOTED. LARGE VOIDS

(2cm x 7mm, 5mm x 5mm) NOTED. SHALE CONTENT
SEEMED HIGH.

TOP



OK

HR - 358 Concrete Cores 1994

SAMPLE IDENTIFICATION: 42, HAMILTON Co., IA 175, STA 190, EB LANE
(joint, good, fly ash)

GENERAL SAMPLE OBSERVATIONS:

Sample Dimensions: 10.1 cm WIDTH, 19.5 cm LENGTH, FULL SLAB

Surface Conditions:

Top- TINES, 6mm MAX DEPTH, 12mm MAX WIDTH

@ 0.1 - 2 cm INTERVALS

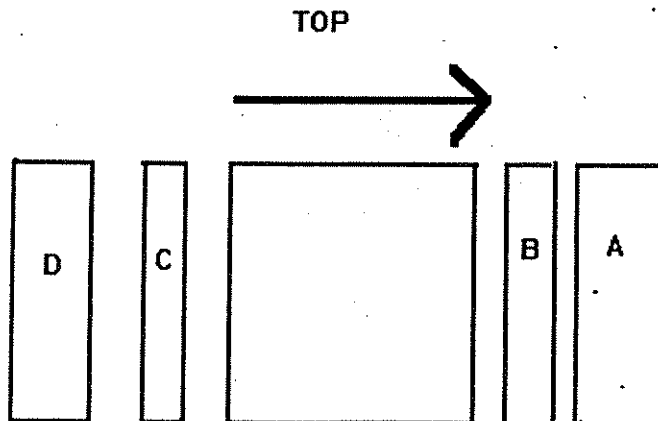
Bottom- CAST ON GRAVEL SUBGRADE

Reinforcement: NONE PRESENT

Cracks and Other

Distinctive Features: NO CRACKS NOTED. NUMEROUS VOIDS

approx 1cm diameter AVERAGE. SHALE CONTENT
NDA.



OK

HR - 358 Concrete Cores 1994

SAMPLE IDENTIFICATION: 413, UNION CO., IA 25, STA 180+20, SB LANE
(mid panel, class I stone)

GENERAL SAMPLE OBSERVATIONS:

Sample Dimensions: 10.1 cm WIDTH, 22 cm LENGTH, Full SURF

Surface Conditions:

Top- SMOOTH SURFACE, POSSIBLY DISTRACT

COIR

Bottom- CAST ON COMPACTED SOIL SUBGRADE

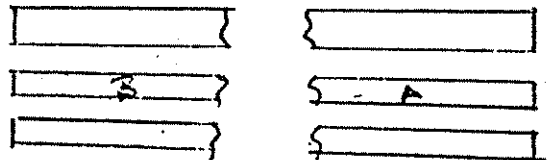
Reinforcement: NONE PRESENT

Cracks and Other

Distinctive Features: CRACKED THROUGH CORE @ 8.5 CM

DEPTH FROM TOP SURFACE PARALLEL TO TOP
AND BREAKING SAMPLE IN TWO PIECES.

OTHER CRACKS RUNNING PARALLEL TO TOP SURFACE
@ 1.5, 5, 10.5, 15.5 CM FROM TOP SURFACE



→
TOP



OK

HR - 358 Concrete Cores 1994

SAMPLE IDENTIFICATION: 44, UNION Co., IA 25, STA 230+00, SB LANE
(mid panel, class 1 stone)

GENERAL SAMPLE OBSERVATIONS:

Sample Dimensions: 10.0 cm WIDTH, UNKNOWN LENGTH, FULL SLAB

Surface Conditions:

Top- SMOOTH TOP SURFACE, OVERLAID

WITH ASPHALT

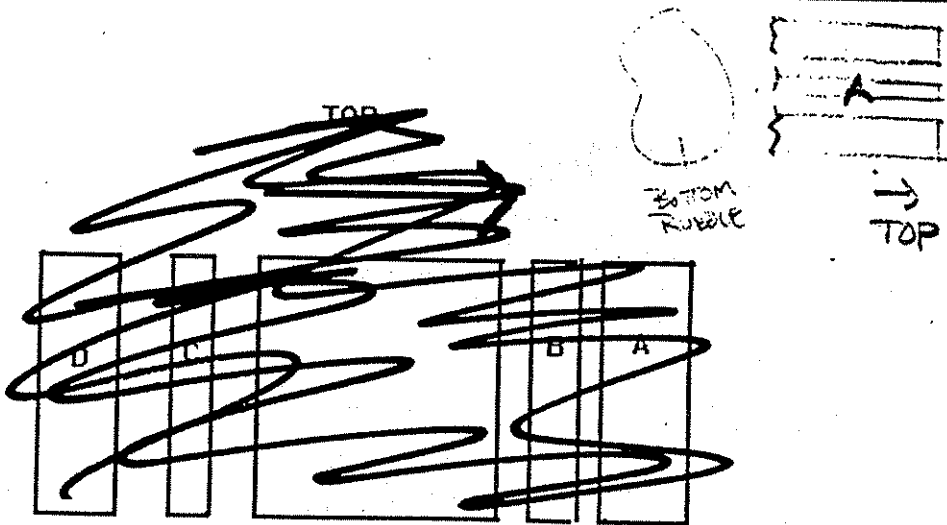
Bottom-

Reinforcement: NONE PRESENT

Cracks and Other

Distinctive Features: BOTTOM PORTION ALL RUBBLE, TOP

PORTION APPROX. 5CM THICK WITH TWO MAJOR
CRACKS PARALLEL TO TOP SURFACE @
1 & 3 cm FROM TOP. AGGREGATES REACTING



OK

HR - 358 Concrete Cores 1994

SAMPLE IDENTIFICATION: 45, UNION CO., IA 25, STA 231+00, SB LANE
(mid panel, class 1 stone)

GENERAL SAMPLE OBSERVATIONS:

Sample Dimensions: 101 cm WIDTH, UNKNOWN LENGTH, FULL SLAB

Surface Conditions:

Top- SMOOTH ^{TOP} SURFACE OVERLAIN WITH ASPHALT

Bottom- CAST ON COMPACTED SOIL & GRAVEL

Reinforcement: NONE PRESENT

Cracks and Other

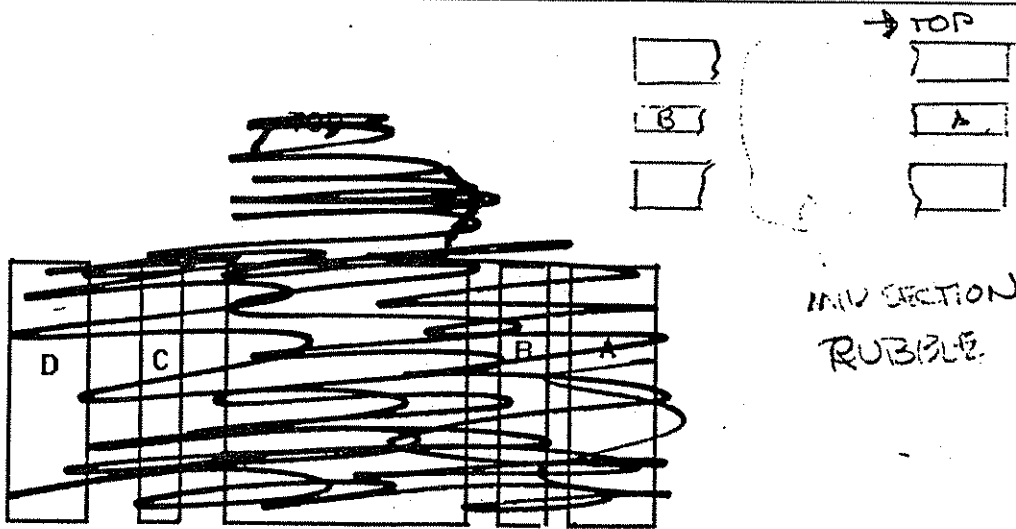
Distinctive Features: MID SECTION COMPLETELY CRUMPLED

OUT. TOP SECTION APPROX 5cm THICK WITH

CRACKS RUNNING PARALLEL TO TOP SURFACE

BOTTOM SECTION ~ 5cm THICK WITH SAME CRACKING

PATTERN. -APPEARS TO HAVE SOME AGGREGATE REACTION



OK

HR 7358 Concrete Cores 1994

SAMPLE IDENTIFICATION: 46, BUCHANAN CO., US 20, STA 57+60, EB LANE
(JOINT, VIRATOR TRAIL)

GENERAL SAMPLE OBSERVATIONS:

Sample Dimensions: 17.1 cm WIDTH, 23.5 cm LENGTH, Full SLAB

Surface Conditions:

Top- TINES, 2mm MAX DEPTH, 5mm MAX WIDTH

@ 1-2cm INTERVALS

Bottom- CAST ON BASE COURSE w/ ASPHALT SEAL

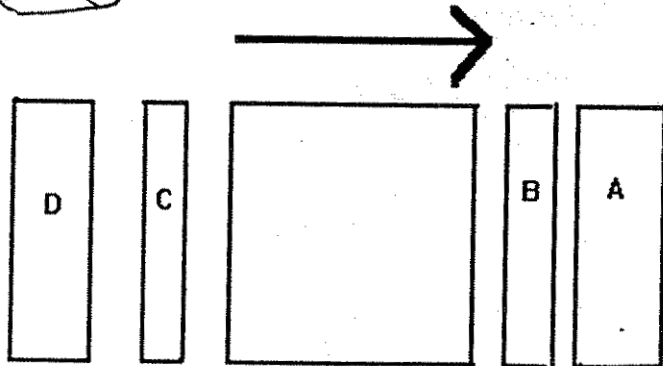
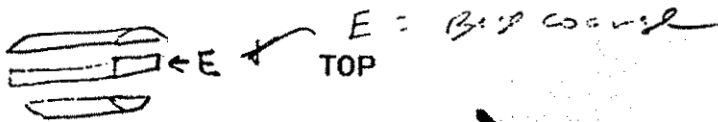
Reinforcement: NONE PRESENT

Cracks and Other

Distinctive Features: NO CRACKS PRESENT, NUMEROUS

SMALL HOLES (0.5cm) ESPECIALLY NOTED AROUND
LARGE AGGREGATE,

ALSO TOOK A CROSS SECTION OF BASE COURSE.



OK

HR - 358 Concrete Cores 1994

SAMPLE IDENTIFICATION: 47, BUCHANAN Co., US. 20, STA 157+60, EB LANE
(MID PANEL, U.I.B. TRAIL)

GENERAL SAMPLE OBSERVATIONS:

Sample Dimensions: 10.1 cm WIDTH, 23.5cm LENGTH, FULL SLAB

Surface Conditions:

Top- TINES, MAX DEPTH 7mm, MAX WIDTH 8mm,

ⓐ 0.2 - 1.4 cm INTERVALS

Bottom- CAST ON BASE COURSE W/ ASPHALT SEAL

Reinforcement: NONE PRESENT

Cracks and Other

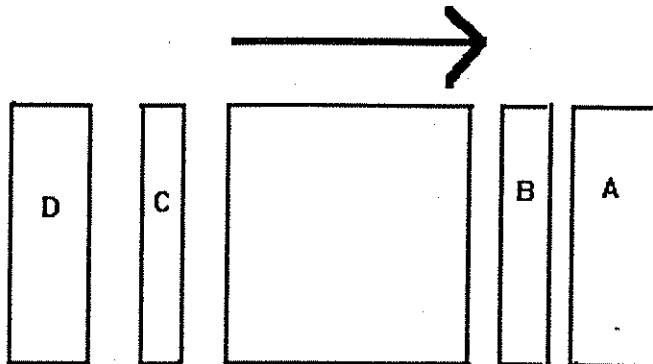
Distinctive Features: CRACKED @ 0.5cm FROM BASE, VOIDS CONCENTRATED

AROUND AGGREGATE. ALSO TOOK A SAMPLE

FROM BASE COURSE.

~~TOP~~ ^{? base course??}
TOP ^{? where is it??} NO 47
base course

DIDNT TAKE
BASE COURSE CUT



OK

HR - 358 Concrete Cores 1994

SAMPLE IDENTIFICATION: 48, BUCHANAN Co., U.S. 20, STA 57+60, EB LANE
(MID PANEL, NO VIB TRAIL)

GENERAL SAMPLE OBSERVATIONS:

Sample Dimensions: 10.1 CM WIDTH, 23.5 CM LENGTH, FULL SLAB

Surface Conditions:

Top-TINES, 4mm MAX DEPTH, 6mm MAX WIDTH,

@ 1-2 CM INTERVALS

Bottom-CASTON A 10CM BASE COURSE W/ ASPHALT SEAL

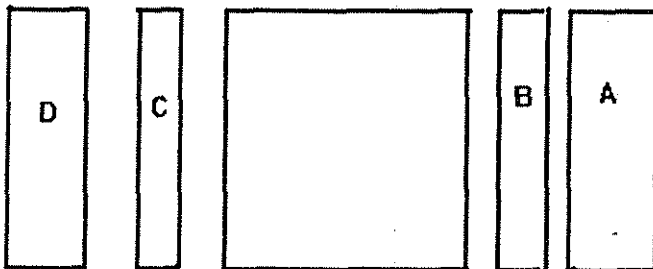
Reinforcement: NONE PRESENT

Cracks and Other

Distinctive Features: NO CRACKS NOTED, A LARGE NUMBER

OF VOIDS CONCENTRATED AROUND LARGE
AGGREGATE.

TOP



OK

HR - 358 Concrete Cores 1994

SAMPLE IDENTIFICATION: 49, BUCHANAN Co., U.S. 20, STA 385+64, EB LANE
(JOINT, NO VIS TRAIL)

GENERAL SAMPLE OBSERVATIONS:

Sample Dimensions: 10.1cm WIDTH, 28.5cm LENGTH, FULL SLAB

Surface Conditions:

Top- 2mm MAX DEPTH, 6mm MAX WIDTH

@ 1-2cm INTERVALS

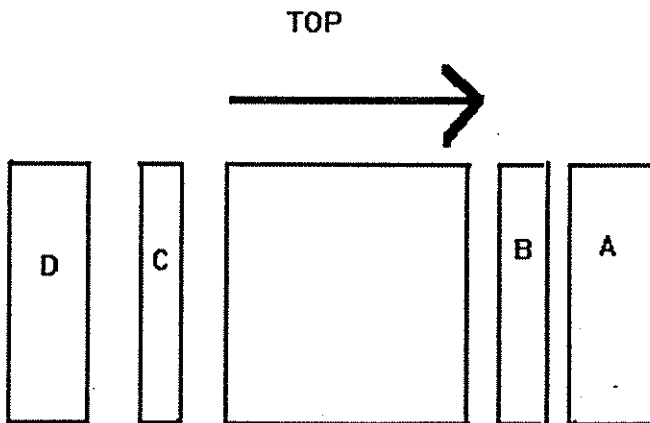
Bottom- CAST ON 11cm BASE COURSE W/ ASPHALT SEAL

Reinforcement: REINFORCEMENT @ BASE OF SLAB

Cracks and Other

Distinctive Features: NO CRACKS NOTED. VOIDS CONCENTRATED

AROUND AGGREGATE.



OK

HR - 358 Concrete Cores 1994

SAMPLE IDENTIFICATION: 50, BUCHANAN Co., US. 20, STA 385+64, EB LANE
(MID PANEL, VIR TRAIL)

GENERAL SAMPLE OBSERVATIONS:

Sample Dimensions: 10.1 cm WIDTH, 20.2 cm LENGTH, FULL SLAB

Surface Conditions:

Top- TINES, 4mm MAX DEPTH, 6mm MAX WIDTH

@ 1-2 cm INTERVALS

Bottom- CASTON 10cm BASE COURSE w/ ASPHALT SEAL

Reinforcement: NONE PRESENT

Cracks and Other

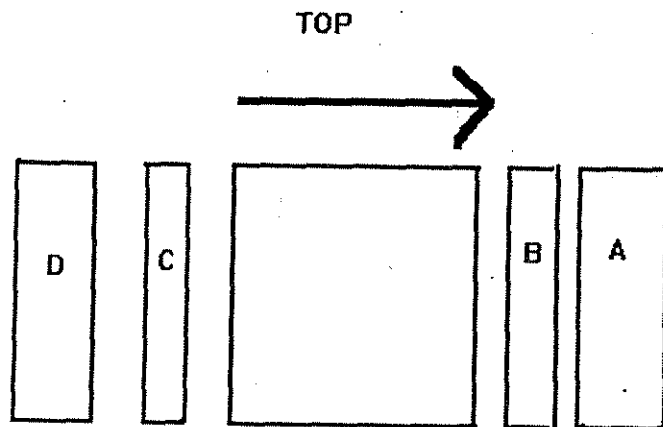
Distinctive Features: CRACK @ 19 cm FROM TOP (MAY HAVE

BEEN THE RESULT OF PRYING BASE COURSE OFF) DOESN'T

EXTEND THROUGH SAMPLE. NUMEROUS VOIDS CONCENTRATED

AROUND AGGREGATE. MANY VOIDS IN AGGREGATE

THROUGHOUT ENTIRE SAMPLE.



-OK

HR - 358 Concrete Cores 1994

SAMPLE IDENTIFICATION: 51 BUCHANAN Co., U.S. 20, STA 385+64, EB LANE
(POINT, VIB. TRAIL)

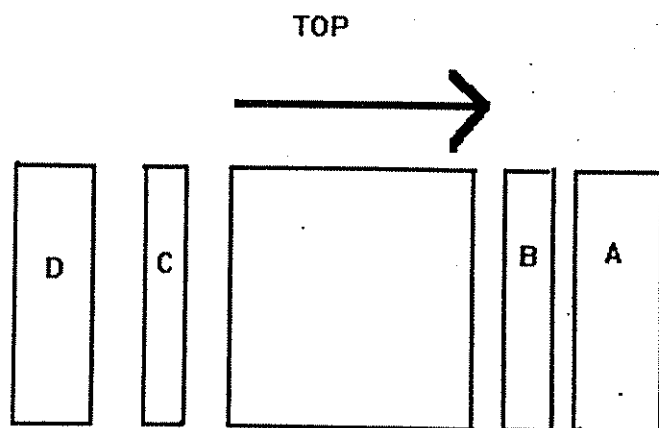
GENERAL SAMPLE OBSERVATIONS:

Sample Dimensions: 10.1 cm WIDTH, 20 cm LENGTH, FULL SLAB

Surface Conditions:

Top- TINES, MAX DEPTH 4mm, MAX WIDTH 6mm,@ 1-2 cm INTERVALSBottom- CAST ON 9cm BASE COURSE W/ ASPHALT SEALReinforcement: NONE PRESENT

Cracks and Other

Distinctive Features: NO CRACKS NOTED, APPROXIMATELY1 cm OF SPALLING OCCURED ON PART OFTHE SAMPLE BOTTOM. APPEARS TO HAVEAGGREGATE RXNS. VOIDS IN MAN? OF AGGREGATE;VOIDS IN PASTE CONCENTRATE AROUND AGGREGATE.

OK

HR - 358 Concrete Cores 1994

SAMPLE IDENTIFICATION: 52, BUCHANAN CO., U.S. 20, STD 385+64, EB LANE
(MID PANEL, NO VIB TRAIL)

GENERAL SAMPLE OBSERVATIONS:

Sample Dimensions: 10.1 cm WIDTH X 20.5 cm LENGTH, FULL SLAB

Surface Conditions:

Top-TINES, MAX DEPTH 4mm, MAX WIDTH 5mm,

@ 1-2 cm INTERVALS,

Bottom-CAST ON 10cm BASE COURSE W/ ASPHALT SEAL

Reinforcement: NONE PRESENT

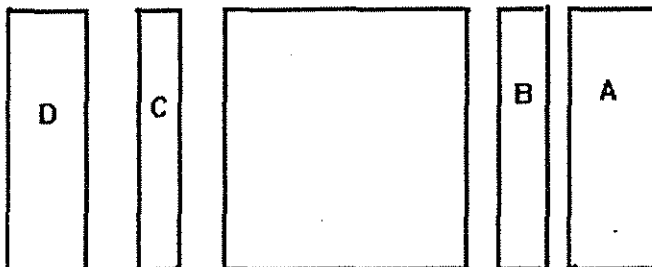
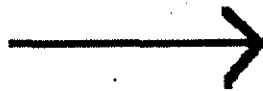
Cracks and Other

Distinctive Features: CRACKED 0.5 cm FROM BOTTOM OF SAMPLE

W/ SOME SPALL OFF. VOIDS CONCENTRATED AROUND

AGGREGATE. ALSO, VOIDS IN MUCH OF AGGREGATE.

TOP



HR - 358 Concrete Cores 1994

SAMPLE IDENTIFICATION: 53, BUCHANAN Co., U.S. 20, STA 385+64, EB LANE
(JOINT, NO VIB TRAIL)

GENERAL SAMPLE OBSERVATIONS:

Sample Dimensions: 10.1 cm WIDTH, 20 cm LENGTH, FULL SLAB

Surface Conditions:

Top- TINES, MAX DEPTH 4mm, MAX WIDTH 5mm,

@ 1-2 cm INTERVALS

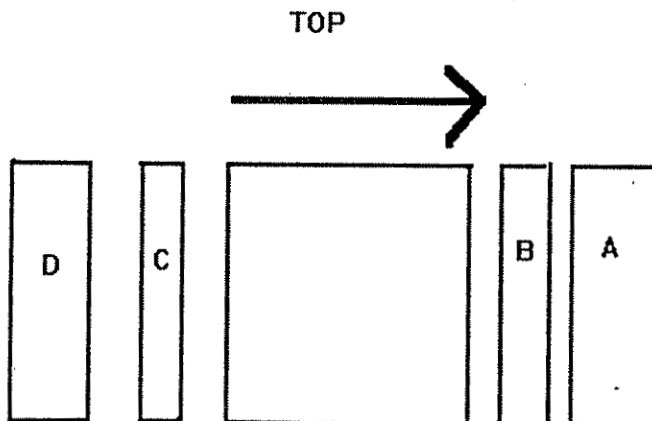
Bottom- CAST ON 10cm BASE COURSE W/ ASPALT SEAL

Reinforcement: NONE PRESENT

Cracks and Other

Distinctive Features: NO CRACKS NOTED. VOIDS CONCENTRATED

AROUND AGGREGATE. ALSO, VOIDS IN MUCH
OF AGGREGATE. LARGE VOIDS CONCENTRATED
IN TOP 1/3 OF PASTE.



AK

APPENDIX B (SUMMARY OF SHALE COUNTS)

Core 1
I-35
Story County

	Total Area (mm ²)	Largest Shale (mm)	Number of Shale	Area per Shale (mm ²)	Total Area of Shale (mm ²)	Percent Shale	Average
Section A	8107	2	7	3.14	21.99	0.27	
Section B Top Surface	8107	5	7	19.63	137.44	1.70	
Section B Bottom Surface	8107	3	11	7.07	77.75	0.96	
Section C Top Surface	8107	3.5	7	9.62	67.35	0.83	
Section C Bottom Surface	8107	2	5	3.14	15.71	0.19	
Section D	8107	3	9	7.07	63.62	0.78	
sum	48643.92				383.86		0.789129

	Total Area (mm ²)	Largest Shale (mm)	Number of Shale	Area per Shale (mm ²)	Total Area of Shale (mm ²)	Percent Shale	Average
Section L Face 1							
Depth							
1"	2581	2	3	3.14	9.42	0.37	
2"	2581	5	3	19.63	58.90	2.28	
3"	2581	0	0	0.00	0.00	0.00	
4"	2581	3	4	7.07	28.27	1.10	
5"	2581	3	5	7.07	35.34	1.37	
6"	2581	2	4	3.14	12.57	0.49	
6.5"	1290	2	2	3.14	6.28	0.49	
sum	16774				150.80		0.86955

	Total Area (mm ²)	Largest Shale (mm)	Number of Shale	Area per Shale (mm ²)	Total Area of Shale (mm ²)	Percent Shale	Average
Section L Face 2							
Depth							
1"	2581	2	6	3.14	18.85	0.73	
2"	2581	8	2	50.27	100.53	3.90	
3"	2581	3	3	7.07	21.21	0.82	
4"	2581	3.5	4	9.62	38.48	1.49	
5"	2581	2	3	3.14	9.42	0.37	
6"	2581	2	5	3.14	15.71	0.61	
6.5"	1290	1	3	0.79	2.36	0.18	
sum	16774				206.56		1.156501

	Total Area (mm ²)	Largest Shale (mm)	Number of Shale	Area per Shale (mm ²)	Total Area of Shale (mm ²)	Percent Shale	Average
Section L Face 3							
Depth							
1"	2581	1	2	0.79	1.57	0.06	
2"	2581	4	4	12.57	50.27	1.95	
3"	2581	4	5	12.57	62.83	2.43	
4"	2581	3	6	7.07	42.41	1.64	
5"	2581	4	2	12.57	25.13	0.97	
6"	2581	5	5	19.63	98.17	3.80	
6.5"	1290	3	2	7.07	14.14	1.10	
sum	16774				294.52		1.708665

	Total Area (mm ²)	Largest Shale (mm)	Number of Shale	Area per Shale (mm ²)	Total Area of Shale (mm ²)	Percent Shale	Average
Section L Face 4							
Depth							
1"	2581	7	4	38.48	153.94	5.97	
2"	2581	3	5	7.07	35.34	1.37	
3"	2581	3	6	7.07	42.41	1.64	
4"	2581	2	4	3.14	12.57	0.49	
5"	2581	1	3	0.79	2.36	0.09	
6"	2581	1	2	0.79	1.57	0.06	
6.5"	1290	5	2	19.63	39.27	3.04	
sum	16774				287.46		1.808663

Average Percent Shale 1.14 diameter check 1.135053

Core 2
I-35
Story County

	Total Area (mm ²)	Largest Shale (mm)	Number of Shale	Area per Shale (mm ²)	Total Area of Shale (mm ²)	Percent Shale	Average
Section A	8107	3	9	7.07	63.62	0.78	
Section B Top Surface	8107	2.5	7	4.91	34.36	0.42	
Section B Bottom Surface	8107	3	10	7.07	70.69	0.87	
Section C Top Surface	8107	3	5	7.07	35.34	0.44	
Section C Bottom Surface	8107	4	6	12.57	75.40	0.93	
Section D	8107	2	11	3.14	34.56	0.43	
sum	48643.92				313.96		0.645431

	Total Area (mm ²)	Largest Shale (mm)	Number of Shale	Area per Shale (mm ²)	Total Area of Shale (mm ²)	Percent Shale	Average
Section L Face 1							
Depth							
1"	2581	5	6	19.63	117.81	4.57	
2"	2581	4	5	12.57	62.83	2.43	
3"	2581	0	0	0.00	0.00	0.00	
4"	2581	1	2	0.79	1.57	0.06	
5"	2581	1	3	0.79	2.36	0.09	
6"	2581	4	2	12.57	25.13	0.97	
sum	15484				209.70		1.354324

	Total Area (mm ²)	Largest Shale (mm)	Number of Shale	Area per Shale (mm ²)	Total Area of Shale (mm ²)	Percent Shale	Average
Section L Face 2							
Depth							
1"	2581	2	4	3.14	12.57	0.49	
2"	2581	5	5	19.63	98.17	3.80	
3"	2581	0	0	0.00	0.00	0.00	
4"	2581	3	3	7.07	21.21	0.82	
5"	2581	3	3	7.07	21.21	0.82	
6"	2581	3.5	5	9.62	48.11	1.86	
sum	15484				201.26		1.299796

	Total Area (mm ²)	Largest Shale (mm)	Number of Shale	Area per Shale (mm ²)	Total Area of Shale (mm ²)	Percent Shale	Average
Section L Face 3							
Depth							
1"	2581	2.5	3	4.91	14.73	0.57	
2"	2581	2	4	3.14	12.57	0.49	
3"	2581	0	0	0.00	0.00	0.00	
4"	2581	5.5	4	23.76	95.03	3.68	
5"	2581	2	4	3.14	12.57	0.49	
6"	2581	2	6	3.14	18.85	0.73	
sum	15484				153.74		0.992917

	Total Area (mm ²)	Largest Shale (mm)	Number of Shale	Area per Shale (mm ²)	Total Area of Shale (mm ²)	Percent Shale	Average
Section L Face 4							
Depth							
1"	2581	2	5	3.14	15.71	0.61	
2"	2581	3	6	7.07	42.41	1.64	
3"	2581	0	0	0.00	0.00	0.00	
4"	2581	3.5	7	9.62	67.35	2.61	
5"	2581	1	1	0.79	0.79	0.03	
6"	2581	2	4	3.14	12.57	0.49	
sum	15484				138.82		0.896542

Average Percent Shale diameter check
0.92 0.92014

Core 3
I-35
Story County

	Total Area (mm ²)	Largest Shale (mm)	Number of Shale	Area per Shale (mm ²)	Total Area of Shale (mm ²)	Percent Shale	Average
Section A	8107	4	8	12.57	100.53	1.24	
Section B Top Surface	8107	4	7	12.57	87.96	1.09	
Section B Bottom Surface	8107	2	8	3.14	25.13	0.31	
Section C Top Surface	8107	3	11	7.07	77.75	0.96	
Section C Bottom Surface	8107	4	16	12.57	201.06	2.48	
Section D	8107	4	7	12.57	87.96	1.09	
sum	48643.92				580.41		1.193179

	Total Area (mm ²)	Largest Shale (mm)	Number of Shale	Area per Shale (mm ²)	Total Area of Shale (mm ²)	Percent Shale	Average
Section L							
Face 1							
Depth							
1"	2581	2	7	3.14	21.99	0.85	
2"	2581	2	7	3.14	21.99	0.85	
3"	2581	2	8	3.14	25.13	0.97	
4"	2581	2	4	3.14	12.57	0.49	
5"	2581	1	6	0.79	4.71	0.18	
6"	2581	5	8	19.63	157.08	6.09	
6.5"	1290	5	5	19.63	98.17	7.61	
sum	16774				341.65		2.434739

	Total Area (mm ²)	Largest Shale (mm)	Number of Shale	Area per Shale (mm ²)	Total Area of Shale (mm ²)	Percent Shale	Average
Section L							
Face 2							
Depth							
1"	2581	2	4	3.14	12.57	0.49	
2"	2581	1	4	0.79	3.14	0.12	
3"	2581	4	8	12.57	100.53	3.90	
4"	2581	2	7	3.14	21.99	0.85	
5"	2581	1	2	0.79	1.57	0.06	
6"	2581	2	6	3.14	18.85	0.73	
6.5"	1290	1	7	0.79	5.50	0.43	
sum	16774				164.15		0.939114

	Total Area (mm ²)	Largest Shale (mm)	Number of Shale	Area per Shale (mm ²)	Total Area of Shale (mm ²)	Percent Shale	Average
Section L							
Face 3							
Depth							
1"	2581	4	10	12.57	125.66	4.87	
2"	2581	3	6	7.07	42.41	1.64	
3"	2581	3	9	7.07	63.62	2.47	
4"	2581	5	9	19.63	176.71	6.85	
5"	2581	5	7	19.63	137.44	5.33	
6"	2581	2	4	3.14	12.57	0.49	
6.5"	1290	2	6	3.14	18.85	1.46	
sum	16774				577.27		3.299941

	Total Area (mm ²)	Largest Shale (mm)	Number of Shale	Area per Shale (mm ²)	Total Area of Shale (mm ²)	Percent Shale	Average
Section L							
Face 4							
Depth							
1"	2581	2	4	3.14	12.57	0.49	
2"	2581	5	9	19.63	176.71	6.85	
3"	2581	3	6	7.07	42.41	1.64	
4"	2581	6	6	28.27	169.65	6.57	
5"	2581	3	8	7.07	56.55	2.19	
6"	2581	3	7	7.07	49.48	1.92	
6.5"	1290	2	6	3.14	18.85	1.46	
sum	16774				526.22		3.017337

Average Percent Shale diameter check
1.89 1.905998

Core 4
I-35
Story County

	Total Area (mm ²)	Largest Shale (mm)	Number of Shale	Area per Shale (mm ²)	Total Area of Shale (mm ²)	Percent Shale	Average
Section A	8107	2.5	10	4.91	49.09	0.61	
Section B Top Surface	8107	3	6	7.07	42.41	0.52	
Section B Bottom Surface	8107	3	10	7.07	70.69	0.87	
Section C Top Surface	8107	6.5	9	33.18	298.65	3.68	
Section C Bottom Surface	8107	2	4	3.14	12.57	0.16	
Section D	8107	5	8	19.63	157.08	1.94	
sum	48643.92				630.48		1.296109

	Total Area (mm ²)	Largest Shale (mm)	Number of Shale	Area per Shale (mm ²)	Total Area of Shale (mm ²)	Percent Shale	Average
Section L Face 1							
Depth							
1"	2581	2	2	3.14	6.28	0.24	
2"	2581	2	4	3.14	12.57	0.49	
3"	2581	3	2	7.07	14.14	0.55	
4"	2581	2	3	3.14	9.42	0.37	
5"	2581	3.5	5	9.62	48.11	1.86	
6"	2581	4	4	12.57	50.27	1.95	
6.75"	1935	2	3	3.14	9.42	0.49	
sum	17419				150.21		0.848898

	Total Area (mm ²)	Largest Shale (mm)	Number of Shale	Area per Shale (mm ²)	Total Area of Shale (mm ²)	Percent Shale	Average
Section L Face 2							
Depth							
1"	2581	2	3	3.14	9.42	0.37	
2"	2581	2	3	3.14	9.42	0.37	
3"	2581	3	6	7.07	42.41	1.64	
4"	2581	2	3	3.14	9.42	0.37	
5"	2581	2	5	3.14	15.71	0.61	
6"	2581	3	4	7.07	28.27	1.10	
6.75"	1935	1	1	0.79	0.79	0.04	
sum	17419				115.45		0.640568

	Total Area (mm ²)	Largest Shale (mm)	Number of Shale	Area per Shale (mm ²)	Total Area of Shale (mm ²)	Percent Shale	Average
Section L Face 3							
Depth							
1"	2581	3	2	7.07	14.14	0.55	
2"	2581	4	2	12.57	25.13	0.97	
3"	2581	2	3	3.14	9.42	0.37	
4"	2581	2	2	3.14	6.28	0.24	
5"	2581	3.5	2	9.62	19.24	0.75	
6"	2581	2	3	3.14	9.42	0.37	
6.75"	1935	3	3	7.07	21.21	1.10	
sum	17419				104.85		0.619554

	Total Area (mm ²)	Largest Shale (mm)	Number of Shale	Area per Shale (mm ²)	Total Area of Shale (mm ²)	Percent Shale	Average
Section L Face 4							
Depth							
1"	2581	2	4	3.14	12.57	0.49	
2"	2581	2	2	3.14	6.28	0.24	
3"	2581	3	2	7.07	14.14	0.55	
4"	2581	5	5	19.63	98.17	3.80	
5"	2581	3	2	7.07	14.14	0.55	
6"	2581	2	6	3.14	18.85	0.73	
6.75"	1935	1	2	0.79	1.57	0.08	
sum	17419				165.72		0.920273

Average Percent Shale diameter 0.99 check 0.97883

Core 5
I-35
Story County

	Total Area (mm ²)	Largest Shale (mm)	Number of Shale	Area per Shale (mm ²)	Total Area of Shale (mm ²)	Percent Shale	Average
Section A	8107	1	6	0.79	4.71	0.06	
Section B Top Surface	8107	3	8	7.07	56.55	0.70	
Section B Bottom Surface	8107	3	9	7.07	63.62	0.78	
Section C Top Surface	8107	2	9	3.14	28.27	0.35	
Section C Bottom Surface	8107	6	9	28.27	254.47	3.14	
Section D	8107	2	5	3.14	15.71	0.19	
sum	48643.92				423.33		0.870262

	Total Area (mm ²)	Largest Shale (mm)	Number of Shale	Area per Shale (mm ²)	Total Area of Shale (mm ²)	Percent Shale	Average
Section L Face 1							
Depth							
1"	2581	5	7	19.63	137.44	5.33	
2"	2581	2	3	3.14	9.42	0.37	
3"	2581	2	5	3.14	15.71	0.61	
4"	2581	3	4	7.07	28.27	1.10	
5"	2581	2	6	3.14	18.85	0.73	
6"	2581	4	8	12.57	100.53	3.90	
6.5"	1290	5	6	19.63	117.81	9.13	
sum	16774				428.04		3.021685

	Total Area (mm ²)	Largest Shale (mm)	Number of Shale	Area per Shale (mm ²)	Total Area of Shale (mm ²)	Percent Shale	Average
Section L Face 2							
Depth							
1"	2581	3.5	10	9.62	96.21	3.73	
2"	2581	2	6	3.14	18.85	0.73	
3"	2581	2	10	3.14	31.42	1.22	
4"	2581	3	4	7.07	28.27	1.10	
5"	2581	2	4	3.14	12.57	0.49	
6"	2581	2	5	3.14	15.71	0.61	
6.5"	1290	2	3	3.14	9.42	0.73	
sum	16774				212.45		1.228239

	Total Area (mm ²)	Largest Shale (mm)	Number of Shale	Area per Shale (mm ²)	Total Area of Shale (mm ²)	Percent Shale	Average
Section L Face 3							
Depth							
1"	2581	2	6	3.14	18.85	0.73	
2"	2581	5	8	19.63	157.08	6.09	
3"	2581	5	5	19.63	98.17	3.80	
4"	2581	2	5	3.14	15.71	0.61	
5"	2581	2	5	3.14	15.71	0.61	
6"	2581	2	7	3.14	21.99	0.85	
6.5"	1290	3.5	8	9.62	76.97	5.97	
sum	16774				404.48		2.66517

	Total Area (mm ²)	Largest Shale (mm)	Number of Shale	Area per Shale (mm ²)	Total Area of Shale (mm ²)	Percent Shale	Average
Section L Face 4							
Depth							
1"	2581	3	2	7.07	14.14	0.55	
2"	2581	2	9	3.14	28.27	1.10	
3"	2581	1	1	0.79	0.79	0.03	
4"	2581	2	7	3.14	21.99	0.85	
5"	2581	2	5	3.14	15.71	0.61	
6"	2581	3	5	7.07	35.34	1.37	
6.5"	1290	3	4	7.07	28.27	2.19	
sum	16774				144.51		0.956505

Average Percent Shale diameter 1.39 check 1.506578

Core 6
I-35
Story County

	Total Area (mm ²)	Largest Shale (mm)	Number of Shale	Area per Shale (mm ²)	Total Area of Shale (mm ²)	Percent Shale	Average
Section A	8107	4	15	12.57	188.50	2.33	
Section B Top Surface	8107	4	15	12.57	188.50	2.33	
Section B Bottom Surface	8107	3	5	7.07	35.34	0.44	
Section C Top Surface	8107	3	13	7.07	91.89	1.13	
Section C Bottom Surface	8107	2	15	3.14	47.12	0.58	
Section D	8107	3	16	7.07	113.10	1.40	
sum	48643.92				664.45		1.36594

	Total Area (mm ²)	Largest Shale (mm)	Number of Shale	Area per Shale (mm ²)	Total Area of Shale (mm ²)	Percent Shale	Average
Section L Face 1							
Depth							
1"	2581	3	4	7.07	28.27	1.10	
2"	2581	3	5	7.07	35.34	1.37	
3"	2581	2	1	3.14	3.14	0.12	
4"	2581	2	3	3.14	9.42	0.37	
5"	2581	3	7	7.07	49.48	1.92	
6"	2581	2	5	3.14	15.71	0.61	
6.5"	1290	2	5	3.14	15.71	1.22	
sum	16774				157.08		0.956505

	Total Area (mm ²)	Largest Shale (mm)	Number of Shale	Area per Shale (mm ²)	Total Area of Shale (mm ²)	Percent Shale	Average
Section L Face 2							
Depth							
1"	2581	2	3	3.14	9.42	0.37	
2"	2581	1	5	0.79	3.93	0.15	
3"	2581	2	4	3.14	12.57	0.49	
4"	2581	2	6	3.14	18.85	0.73	
5"	2581	2	4	3.14	12.57	0.49	
6"	2581	3	6	7.07	42.41	1.64	
6.5"	1290	2	6	3.14	18.85	1.46	
sum	16774				118.60		0.760856

	Total Area (mm ²)	Largest Shale (mm)	Number of Shale	Area per Shale (mm ²)	Total Area of Shale (mm ²)	Percent Shale	Average
Section L Face 3							
Depth							
1"	2581	2	5	3.14	15.71	0.61	
2"	2581	2	4	3.14	12.57	0.49	
3"	2581	2	3	3.14	9.42	0.37	
4"	2581	1	2	0.79	1.57	0.06	
5"	2581	1	4	0.79	3.14	0.12	
6"	2581	3	9	7.07	63.62	2.47	
6.5"	1290	2	3	3.14	9.42	0.73	
sum	16774				115.45		0.691292

	Total Area (mm ²)	Largest Shale (mm)	Number of Shale	Area per Shale (mm ²)	Total Area of Shale (mm ²)	Percent Shale	Average
Section L Face 4							
Depth							
1"	2581	2	3	3.14	9.42	0.37	
2"	2581	2	4	3.14	12.57	0.49	
3"	2581	3	6	7.07	42.41	1.64	
4"	2581	2	4	3.14	12.57	0.49	
5"	2581	1	7	0.79	5.50	0.21	
6"	2581	5	8	19.63	157.08	6.09	
6.5"	1290	1	3	0.79	2.36	0.18	
sum	16774				241.90		1.35215

Average Percent Shale 1.12 diameter check 1.119134

Core 7
I-35
Story County

	Total Area (mm ²)	Largest Shale (mm)	Number of Shale	Area per Shale (mm ²)	Total Area of Shale (mm ²)	Percent Shale	Average
Section A	8107	5	11	19.63	215.98	2.66	
Section B Top Surface	8107	3	9	7.07	63.62	0.78	
Section B Bottom Surface	8107	3	8	7.07	56.55	0.70	
Section C Top Surface	8107	4	12	12.57	150.80	1.86	
Section C Bottom Surface	8107	2	6	3.14	18.85	0.23	
Section D	8107	2	11	3.14	34.56	0.43	
sum	48643.92				540.35		1.110836

	Total Area (mm ²)	Largest Shale (mm)	Number of Shale	Area per Shale (mm ²)	Total Area of Shale (mm ²)	Percent Shale	Average
Section L							
Face 1							
Depth							
1"	2581	3	4	7.07	28.27	1.10	
2"	2581	5	8	19.63	157.08	6.09	
3"	2581	2	6	3.14	18.85	0.73	
4"	2581	2	5	3.14	15.71	0.61	
5"	2581	3	4	7.07	28.27	1.10	
6"	2581	2	5	3.14	15.71	0.61	
6.5"	1290	2	5	3.14	15.71	1.22	
sum	16774				279.60		1.634753

	Total Area (mm ²)	Largest Shale (mm)	Number of Shale	Area per Shale (mm ²)	Total Area of Shale (mm ²)	Percent Shale	Average
Section L							
Face 2							
Depth							
1"	2581	2	8	3.14	25.13	0.97	
2"	2581	2	10	3.14	31.42	1.22	
3"	2581	3	6	7.07	42.41	1.64	
4"	2581	4	7	12.57	87.96	3.41	
5"	2581	1	9	0.79	7.07	0.27	
6"	2581	2	7	3.14	21.99	0.85	
6.5"	1290	2	3	3.14	9.42	0.73	
sum	16774				225.41		1.299977

	Total Area (mm ²)	Largest Shale (mm)	Number of Shale	Area per Shale (mm ²)	Total Area of Shale (mm ²)	Percent Shale	Average
Section L							
Face 3							
Depth							
1"	2581	4	9	12.57	113.10	4.38	
2"	2581	2	5	3.14	15.71	0.61	
3"	2581	2	9	3.14	28.27	1.10	
4"	2581	2	7	3.14	21.99	0.85	
5"	2581	2	9	3.14	28.27	1.10	
6"	2581	4	8	12.57	100.53	3.90	
6.5"	1290	3	4	7.07	28.27	2.19	
sum	16774				336.15		2.017355

	Total Area (mm ²)	Largest Shale (mm)	Number of Shale	Area per Shale (mm ²)	Total Area of Shale (mm ²)	Percent Shale	Average
Section L							
Face 4							
Depth							
1"	2581	5	6	19.63	117.81	4.57	
2"	2581	2	7	3.14	21.99	0.85	
3"	2581	2	6	3.14	18.85	0.73	
4"	2581	4	4	12.57	50.27	1.95	
5"	2581	2	4	3.14	12.57	0.49	
6"	2581	4	3	12.57	37.70	1.46	
6.5"	1290	3	5	7.07	35.34	2.74	
sum	16774				294.52		1.826054

Average Percent Shale 1.45 check 1.449215

Core 8
I-35
Story County

	Total Area (mm ²)	Largest Shale (mm)	Number of Shale	Area per Shale (mm ²)	Total Area of Shale (mm ²)	Percent Shale	Average
Section A	8107	4	13	12.57	163.36	2.02	
Section B Top Surface	8107	3	16	7.07	113.10	1.40	
Section B Bottom Surface	8107	6	12	28.27	339.29	4.19	
Section C Top Surface	8107	4	13	12.57	163.36	2.02	
Section C Bottom Surface	8107	5	10	19.63	196.35	2.42	
Section D	8107	3	10	7.07	70.69	0.87	
sum	48643.92				1046.15		2.150629

	Total Area (mm ²)	Largest Shale (mm)	Number of Shale	Area per Shale (mm ²)	Total Area of Shale (mm ²)	Percent Shale	Average
Section L							
Face 1							
Depth							
1"	2581	2	8	3.14	25.13	0.97	
2"	2581	2	10	3.14	31.42	1.22	
3"	2581	2	13	3.14	40.84	1.58	
4"	2581	4	9	12.57	113.10	4.38	
5"	2581	4	8	12.57	100.53	3.90	
6"	2581	2	6	3.14	18.85	0.73	
6.5"	1290	2	4	3.14	12.57	0.97	
sum	16774				342.43		1.965182

	Total Area (mm ²)	Largest Shale (mm)	Number of Shale	Area per Shale (mm ²)	Total Area of Shale (mm ²)	Percent Shale	Average
Section L							
Face 2							
Depth							
1"	2581	4	5	12.57	62.83	2.43	
2"	2581	3	4	7.07	28.27	1.10	
3"	2581	3	9	7.07	63.62	2.47	
4"	2581	1	6	0.79	4.71	0.18	
5"	2581	2	12	3.14	37.70	1.46	
6"	2581	5	8	19.63	157.08	6.09	
6.5"	1290	2	4	3.14	12.57	0.97	
sum	16774				366.78		2.099963

	Total Area (mm ²)	Largest Shale (mm)	Number of Shale	Area per Shale (mm ²)	Total Area of Shale (mm ²)	Percent Shale	Average
Section L							
Face 3							
Depth							
1"	2581	2	7	3.14	21.99	0.85	
2"	2581	4	9	12.57	113.10	4.38	
3"	2581	4	7	12.57	87.96	3.41	
4"	2581	2	6	3.14	18.85	0.73	
5"	2581	4	6	12.57	75.40	2.92	
6"	2581	2	7	3.14	21.99	0.85	
6.5"	1290	3	5	7.07	35.34	2.74	
sum	16774				374.63		2.269525

	Total Area (mm ²)	Largest Shale (mm)	Number of Shale	Area per Shale (mm ²)	Total Area of Shale (mm ²)	Percent Shale	Average
Section L							
Face 4							
Depth							
1"	2581	2	5	3.14	15.71	0.61	
2"	2581	2	6	3.14	18.85	0.73	
3"	2581	2	4	3.14	12.57	0.49	
4"	2581	2	4	3.14	12.57	0.49	
5"	2581	4	6	12.57	75.40	2.92	
6"	2581	2	5	3.14	15.71	0.61	
6.5"	1290	4	8	12.57	100.53	7.79	
sum	16774				251.33		1.947791

Average Percent Shale 2.06 check 2.104246

UPDATED with proper calculation for area ON 10-2-95

Core 10
U.S. 520
Webster County

Calculated by TP using diameter

	Total Area (mm ²)	Largest Shale (mm)	Number of Shale	Area per Shale (mm ²)	Total Area of Shale (mm ²)	Percent Shale	Average
Section A	8107	2	6	3.14	18.85	0.23	
Section B Top Surface	8107	3	10	7.07	70.69	0.87	
Section B Bottom Surface	8107	8	11	50.27	552.92	6.82	
Section C Top Surface	8107	1.5	3	1.77	5.30	0.07	
Section C Bottom Surface	8107	5	3	19.63	58.90	0.73	
Section D	8107	4	5	12.57	62.83	0.78	
sum	48643.92				769.49		1.581891

	Total Area (mm ²)	Largest Shale (mm)	Number of Shale	Area per Shale (mm ²)	Total Area of Shale (mm ²)	Percent Shale	Average
Section L Face 1							
Depth							
1"	2581	2	2	3.14	6.28	0.24	
2"	2581	3	3	7.07	21.21	0.82	
3"	2581	2	5	3.14	15.71	0.61	
4"	2581	2	3	3.14	9.42	0.37	
5"	2581	1	2	0.79	1.57	0.06	
6"	2581	2	3	3.14	9.42	0.37	
sum	15484				63.62		0.410862

	Total Area (mm ²)	Largest Shale (mm)	Number of Shale	Area per Shale (mm ²)	Total Area of Shale (mm ²)	Percent Shale	Average
Section L Face 2							
Depth							
1"	2581	5	2	19.63	39.27	1.52	
2"	2581	4	6	12.57	75.40	2.92	
3"	2581	6	4	28.27	113.10	4.38	
4"	2581	3	3	7.07	21.21	0.82	
5"	2581	1	6	0.79	4.71	0.18	
6"	2581	2	3	3.14	9.42	0.37	
sum	15484				263.11		1.699245

	Total Area (mm ²)	Largest Shale (mm)	Number of Shale	Area per Shale (mm ²)	Total Area of Shale (mm ²)	Percent Shale	Average
Section L Face 3							
Depth							
1"	2581	2	2	3.14	6.28	0.24	
2"	2581	2	4	3.14	12.57	0.49	
3"	2581	2	3	3.14	9.42	0.37	
4"	2581	2.8	5	6.16	30.79	1.19	
5"	2581	2	7	3.14	21.99	0.85	
6"	2581	3	5	7.07	35.34	1.37	
sum	15484				116.40		0.751726

	Total Area (mm ²)	Largest Shale (mm)	Number of Shale	Area per Shale (mm ²)	Total Area of Shale (mm ²)	Percent Shale	Average
Section L Face 4							
Depth							
1"	2581	2	2	3.14	6.28	0.24	
2"	2581	2	2	3.14	6.28	0.24	
3"	2581	1	3	0.79	2.36	0.09	
4"	2581	2	3	3.14	9.42	0.37	
5"	2581	2	2	3.14	6.28	0.24	
6"	2581	1	3	0.79	2.36	0.09	
sum	15484				32.99		0.21304

Average Percent Shale 1.13 diameter check 1.126432

Core 11
U.S. 520
Webster County

	Total Area (mm ²)	Largest Shale (mm)	Number of Shale	Area per Shale (mm ²)	Total Area of Shale (mm ²)	Percent Shale	Average
Section A	8107	2	9	3.14	28.27	0.35	
Section B Top Surface	8107	4	5	12.57	62.83	0.78	
Section B Bottom Surface	8107	2	4	3.14	12.57	0.16	
Section C Top Surface	8107	4	3	12.57	37.70	0.47	
Section C Bottom Surface	8107	2.5	4	4.91	19.63	0.24	
Section D	8107	2	6	3.14	18.85	0.23	
sum	48643.92				179.86		0.36974

	Total Area (mm ²)	Largest Shale (mm)	Number of Shale	Area per Shale (mm ²)	Total Area of Shale (mm ²)	Percent Shale	Average
Section L Face 1							
Depth							
1"	2581	2	8	3.14	25.13	0.97	
2"	2581	1	6	0.79	4.71	0.18	
3"	2581	1	2	0.79	1.57	0.06	
4"	2581	3.5	6	9.62	57.73	2.24	
5"	2581	2.7	4	5.73	22.90	0.89	
6"	2581	2	6	3.14	18.85	0.73	
sum	15484				130.89		0.845362

	Total Area (mm ²)	Largest Shale (mm)	Number of Shale	Area per Shale (mm ²)	Total Area of Shale (mm ²)	Percent Shale	Average
Section L Face 2							
Depth							
1"	2581	5	5	19.63	98.17	3.80	
2"	2581	2	7	3.14	21.99	0.85	
3"	2581	1	3	0.79	2.36	0.09	
4"	2581	4	6	12.57	75.40	2.92	
5"	2581	2	2	3.14	6.28	0.24	
6"	2581	1	3	0.79	2.36	0.09	
sum	15484				206.56		1.334034

	Total Area (mm ²)	Largest Shale (mm)	Number of Shale	Area per Shale (mm ²)	Total Area of Shale (mm ²)	Percent Shale	Average
Section L Face 3							
Depth							
1"	2581	1	6	0.79	4.71	0.18	
2"	2581	1	2	0.79	1.57	0.06	
3"	2581	1	5	0.79	3.93	0.15	
4"	2581	2.5	4	4.91	19.63	0.76	
5"	2581	2	4	3.14	12.57	0.49	
6"	2581	3	7	7.07	49.48	1.92	
sum	15484				91.89		0.593468

	Total Area (mm ²)	Largest Shale (mm)	Number of Shale	Area per Shale (mm ²)	Total Area of Shale (mm ²)	Percent Shale	Average
Section L Face 4							
Depth							
1"	2581	2	3	3.14	9.42	0.37	
2"	2581	1	4	0.79	3.14	0.12	
3"	2581	2	4	3.14	12.57	0.49	
4"	2581	1	3	0.79	2.36	0.09	
5"	2581	3.5	5	9.62	48.11	1.86	
6"	2581	3	3	7.07	21.21	0.82	
sum	15484				96.80		0.62517

Average Percent Shale 0.64 diameter check 0.638459

Core 13
U.S. 520
Webster County

	Total Area (mm ²)	Largest Shale (mm)	Number of Shale	Area per Shale (mm ²)	Total Area of Shale (mm ²)	Percent Shale	Average
Section A	8107	5	9	19.63	176.71	2.18	
Section B Top Surface	8107	5.5	6	23.76	142.55	1.76	
Section B Bottom Surface	8107	3.5	6	9.62	57.73	0.71	
Section C Top Surface	8107	3	6	7.07	42.41	0.52	
Section C Bottom Surface	8107	2	7	3.14	21.99	0.27	
Section D	8107	2	4	3.14	12.57	0.16	
sum	48643.92				453.96		0.933231

	Total Area (mm ²)	Largest Shale (mm)	Number of Shale	Area per Shale (mm ²)	Total Area of Shale (mm ²)	Percent Shale	Average
Section L Face 1							
Depth							
1"	2581	1	1	0.79	0.79	0.03	
2"	2581	5	5	19.63	98.17	3.80	
3"	2581	2	6	3.14	18.85	0.73	
4"	2581	1	3	0.79	2.36	0.09	
5"	2581	4	4	12.57	50.27	1.95	
6"	2581	9.5	6	70.88	425.29	16.48	
sum	15484				595.72		3.847395

	Total Area (mm ²)	Largest Shale (mm)	Number of Shale	Area per Shale (mm ²)	Total Area of Shale (mm ²)	Percent Shale	Average
Section L Face 2							
Depth							
1"	2581	2	6	3.14	18.85	0.73	
2"	2581	2	3	3.14	9.42	0.37	
3"	2581	2	3	3.14	9.42	0.37	
4"	2581	2	2	3.14	6.28	0.24	
5"	2581	2	2	3.14	6.28	0.24	
6"	2581	5	4	19.63	78.54	3.04	
sum	15484				128.81		0.831869

	Total Area (mm ²)	Largest Shale (mm)	Number of Shale	Area per Shale (mm ²)	Total Area of Shale (mm ²)	Percent Shale	Average
Section L Face 3							
Depth							
1"	2581	1	3	0.79	2.36	0.09	
2"	2581	1.5	1	1.77	1.77	0.07	
3"	2581	1	4	0.79	3.14	0.12	
4"	2581	2	5	3.14	15.71	0.61	
5"	2581	2	3	3.14	9.42	0.37	
6"	2581	1	4	0.79	3.14	0.12	
sum	15484				35.54		0.229525

	Total Area (mm ²)	Largest Shale (mm)	Number of Shale	Area per Shale (mm ²)	Total Area of Shale (mm ²)	Percent Shale	Average
Section L Face 4							
Depth							
1"	2581	1	1	0.79	0.79	0.03	
2"	2581	3	2	7.07	14.14	0.55	
3"	2581	1.5	5	1.77	8.84	0.34	
4"	2581	3	4	7.07	28.27	1.10	
5"	2581	3	2	7.07	14.14	0.55	
6"	2581	3.5	2	9.62	19.24	0.75	
sum	15484				85.41		0.551621

Average Percent Shale 1.18 check 1.175123

Core 14
U.S. 520
Webster County

	Total Area (mm ²)	Largest Shale (mm)	Number of Shale	Area per Shale (mm ²)	Total Area of Shale (mm ²)	Percent Shale	Average
Section A	8107	4	8	12.57	100.53	1.24	
Section B Top Surface	8107	1	6	0.79	4.71	0.06	
Section B Bottom Surface	8107	2	8	3.14	25.13	0.31	
Section C Top Surface	8107	5	7	19.63	137.44	1.70	
Section C Bottom Surface	8107	3	6	7.07	42.41	0.52	
Section D	8107	6	14	28.27	395.84	4.88	
sum	48643.92				706.07		1.451513

	Total Area (mm ²)	Largest Shale (mm)	Number of Shale	Area per Shale (mm ²)	Total Area of Shale (mm ²)	Percent Shale	Average
Section L							
Face 1							
Depth							
1"	2581	2	7	3.14	21.99	0.85	
2"	2581	1	4	0.79	3.14	0.12	
3"	2581	3	8	7.07	56.55	2.19	
4"	2581	3	4	7.07	28.27	1.10	
5"	2581	1	2	0.79	1.57	0.06	
6"	2581	2	7	3.14	21.99	0.85	
sum	15484				133.52		0.862303

	Total Area (mm ²)	Largest Shale (mm)	Number of Shale	Area per Shale (mm ²)	Total Area of Shale (mm ²)	Percent Shale	Average
Section L							
Face 2							
Depth							
1"	2581	2.5	5	4.91	24.54	0.95	
2"	2581	4	8	12.57	100.53	3.90	
3"	2581	2	4	3.14	12.57	0.49	
4"	2581	3	3	7.07	21.21	0.82	
5"	2581	1	5	0.79	3.93	0.15	
6"	2581	2	3	3.14	9.42	0.37	
sum	15484				172.20		1.112118

	Total Area (mm ²)	Largest Shale (mm)	Number of Shale	Area per Shale (mm ²)	Total Area of Shale (mm ²)	Percent Shale	Average
Section L							
Face 3							
Depth							
1"	2581	2	7	3.14	21.99	0.85	
2"	2581	2	6	3.14	18.85	0.73	
3"	2581	4	3	12.57	37.70	1.46	
4"	2581	3	3	7.07	21.21	0.82	
5"	2581	3	3	7.07	21.21	0.82	
6"	2581	1	2	0.79	1.57	0.06	
sum	15484				122.52		0.79129

	Total Area (mm ²)	Largest Shale (mm)	Number of Shale	Area per Shale (mm ²)	Total Area of Shale (mm ²)	Percent Shale	Average
Section L							
Face 4							
Depth							
1"	2581	1	2	0.79	1.57	0.06	
2"	2581	5	12	19.63	235.62	9.13	
3"	2581	5	4	19.63	78.54	3.04	
4"	2581	2	5	3.14	15.71	0.61	
5"	2581	3	5	7.07	35.34	1.37	
6"	2581	2	4	3.14	12.57	0.49	
sum	15484				379.35		2.449956

Average Percent Shale 1.37 diameter check 1.363302

Core 15
U.S. 520
Webster County

	Total Area (mm ²)	Largest Shale (mm)	Number of Shale	Area per Shale (mm ²)	Total Area of Shale (mm ²)	Percent Shale	Average
Section A	8107	1	4	0.79	3.14	0.04	
Section B Top Surface	8107	6.5	4	33.18	132.73	1.64	
Section B Bottom Surface	8107	5	7	19.63	137.44	1.70	
Section C Top Surface	8107	3	8	7.07	56.55	0.70	
Section C Bottom Surface	8107	2	8	3.14	25.13	0.31	
Section D	8107	3	11	7.07	77.75	0.96	
sum	48643.92				432.75		0.889637

	Total Area (mm ²)	Largest Shale (mm)	Number of Shale	Area per Shale (mm ²)	Total Area of Shale (mm ²)	Percent Shale	Average
Section L							
Face 1							
Depth							
1"	2581	2.5	5	4.91	24.54	0.95	
2"	2581	3	4	7.07	28.27	1.10	
3"	2581	2	6	3.14	18.85	0.73	
4"	2581	2	5	3.14	15.71	0.61	
5"	2581	3	4	7.07	28.27	1.10	
6"	2581	2	4	3.14	12.57	0.49	
7"	2581	2	5	3.14	15.71	0.61	
sum	18064				143.92		0.796725

	Total Area (mm ²)	Largest Shale (mm)	Number of Shale	Area per Shale (mm ²)	Total Area of Shale (mm ²)	Percent Shale	Average
Section L							
Face 2							
Depth							
1"	2581	4	6	12.57	75.40	2.92	
2"	2581	3	5	7.07	35.34	1.37	
3"	2581	2	5	3.14	15.71	0.61	
4"	2581	2	5	3.14	15.71	0.61	
5"	2581	1	2	0.79	1.57	0.06	
6"	2581	2	3	3.14	9.42	0.37	
7"	2581	2	3	3.14	9.42	0.37	
sum	18064				162.58		0.899984

	Total Area (mm ²)	Largest Shale (mm)	Number of Shale	Area per Shale (mm ²)	Total Area of Shale (mm ²)	Percent Shale	Average
Section L							
Face 3							
Depth							
1"	2581	3	4	7.07	28.27	1.10	
2"	2581	2	6	3.14	18.85	0.73	
3"	2581	1	3	0.79	2.36	0.09	
4"	2581	5	9	19.63	176.71	6.85	
5"	2581	2	8	3.14	25.13	0.97	
6"	2581	2	6	3.14	18.85	0.73	
7"	2581	1	4	0.79	3.14	0.12	
sum	18064				273.32		1.513016

	Total Area (mm ²)	Largest Shale (mm)	Number of Shale	Area per Shale (mm ²)	Total Area of Shale (mm ²)	Percent Shale	Average
Section L							
Face 4							
Depth							
1"	2581	2	4	3.14	12.57	0.49	
2"	2581	2	4	3.14	12.57	0.49	
3"	2581	3	3	7.07	21.21	0.82	
4"	2581	4	4	12.57	50.27	1.95	
5"	2581	3	2	7.07	14.14	0.55	
6"	2581	1	3	0.79	2.36	0.09	
7"	2581	1	3	0.79	2.36	0.09	
sum	18064				115.45		0.639119

Average Percent Shale diameter check
0.93 0.933011

Core 16
U.S. 520
Webster County

	Total Area (mm ²)	Largest Shale (mm)	Number of Shale	Area per Shale (mm ²)	Total Area of Shale (mm ²)	Percent Shale	Average
Section A	8107	5	8	19.63	157.08	1.94	
Section B Top Surface	8107	2	8	3.14	25.13	0.31	
Section B Bottom Surface	8107	2	10	3.14	31.42	0.39	
Section C Top Surface	8107	2	9	3.14	28.27	0.35	
Section C Bottom Surface	8107	4	8	12.57	100.53	1.24	
Section D	8107	1	13	0.79	10.21	0.13	
sum	48643.92				352.64		0.724949

	Total Area (mm ²)	Largest Shale (mm)	Number of Shale	Area per Shale (mm ²)	Total Area of Shale (mm ²)	Percent Shale	Average
Section L Face 1							
Depth							
1"	2581	1.5	4	1.77	7.07	0.27	
2"	2581	2	4	3.14	12.57	0.49	
3"	2581	2	6	3.14	18.85	0.73	
4"	2581	2	3	3.14	9.42	0.37	
5"	2581	2	4	3.14	12.57	0.49	
6"	2581	2	3	3.14	9.42	0.37	
6.5"	1290	1	2	0.79	1.57	0.12	
sum	16774				71.47		0.404341

	Total Area (mm ²)	Largest Shale (mm)	Number of Shale	Area per Shale (mm ²)	Total Area of Shale (mm ²)	Percent Shale	Average
Section L Face 2							
Depth							
1"	2581	3	5	7.07	35.34	1.37	
2"	2581	2	2	3.14	6.28	0.24	
3"	2581	4	5	12.57	62.83	2.43	
4"	2581	3	4	7.07	28.27	1.10	
5"	2581	3	3	7.07	21.21	0.82	
6"	2581	1	5	0.79	3.93	0.15	
6.5"	1290	1	4	0.79	3.14	0.24	
sum	16774				161.01		0.908679

	Total Area (mm ²)	Largest Shale (mm)	Number of Shale	Area per Shale (mm ²)	Total Area of Shale (mm ²)	Percent Shale	Average
Section L Face 3							
Depth							
1"	2581	2	6	3.14	18.85	0.73	
2"	2581	1	4	0.79	3.14	0.12	
3"	2581	5	6	19.63	117.81	4.57	
4"	2581	2	6	3.14	18.85	0.73	
5"	2581	3	4	7.07	28.27	1.10	
6"	2581	2	5	3.14	15.71	0.61	
6.5"	1290	1	4	0.79	3.14	0.24	
sum	16774				205.77		1.156501

	Total Area (mm ²)	Largest Shale (mm)	Number of Shale	Area per Shale (mm ²)	Total Area of Shale (mm ²)	Percent Shale	Average
Section L Face 4							
Depth							
1"	2581	1	5	0.79	3.93	0.15	
2"	2581	1	5	0.79	3.93	0.15	
3"	2581	1	3	0.79	2.36	0.09	
4"	2581	2	4	3.14	12.57	0.49	
5"	2581	3	6	7.07	42.41	1.64	
6"	2581	3	5	7.07	35.34	1.37	
6.5"	1290	1	3	0.79	2.36	0.18	
sum	16774				102.89		0.582598

Average Percent Shale

diameter
0.77

check
0.747025

Core 17
U.S. 520
Webster County

	Total Area (mm ²)	Largest Shale (mm)	Number of Shale	Area per Shale (mm ²)	Total Area of Shale (mm ²)	Percent Shale	Average
Section A	8107	1	6	0.79	4.71	0.06	
Section B Top Surface	8107	2	3	3.14	9.42	0.12	
Section B Bottom Surface	8107	4	6	12.57	75.40	0.93	
Section C Top Surface	8107	6	6	28.27	169.65	2.09	
Section C Bottom Surface	8107	6	4	28.27	113.10	1.40	
Section D	8107	7	6	38.48	230.91	2.85	
sum	48643.92				603.19		1.240002

	Total Area (mm ²)	Largest Shale (mm)	Number of Shale	Area per Shale (mm ²)	Total Area of Shale (mm ²)	Percent Shale	Average
Section L							
Face 1							
Depth							
1"	2581	1	2	0.79	1.57	0.06	
2"	2581	2	4	3.14	12.57	0.49	
3"	2581	1	2	0.79	1.57	0.06	
4"	2581	1	2	0.79	1.57	0.06	
5"	2581	1	3	0.79	2.36	0.09	
6"	2581	1	5	0.79	3.93	0.15	
sum	15484				23.56		0.152171

	Total Area (mm ²)	Largest Shale (mm)	Number of Shale	Area per Shale (mm ²)	Total Area of Shale (mm ²)	Percent Shale	Average
Section L							
Face 2							
Depth							
1"	2581	2	1	3.14	3.14	0.12	
2"	2581	2	3	3.14	9.42	0.37	
3"	2581	1	1	0.79	0.79	0.03	
4"	2581	2	3	3.14	9.42	0.37	
5"	2581	1	2	0.79	1.57	0.06	
6"	2581	2	3	3.14	9.42	0.37	
sum	15484				33.77		0.218112

	Total Area (mm ²)	Largest Shale (mm)	Number of Shale	Area per Shale (mm ²)	Total Area of Shale (mm ²)	Percent Shale	Average
Section L							
Face 3							
Depth							
1"	2581	1	4	0.79	3.14	0.12	
2"	2581	2	2	3.14	6.28	0.24	
3"	2581	1	2	0.79	1.57	0.06	
4"	2581	1	3	0.79	2.36	0.09	
5"	2581	1	1	0.79	0.79	0.03	
6"	2581	4	3	12.57	37.70	1.46	
sum	15484				51.84		0.334777

	Total Area (mm ²)	Largest Shale (mm)	Number of Shale	Area per Shale (mm ²)	Total Area of Shale (mm ²)	Percent Shale	Average
Section L							
Face 4							
Depth							
1"	2581	0	0	0.00	0.00	0.00	
2"	2581	6	3	28.27	84.82	3.29	
3"	2581	3.5	6	9.62	57.73	2.24	
4"	2581	1	3	0.79	2.36	0.09	
5"	2581	2	7	3.14	21.99	0.85	
6"	2581	3.5	4	9.62	38.48	1.49	
sum	15484				205.38		1.326426

Average Percent Shale diameter check
0.83 0.829935

Core 18
U.S. 520
Webster County

	Total Area (mm ²)	Largest Shale (mm)	Number of Shale	Area per Shale (mm ²)	Total Area of Shale (mm ²)	Percent Shale	Average
Section A	8107	2	5	3.14	15.71	0.19	
Section B Top Surface	8107	3	6	7.07	42.41	0.52	
Section B Bottom Surface	8107	2	15	3.14	47.12	0.58	
Section C Top Surface	8107	3	7	7.07	49.48	0.61	
Section C Bottom Surface	8107	2	8	3.14	25.13	0.31	
Section D	8107	3	6	7.07	42.41	0.52	
sum	48643.92				222.27		0.456928

	Total Area (mm ²)	Largest Shale (mm)	Number of Shale	Area per Shale (mm ²)	Total Area of Shale (mm ²)	Percent Shale	Average
Section L							
Face 1							
Depth							
1"	2581	1	6	0.79	4.71	0.18	
2"	2581	1	3	0.79	2.36	0.09	
3"	2581	4.5	3	15.90	47.71	1.85	
4"	2581	3	4	7.07	28.27	1.10	
5"	2581	1	4	0.79	3.14	0.12	
6"	2581	1	5	0.79	3.93	0.15	
sum	15484				90.12		0.582055

	Total Area (mm ²)	Largest Shale (mm)	Number of Shale	Area per Shale (mm ²)	Total Area of Shale (mm ²)	Percent Shale	Average
Section L							
Face 2							
Depth							
1"	2581	1	3	0.79	2.36	0.09	
2"	2581	1	3	0.79	2.36	0.09	
3"	2581	1	6	0.79	4.71	0.18	
4"	2581	3	6	7.07	42.41	1.64	
5"	2581	3	3	7.07	21.21	0.82	
6"	2581	1	2	0.79	1.57	0.06	
sum	15484				74.61		0.481875

	Total Area (mm ²)	Largest Shale (mm)	Number of Shale	Area per Shale (mm ²)	Total Area of Shale (mm ²)	Percent Shale	Average
Section L							
Face 3							
Depth							
1"	2581	2	5	3.14	15.71	0.61	
2"	2581	2	4	3.14	12.57	0.49	
3"	2581	1	1	0.79	0.79	0.03	
4"	2581	1	2	0.79	1.57	0.06	
5"	2581	2	4	3.14	12.57	0.49	
6"	2581	1	1	0.79	0.79	0.03	
sum	15484				43.98		0.284053

	Total Area (mm ²)	Largest Shale (mm)	Number of Shale	Area per Shale (mm ²)	Total Area of Shale (mm ²)	Percent Shale	Average
Section L							
Face 4							
Depth							
1"	2581	4	5	12.57	62.83	2.43	
2"	2581	1	5	0.79	3.93	0.15	
3"	2581	1	4	0.79	3.14	0.12	
4"	2581	2	5	3.14	15.71	0.61	
5"	2581	5	3	19.63	58.90	2.28	
6"	2581	2	3	3.14	9.42	0.37	
sum	15484				153.94		0.994185

Average Percent Shale 0.53 diameter check 0.528965

Core 20
U.S. 520
Webster County

	Total Area (mm ²)	Largest Shale (mm)	Number of Shale	Area per Shale (mm ²)	Total Area of Shale (mm ²)	Percent Shale	Average
Section A	8107	5	7	19.63	137.44	1.70	
Section B Top Surface	8107	4	6	12.57	75.40	0.93	
Section B Bottom Surface	8107	3	6	7.07	42.41	0.52	
Section C Top Surface	8107	3	5	7.07	35.34	0.44	
Section C Bottom Surface	8107	3	4	7.07	28.27	0.35	
Section D	8107	6	8	28.27	226.19	2.79	
sum	48643.92				545.07		1.120523

	Total Area (mm ²)	Largest Shale (mm)	Number of Shale	Area per Shale (mm ²)	Total Area of Shale (mm ²)	Percent Shale	Average
Section L							
Face 1							
Depth							
1"	2581	5	4	19.63	78.54	3.04	
2"	2581	1	1	0.79	0.79	0.03	
3"	2581	4	1	12.57	12.57	0.49	
4"	2581	0	0	0.00	0.00	0.00	
5"	2581	2	2	3.14	6.28	0.24	
6"	2581	2	3	3.14	9.42	0.37	
sum	15484				107.60		0.694915

	Total Area (mm ²)	Largest Shale (mm)	Number of Shale	Area per Shale (mm ²)	Total Area of Shale (mm ²)	Percent Shale	Average
Section L							
Face 2							
Depth							
1"	2581	2	3	3.14	9.42	0.37	
2"	2581	1	3	0.79	2.36	0.09	
3"	2581	2	2	3.14	6.28	0.24	
4"	2581	2	2	3.14	6.28	0.24	
5"	2581	3	4	7.07	28.27	1.10	
6"	2581	3.5	1	9.62	9.62	0.37	
sum	15484				62.24		0.401986

	Total Area (mm ²)	Largest Shale (mm)	Number of Shale	Area per Shale (mm ²)	Total Area of Shale (mm ²)	Percent Shale	Average
Section L							
Face 3							
Depth							
1"	2581	1	5	0.79	3.93	0.15	
2"	2581	1	1	0.79	0.79	0.03	
3"	2581	0	0	0.00	0.00	0.00	
4"	2581	2	2	3.14	6.28	0.24	
5"	2581	2	3	3.14	9.42	0.37	
6"	2581	2	2	3.14	6.28	0.24	
sum	15484				26.70		0.172461

	Total Area (mm ²)	Largest Shale (mm)	Number of Shale	Area per Shale (mm ²)	Total Area of Shale (mm ²)	Percent Shale	Average
Section L							
Face 4							
Depth							
1"	2581	1	1	0.79	0.79	0.03	
2"	2581	1	2	0.79	1.57	0.06	
3"	2581	1	3	0.79	2.36	0.09	
4"	2581	6	1	28.27	28.27	1.10	
5"	2581	0	0	0.00	0.00	0.00	
6"	2581	5	1	19.63	19.63	0.76	
sum	15484				52.62		0.339849

Average Percent Shale 0.72 diameter check 0.718247

Core 21
I-80
Dallas County

	Total Area (mm ²)	Largest Shale (mm)	Number of Shale	Area per Shale (mm ²)	Total Area of Shale (mm ²)	Percent Shale	Average
Section A	8107	6.5	13	33.18	431.38	5.32	
Section B Top Surface	8107	5	10	19.63	196.35	2.42	
Section B Bottom Surface	8107	2.5	14	4.91	68.72	0.85	
Section C Top Surface	8107	2	7	3.14	21.99	0.27	
Section C Bottom Surface	8107	2	6	3.14	18.85	0.23	
Section D	8107	4	5	12.57	62.83	0.78	
sum	48643.92				800.12		1.64486

	Total Area (mm ²)	Largest Shale (mm)	Number of Shale	Area per Shale (mm ²)	Total Area of Shale (mm ²)	Percent Shale	Average
Section L							
Face 1							
Depth							
1"	2581	5	8	19.63	157.08	6.09	
2"	2581	3	7	7.07	49.48	1.92	
3"	2581	2	6	3.14	18.85	0.73	
4"	2581	2	4	3.14	12.57	0.49	
5"	2581	2	5	3.14	15.71	0.61	
6"	2581	3	3	7.07	21.21	0.82	
7"	2581	4	4	12.57	50.27	1.95	
8"	2581	2	3	3.14	9.42	0.37	
sum	20645				334.58		1.620623

	Total Area (mm ²)	Largest Shale (mm)	Number of Shale	Area per Shale (mm ²)	Total Area of Shale (mm ²)	Percent Shale	Average
Section L							
Face 2							
Depth							
1"	2581	3	8	7.07	56.55	2.19	
2"	2581	3	6	7.07	42.41	1.64	
3"	2581	2	6	3.14	18.85	0.73	
4"	2581	2	6	3.14	18.85	0.73	
5"	2581	2	5	3.14	15.71	0.61	
6"	2581	2	4	3.14	12.57	0.49	
7"	2581	2	4	3.14	12.57	0.49	
8"	2581	2.5	4	4.91	19.63	0.76	
sum	20645				197.13		0.954874

	Total Area (mm ²)	Largest Shale (mm)	Number of Shale	Area per Shale (mm ²)	Total Area of Shale (mm ²)	Percent Shale	Average
Section L							
Face 3							
Depth							
1"	2581	2	9	3.14	28.27	1.10	
2"	2581	3	6	7.07	42.41	1.64	
3"	2581	2	5	3.14	15.71	0.61	
4"	2581	2	6	3.14	18.85	0.73	
5"	2581	2	4	3.14	12.57	0.49	
6"	2581	6	4	28.27	113.10	4.38	
7"	2581	3	4	7.07	28.27	1.10	
8"	2581	2	4	3.14	12.57	0.49	
sum	20645				271.75		1.316281

	Total Area (mm ²)	Largest Shale (mm)	Number of Shale	Area per Shale (mm ²)	Total Area of Shale (mm ²)	Percent Shale	Average
Section L							
Face 4							
Depth							
1"	2581	3	6	7.07	42.41	1.64	
2"	2581	4	6	12.57	75.40	2.92	
3"	2581	2	7	3.14	21.99	0.85	
4"	2581	3	6	7.07	42.41	1.64	
5"	2581	3	6	7.07	42.41	1.64	
6"	2581	2	4	3.14	12.57	0.49	
7"	2581	3	6	7.07	42.41	1.64	
8"	2581	2	3	3.14	9.42	0.37	
sum	20645				289.03		1.399975

Average Percent Shale 1.44 check 1.442274

Core 22
I-80
Dallas County

	Total Area (mm ²)	Largest Shale (mm)	Number of Shale	Area per Shale (mm ²)	Total Area of Shale (mm ²)	Percent Shale	Average
Section A	8107	3	10	7.07	70.69	0.87	
Section B Top Surface	8107	2	10	3.14	31.42	0.39	
Section B Bottom Surface	8107	2	11	3.14	34.56	0.43	
Section C Top Surface	8107	5.5	5	23.76	118.79	1.47	
Section C Bottom Surface	8107	4	10	12.57	125.66	1.55	
Section D	8107	3	7	7.07	49.48	0.61	
sum	48643.92				430.59		0.885197

	Total Area (mm ²)	Largest Shale (mm)	Number of Shale	Area per Shale (mm ²)	Total Area of Shale (mm ²)	Percent Shale	Average
Section L Face 1							
Depth							
1"	2581	3	6	7.07	42.41	1.64	
2"	2581	2	3	3.14	9.42	0.37	
3"	2581	2	4	3.14	12.57	0.49	
4"	2581	3	7	7.07	49.48	1.92	
5"	2581	2	3	3.14	9.42	0.37	
6"	2581	1	3	0.79	2.36	0.09	
7"	2581	2	5	3.14	15.71	0.61	
8"	2581	2	8	3.14	25.13	0.97	
sum	20645				166.50		0.806507

	Total Area (mm ²)	Largest Shale (mm)	Number of Shale	Area per Shale (mm ²)	Total Area of Shale (mm ²)	Percent Shale	Average
Section L Face 2							
Depth							
1"	2581	2	4	3.14	12.57	0.49	
2"	2581	2	5	3.14	15.71	0.61	
3"	2581	2	5	3.14	15.71	0.61	
4"	2581	2	4	3.14	12.57	0.49	
5"	2581	2	3	3.14	9.42	0.37	
6"	2581	2	4	3.14	12.57	0.49	
7"	2581	2	4	3.14	12.57	0.49	
8"	2581	3	3	7.07	21.21	0.82	
sum	20645				112.31		0.544012

	Total Area (mm ²)	Largest Shale (mm)	Number of Shale	Area per Shale (mm ²)	Total Area of Shale (mm ²)	Percent Shale	Average
Section L Face 3							
Depth							
1"	2581	2	4	3.14	12.57	0.49	
2"	2581	2	5	3.14	15.71	0.61	
3"	2581	2	2	3.14	6.28	0.24	
4"	2581	3	3	7.07	21.21	0.82	
5"	2581	4	4	12.57	50.27	1.95	
6"	2581	2	2	3.14	6.28	0.24	
7"	2581	2	4	3.14	12.57	0.49	
8"	2581	3	2	7.07	14.14	0.55	
sum	20645				139.02		0.673358

	Total Area (mm ²)	Largest Shale (mm)	Number of Shale	Area per Shale (mm ²)	Total Area of Shale (mm ²)	Percent Shale	Average
Section L Face 4							
Depth							
1"	2581	3	6	7.07	42.41	1.64	
2"	2581	2	7	3.14	21.99	0.85	
3"	2581	2	4	3.14	12.57	0.49	
4"	2581	2	3	3.14	9.42	0.37	
5"	2581	2	5	3.14	15.71	0.61	
6"	2581	2	4	3.14	12.57	0.49	
7"	2581	1	4	0.79	3.14	0.12	
8"	2581	2	3	3.14	9.42	0.37	
sum	20645				127.23		0.616293

Average Percent Shale

0.74check
0.743507

Core 23
I-80
Dallas County

	Total Area (mm ²)	Largest Shale (mm)	Number of Shale	Area per Shale (mm ²)	Total Area of Shale (mm ²)	Percent Shale	Average
Section A	8107	4	9	12.57	113.10	1.40	
Section B Top Surface	8107	3	17	7.07	120.17	1.48	
Section B Bottom Surface	8107	5	9	19.63	176.71	2.18	
Section C Top Surface	8107	2	6	3.14	18.85	0.23	
Section C Bottom Surface	8107	3	10	7.07	70.69	0.87	
Section D	8107	2	9	3.14	28.27	0.35	
sum	48643.92				527.79		1.085002

Section L Face 1 Depth	Total Area (mm ²)	Largest Shale (mm)	Number of Shale	Area per Shale (mm ²)	Total Area of Shale (mm ²)	Percent Shale	Average
1"	2581	0	0	0.00	0.00	0.00	
2"	2581	0	0	0.00	0.00	0.00	
3"	2581	0	0	0.00	0.00	0.00	
4"	2581	0	0	0.00	0.00	0.00	
5"	2581	0	0	0.00	0.00	0.00	
6"	2581	0	0	0.00	0.00	0.00	
7"	2581	0	0	0.00	0.00	0.00	
8"	2581	0	0	0.00	0.00	0.00	
sum	20645				0.00		0

Section L Face 2 Depth	Total Area (mm ²)	Largest Shale (mm)	Number of Shale	Area per Shale (mm ²)	Total Area of Shale (mm ²)	Percent Shale	Average
1"	2581	0	0	0.00	0.00	0.00	
2"	2581	0	0	0.00	0.00	0.00	
3"	2581	0	0	0.00	0.00	0.00	
4"	2581	0	0	0.00	0.00	0.00	
5"	2581	0	0	0.00	0.00	0.00	
6"	2581	0	0	0.00	0.00	0.00	
7"	2581	0	0	0.00	0.00	0.00	
8"	2581	0	0	0.00	0.00	0.00	
sum	20645				0.00		0

Section L Face 3 Depth	Total Area (mm ²)	Largest Shale (mm)	Number of Shale	Area per Shale (mm ²)	Total Area of Shale (mm ²)	Percent Shale	Average
1"	2581	0	0	0.00	0.00	0.00	
2"	2581	0	0	0.00	0.00	0.00	
3"	2581	0	0	0.00	0.00	0.00	
4"	2581	0	0	0.00	0.00	0.00	
5"	2581	0	0	0.00	0.00	0.00	
6"	2581	0	0	0.00	0.00	0.00	
7"	2581	0	0	0.00	0.00	0.00	
8"	2581	0	0	0.00	0.00	0.00	
sum	20645				0.00		0

Section L Face 4 Depth	Total Area (mm ²)	Largest Shale (mm)	Number of Shale	Area per Shale (mm ²)	Total Area of Shale (mm ²)	Percent Shale	Average
1"	2581	0	0	0.00	0.00	0.00	
2"	2581	0	0	0.00	0.00	0.00	
3"	2581	0	0	0.00	0.00	0.00	
4"	2581	0	0	0.00	0.00	0.00	
5"	2581	0	0	0.00	0.00	0.00	
6"	2581	0	0	0.00	0.00	0.00	
7"	2581	0	0	0.00	0.00	0.00	
8"	2581	0	0	0.00	0.00	0.00	
sum	20645				0.00		0

Average Percent Shale 1.09 check 1.085004

Core 24
I-80
Dallas County

	Total Area (mm ²)	Largest Shale (mm)	Number of Shale	Area per Shale (mm ²)	Total Area of Shale (mm ²)	Percent Shale	Average
Section A	8107	4	15	12.57	188.50	2.33	
Section B Top Surface	8107	2	10	3.14	31.42	0.39	
Section B Bottom Surface	8107	2	11	3.14	34.56	0.43	
Section C Top Surface	8107	2	8	3.14	25.13	0.31	
Section C Bottom Surface	8107	2	11	3.14	34.56	0.43	
Section D	8107	2	7	3.14	21.99	0.27	
sum	48643.92				336.15		0.691043

	Total Area (mm ²)	Largest Shale (mm)	Number of Shale	Area per Shale (mm ²)	Total Area of Shale (mm ²)	Percent Shale	Average
Section L Face 1							
Depth							
1"	2581	3	4	7.07	28.27	1.10	
2"	2581	3	4	7.07	28.27	1.10	
3"	2581	4	8	12.57	100.53	3.90	
4"	2581	2	3	3.14	9.42	0.37	
5"	2581	3	6	7.07	42.41	1.64	
6"	2581	4	6	12.57	75.40	2.92	
7"	2581	2	3	3.14	9.42	0.37	
8"	2581	3	5	7.07	35.34	1.37	
sum	20645				329.08		1.593993

	Total Area (mm ²)	Largest Shale (mm)	Number of Shale	Area per Shale (mm ²)	Total Area of Shale (mm ²)	Percent Shale	Average
Section L Face 2							
Depth							
1"	2581	2	4	3.14	12.57	0.49	
2"	2581	3	3	7.07	21.21	0.82	
3"	2581	3	5	7.07	35.34	1.37	
4"	2581	4	5	12.57	62.83	2.43	
5"	2581	1	3	0.79	2.36	0.09	
6"	2581	3	4	7.07	28.27	1.10	
7"	2581	2	6	3.14	18.85	0.73	
8"	2581	2	4	3.14	12.57	0.49	
sum	20645				193.99		0.939657

	Total Area (mm ²)	Largest Shale (mm)	Number of Shale	Area per Shale (mm ²)	Total Area of Shale (mm ²)	Percent Shale	Average
Section L Face 3							
Depth							
1"	2581	2	3	3.14	9.42	0.37	
2"	2581	3	3	7.07	21.21	0.82	
3"	2581	4	4	12.57	50.27	1.95	
4"	2581	3	2	7.07	14.14	0.55	
5"	2581	2	3	3.14	9.42	0.37	
6"	2581	3	3	7.07	21.21	0.82	
7"	2581	2	2	3.14	6.28	0.24	
8"	2581	3	3	7.07	21.21	0.82	
sum	20645				153.15		0.741835

	Total Area (mm ²)	Largest Shale (mm)	Number of Shale	Area per Shale (mm ²)	Total Area of Shale (mm ²)	Percent Shale	Average
Section L Face 4							
Depth							
1"	2581	5	6	19.63	117.81	4.57	
2"	2581	2	5	3.14	15.71	0.61	
3"	2581	2	4	3.14	12.57	0.49	
4"	2581	2	2	3.14	6.28	0.24	
5"	2581	2	3	3.14	9.42	0.37	
6"	2581	2	3	3.14	9.42	0.37	
7"	2581	2	2	3.14	6.28	0.24	
8"	2581	2	6	3.14	18.85	0.73	
sum	20645				196.35		0.95107

Average shale = 0.92

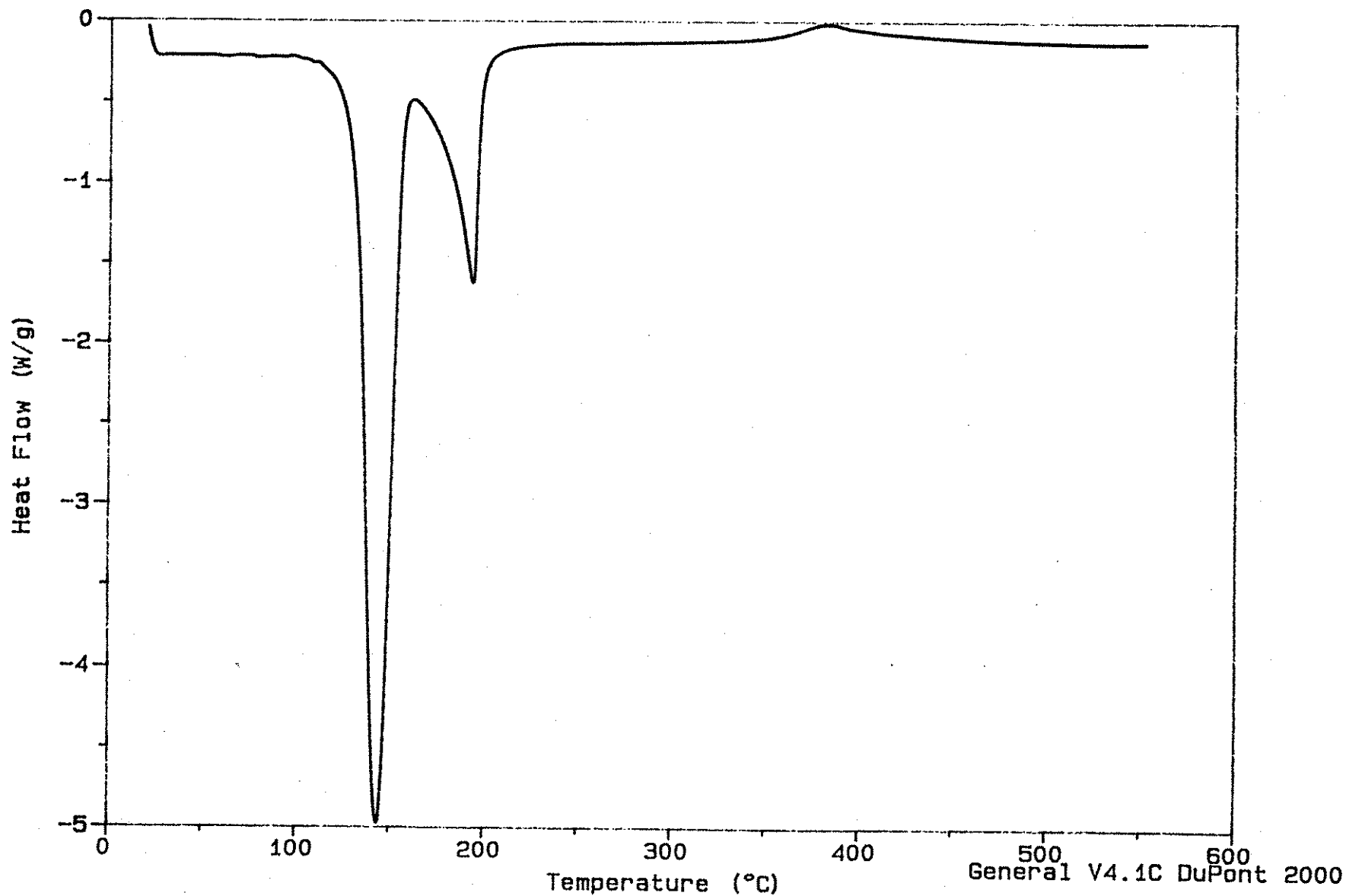
APPENDIX C (DSC RESULTS, PRELIMINARY)



Sample: GYPSUM 7/18/94
Size: 10.5000 mg
Method: 10°C/min
Comment: In N2 @ 50 ml/min

DSC

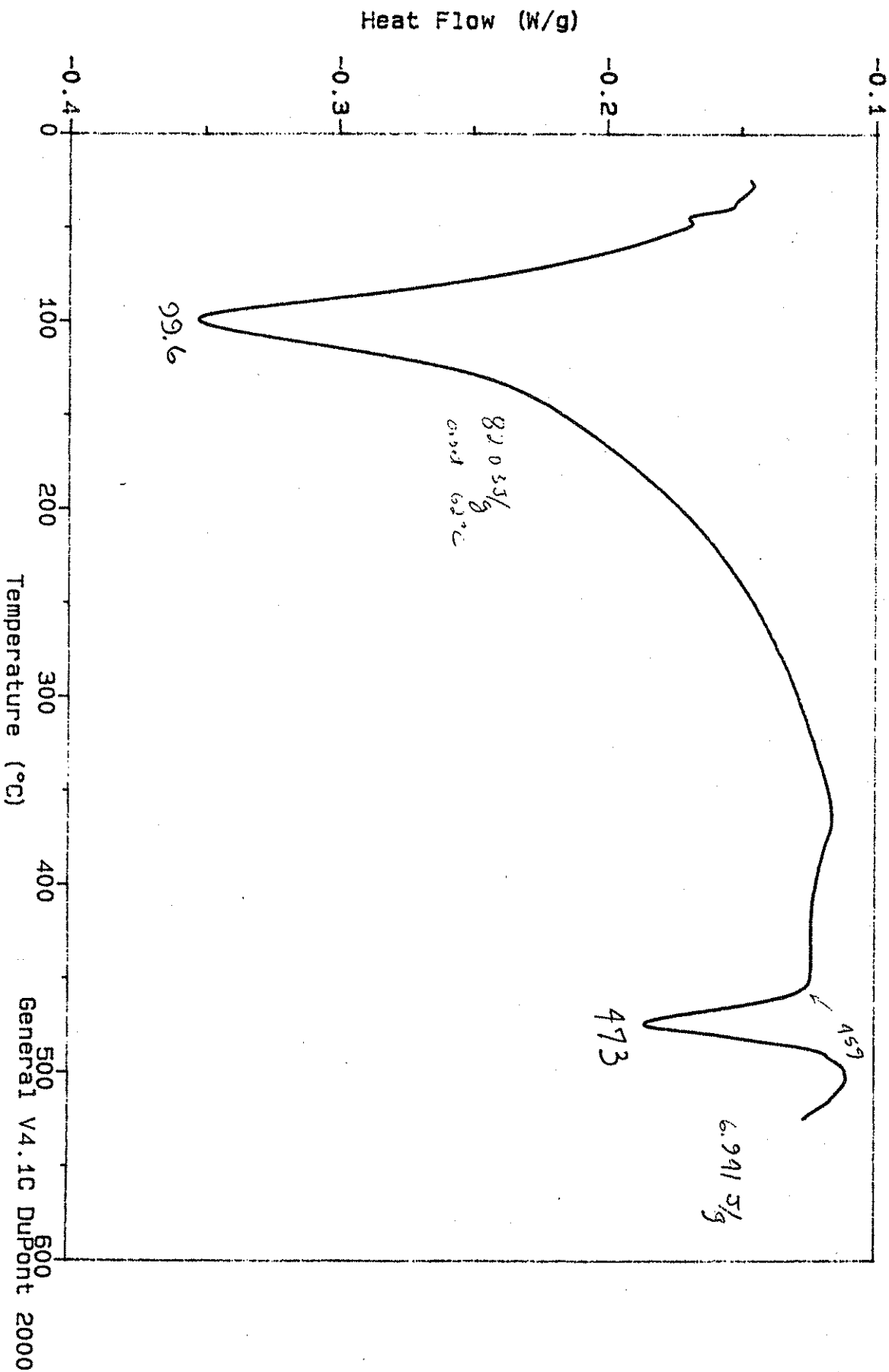
File: C: SCOTT.720
Operator: J. AMENSON
Run Date: 15-Sep-95 07:02



Sample: C2S 90 DAYS, 1st run
Size: 10.3000 mg
Method: 10°C/min
Comment: In N2 @ 50 ml/min

DSC

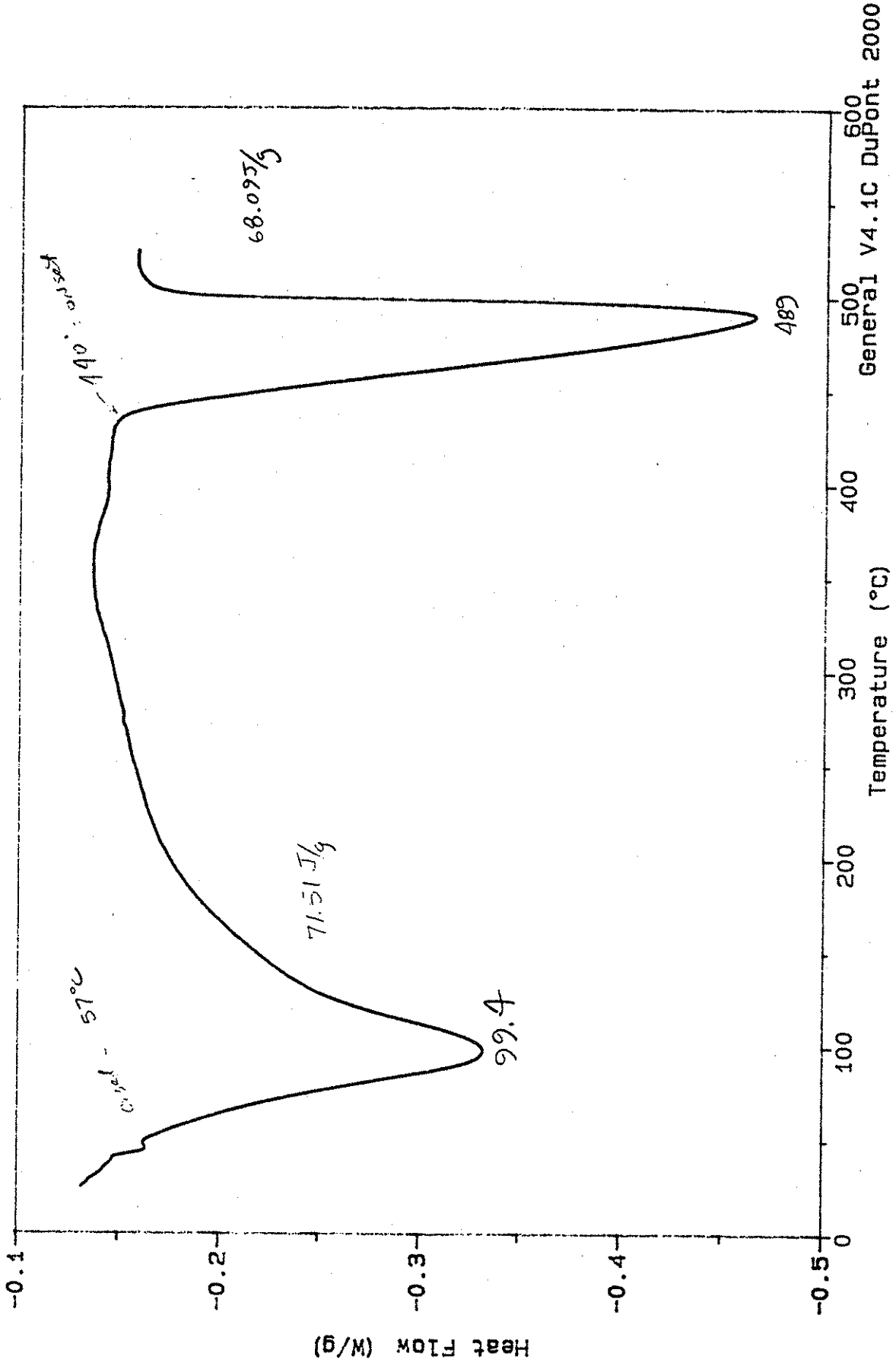
File: CHENG.036
Operator: J. AMENSON
Run Date: 23-Aug-95 10:53



Sample: C35 90 DAYS, 2nd run
Size: 10.4000 mg
Method: 10°C/min
Comment: In N2 @ 50 ml/min

DSC

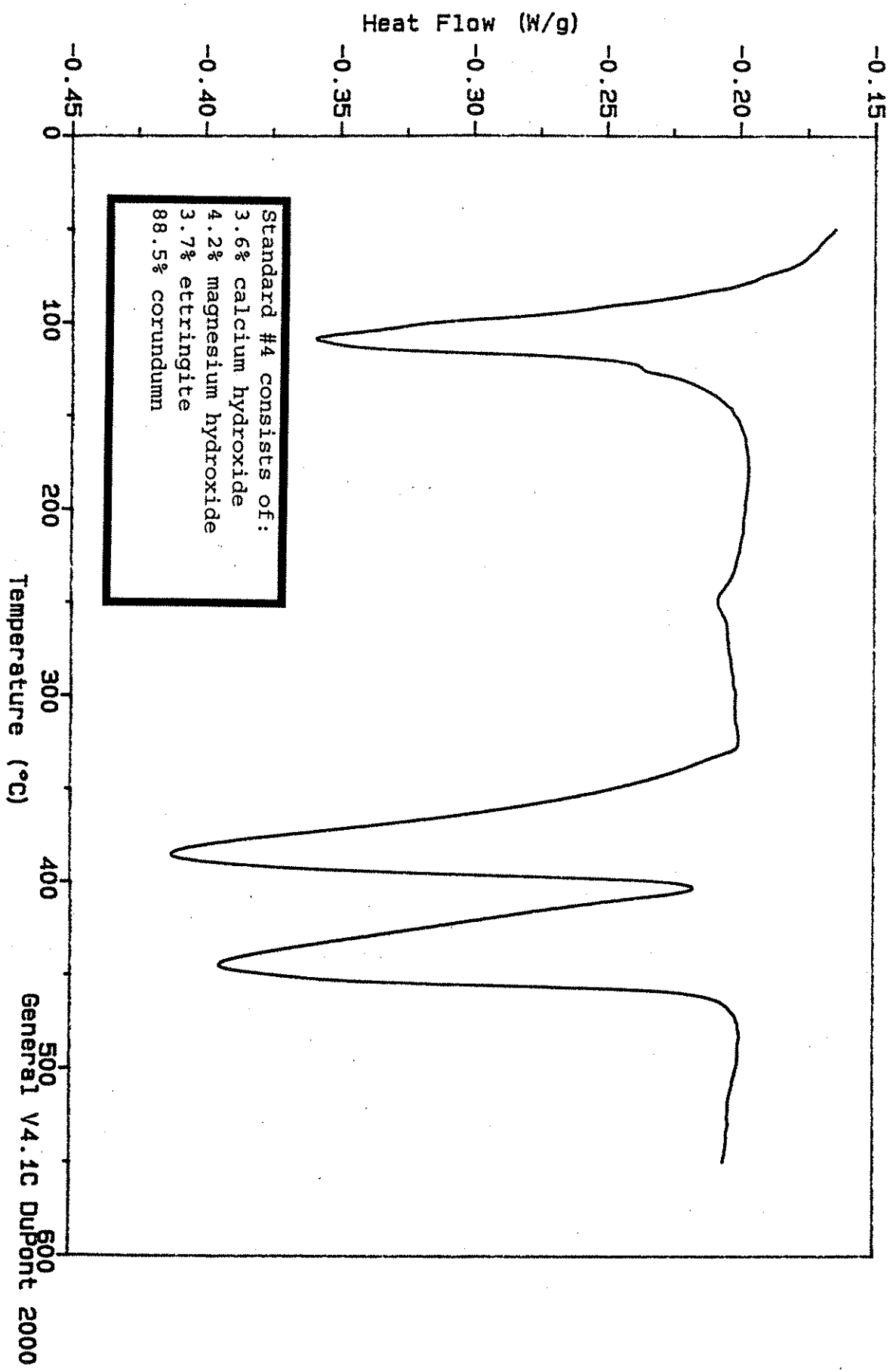
File: CHENG.035
Operator: J. AMENSON
Run Date: 23-Aug-95 09:51



Sample: STANDARD #4
Size: 10.3000 mg
Method: 10°C/min
Comment: In N2 @ 50 ml/min

DSC

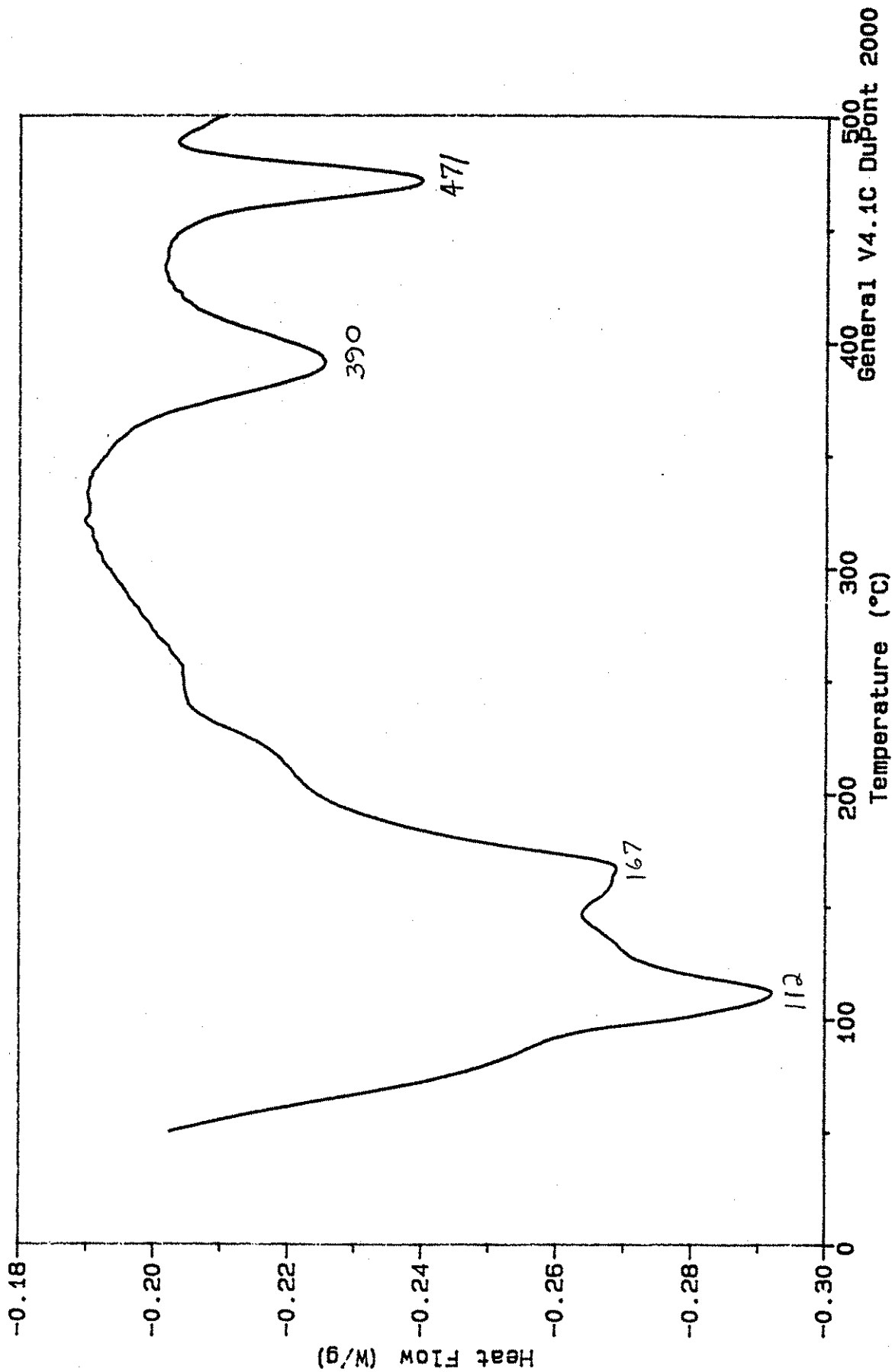
File: C:SCOTT.764
Operator: J. AMENSON



Sample: CM1-1
Size: 10.5000 mg
Method: 10°C/min
Comment: In N2 @ 50 ml/min

DSC

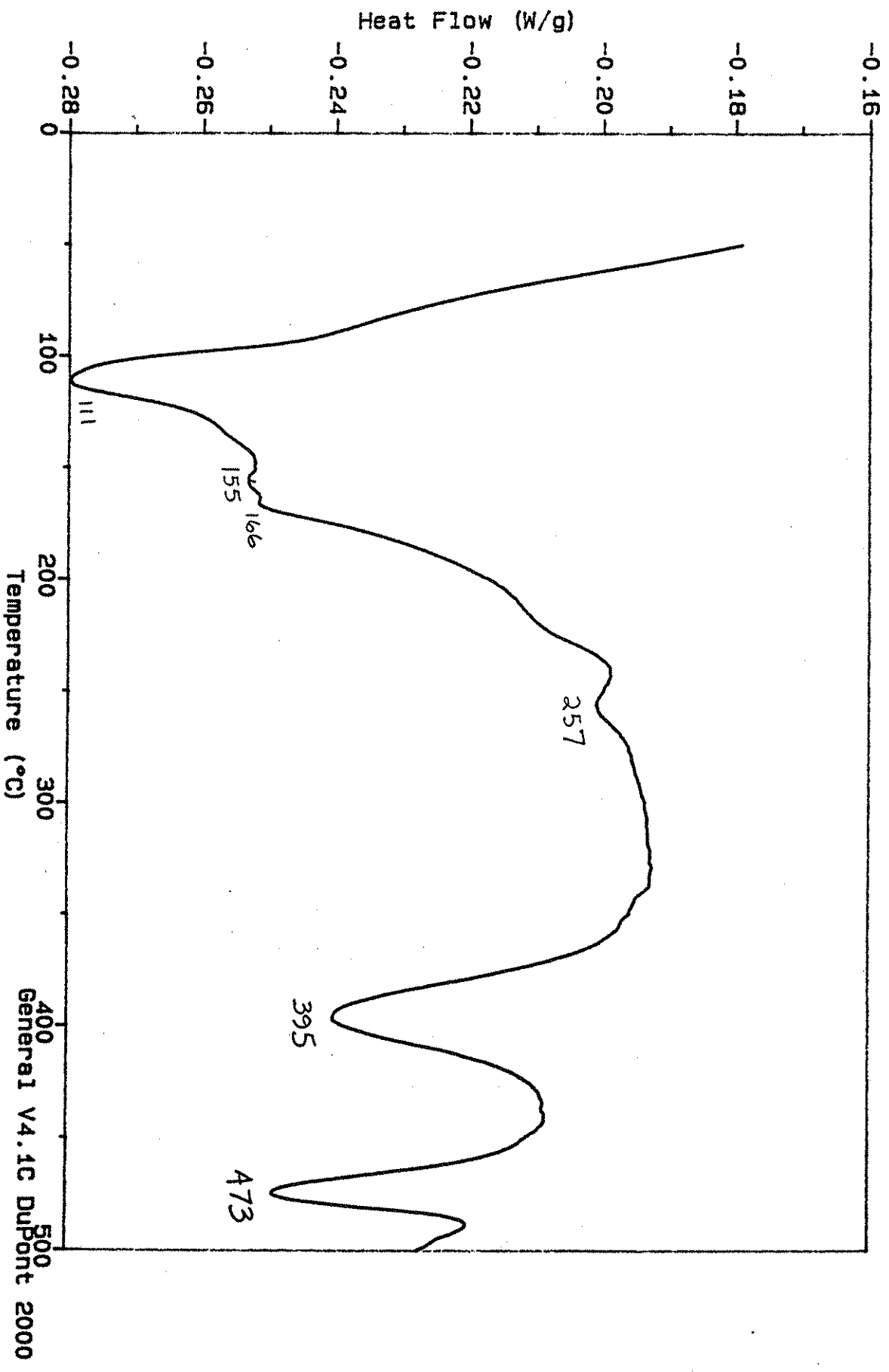
File: C:SCOTT.673
Operator: J. AMENSON
Run Date: 2-Jun-95 08:31



Sample: CM1-2
Size: 10.3000 mg
Method: 10°C/min
Comment: In N2 @ 50 ml/min

DSC

File: C:SCOTT.671
Operator: J. AMENSON
Run Date: 2-Jun-95 06:04

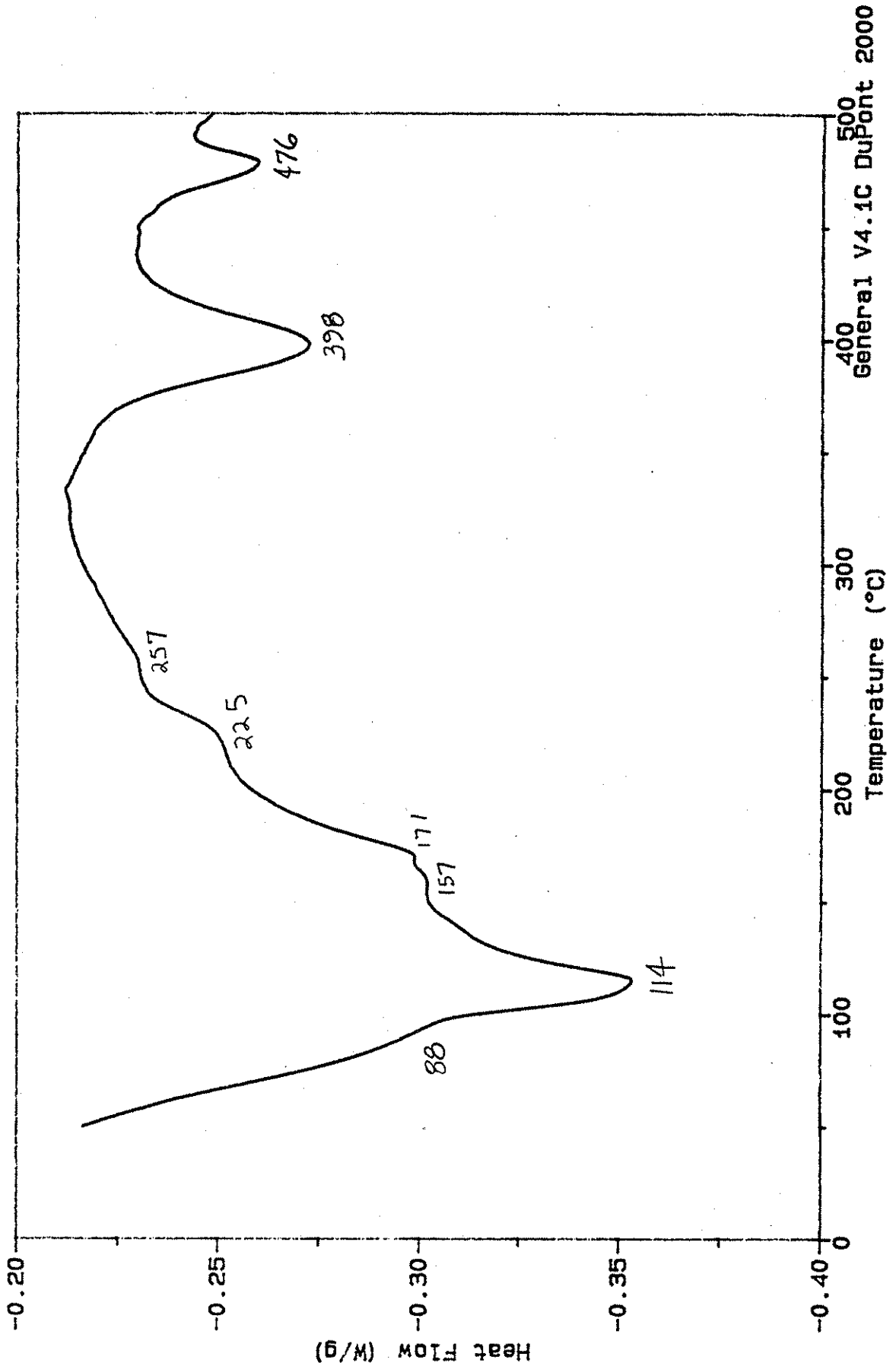


General V4.1C DuPont 2000

Sample: CM1-5
Size: 10.4000 mg
Method: 10°C/min
Comment: In N2 @ 50 ml/min

DSC

File: C:SCOTT.672
Operator: J. AMENSON
Run Date: 2-JUN-95 07:24

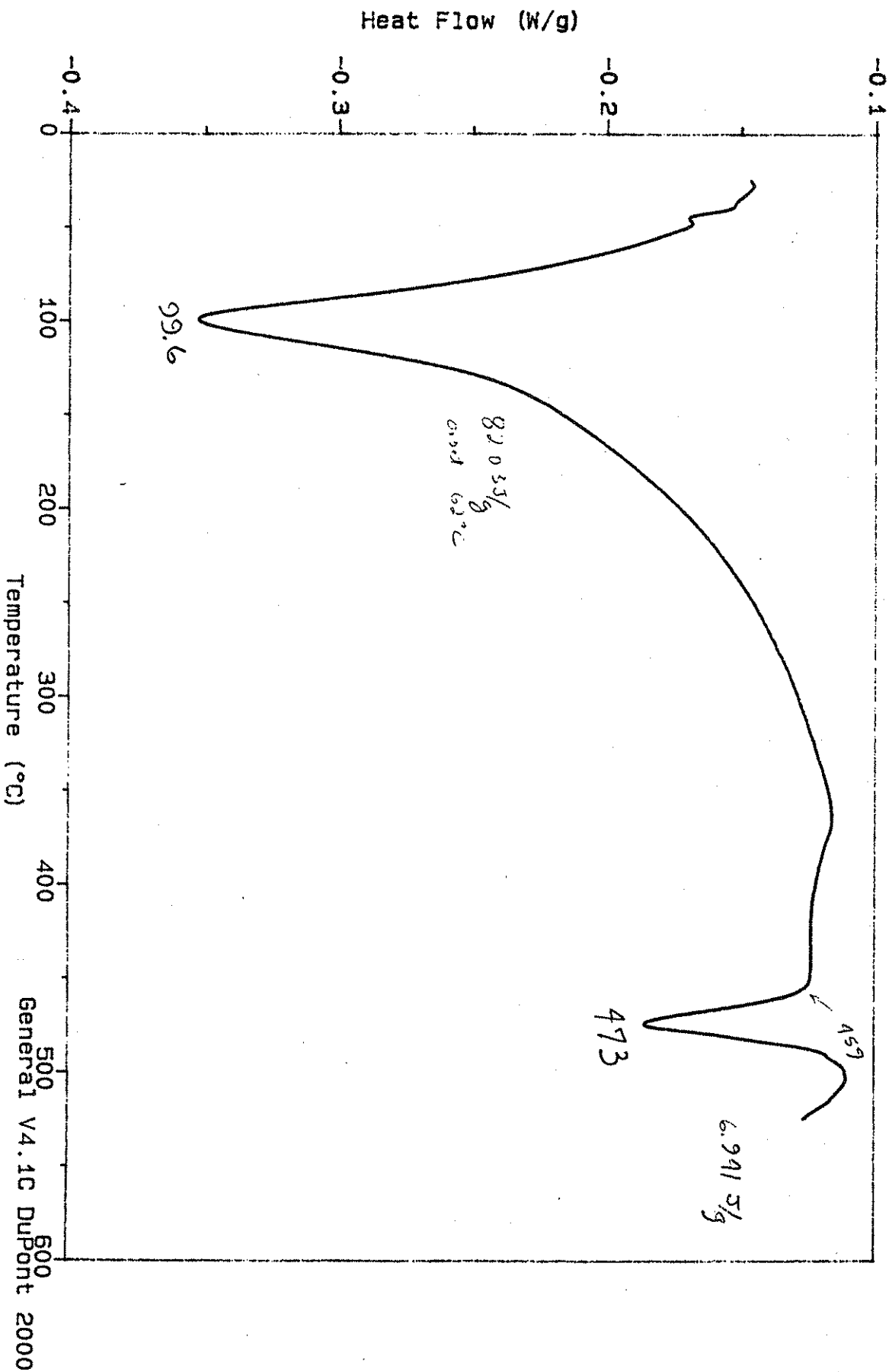


General V4.1C DuPont 2000

Sample: C2S 90 DAYS. 1st run
Size: 10.3000 mg
Method: 10°C/min
Comment: In N2 @ 50 ml/min

DSC

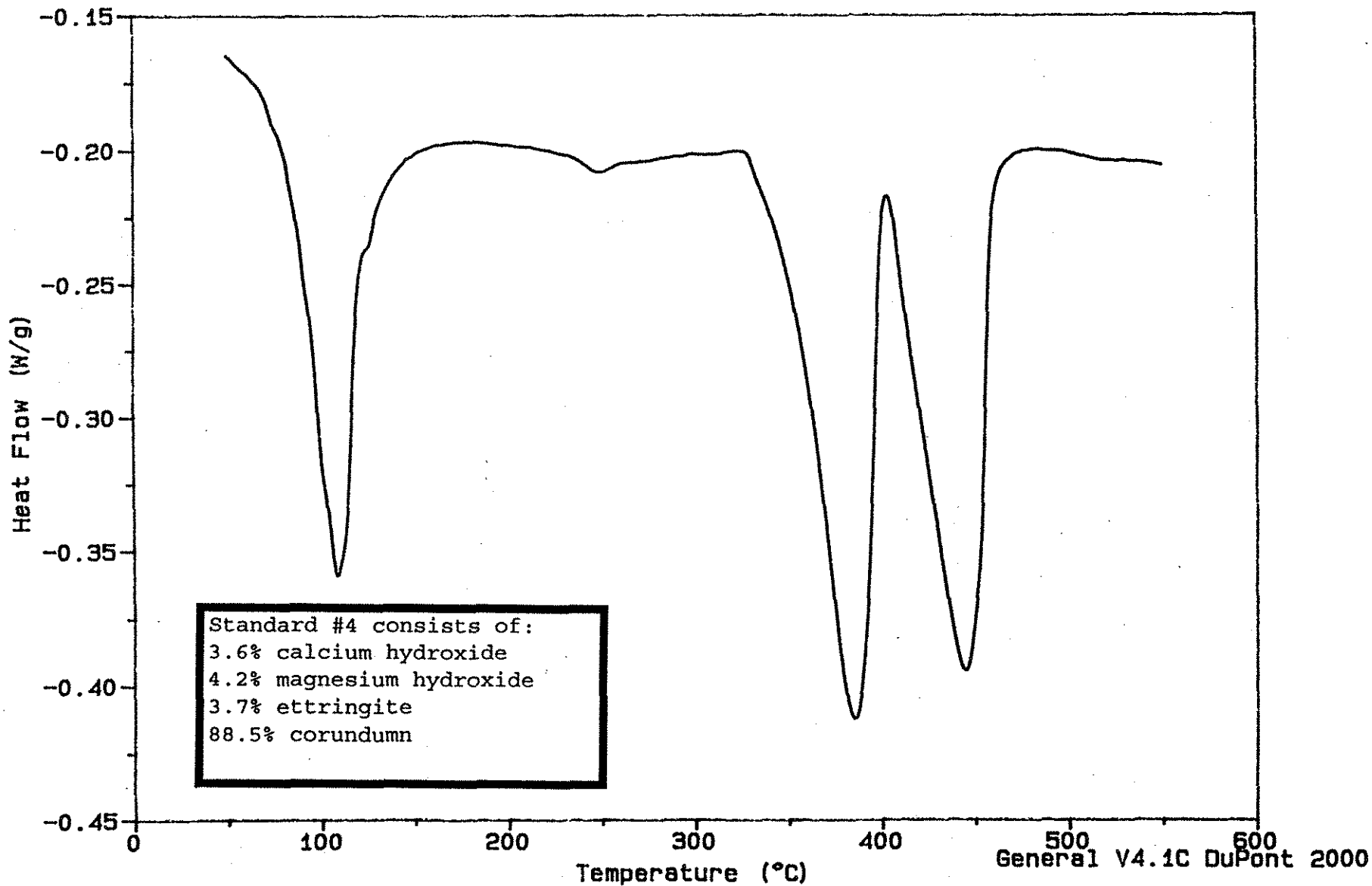
File: CHENG.036
Operator: J. AMENSON
Run Date: 23-Aug-95 10:53



Sample: STANDARD #4
Size: 10.3000 mg
Method: 10°C/min
Comment: In N2 @ 50 ml/min

DSC

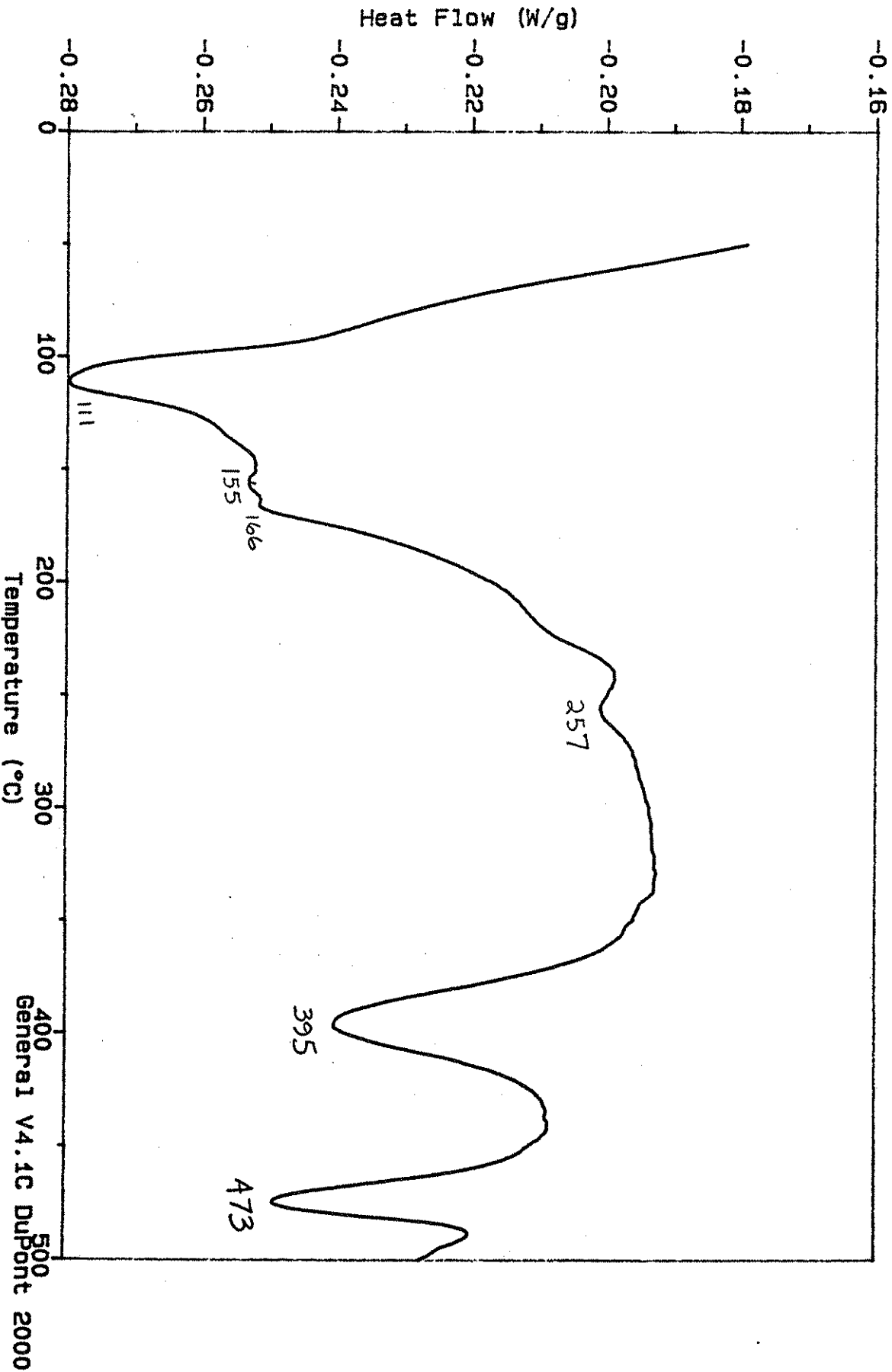
File: C: SCOTT.764
Operator: J. AMENSON



Sample: CM1-2
Size: 10.3000 mg
Method: 10°C/min
Comment: In N2 @ 50 ml/min

DSC

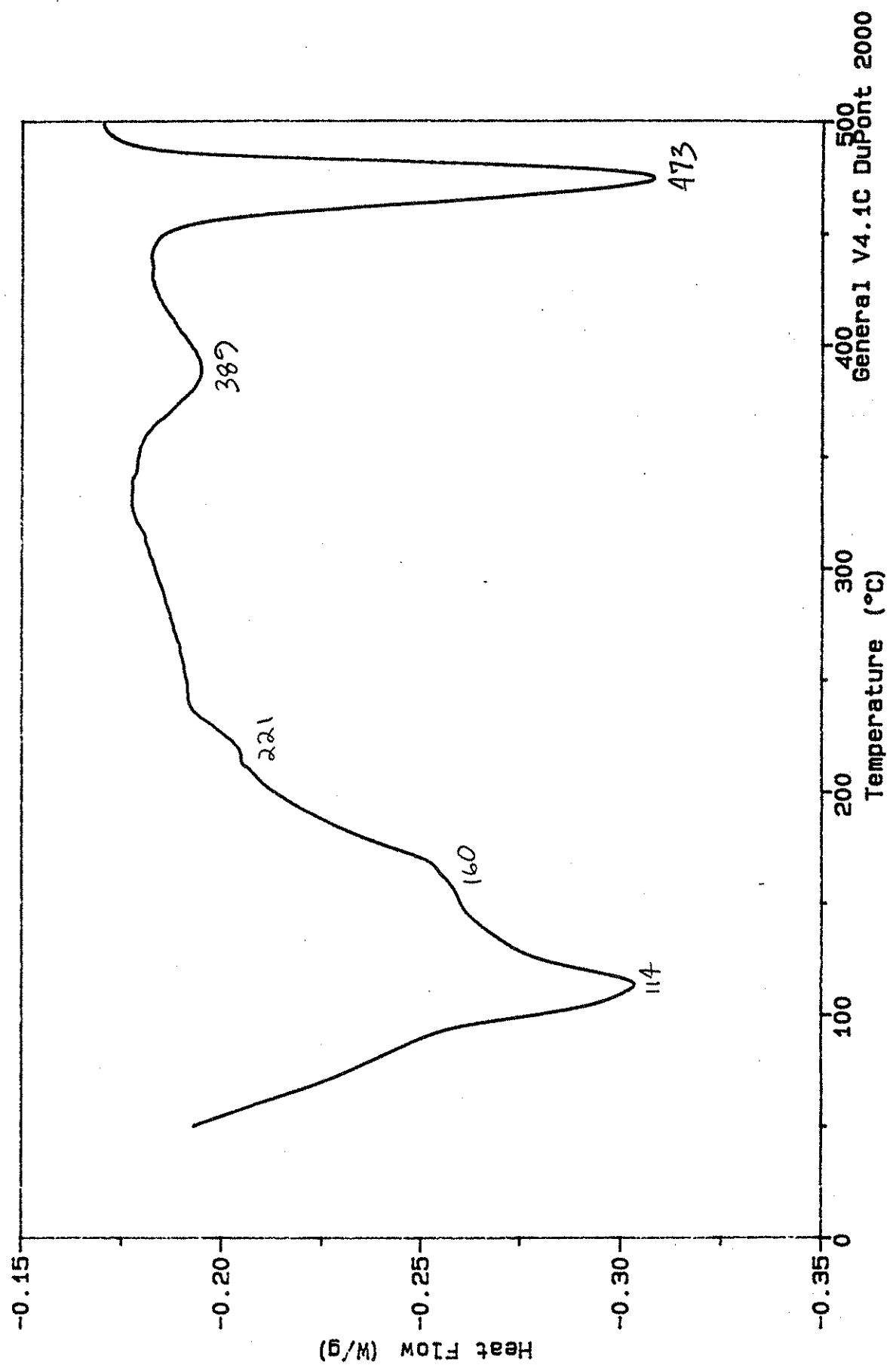
File: C:SCOTT.671
Operator: J. AMENSON
Run Date: 2-Jun-95 06:04



File: C: SCOTT.674
Operator: J. AMENSON
Run Date: 2-Jun-95 10:59

DSC

Sample: CM1-6
Size: 10.3000 mg
Method: 10°C/min
Comment: In N2 @ 50 ml/min

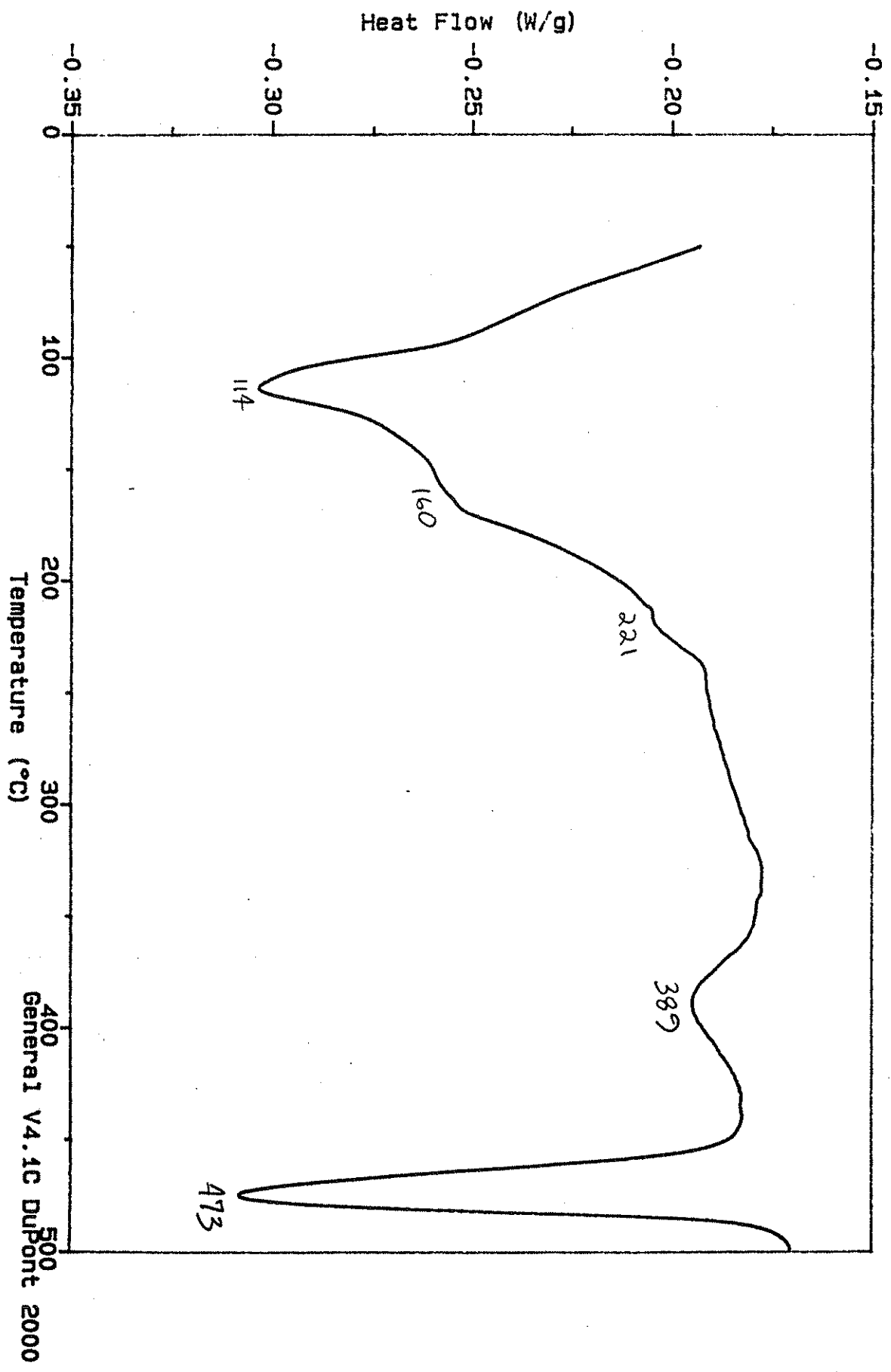


500
General V4.1C DuPont 2000

Sample: CM1-6
Size: 10.3000 mg
Method: 10°C/min
Comment: In N2 @ 50 ml/min

DSC

File: C:SCOTT.674
Operator: J. AMENSON
Run Date: 2-Jun-95 10:59

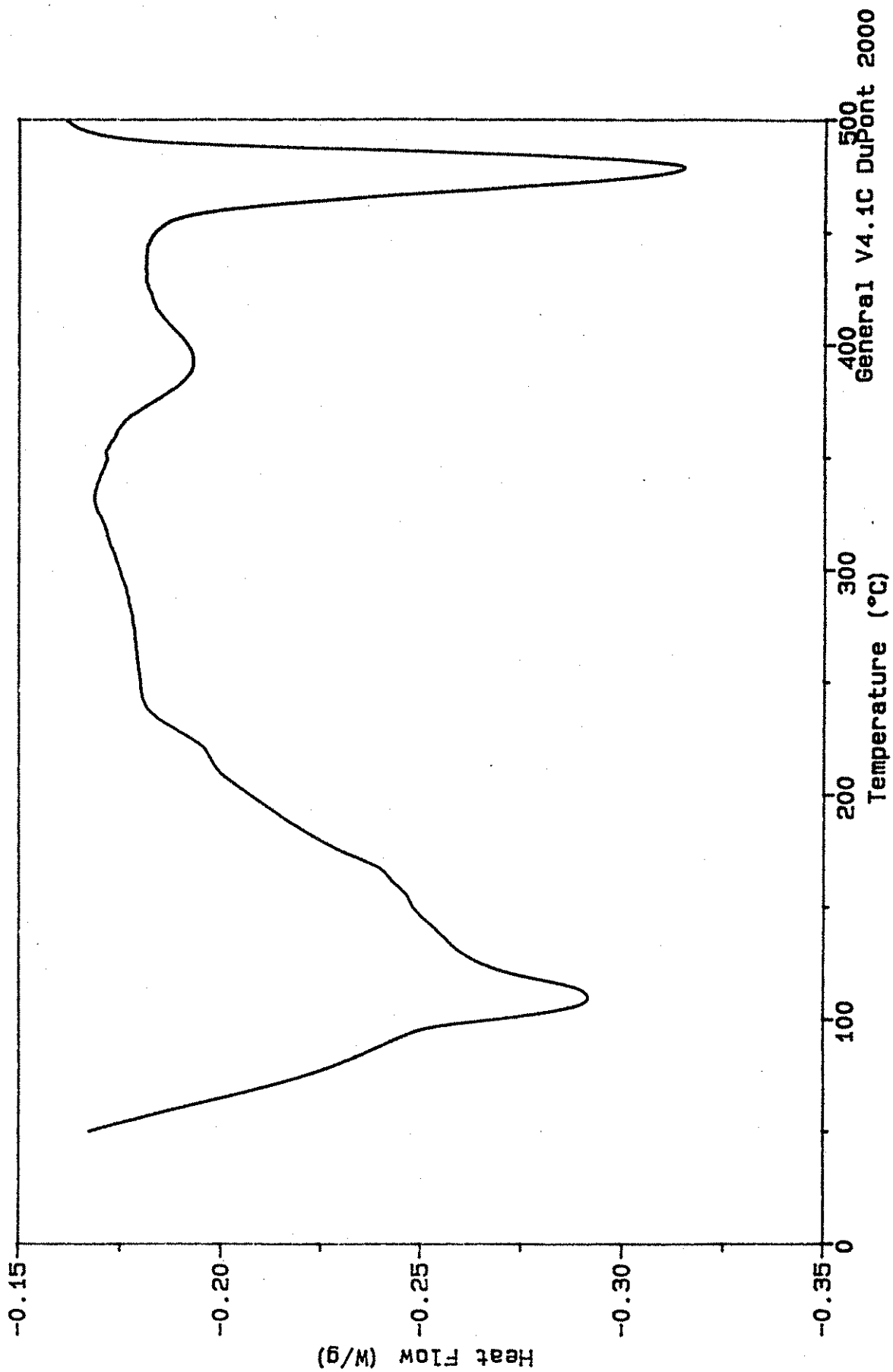


General V4.1C DuPont 2000

File: C:SCOTT.675
Operator: J. AMENSON
Run Date: 5-Jun-95 08:48

DSC

Sample: CM1-11
Size: 10.2000 mg
Method: 10°C/min
Comment: In N2 @ 50 ml/min

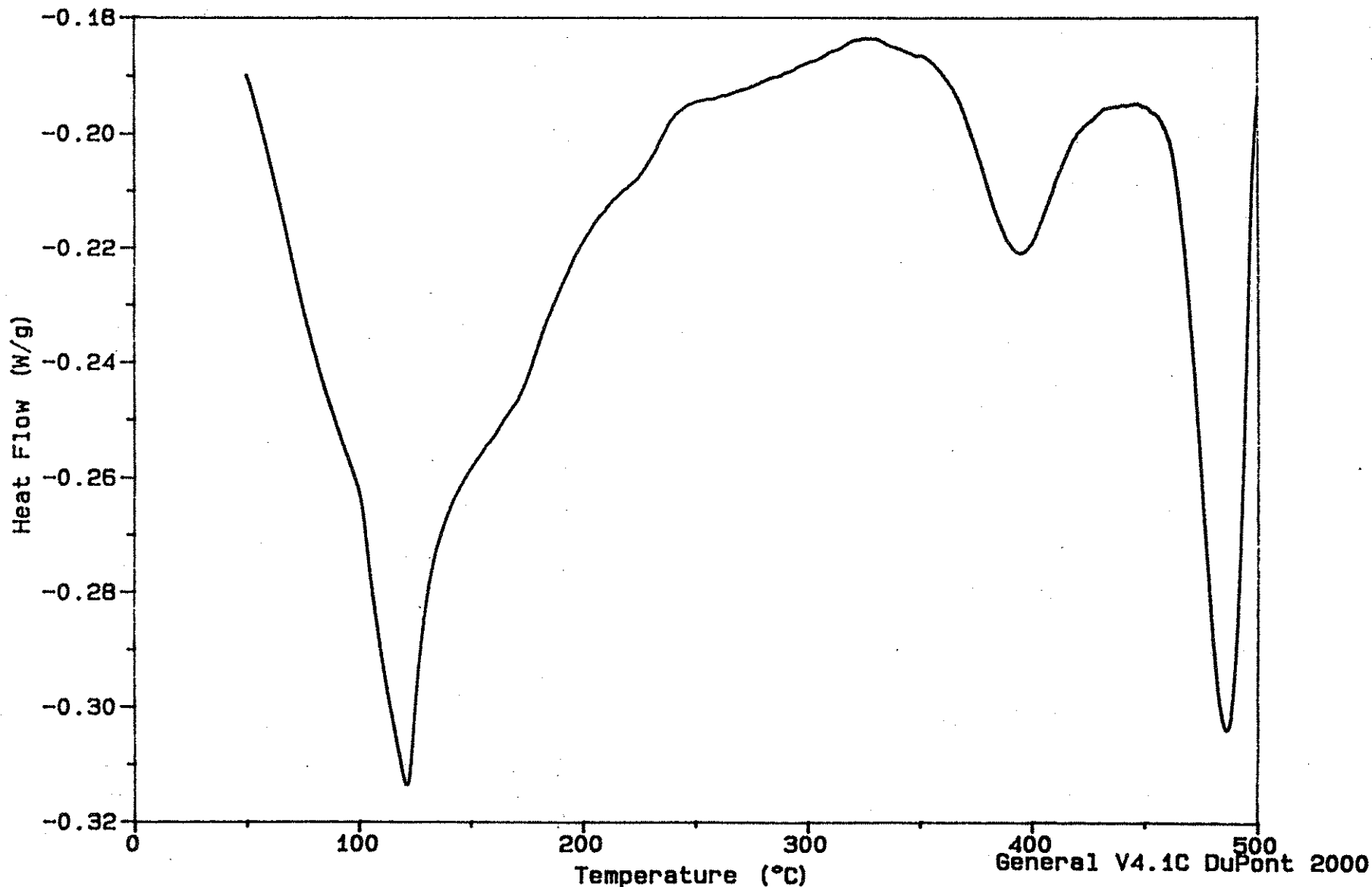


General V4.1C DuPont 2000

Sample: CM1-12
Size: 10.5000 mg
Method: 10°C/min
Comment: In N2 @ 50 ml/min

DSC

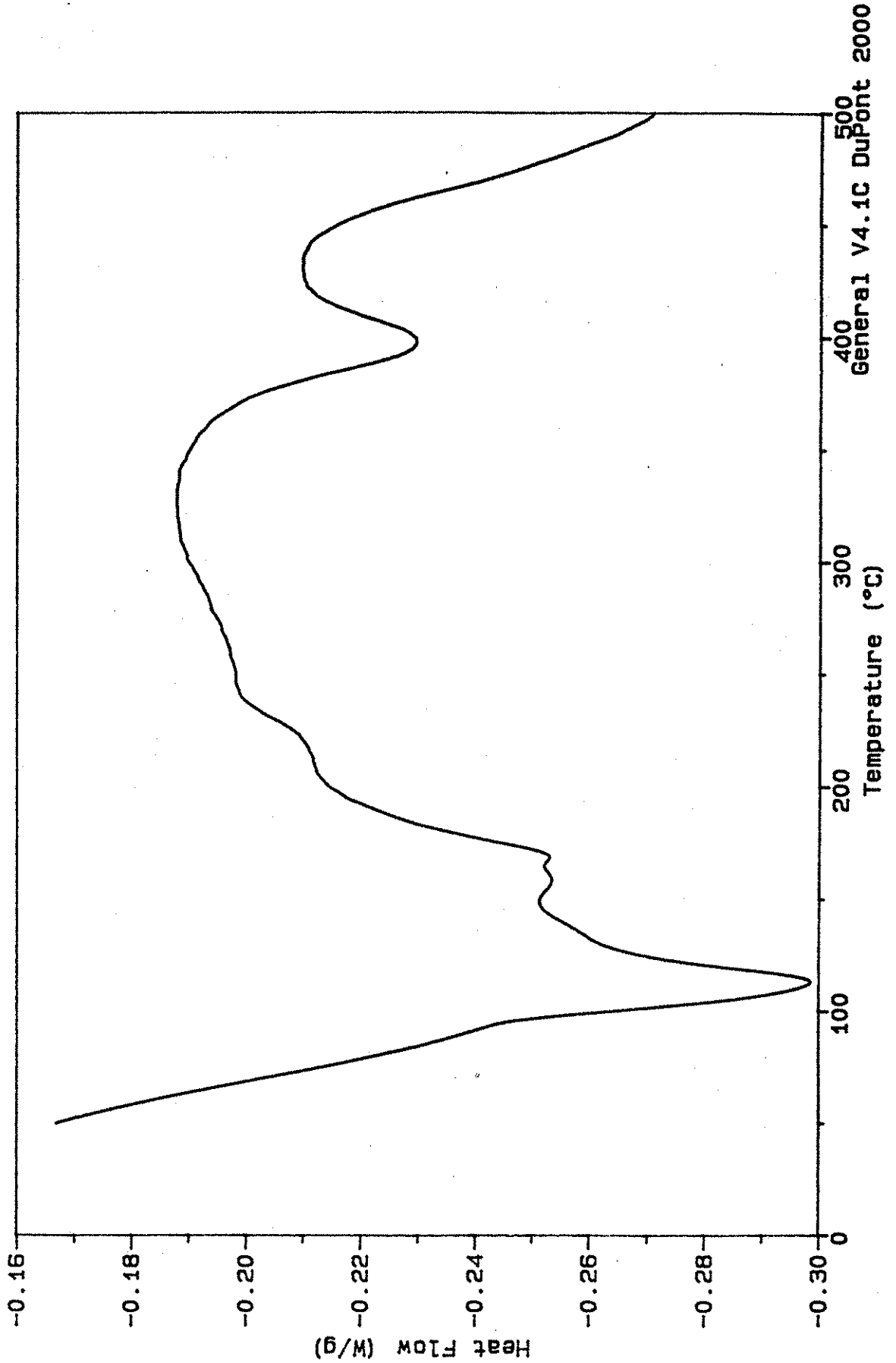
File: C: SCOTT.676
Operator: J. AMENSON
Run Date: 5-Jun-95 09:49



Sample: CORE 1
Size: 10.2000 mg
Method: 10°C/min
Comment: In N2 @ 50 ml/min

DSC

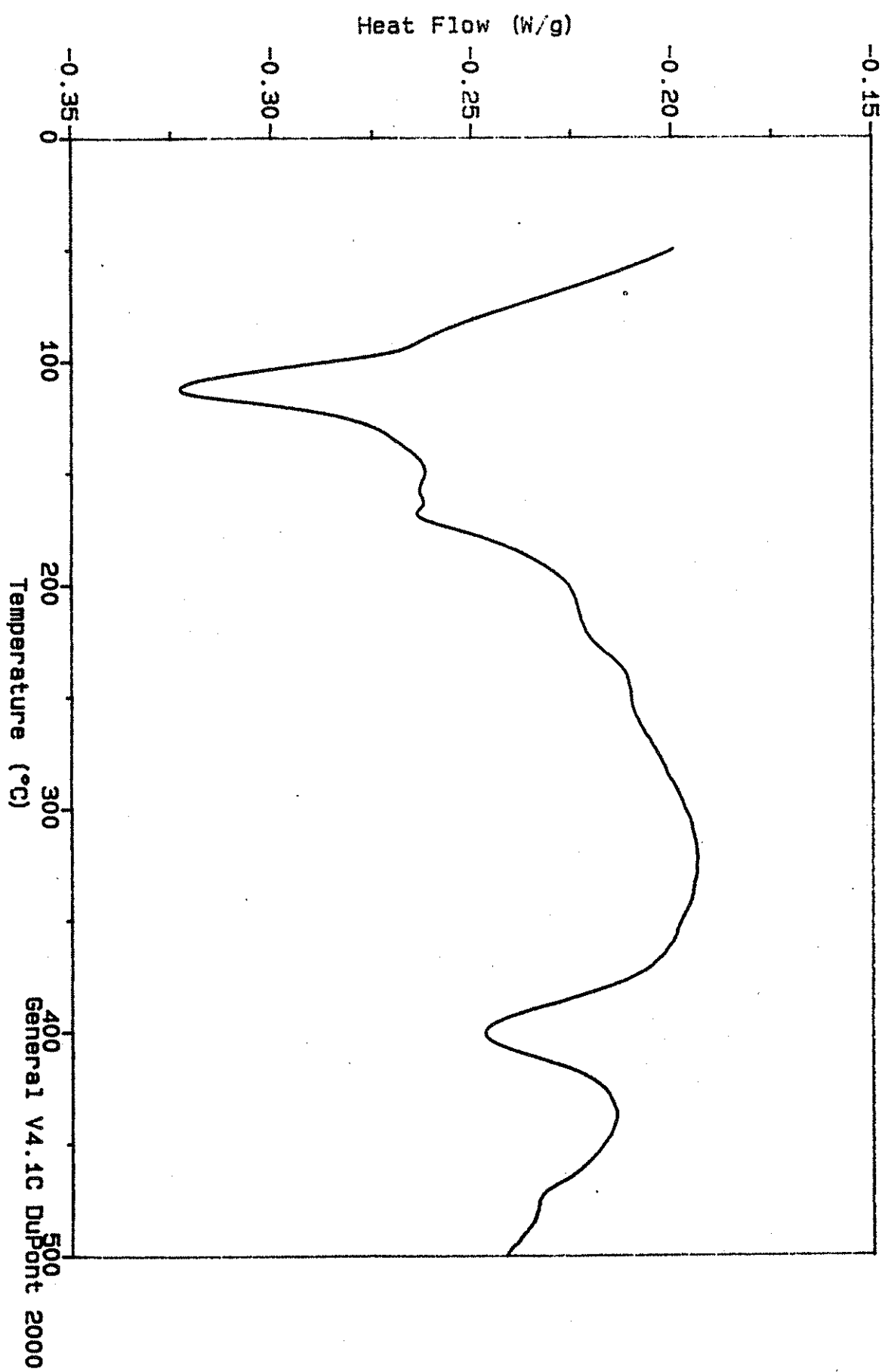
File: C: SCOTT.648
Operator: J. AMENSON
Run Date: 23-May-95 13:37



Sample: CORE 2
Size: 10.4000 mg
Method: 10°C/min
Comment: In N2 @ 50 ml/min

DSC

File: C:SCOTT.649
Operator: J. AMENSON
Run Date: 23-May-95 14: 42

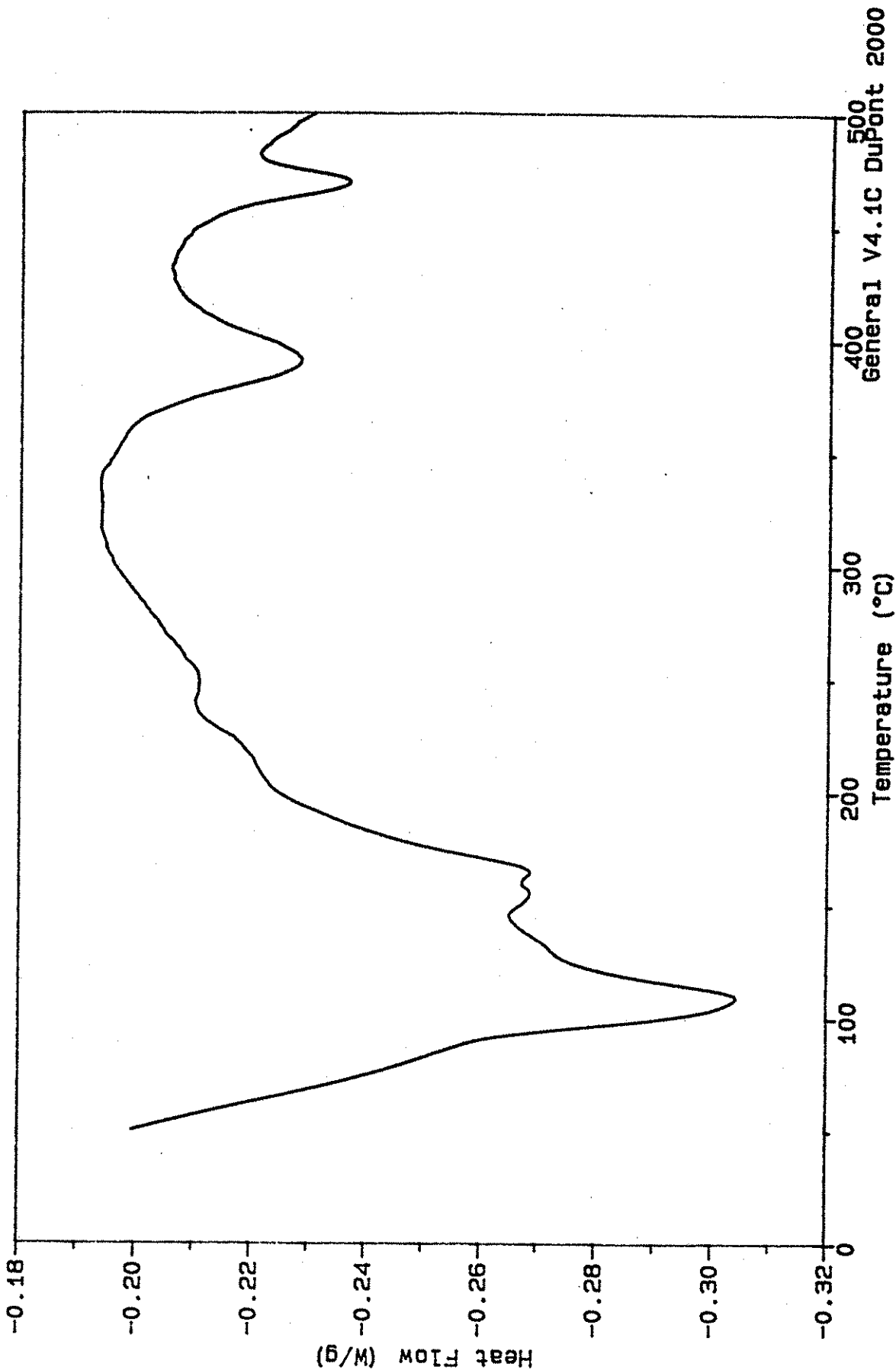


General V4.1C DuPont 2000

Sample: CORE 3
Size: 10.4000 mg
Method: 10°C/min
Comment: In N2 @ 50 ml/min

DSC

File: C: SCOTT.650
Operator: J. AMENSON
Run Date: 23-May-95 15: 57

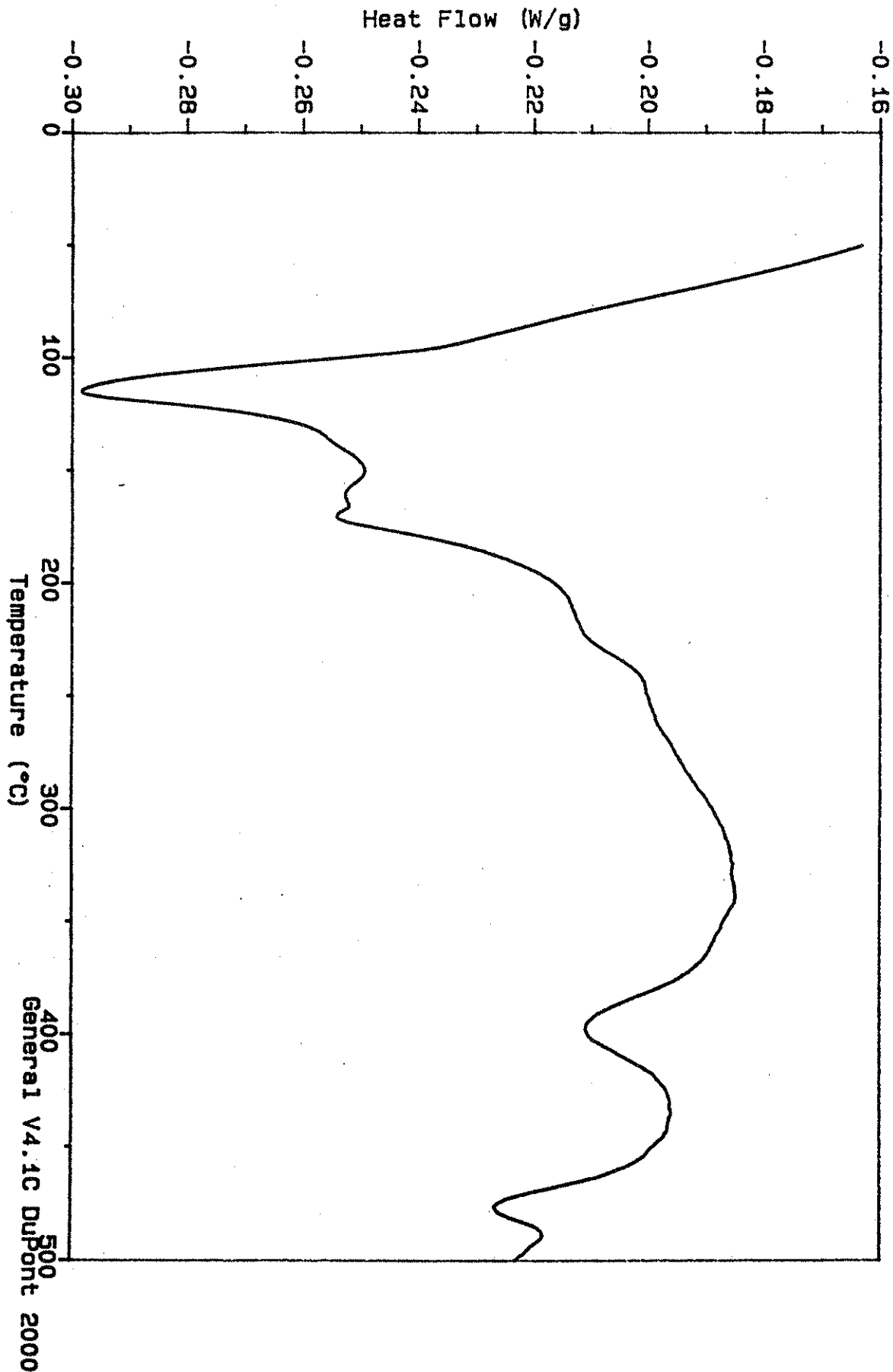


General V4.1C DuPont 2000

Sample: CORE 4
Size: 10.4000 mg
Method: 10°C/min
Comment: In N2 @ 50 ml/min

DSC

File: C:SCOTT.651
Operator: J. AMENSON
Run Date: 24-May-95 07:23

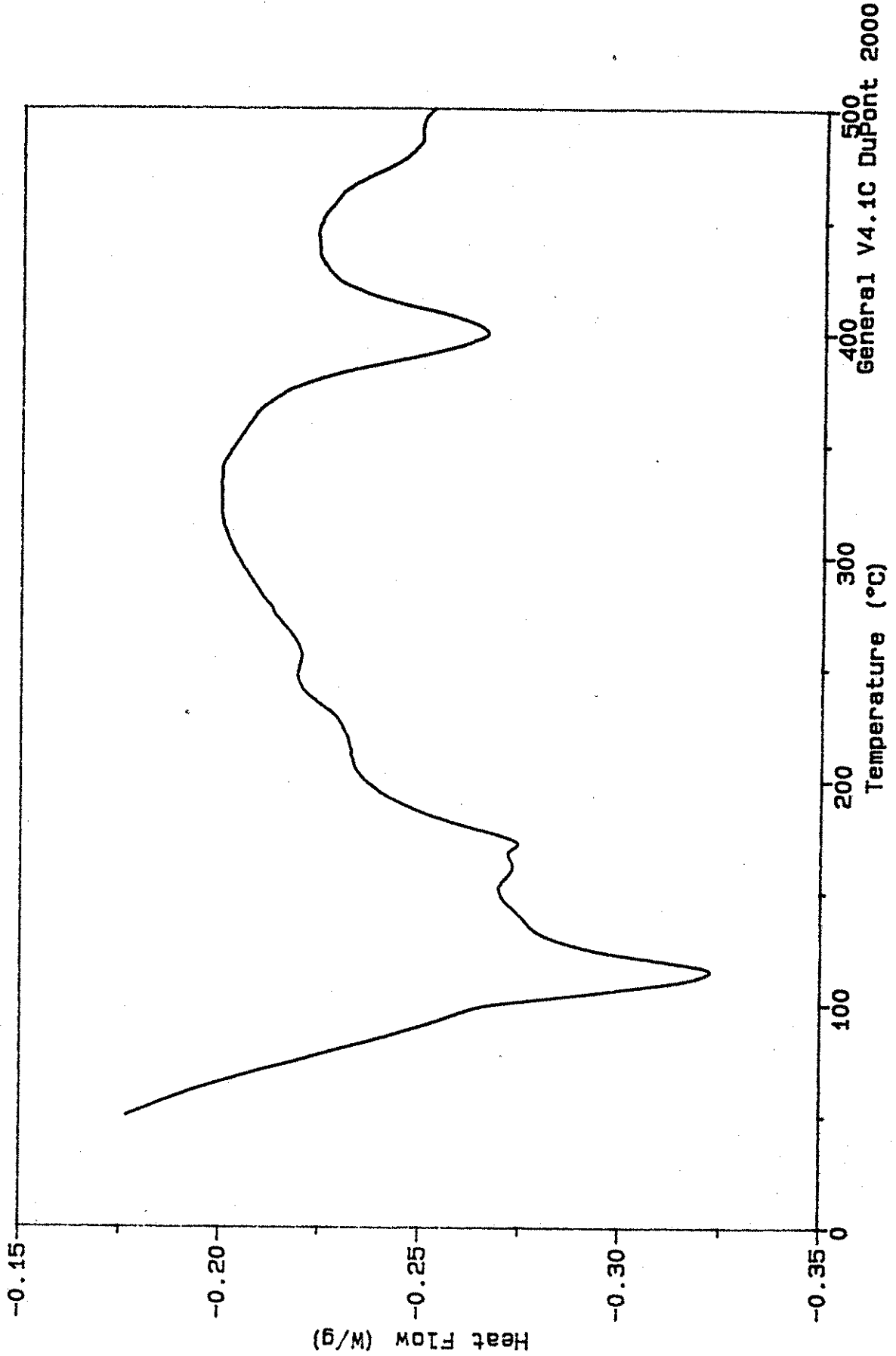


General V4.1C DuPont 2000

Sample: CORE 5
Size: 10.5000 mg
Method: 10 °C/min
Comment: In N2 @ 50 ml/min

DSC

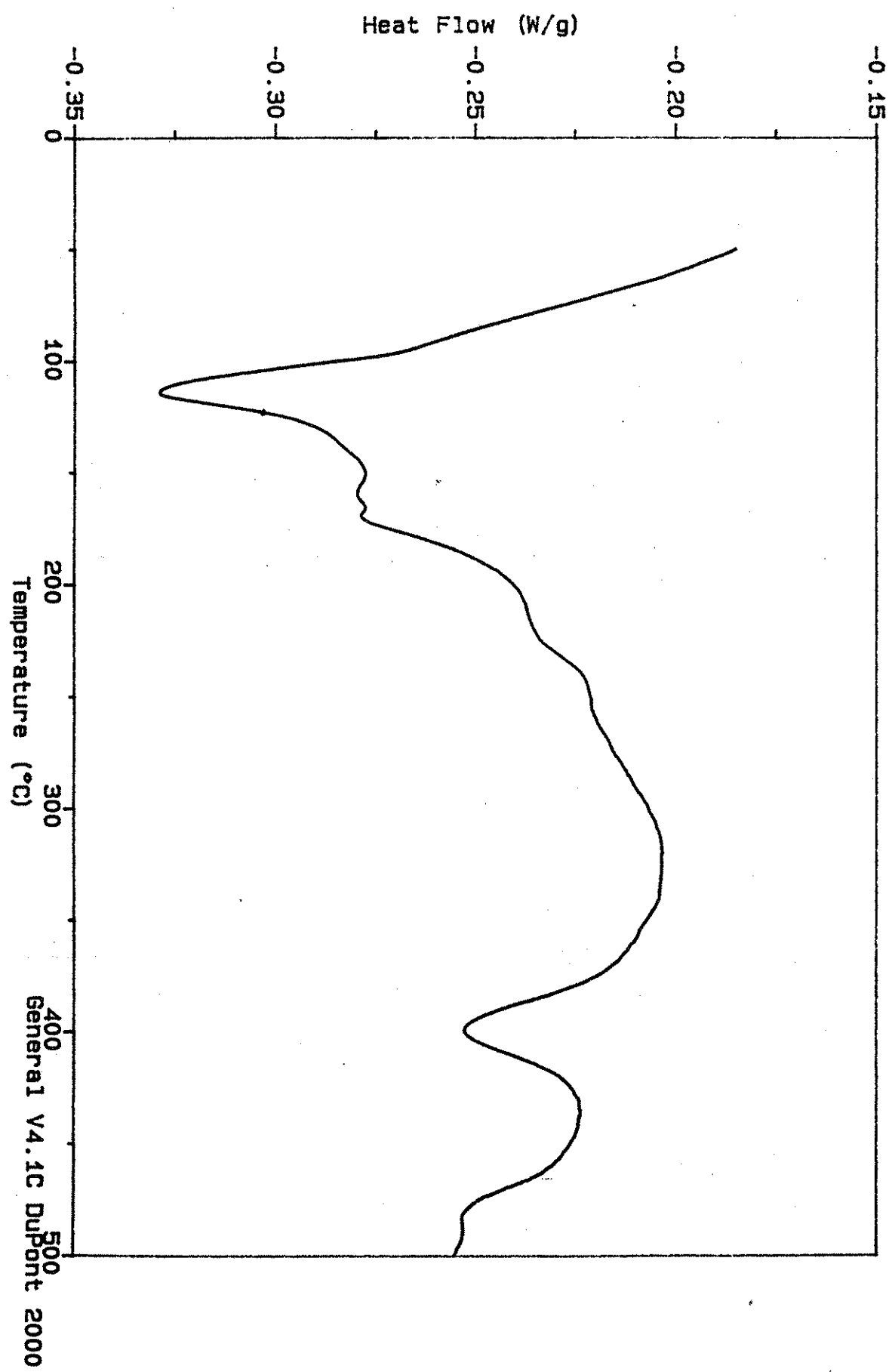
File: C: SCOTT.652
Operator: J. AMENSON
Run Date: 24-May-95 09:45



Sample: CORE 6
Size: 10.5000 mg
Method: 10°C/min
Comment: In N2 @ 50 ml/min

DSC

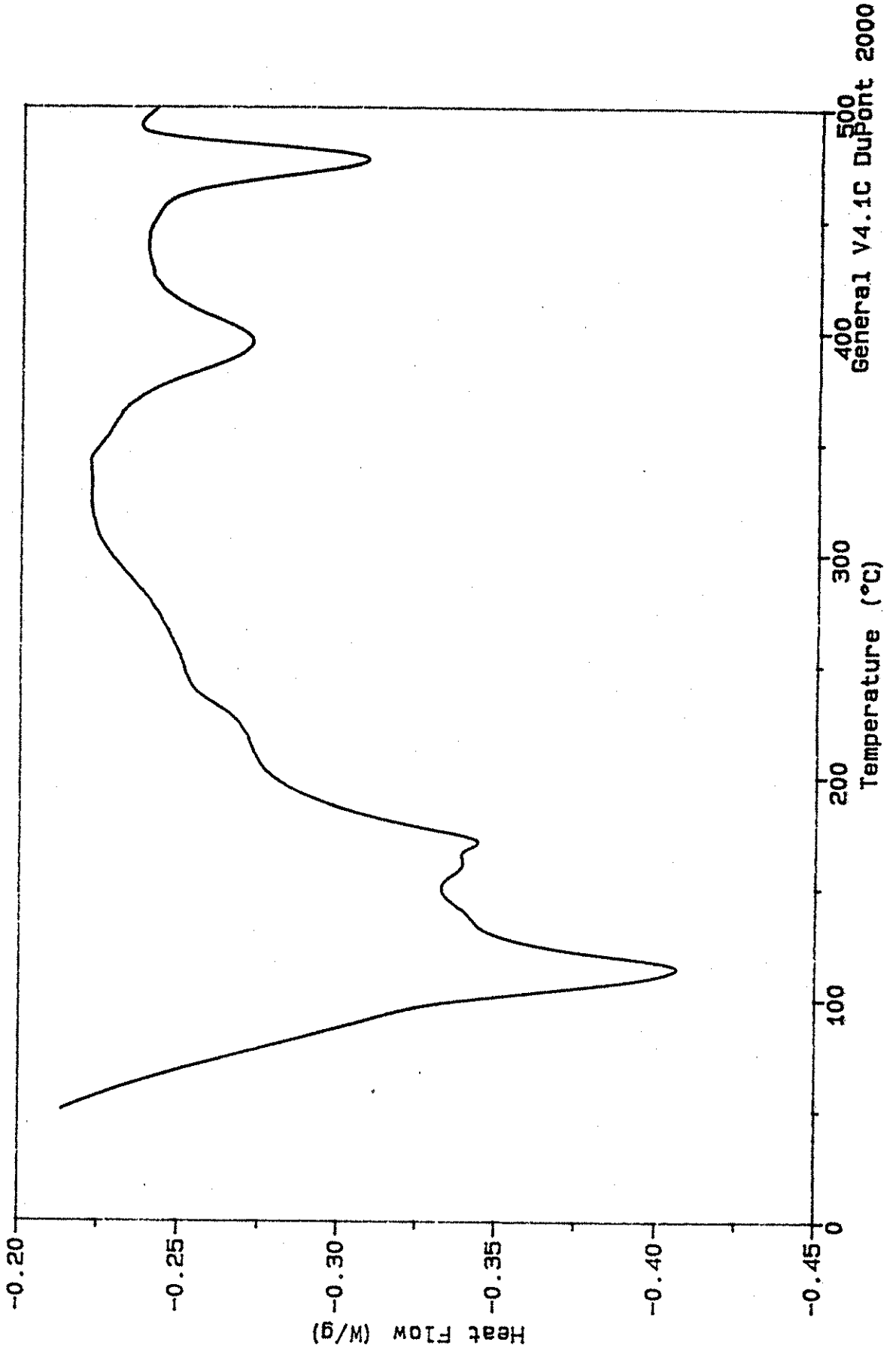
File: C:SCOTT.653
Operator: J. AMENSON
Run Date: 24-May-95 11:04



Sample: CORE 7
Size: 10.4000 mg
Method: 10 °C/min
Comment: In N2 @ 50 ml/min

DSC

File: C:SCOTT.654
Operator: J. AMENSON
Run Date: 24-May-95 12:30

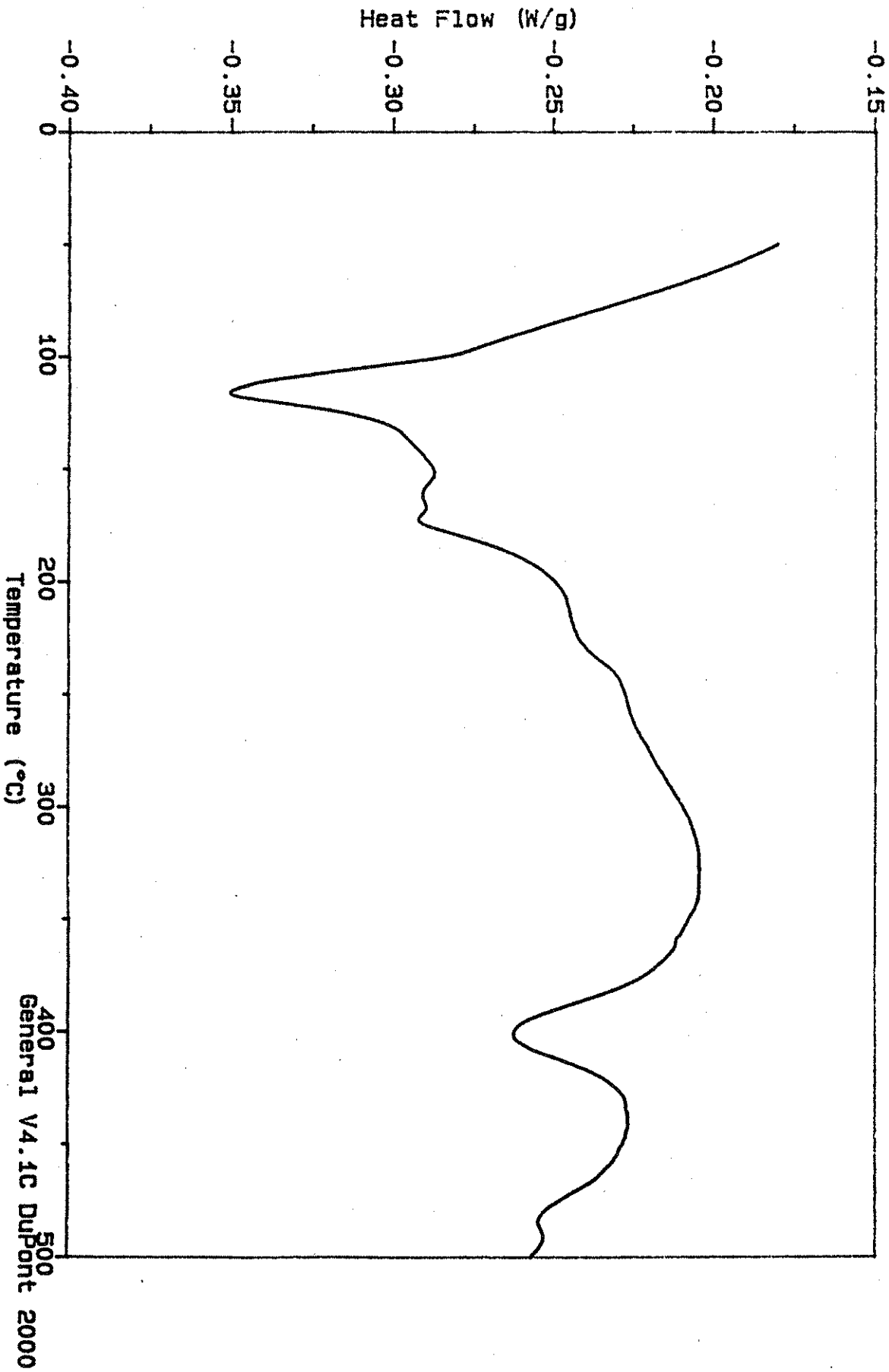


General V4.1C DuPont 2000

Sample: CORE B
Size: 10.4000 mg
Method: 10°C/min
Comment: In N2 @ 50 ml/min

DSC

File: C:SCOTT.655
Operator: J. AMENSON
Run Date: 25-May-95 14:36

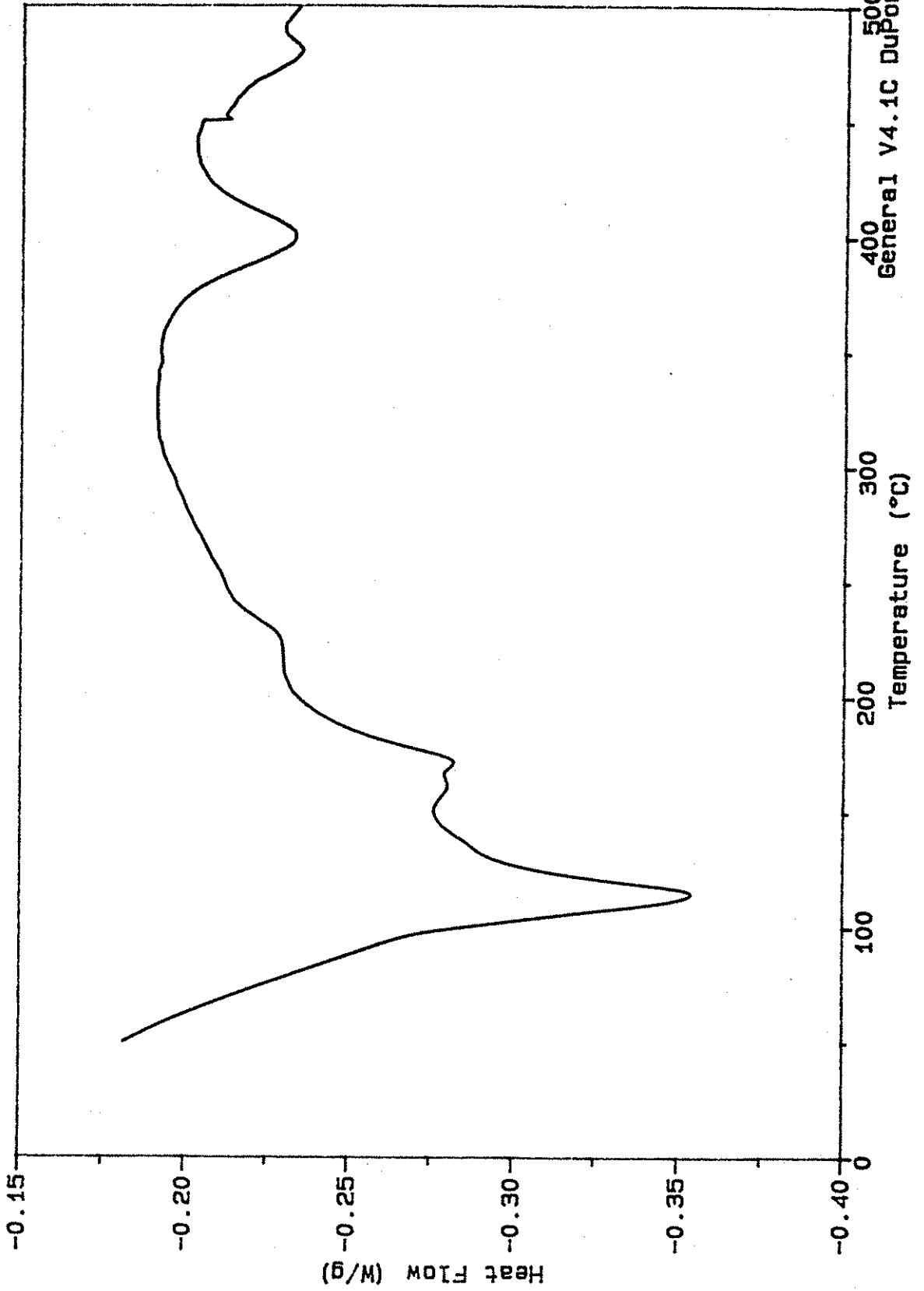


400
General V4.1C DuPont 2000

File: C:SCOTT.656
Operator: J. AMENSON
Run Date: 25-May-95 16:11

DSC

Sample: CORE 10
Size: 10.5000 mg
Method: 10°C/min
Comment: In N2 @ 50 ml/min

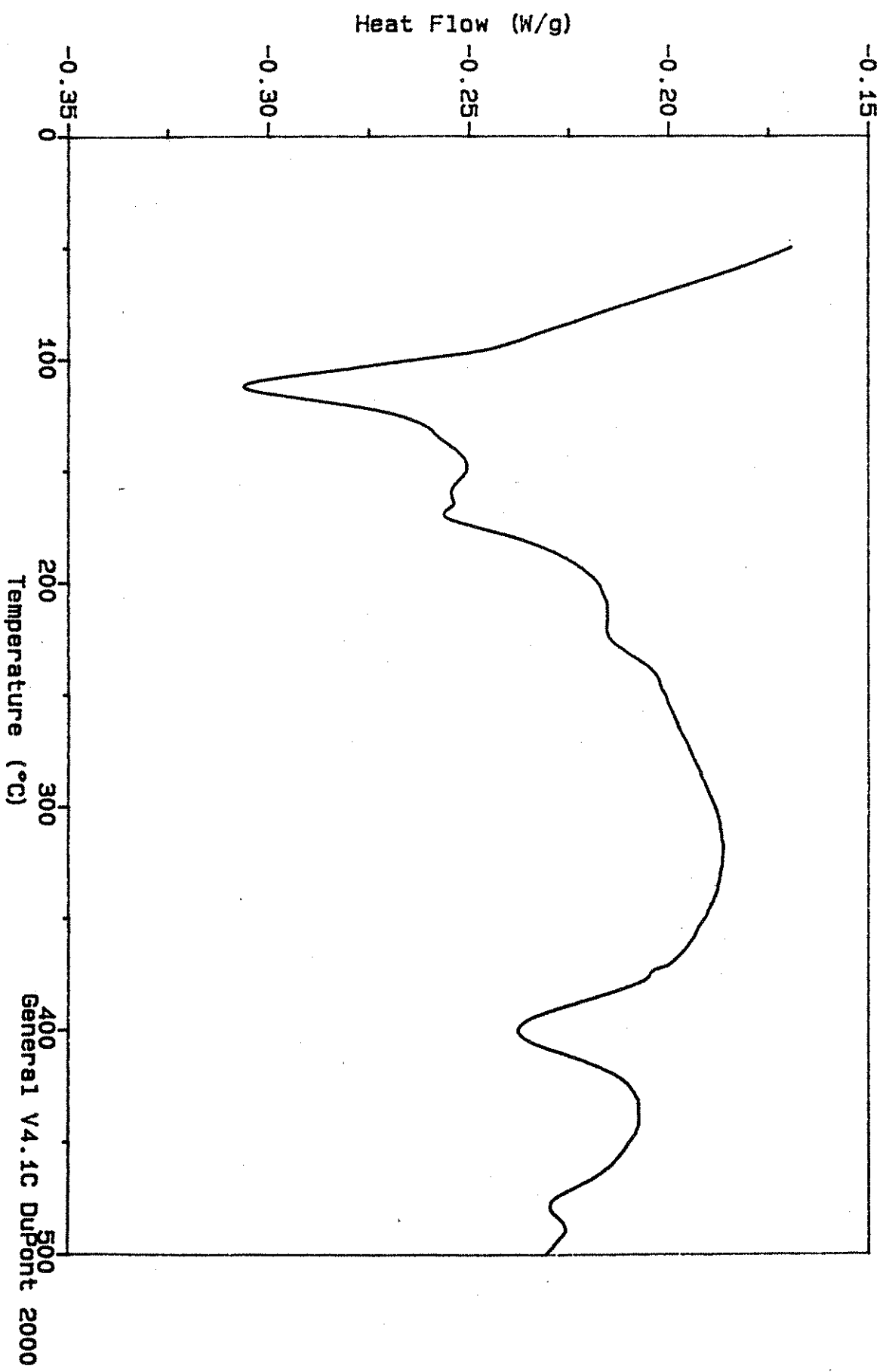


General V4.1C DuPont 2000

Sample: CORE 11
Size: 10.3000 mg
Method: 10°C/min
Comment: In N2 @ 50 ml/min

DSC

File: C:SCOTT.657
Operator: J. AMENSON
Run Date: 26-May-95 07:28

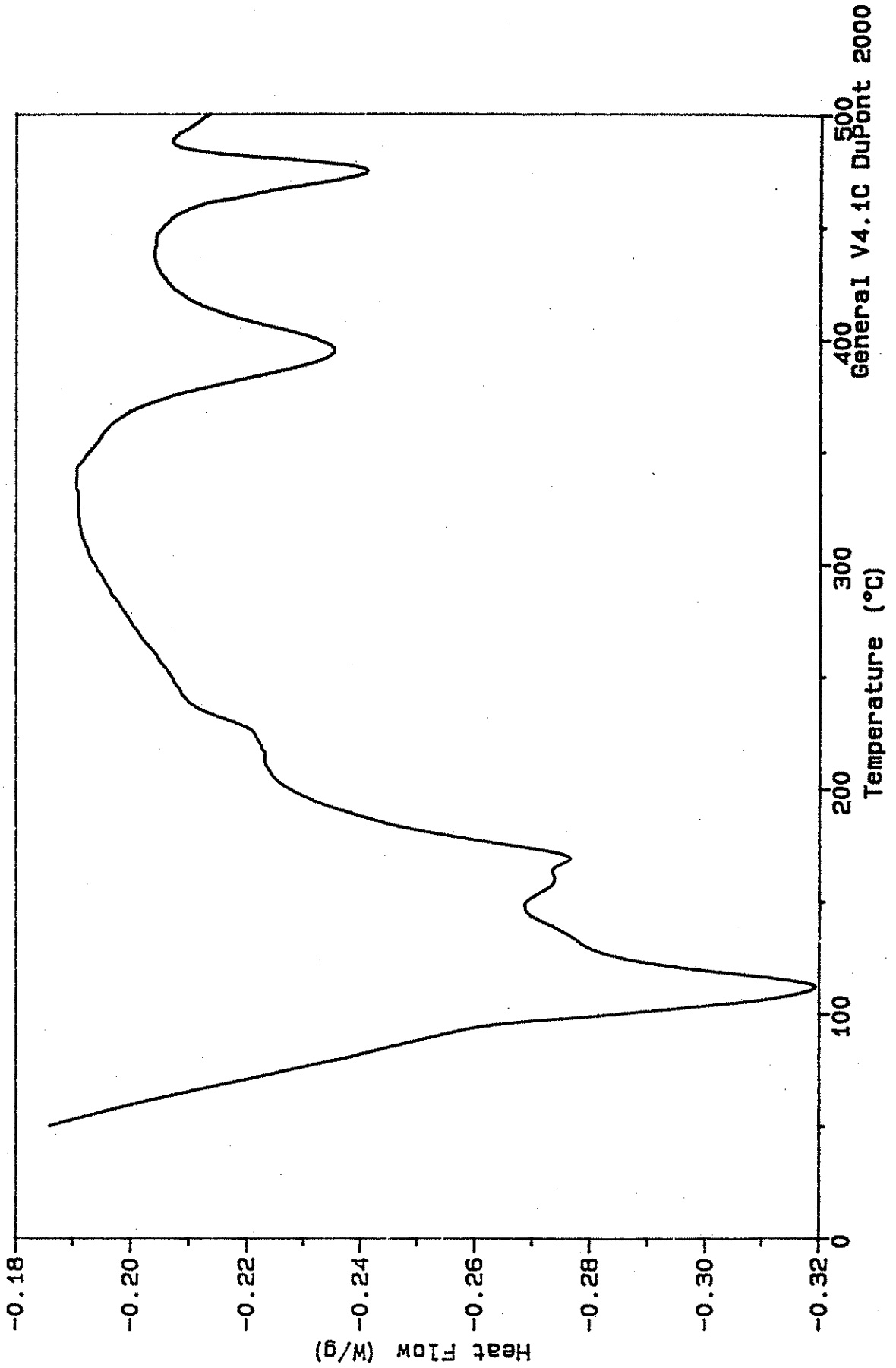


General V4.1C DuPont 2000

File: C: SCOTT.658
Operator: J. AMENSON
Run Date: 26-May-95 08:46

DSC

Sample: CORE 12
Size: 10.2000 mg
Method: 10°C/min
Comment: In N2 @ 50 ml/min

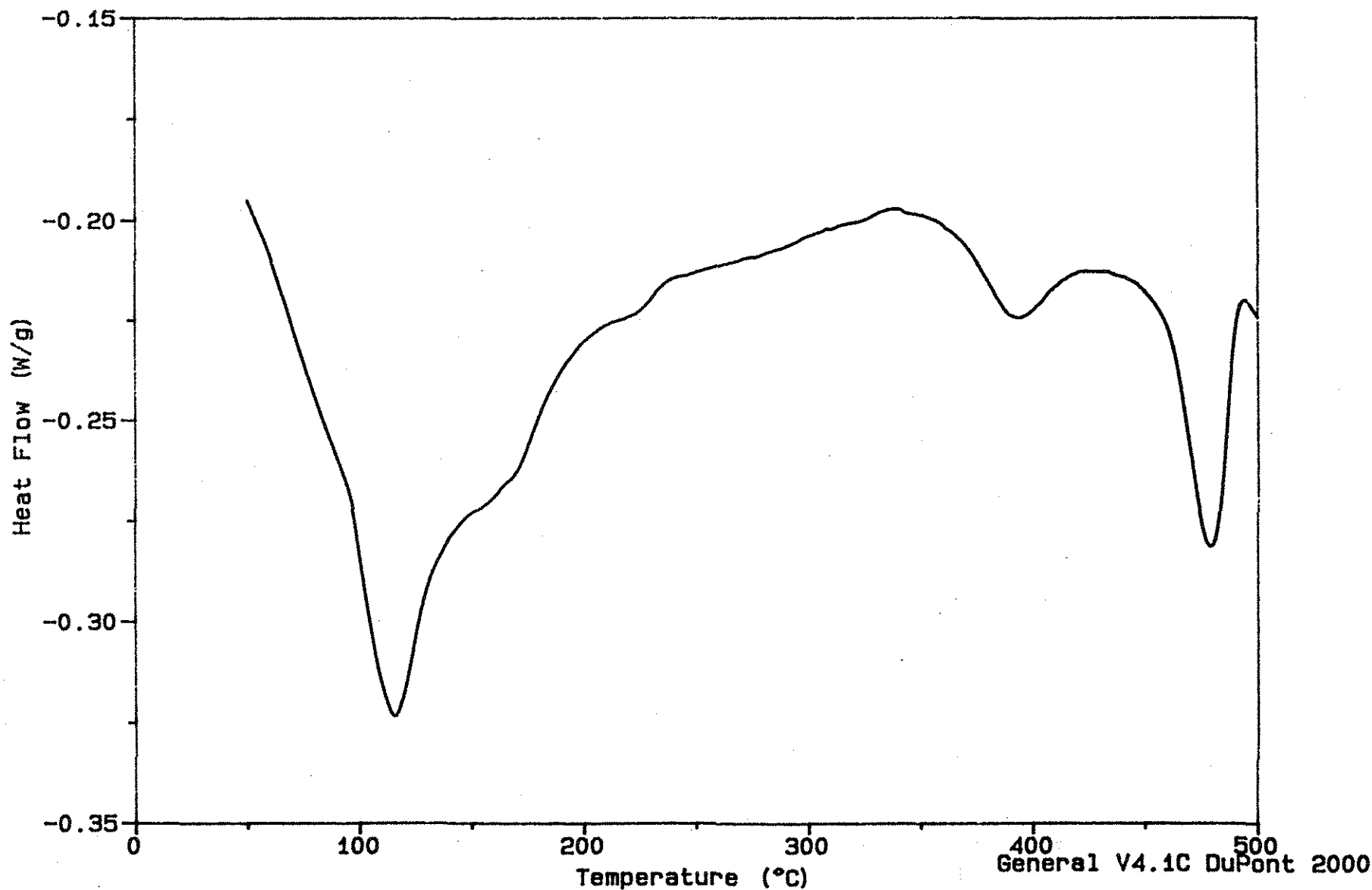


500
400
General V4.1C DuPont 2000

Sample: CORE 13
Size: 10.2000 mg
Method: 10°C/min
Comment: In N2 @ 50 ml/min

DSC

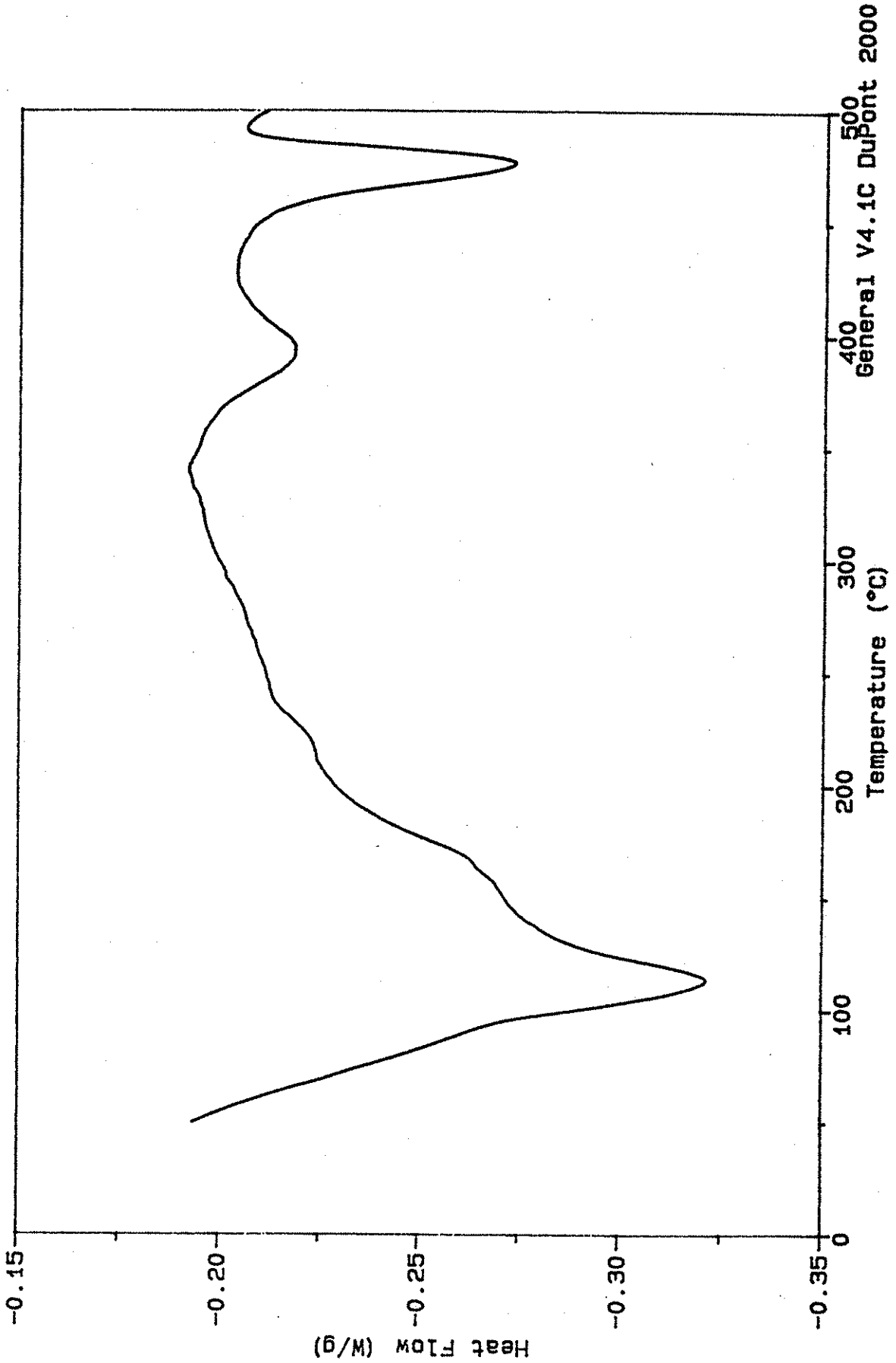
File: C: SCOTT.659
Operator: J. AMENSON
Run Date: 26-May-95 09:49



Sample: CORE 14
Size: 10.4000 mg
Method: 10°C/min
Comment: In N2 @ 50 ml/min

DSC

File: C: SCOTT.660
Operator: J. AMENSON
Run Date: 26-May-95 10: 57

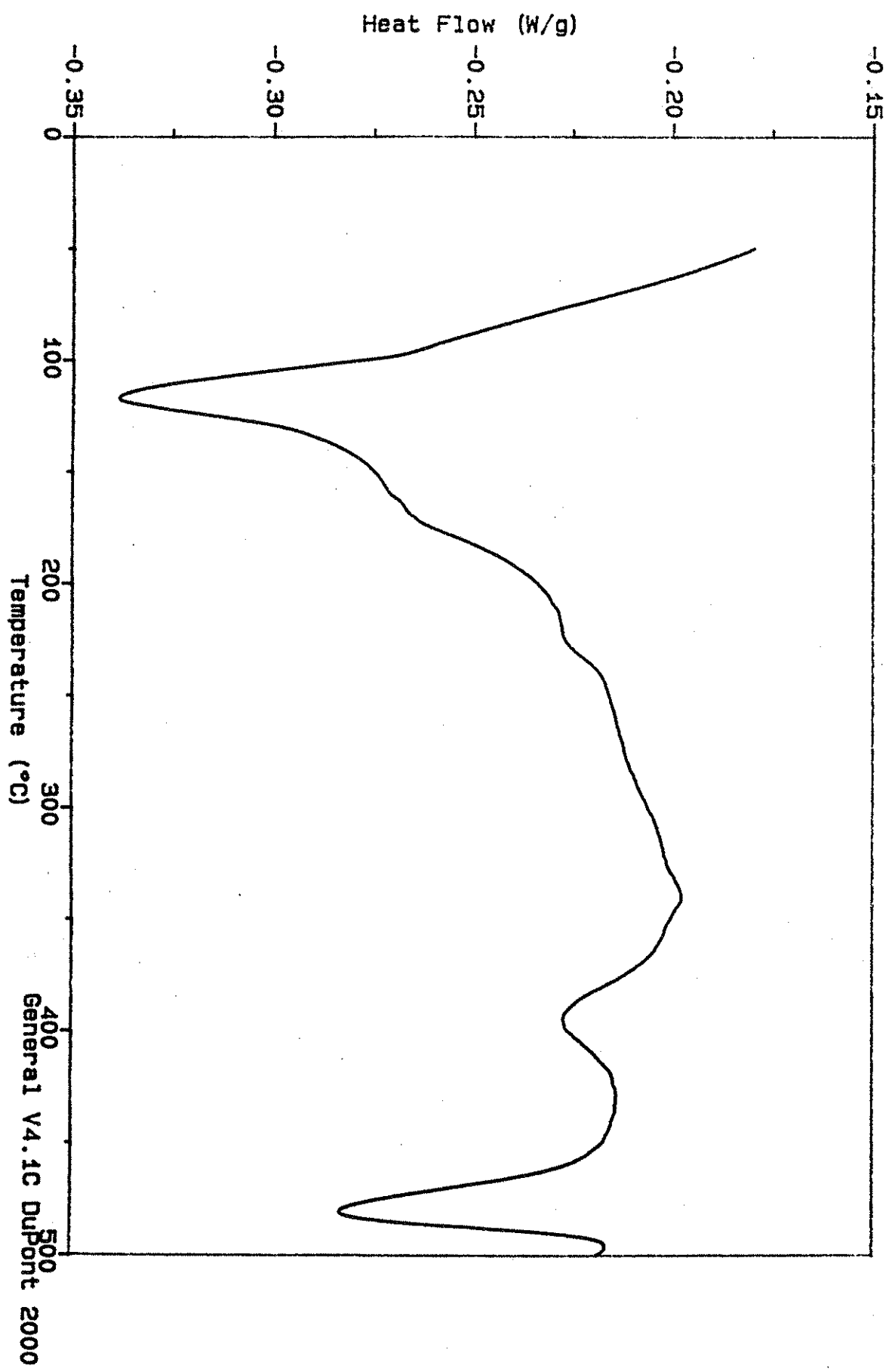


General V4.1C DuPont 2000

Sample: CORE 15
Size: 10.0000 mg
Method: 10°C/min
Comment: In N2 @ 50 ml/min

DSC

File: C:SCOTT.661
Operator: J. AMENSON
Run Date: 26-May-95 13:01

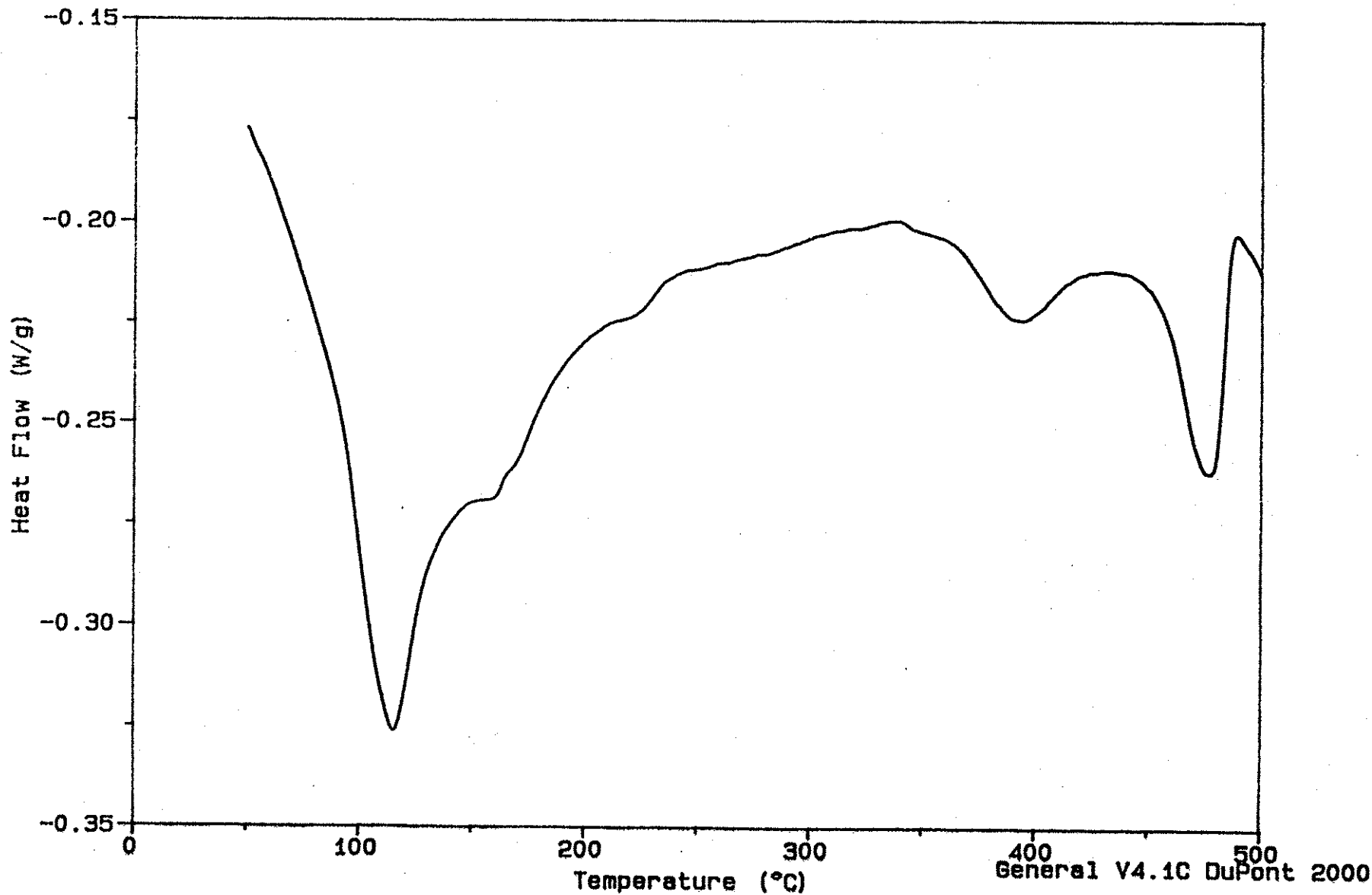


General V4.1C DuPont 2000

Sample: CORE 16
Size: 10.2000 mg
Method: 10°C/min
Comment: In N2 @ 50 ml/min

DSC

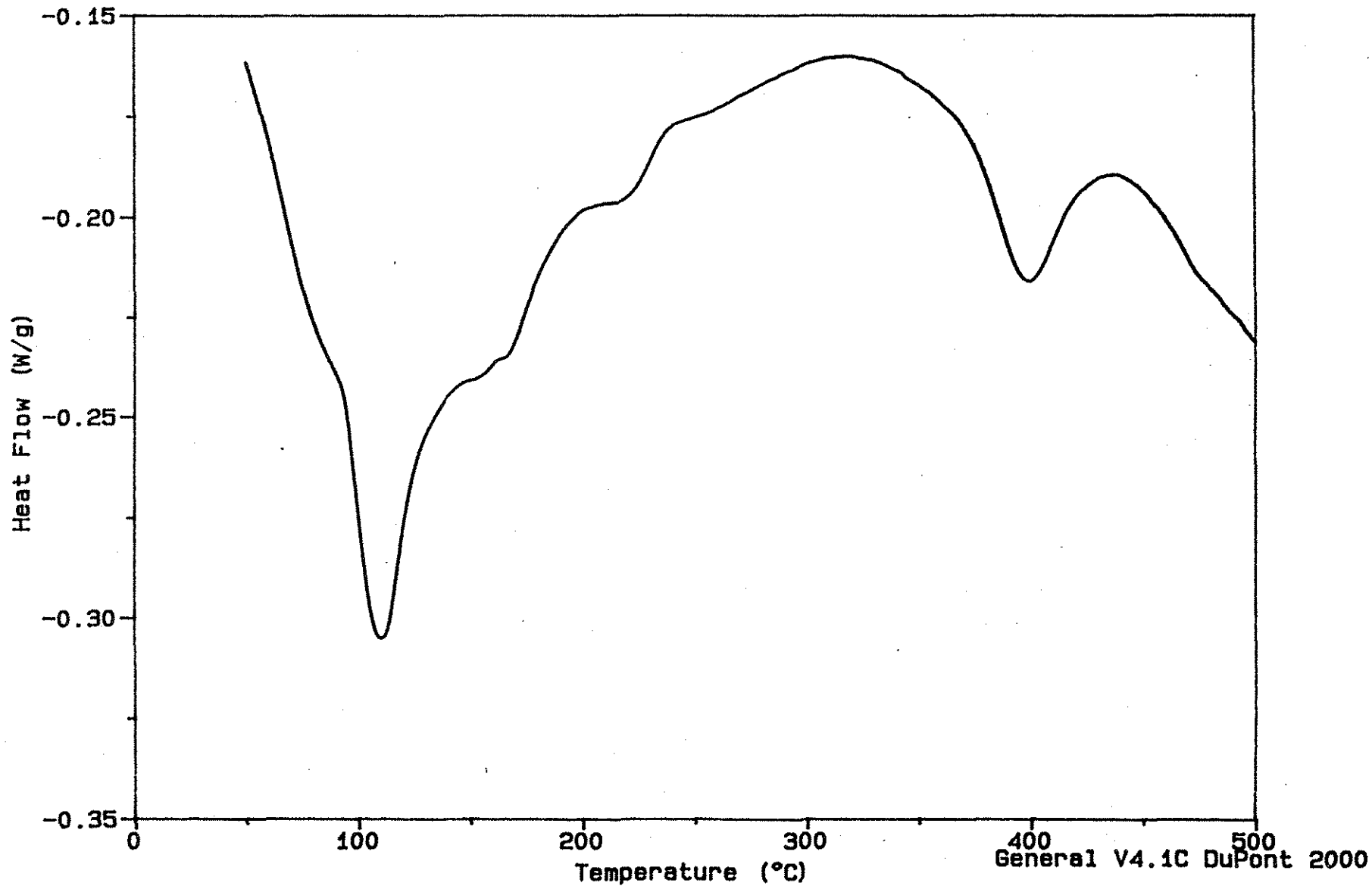
File: C: SCOTT.662
Operator: J. AMENSON
Run Date: 26-May-95 14:17



Sample: CORE 17
Size: 10.4000 mg
Method: 10°C/min
Comment: In N2 @ 50 ml/min

DSC

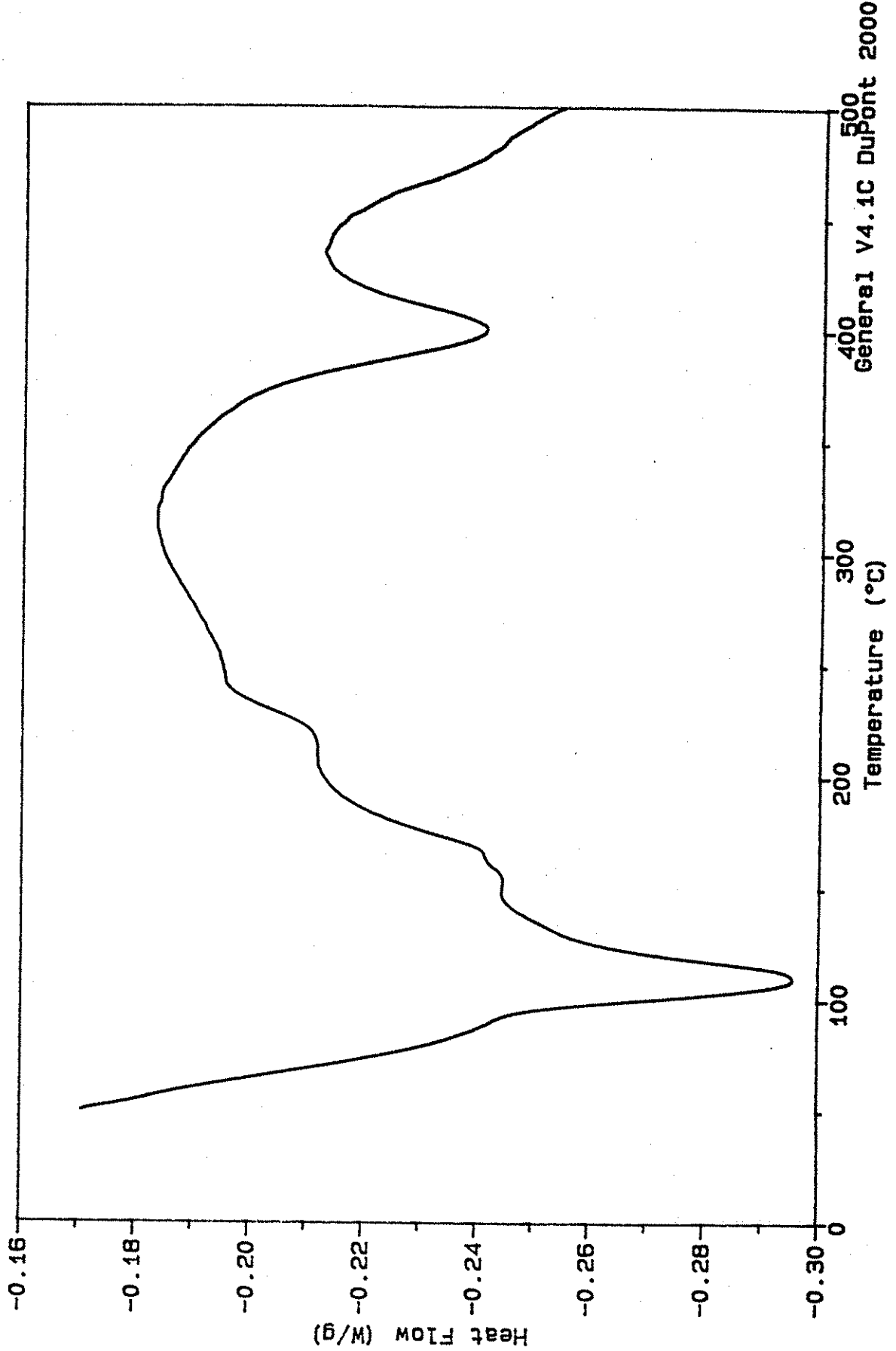
File: C:SCOTT.663
Operator: J. AMENSON
Run Date: 31-May-95 14:57



Sample: CORE 18
Size: 10.1000 mg
Method: 10°C/min
Comment: In N2 @ 50 ml/min

DSC

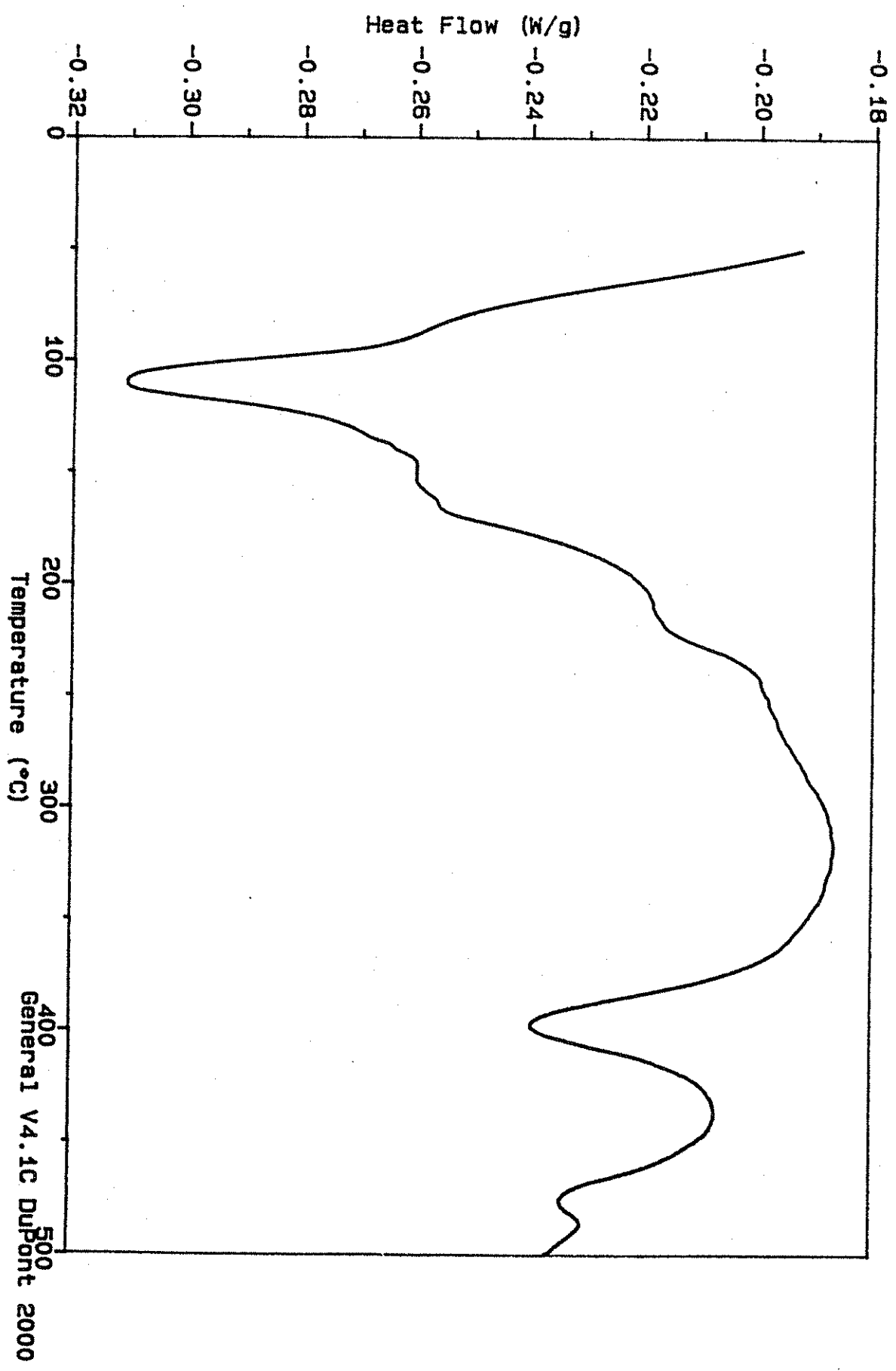
File: C:SCOTT.664
Operator: J. AMENSON
Run Date: 1-Jun-95 06:06



Sample: CORE 19
Size: 10.1000 mg
Method: 10°C/min
Comment: In N2 @ 50 ml/min

DSC

File: C:SCOTT.665
Operator: J. AMENSON
Run Date: 1-Jun-95 07:17

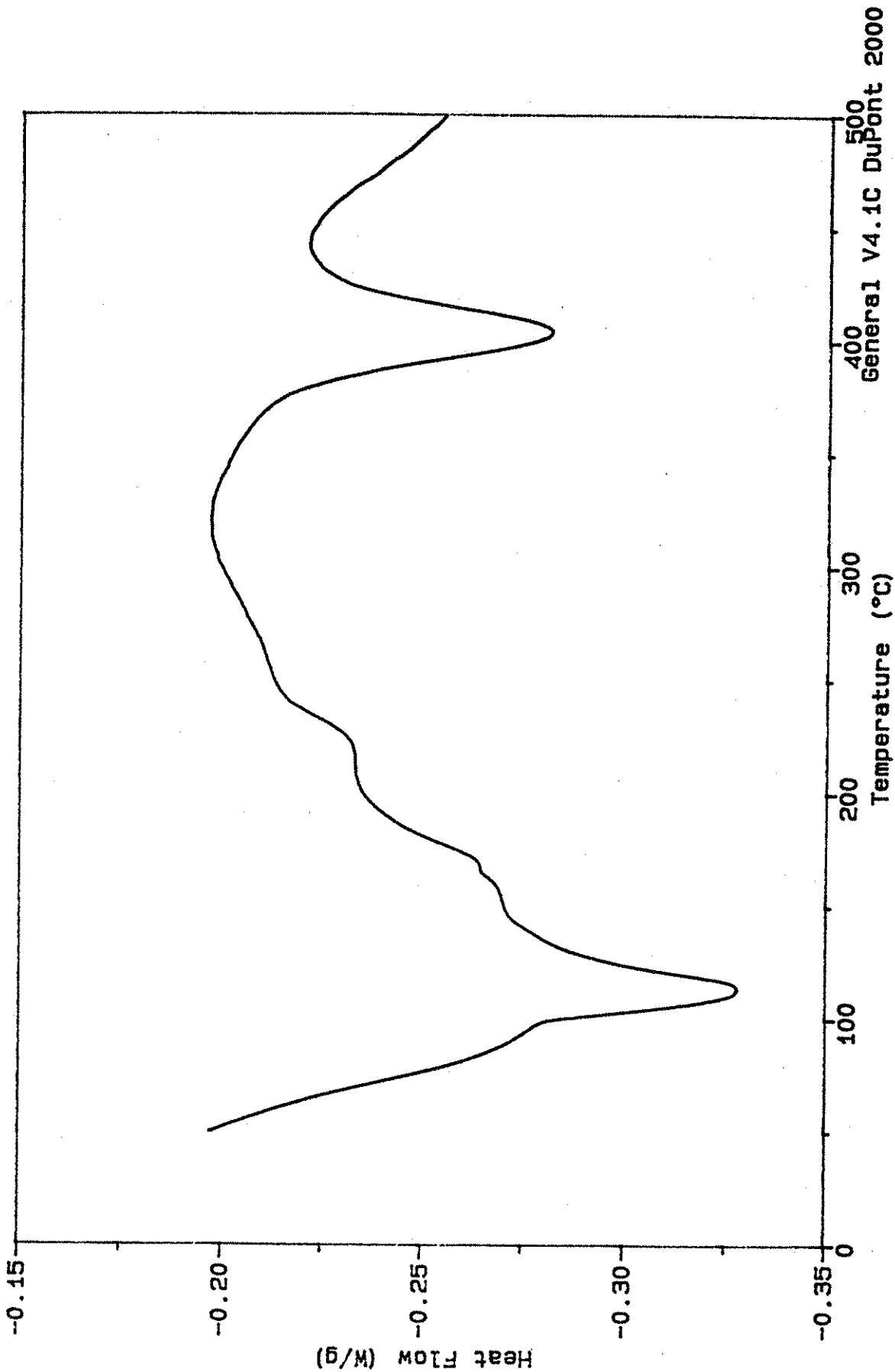


General V4.1C DuPont 2000

Sample: CORE 20
Size: 10.1000 mg
Method: 10°C/min
Comment: In N2 @ 50 ml/min

DSC

File: C:SCOTT.666
Operator: J. AMENSON
Run Date: 1-Jun-95 08:38

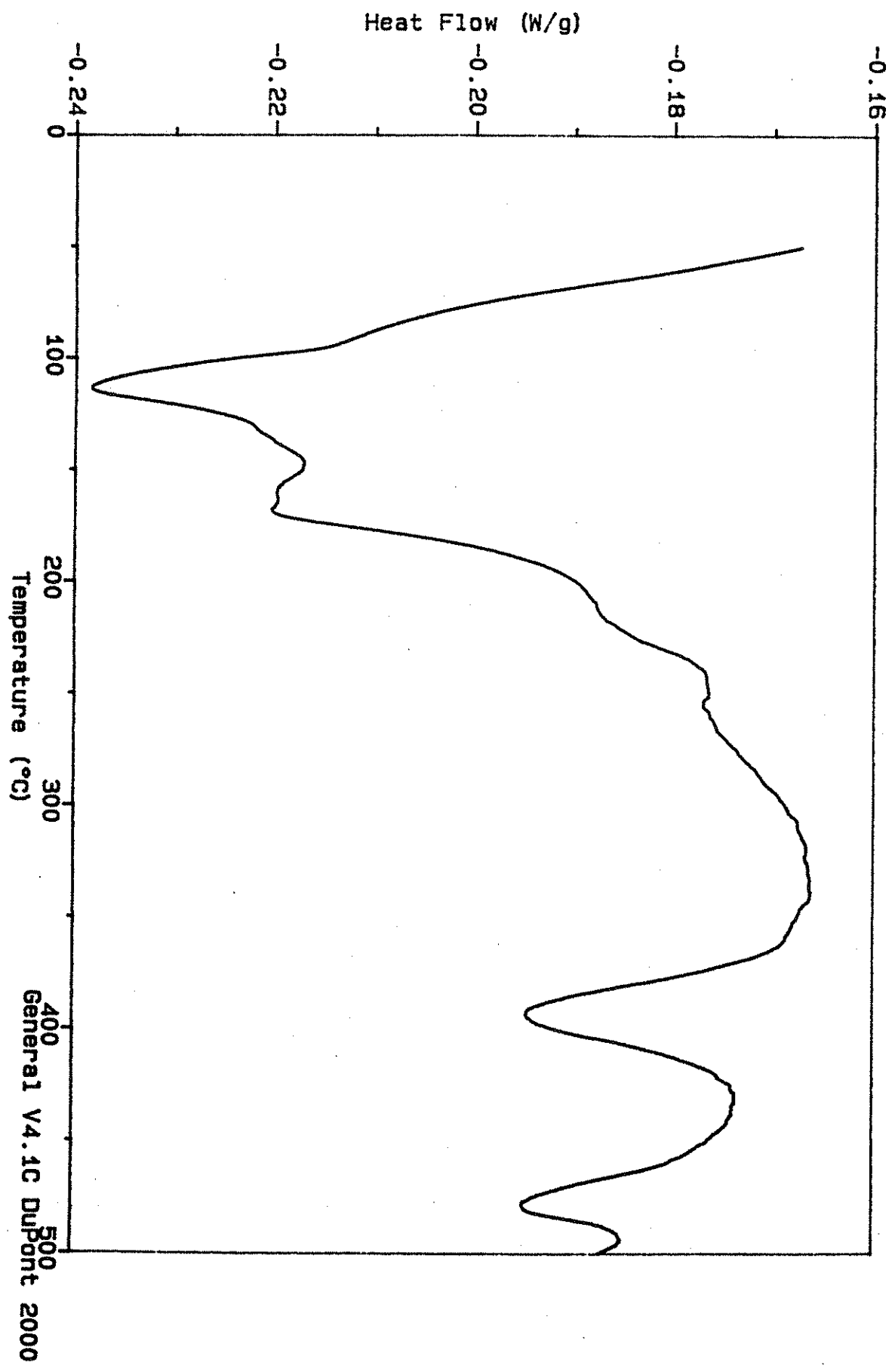


General V4.1C DuPont 2000

Sample: CORE 21
Size: 10.4000 mg
Method: 10°C/min
Comment: In N2 @ 50 ml/min

DSC

File: C:SCOTT.667
Operator: J. AMENSON
Run Date: 1-Jun-95 09:48

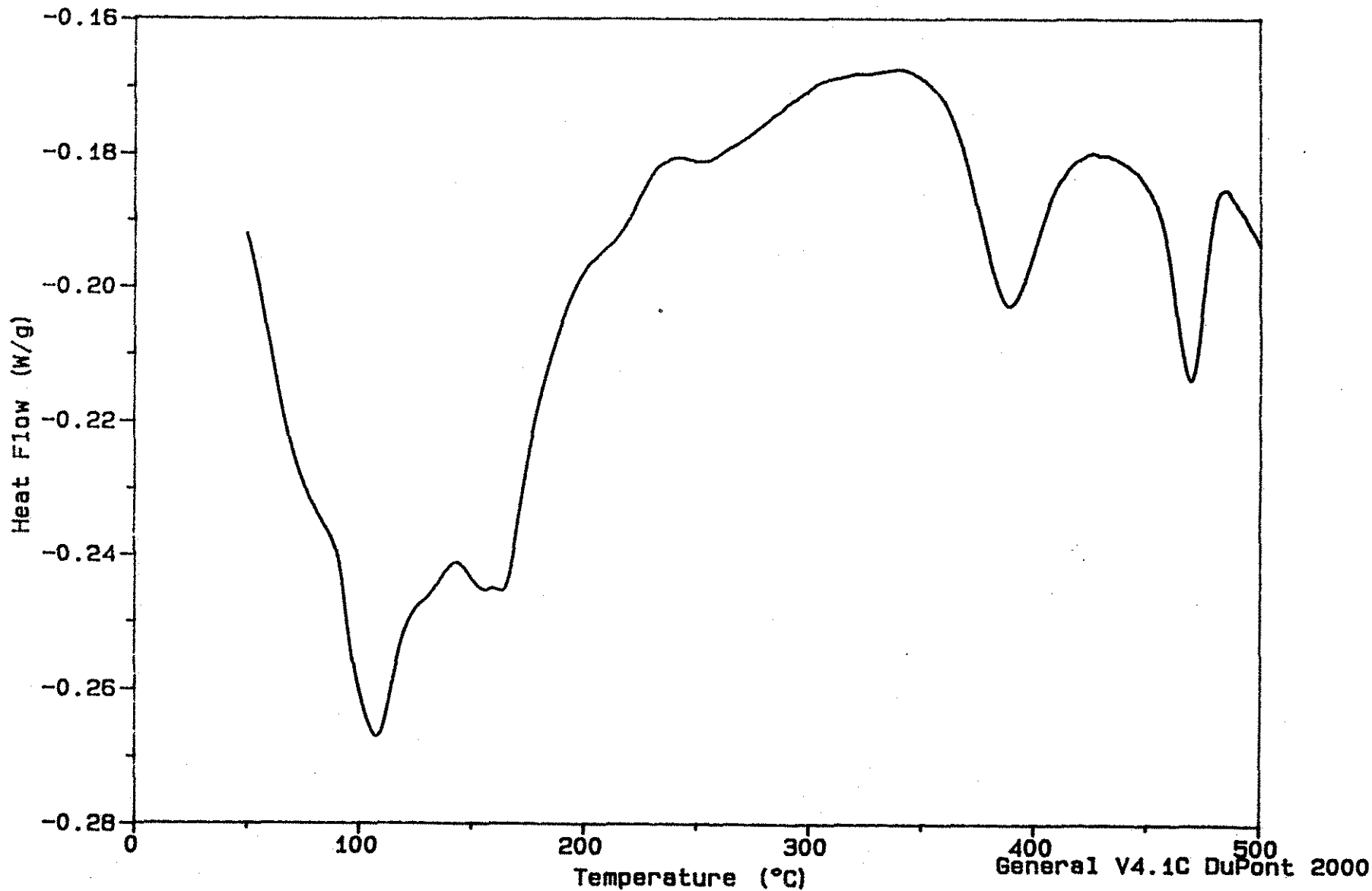


General V4.1C DuPont 2000

Sample: CORE 22
Size: 10.2000 mg
Method: 10°C/min
Comment: In N2 @ 50 ml/min

DSC

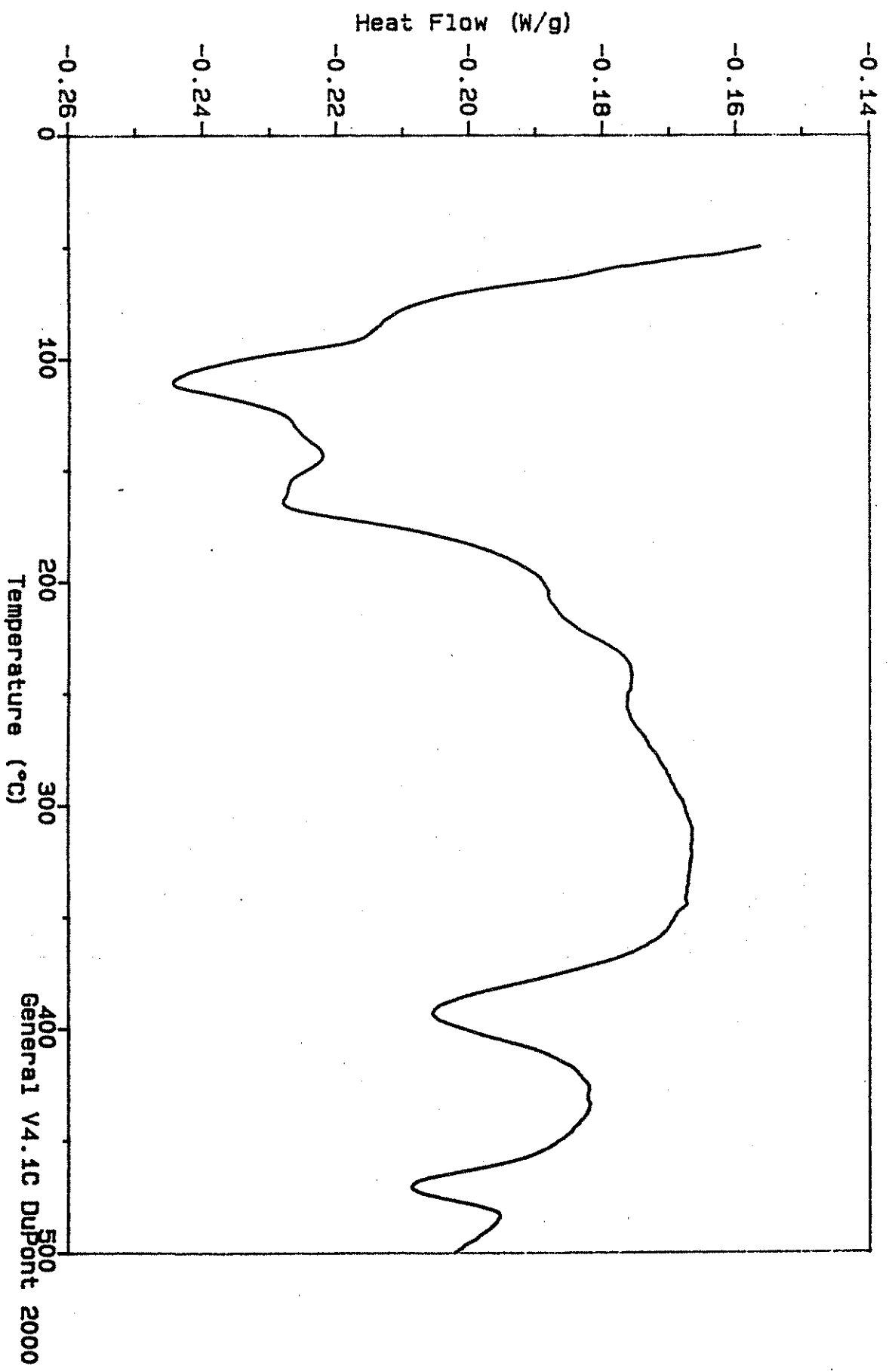
File: C: SCOTT.668
Operator: J. AMENSON
Run Date: 1-Jun-95 10:49



Sample: CORE 24
Size: 10.3000 mg
Method: 10°C/min
Comment: In N2 @ 50 ml/min

DSC

File: C:SCOTT.669
Operator: J. AMENSON
Run Date: 1-Jun-95 13:24

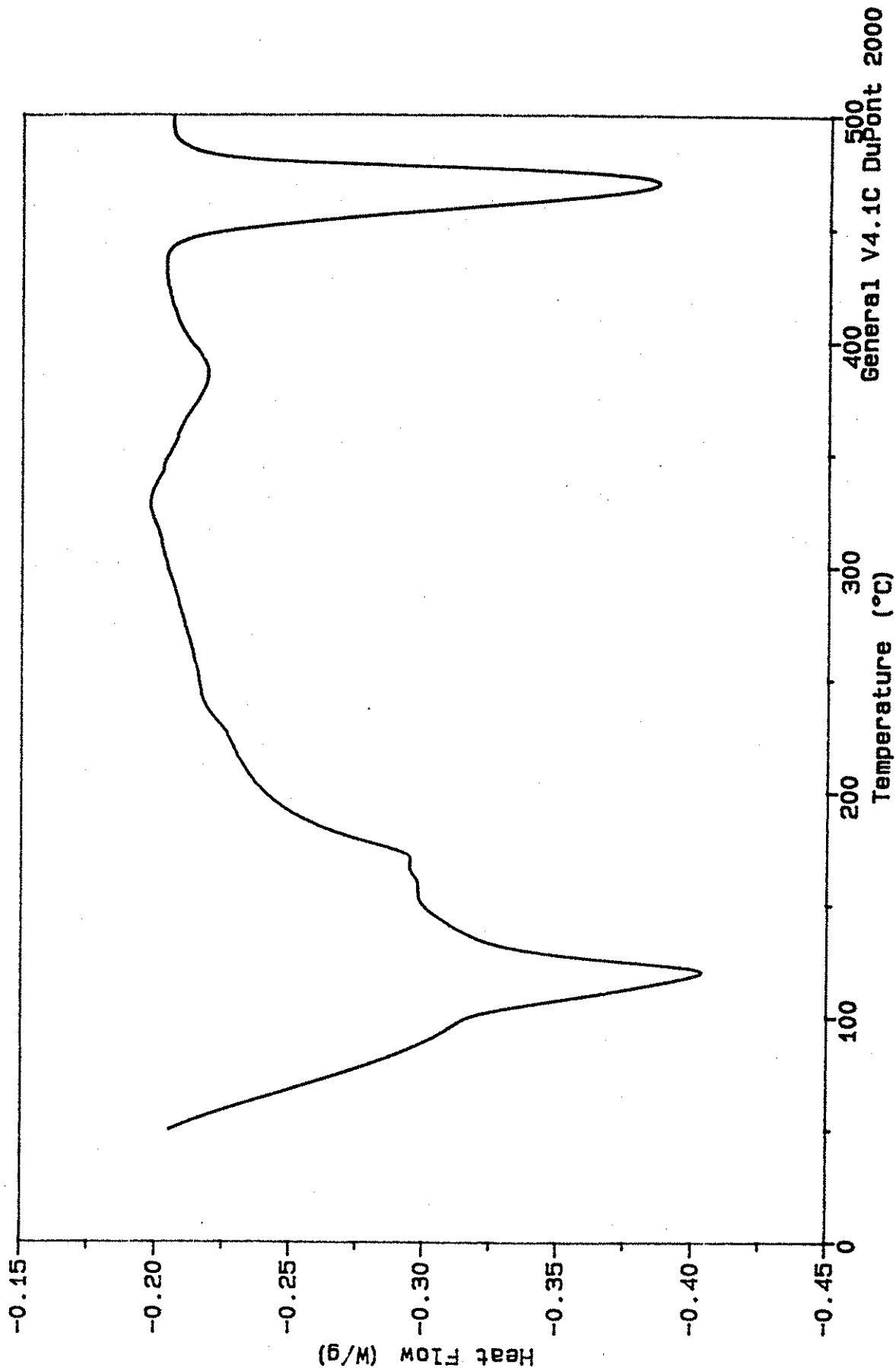


General V4.1C DuPont 2000

Sample: IO-1 #53
Size: 10.2000 mg
Method: 10°C/min
Comment: In N2 @ 50 ml/min

DSC

File: C:\SCOTT.677
Operator: J. AMENSON
Run Date: 5-Jun-95 10:50



General V4.1C DuPont 2000

Sample: I15-1 #55
Size: 10.3000 mg
Method: 10°C/min
Comment: In N2 @ 50 ml/min

DSC

File: C: SCOTT.678
Operator: J. AMENSON
Run Date: 5-Jun-95 11:54

